ВЕСТНИК ТРАНСПЛАНТОЛОГИИ И ИСКУССТВЕННЫХ ОРГАНОВ

VESTNIK TRANSPLANTOLOGII I ISKUSSTVENNYKH ORGANOV

RUSSIAN JOURNAL OF TRANSPLANTOLOGY AND ARTIFICIAL ORGANS

УЧРЕДИТЕЛЬ: ОБЩЕРОССИЙСКАЯ ОБЩЕСТВЕННАЯ ОРГАНИЗАЦИЯ ТРАНСПЛАНТОЛОГОВ «РОССИЙСКОЕ ТРАНСПЛАНТОЛОГИЧЕСКОЕ ОБЩЕСТВО»

THE OFFICIAL JOURNAL OF ALL-RUSSIAN PUBLIC ORGANIZATION OF TRANSPLANTOLOGISTS "RUSSIAN TRANSPLANT SOCIETY"

2024. Том XXVI. № 4

2024. Vol. XXVI. № 4

Научно-практический журнал основан в 1999 г.
Регистр. № 018616

Scientific and Practical Journal was founded in 1999
Reg. № 018616

Журнал «Вестник трансплантологии и искусственных органов» включен ВАК РФ в перечень российских рецензируемых научных изданий, в которых должны быть опубликованы результаты диссертационных работ

Журнал «Вестник трансплантологии и искусственных органов» включен ФГБУ «НМИЦ ТИО им. ак. В.И. Шумакова» Минздрава России в перечень российских рецензируемых научных изданий, в которых должны быть опубликованы основные результаты исследований в рамках диссертаций, представляемых к защите в диссертационный совет ФГБУ «НМИЦ ТИО им. ак. В.И. Шумакова» Минздрава России

Журнал «Вестник трансплантологии и искусственных органов» индексируется в Scopus и размещен на платформе Web of Science Core Collection: Emerging Science Citation Index

"Russian Journal of Transplantology and Artificial Organs" is included in the list of leading peer-reviewed scientific publication editions, produced in the Russian Federation and is recommended for publication of primary results of dissertation research

"Russian Journal of transplantology and artificial organs" is included by the Federal State Budgetary Institution "Shumakov National Medical Research Center of Transplantology and Artificial Organs" of the Ministry of Health of Russia in the list of Russian peer-reviewed scientific publications in which the main results of research should be published within the framework of dissertations submitted for defense to the dissertation council of Shumakov National Medical Research Center of Transplantology and Artificial Organs

"Russian Journal of Transplantology and Artificial Organs" is indexed in Scopus and in the Emerging Science Citation Index of the Web of Science Core Collection

ISSN 1995-1191

Адрес для корреспонденции:

Россия, 123182, Москва, ул. Щукинская, 1
Тел./факс +7 (499) 193 87 62
E-mail: vestniktranspl@gmail.com
Интернет-сайт журнала: http://journal.transpl.ru
Научная электронная библиотека: http://elibrary.ru

Address for correspondence:

1, Shchukinskaya st., Moscow 123182, Russia
Tel./Fax +7 (499) 193 87 62
E-mail: vestniktranspl@gmail.com
Journal's web site: http://journal.transpl.ru
Scientific eLibrary: http://elibrary.ru

Подписной индекс в каталоге почты России – ПН380

СОДЕРЖАНИЕ

СТРАНИЦА ГЛАВНОГО РЕДАКТОРА

КЛИНИЧЕСКАЯ ТРАНСПЛАНТОЛОГИЯ

CONTENTS

EDITORIAL

CLINICAL TRANSPLANTOLOGY

XII ВСЕРОССИЙСКИЙ СЪЕЗД ТРАНСПЛАНТОЛОГОВ (С МЕЖДУНАРОДНЫМ УЧАСТИЕМ)

Глубокоуважаемые коллеги!

30 сентября – 2 октября 2024 года в Москве состоялся XII Всероссийский съезд трансплантологов с международным участием, приуроченный к 55-летию Национального медицинского исследовательского центра трансплантологии и искусственных органов имени академика В.И. Шумакова Минздрава России (юбилею НМИЦ ТИО им. ак. В.И. Шумакова была посвящена страница главного редактора в предыдущем номере нашего журнала).

Всероссийские съезды и конгрессы трансплантологов проводятся традиционно, но в этом году событие получилось особенно праздничным и знаменательным. Во-первых, благодаря юбилейным торжествам, приветствиям и награждениям, которыми были отмечены весь коллектив, руководство Центра и многие заслуженные сотрудники, а также в силу важности и высокого качества профессиональной информации, представленной на съезде. В программу съезда вошли анализ и обсуждение новейших достижений трансплантологии:

– *уникальный клинический опыт трансплантации сердца с обсуждением широкого круга проблем – от пригодности донорского сердца для трансплантации до лечения кардиопатии сердечного трансплантата в отдаленные сроки;*
– *применение вспомогательного кровообращения у взрослых и детей, с трансляцией операции по имплантации отечественной системы механического кровообращения, разработанной в ФГБУ «НМИЦ ТИО им. ак. В.И. Шумакова» Минздрава России;*
– *анализ 10-летнего опыта трансплантации легких в НМИЦ ТИО им. ак. В.И. Шумакова; мастер-класс по интервенционной бронхоскопии в трансплантации легких;*

THE 12TH ALL-RUSSIAN CONGRESS OF TRANSPLANTOLOGISTS (WITH INTERNATIONAL PARTICIPANTS)

Dear colleagues,

The city of Moscow hosted the 12th All-Russian Congress of Transplantologists from September 30 to October 2, 2024. The international event was held to celebrate the 55th anniversary of the Shumakov National Medical Research Center of Transplantology and Artificial Organs ("Shumakov Center"). This anniversary was commemorated on the Editor-in-Chief's page in the last issue of our journal.

All-Russian congresses and conventions of transplantologists are traditional events, but this year's event was particularly festive and noteworthy. This was so firstly due to the anniversary festivities, welcoming speeches and awards that were given to the entire Shumakov Center staff and management, as well as many distinguished employees, and because of the importance and high quality of the expert knowledge presented at the Congress. The program of the event featured some analysis and conversation about the most recent advancements in transplantology such as:

– *Exceptional clinical experience in heart transplantation with a discussion of a wide range of transplant topics – from suitability of donor heart for transplantation to long-term management of transplant cardiomyopathy;*
– *The use of assisted circulation in adults and children, along with a broadcast of the procedure on implantation of a Russian-made mechanical circulatory system, developed at Shumakov Center;*
– *A review of Shumakov Center's ten years of lung transplant experience; a master class on interventional bronchoscopy in lung transplantation;*

– *актовая лекция почетного профессора Б.Л. Миронкова – «Эндоваскулярная хирургия в трансплантологической практике».*

Обсуждались новые подходы к решению «старых» проблем при трансплантации печени, с демонстрацией операции по лапароскопическому изъятию левого латерального сектора печени у родственного донора;

– *важные вопросы физической, социально-педагогической, психологической реабилитации маленьких пациентов после трансплантации органов;*
– *иммунологические и другие факторы риска в трансплантации гемопоэтических стволовых клеток и солидных органов;*
– *технологии клеточной, тканевой инженерии и регенеративной медицины для компенсации или замены функций пораженных органов и тканей человека на молекулярном, клеточном и тканевом уровнях и многое другое.*

Участникам была предоставлена возможность посещения 23 мероприятий с разнообразной тематикой, в рамках которых прозвучало более 120 докладов, посвященных медицинским, организационным аспектам оказания трансплантологической помощи и донорства органов. Специалисты со всей страны и из зарубежья приняли участие в конференциях, методических совещаниях, семинарах, «круглых столах», обсуждениях, мастер-классах и постерной сессии.

Постерная сессия «Зеркало современной трансплантологии» была посвящена 25-летию журнала «Вестник трансплантологии и искусственных органов». Конкурсная комиссия оценила 30 ранее отобранных для презентации стендовых докладов разных научных школ из разных регионов нашей страны. Грамоту признания коллег получил постер «Лапароскопическая резекция печени у родственного донора с получением трансплантата 2-го сегмента с использованием флуоресцентной навигации», представленный сотрудниками НМИЦ ТИО им. ак. В.И. Шумакова. Все остальные постеры удостоились публикации в настоящем номере журнала, учитывая их высокие научную ценность и качество оформления.

С уважением,
главный редактор
академик РАН С.В. Готье

– *A lecture titled "Endovascular surgery in transplantology practice" by emeritus professor Boris Mironkov.*
– *New approaches to solving "old" problems in liver transplantation were discussed, with a demonstration of a laparoscopic procedure to remove the left lateral sector of the liver from a related donor;*
– *Important issues on physical, socio-pedagogical and psychological rehabilitation of young patients after organ transplantation;*
– *Immunological and other risk factors in solid organ and hematopoietic stem cell transplantation;*
– *Cellular, tissue engineering, and regenerative medicine technologies to compensate or replace the functions of diseased human organs and tissues at the molecular, cellular and tissue levels, and much more.*

Participants had the opportunity to attend 23 events covering a range of topics, where more than 120 reports on medical, organizational aspects of transplant care and organ donation were presented. The conferences, methodological meetings, seminars, roundtable discussions, master classes, and a poster session were attended by experts from across the country and overseas.

A poster session titled "Mirror of Modern Transplantology" was dedicated to the 25th anniversary of the Russian Journal of Transplantology and Artificial Organs. The competition committee evaluated 30 poster papers from different scientific schools from different regions in Russia, which had been previously selected for presentation. A poster with the title "Laparoscopic hepatectomy in a related donor with an S2 monosegment graft using fluorescence navigation", presented by some personnel at Shumakov Center, was awarded a certificate of recognition by colleagues. All other posters were accepted for publication in this issue of the journal, given their high research value and excellent design.

Sincerely,

Sergey Gautier,
Fellow, Russian Academy of Sciences
Editor-in-chief, Russian Journal
of Transplantology and Artificial Organs

DOI: 10.15825/1995-1191-2024-4-8-13

KIDNEY TRANSPLANTATION IN CHILDREN WITH A COMPROMISED INFERIOR VENA CAVA: A UNIQUE EXPERIENCE AT SHUMAKOV RESEARCH CENTER

D.A. Saydulaev, A.A. Zharikov, A.A. Kartashev, P.M. Gadzhieva, A.R. Karapityan

Shumakov National Medical Research Center of Transplantology and Artificial Organs, Moscow, Russian Federation

Compromised inferior vena cava (IVC) is a rare but life-threatening condition in low-birth-weight children who require kidney transplantation (KT) to survive. **Objective:** to demonstrate a comprehensive approach to KT in children with IVC atresia. **Materials and methods.** In the period from December 2019 to April 2024, 5 kidney transplants were performed in children with atresia or obliteration of the IVC at Shumakov National Medical Research Center of Transplantology and Artificial Organs. The average age of the children at transplantation was 4.6 ± 2.7 (from 1 to 8 years) years, body weight 13.5 ± 4 (from 8.3 to 19.5) kg. **Results.** Vertical midline transperitoneal approach was performed, the right lobe of the liver, as well as the accessible part of the subhepatic IVC were partially mobilized. The renal graft was positioned on the right side with the formation of venous anastomosis with the accessible part of the subhepatic IVC. All the children had primary graft function. There were no acute rejection episodes at year 1 post-transplant. The average renal graft glomerular filtration rates in recipients at 3 months and at 1 year post-transplant were 95.9 ± 9.6 ml/min per 1.73 m^2 and 80.6 ± 26.2 ml/min per 1.73 m^2, respectively. **Conclusion.** When the iliac veins and/or distal IVC are compromised, venous outflow into an accessible IVC segment is the preferred option. Transplantation in the left orthotopic position and other mentioned revascularization techniques are complex surgical techniques with a higher risk of thrombotic complications in the early postoperative period.

Keywords: kidney transplantation in children, pediatric kidney transplantation, inferior vena cava compromise, inferior vena cava thrombosis.

INTRODUCTION

Venous system compromise, particularly involving the inferior vena cava (IVC), is a rare but potentially life-threatening condition in low-birth-weight children who require kidney transplantation (KT) for survival. Congenital anomalies of the great vessels, prior abdominal surgeries, and prolonged or repeated placement of temporary or permanent central venous catheters for renal replacement therapy (RRT) can result in narrowing or complete obliteration of the IVC lumen. In most instances, IVC compromise significantly challenges the technical feasibility of KT [1].

In children weighing 15 kg or less, vascular anastomosis of the graft typically involves the distal aorta and IVC. However, in cases of IVC atresia or absence, venous anastomosis – performed in a restricted operative field using available central or peripheral veins – may result in impaired venous outflow. This can lead to venous hypertension and increase the risk of graft thrombosis. Historically, children with absent or thrombosed IVCs were considered high-risk candidates for graft loss and were frequently deemed unsuitable for transplantation [1–3].

However, Eneriz-Wiemer et al. [1] reported 6 successful kidney transplants in children with IVC thrombosis using deceased donor grafts, all of which resulted in satisfactory outcomes. In their approach, the authors favored the use of small renal allografts to ensure that venous outflow did not exceed the drainage capacity of the iliac or adjacent collateral veins [2, 4, 5].

Some authors have used segments of the open IVC or iliac vein [6], ovarian vein [7, 8], left renal vein, and even the superior or inferior mesenteric veins or the portal vein [9–11]. Despite these efforts, a universally accepted surgical strategy for KT in the setting of IVC atresia or thrombosis has yet to be established.

Therefore, the aim of this study was to present a comprehensive surgical approach developed at Shumakov National Medical Research Center of Transplantology and Artificial Organs (“Shumakov Center”) for performing KT in pediatric patients with IVC atresia.

Corresponding author: Andrey Zharikov. Address: 1, Shchukinskaya str., Moscow, 123182, Russian Federation. Phone: (962) 983-68-70. E-mail: zharikof94@mail.ru

MATERIALS AND METHODS

Between December 2019 and April 2024, five KTs were performed in pediatric patients with IVC) atresia or obliteration at Shumakov Center. The average age of recipients at the time of transplantation was 4.6 ± 2.7 years (range: 1–8 years), and their body weight ranged from 8.3 to 19.5 kg (mean: 13.5 ± 4 kg). All patients were on RRT prior to transplantation: 4 patients (80%) were on peritoneal dialysis (PD), while 1 (20%) was on long-term hemodialysis (HD).

The leading underlying causes of end-stage kidney disease were congenital anomalies of the kidney and urinary tract in 3 patients (60%), autosomal recessive polycystic kidney disease in 1 patient (20%), and infantile nephrotic syndrome in 1 patient (20%). Notably, none of the patients exhibited clinical signs or symptoms of IVC thrombosis.

KT was performed using deceased donor organs in 4 cases and a living related donor in 1 case. Detailed recipient characteristics are summarized in Table.

All recipients underwent standard pre-transplant evaluation protocols. At the preoperative stage, each patient underwent intravenous bolus contrast-enhanced computed tomography (CT) scan using the GE Revolution EVO CT scanner (General Electric, USA), followed by three-dimensional (3D) image reconstruction. Contrast enhancement was utilized to delineate the vascular anatomy of the abdominal aorta, iliac arteries, IVC, and iliac veins, in order to identify suitable zones for vascular anastomosis (Fig. 1).

Renal function was assessed based on serum creatinine levels and the estimated glomerular filtration rate (eGFR), calculated using the Schwartz formula. Post-transplant follow-up ranged from 1 to 55 (23 ± 19) months.

RESULTS

A vertical midline transperitoneal approach was used for all recipients. Depending on clinical indications and the need to create adequate space for graft placement, patients underwent either unilateral right nephrectomy

Table

Recipient characteristics

Case	Sex	Height, cm	Weight at time of transplantation, kg	Type of RRT	Age at time of transplantation, year	Time on RRT, year	Related or deceased donor	Right or left kidney
1	F	100	13.5	PD	8	3.1	Deceased	Left
2	F	86	12	PD	3	1.9	Deceased	Left
3	M	109	19.5	PD	6	2.2	Deceased	Right
4	F	96	14	HD	5	1.8	Deceased	Right
5	F	71	8.3	PD	1	0.9	Related	Left

Note: RRT, renal replacement therapy; PD, peritoneal dialysis; HD, hemodialysis.

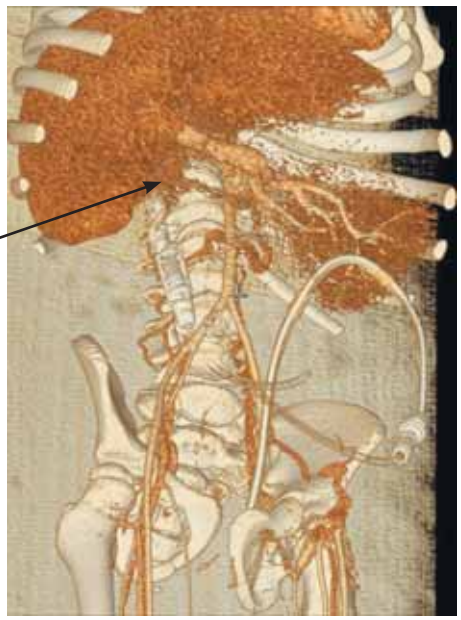

Fig. 1. Contrast-enhanced CT scan to visualize the vascular architecture of the abdominal aorta and iliac arteries

or bilateral nephrectomy (Fig. 2, a). The right lobe of the liver and the accessible area of the subhepatic IVC were partially mobilized (Fig. 2, b).

Following preparatory steps, the renal graft was placed on the right side, with venous anastomosis constructed to the accessible portion of the subhepatic IVC (Fig. 3). The renal artery was anastomosed to the aorta and/or common iliac artery where two graft arteries were present. When the left kidney was used, the graft vein typically provided adequate length. In cases where the right kidney was used, the graft vein was lengthened using a segment of the donor's vena cava (Fig. 4).

In all cases, ureteral-bladder anastomosis was performed using the Lich-Gregoir technique, with the placement of a graft ureteral stent (Fig. 5). The stent was removed on day 21 post-transplantation.

Immunosuppressive therapy followed a standardized regimen consisting of three medications: calcineurin inhibitors, mycophenolic acid, and glucocorticosteroids.

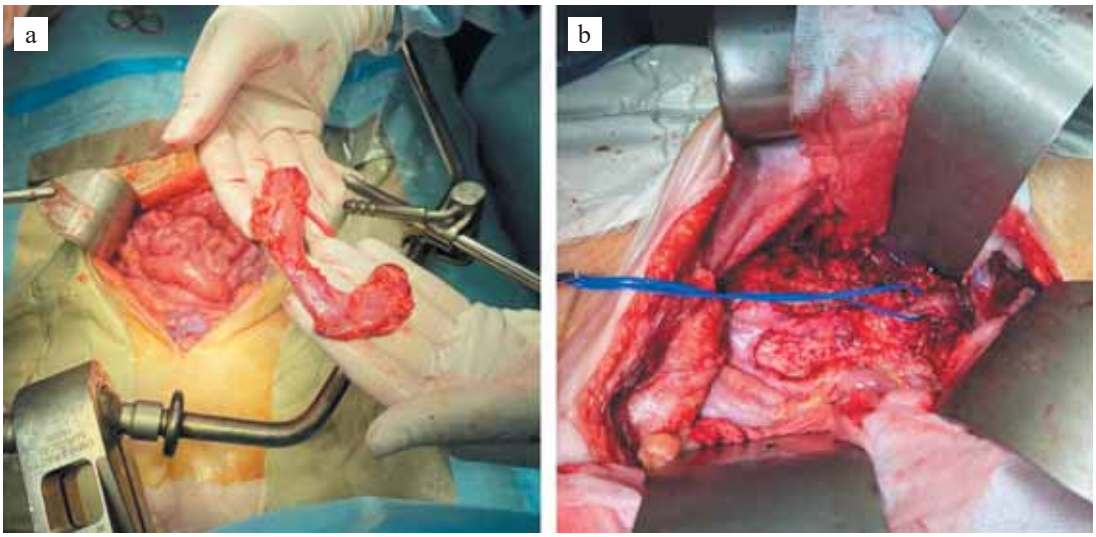

Fig. 2. Intraoperative anatomical features: a, horseshoe kidney nephrectomy; b, mobilized section of the subhepatic inferior vena cava on a holder

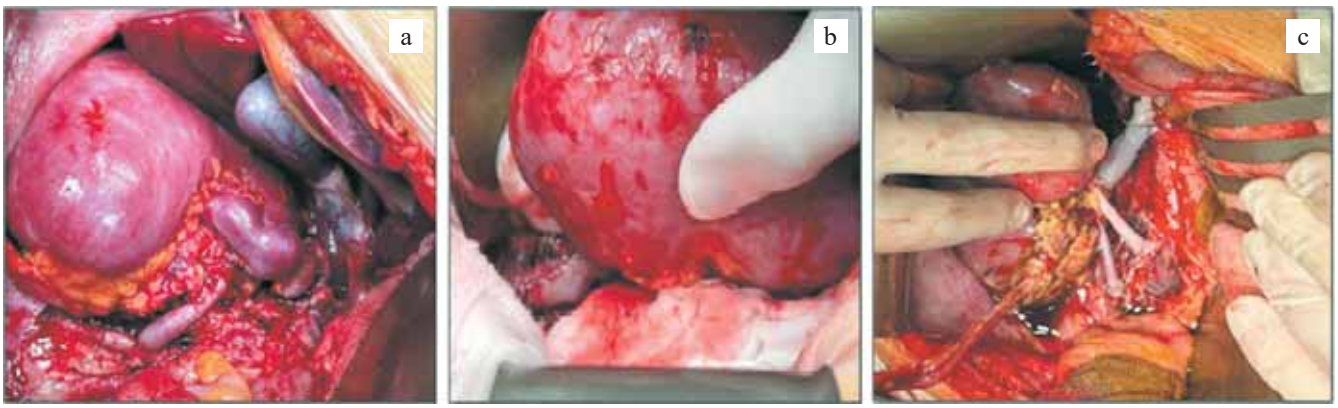

Fig. 3. Features of the formation of vascular anastomoses in conditions of IVC deficiency: a, vascular anastomoses after reperfusion; b, elongation of the renal vein of the graft due to the donor's IVC site; c, vascular anastomoses before reperfusion

Fig. 4. Right kidney, renal vein reconstruction using IVC

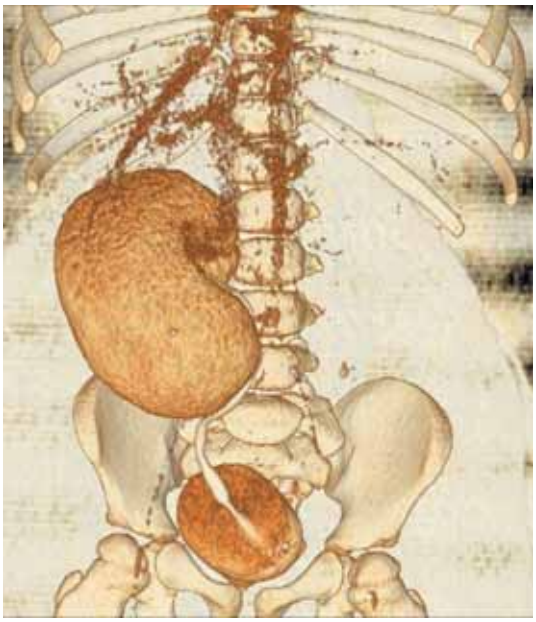

Fig. 5. CT scan – urinary phase

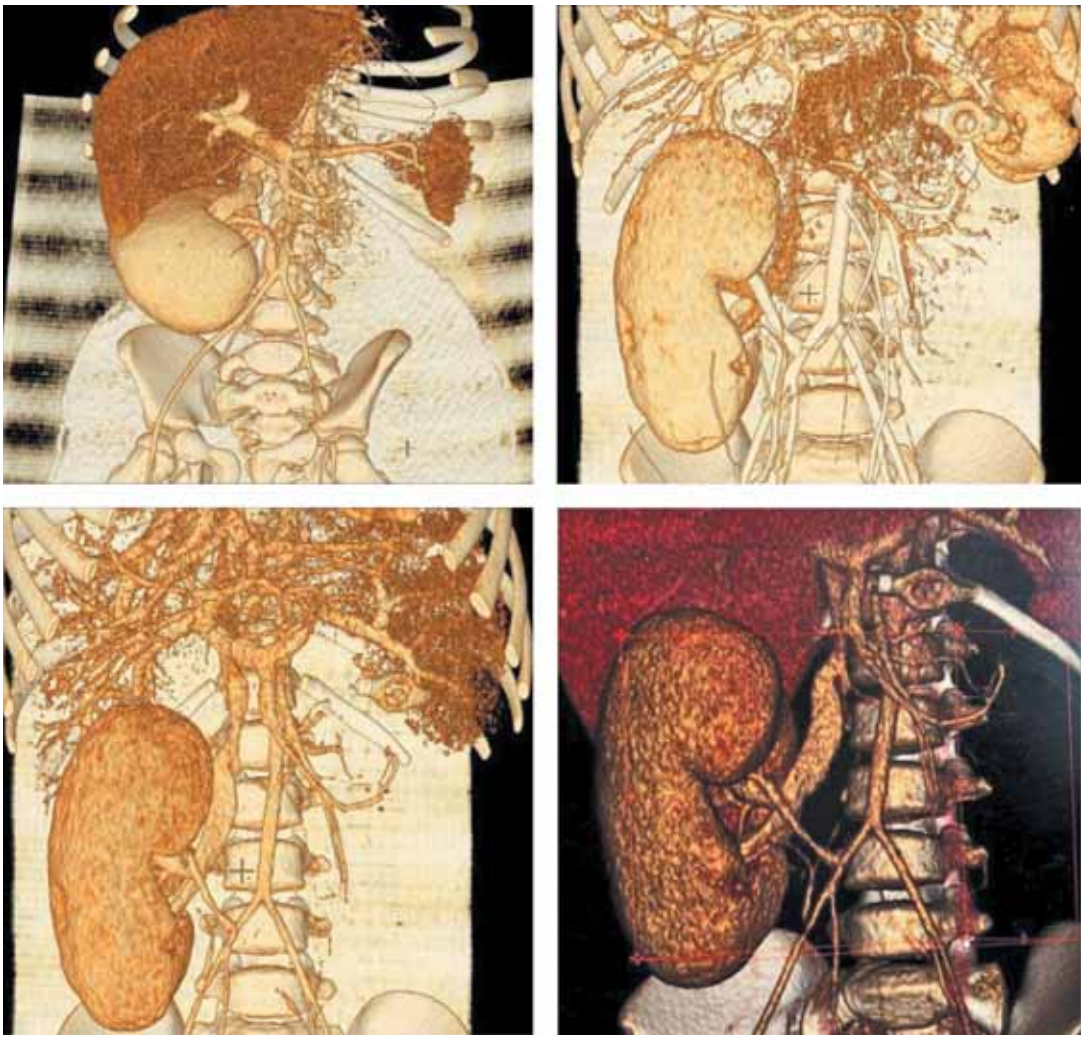

Fig. 6. Intravenous bolus contrast-enhanced CT scan MSCT 3 months after kidney transplantation

All patients exhibited primary kidney graft function, with no instances of acute rejection observed within the first year after transplantation. A follow-up intravenous bolus contrast-enhanced CT scan was performed 3 months post-KT (Fig. 6). The mean eGFR of the renal grafts at 3 months was 95.9 ± 9.6 mL/min/1.73 m^2. By the end of the first year, mean eGFR for the five functioning grafts was 80.6 ± 26.2 mL/min/1.73 m^2.

DISCUSSION

Compromised IVC may be detected in pediatric patients requiring KT for survival. Historically, this condition was regarded as an absolute contraindication to KT due to significant technical challenges and the heightened risk of graft thrombosis resulting from impaired renal venous outflow. Detailed preoperative imaging of the vascular network is therefore crucial, particularly in children with congenital anomalies or a history of repeated central venous catheter placement for RRT. When IVC compromise is suspected, a thorough preoperative assessment of the vascular anatomy is essential to guide surgical planning and ensure the feasibility and safety of KT.

Intravenous bolus contrast-enhanced multislice CT scan combined with 3D reconstruction is an accurate, reliable, and noninvasive tool for assessing organ transplantation feasibility [11]. This imaging technique enables detailed visualization of the patient's vascular anatomy, allowing for identification of optimal sites for vascular anastomosis, particularly in cases of IVC or iliac vein thrombosis or atresia. In our clinical experience, the thrombus-free subhepatic segment of the IVC has proven to be the most suitable site for renal vein anastomosis. This approach aligns with findings reported by Salvatierra et al. [12], who emphasized that, in pediatric recipients with IVC thrombosis receiving large renal allografts, an open segment of the IVC is preferred for the venous anastomosis.

Martinez-Urrutia et al. [5] also reported successful orthotopic left KT in 4 children with infrarenal IVC thrombosis. In these cases, the renal allografts were positioned orthotopically on the left, and venous anas-

tomosis was performed either with the subhepatic IVC or the recipient's native renal vein following ipsilateral nephrectomy. However, this technique presents certain limitations. One significant drawback is the insufficient length of the donor renal vein, particularly when using a right kidney graft, which introduces additional technical complexity during venous anastomosis. Another concern is the potential for external compression of the graft vein by the root of the small-bowel mesentery. In our view, the technical limitations associated with the Martinez-Urrutia technique can be mitigated by lengthening the donor renal vein using a segment of the donor IVC, thereby facilitating more secure and tension-free anastomosis.

Several researchers have proposed the use of the portal venous system for kidney graft revascularization. In these techniques, venous outflow is achieved through the creation of porto-renal or mesenterorenal shunts [10–11]. From a technical standpoint, anastomosis of the donor renal vein to the superior mesenteric vein (SMV) appears relatively straightforward, as the SMV is anatomically accessible and has adequate length for mobilization within the abdominal cavity. However, a significant limitation of this approach lies in the size mismatch between the donor renal vein and the recipient's SMV, which may increase the risk of venous thrombosis. Furthermore, this type of venous reconstruction is associated with a higher risk of graft malposition or rotation [10].

CONCLUSION

A comprehensive preoperative assessment of the potential recipient is essential for determining the most appropriate surgical tactics for KT in children with venous anomalies. In cases where the iliac veins and/or distal IVC are compromised, using an accessible segment of the subhepatic IVC for venous outflow remains the preferred option. Alternative approaches, such as orthotopic transplantation on the left side or revascularization using the portal venous system, represent technically demanding procedures that are associated with an elevated risk of early postoperative thrombotic complications.

The authors declare no conflict of interest.

REFERENCES

1. *Eneriz-Wiemer M, Sarwal MM, Donovan D, Costaglio C, Concepción W, Salvatierra O Jr.* Successful renal transplantation in high-risk small children with a completely thrombosed inferior vena cava. *Transplantation*. 2006; 82 (9): 1148–1152.
2. *Shenoy M, Pararajasingam R, Wright NB, Lewis MA, Parrott N, Riad H, Webb NJ.* Successful renal transplantation in children in the presence of thrombosis of the inferior vena cava. *Pediatr Nephrol*. 2008; 23 (12): 2261–2265.
3. *Stevens RB, Yannam GR, Hill BC, Rigley TH, Penn DM, Skorupa JY*. Successful urgent transplantation of an adult kidney into a child with inferior vena cava thrombosis. *Am J Transplant*. 2009; 9 (8): 1953–1956.
4. *Thomas SE, Hickman RO, Tapper D, Shaw DW, Fouser LS, McDonald RA*. Asymptomatic inferior vena cava abnormalities in three children with end-stage renal disease: risk factors and screening guidelines for pretransplant diagnosis. *Pediatr Transplant*. 2000; 4 (1): 28–34.
5. *Martinez-Urrutia MJ, Pereira PL, Ramirez LA, Romera RL, Melgar AA, Monereo EJ, Larrucea JT.* Renal transplant in children with previous inferior vena cava thrombosis. *Pediatr Transplant*. 2007; 11 (4): 419–421.
6. *Pirenne J, Benedetti E, Kashtan CE , Llédo-Garcia E, Hakim N, Schroeder CH et al.* Kidney transplantation in the absence of the infrarenal vena cava. *Transplantation*. 1995; 59 (12): 1739–1742.
7. *Tao R, Shapiro R.* Successful adult-to-child renal transplantation utilizing the ovarian vein in children with inferior vena cava/iliac vein thrombosis. *Pediatr Transplant*. 2010; 14 (6): E70–E74.
8. *Wong VK, Baker R, Patel J, Menon K, Ahmad N*. Renal transplantation to the ovarian vein: a case report. *Am J Transplant*. 2008; 8 (5): 1064–1066.
9. *Rizzello A, Smyth O, Patel N, Reddy S, Sinha S, Vaidya A*. Successful splenic venous drainage for kidney transplant in case of inferior vena cava thrombosis. *Transplantation*. 2011; 92 (10): e59–e60.
10. *Aguirrezabalaga J, Novas S, Veiga F, Chantada V, Rey I, Gonzalez M, Gomez M*. Renal transplantation with venous drainage through the superior mesenteric vein in cases of thrombosis of the inferior vena cava. *Transplantation*. 2002; 74 (3): 413–415.
11. *Patel P, Krishnamurthi V.* Successful use of the inferior mesenteric vein for renal transplantation. *Am J Transplant*. 2003; 3 (8): 1040–1042.
12. *Salvatierra O Jr, ConcepcionW, Sarwal MM.* Renal transplantation in children with thrombosis of the inferior vena cava requires careful assessmentand planning. *Pediatr Nephrol*. 2008; 23 (12): 2107–2109.
13. *Gil-Vernet JM, Gil-Vernet A, Caralps A, Carretero P, Talbot-Wright R, Andreu J, Campos JA*. Orthotopic renal transplant and results in 139 consecutive cases. *J Urol*. 1989; 142 (2 Pt 1): 248–252.

The article was submitted to the journal on 03.06.2024

DOI: 10.15825/1995-1191-2024-4-14-23

IMPACT OF INTRAOPERATIVE ASSESSMENT OF RENAL ALLOGRAFT ARTERIAL BLOOD FLOW ON VASCULAR COMPLICATIONS AND THEIR PREVENTION STRATEGIES

A.A. Zharikov[1], D.A. Bankeev[1, 2], I.R. Kurbangulov[1], D.V. Kukovyakin[1], A.R. Karapityan[1], M.A. Petryaev[1], A.A. Kartashev[1], Z.A. Porchkhidze[1], D.A. Saydulaev[1]

[1] Shumakov National Medical Research Center of Transplantology and Artificial Organs, Moscow, Russian Federation

[2] Botkin Hospital, Moscow, Russian Federation

Objective: to use intraoperative fluorometry to assess the impact of renal allograft arterial blood flow on vascular complications. **Materials and methods.** The study included 285 patients who underwent kidney transplantation (KT) at Shumakov National Medical Research Center of Transplantology and Artificial Organs (from May 2022 to July 2023). Patients were distributed into 2 comparison groups. Group 1 (49 patients, 17.2%) underwent intraoperative flowmetry, while group 2 (236 patients, 82.8%) did not. Following graft reperfusion, renal transplant arterial blood flow was measured in real time. Next, ureteroneocystostomy was performed, and then the graft was placed in the iliac fossa in its optimal position and the measurement was repeated. **Results.** Intraoperative vascular complications occurred in 6 patients (12.2%) in the intraoperative flowmetry group. Those with vascular complications exhibited statistically significantly lower renal arterial volumetric blood flow (VBF) rate immediately after reperfusion (94 ± 93 *vs.* 291 ± 147; p = 0.002) and after reassessment at the end of ureteroneocystostomy (160 ± 88 *vs.* 349 ± 157; p = 0.006). A VBF of less than 120 mL/min contributed to the intraoperative decision to immediately revise the anastomosis. Following revision and reanastomosis of the arterial channel, there was no significant difference in VBF rate and PI values between recipients with the complications and the group without. **Conclusion.** Prophylactic application of intraoperative fluorometry in KT allows to obtain objective data about the quality of vascular anastomosis and timely prevent irreversible vascular complications, thus preserving the renal graft in the postoperative period.

Keywords: kidney transplantation, vascular complications in renal transplantation, intraoperative fluorometry, prevention of vascular complications.

INTRODUCTION

Vascular complications remain the leading cause of early kidney graft loss following transplantation. These complications may arise from various factors, including technical errors during vascular anastomosis formation, complex arterial reconstruction in cases involving multiple renal arteries, vascular intimal injury, compartment syndrome, diminished arterial inflow due to iliac artery spasm, vascular kinking or torsion, suboptimal graft positioning within the retroperitoneal space, and underlying coagulopathies [1–4].

In clinical practice, the assessment of graft reperfusion injury is frequently based on the surgeon's subjective judgment, supplemented by limited objective indicators such as immediate urine output, and the color and turgor of the graft. Therefore, the availability of reliable intraoperative tools for evaluating graft perfusion is critical. Such tools should be safe, easy to use, and capable of delivering rapid and reproducible results. Most importantly, they must provide a quantitative assessment of arterial blood flow and tissue perfusion. A robust intraoperative evaluation of renal graft hemodynamics is essential for early detection of vascular complications, prediction of graft function, and prevention of graft loss [5].

Intraoperative transit time flowmetry (TTFM) is a non-invasive technique that measures the "transit time" of ultrasound signals transmitted between two transducers across a blood-filled vessel. This method provides objective and real-time information regarding the quality of arterial anastomoses, particularly following arterial reconstructions, and helps identify potential technical errors [6]. The use of intraoperative TTFM to assess the quality of anastomoses of arteriovenous fistulas, aortocoronary shunts, as well as in the performance of native renal artery reconstructions has ben shown to reduce the rate of intraoperative anastomotic revisions from 8% to 3% [6].

This study aimed to evaluate the impact of arterial blood flow quality in renal allograft vessels, as measured

Corresponding author: Andrey Zharikov. Address: 1, Shchukinskaya str., Moscow, 123182, Russian Federation. Phone: (962) 983-68-70. E-mail: zharikof94@mail.ru

by intraoperative TTFM, on the incidence of vascular complications and the effectiveness of subsequent intraoperative interventions.

MATERIALS AND METHODS

Between May 2022 and July 2023, a total of 298 kidney transplants were performed at Shumakov National Medical Research Center of Transplantology and Artificial Organs. The study included 285 patients with end-stage chronic kidney disease who were candidates for kidney transplantation (KT), aged from 1 to 70 years (mean age: 38.1 ± 17.8 years). These included 160 men (56.1%) and 125 women (43.9%). Thirteen patients were excluded from the study due to receiving kidneys from a donation after cardiac death, as such grafts are more frequently associated with delayed graft function.

The patients were divided into two groups for comparison: Group 1 (49 patients, 17.2%) underwent intraoperative TTFM, while Group 2 (236 patients, 82.8%) did not. KT was performed using a standard technique, regardless of donor type. In 90% of cases, vascular anastomoses were created end-to-side with the external iliac vessels. Arterial blood flow in the graft was measured in real time using the Veri-Q system (Medistim ASA, Oslo, Norway) immediately following graft reperfusion (Fig. 1).

Following next was ureteroneocystostomy, where the kidney graft was positioned optimally in the iliac fossa, and a second arterial blood flow measurement was performed. The space between the flow probe and the arterial vessel was filled with sterile saline.

Ultrasound transit-time flowmetry uses a specialized probe sized according to the diameter of the target vessel. The probe emits ultrasound signals in the direction of blood flow, and measures the "transit time" of the signal between transmitting and receiving transducers via a reflector within the bloodstream. During measurement, parameters such as mean volumetric blood flow rate, pulsatility index (PI) and percentage of diastolic volume filling are determined [7–9].

Among these, PI is a key indicator of anastomotic quality and graft perfusion. It is calculated as the difference between maximum and minimum flow velocities divided by the mean flow velocity, and is expressed as an absolute value. A PI in the range of 1–2 is generally considered acceptable, while higher values suggest increased flow resistance – commonly due to vascular stenosis [7, 9].

Mean volumetric blood flow (VBF) is not always a reliable standalone marker of anastomotic integrity, as it is influenced by several variables, including blood viscosity, graft resistance, the caliber of the recipient artery, and the anatomical and functional characteristics of the graft. The percentage of diastolic volume filling reflects the proportion of diastolic-phase blood flow returning through the anastomosis during the cardiac cycle [7, 9].

Immunosuppressive therapy consisted of calcineurin inhibitors, with dose adjustments based on therapeutic drug monitoring, in combination with mycophenolate

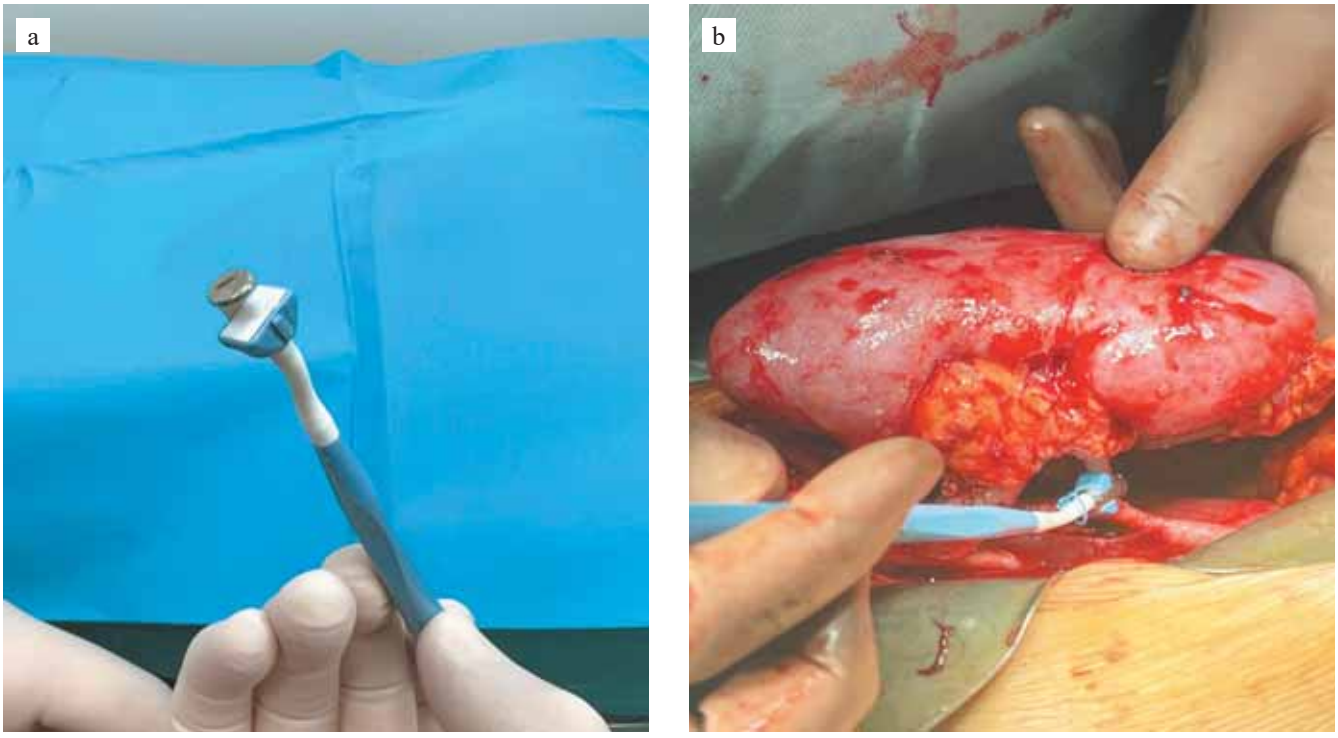

Fig. 1. Intraoperative flowmetry: a, probe; b, intraoperative renal artery flowmetry performed after graft reperfusion

mofetil and/or mycophenolic acid, and methylprednisolone administered in standard dosages.

Following data collection, all patient information was compiled into a unified spreadsheet for analysis. Statistical processing was carried out using SPSS version 26 (IBM SPSS Inc., USA). Parametric variables were expressed as mean ± standard deviation (M ± SD), while nonparametric data were presented as median (Me) and interquartile range (IQR = Q3–Q1).

For dependent sample comparisons, the paired Wilcoxon signed-rank test was employed, while independent groups were compared using the Mann–Whitney U test. Receiver operating characteristic (ROC) curve analysis was used to calculate the area under the curve (AUC), and to determine the sensitivity, specificity, and threshold values for each parameter.

To evaluate the prognostic significance of renal arterial VBF rate and PI in predicting vascular complications, univariate logistic regression analysis was performed. Model calibration was assessed using the Hosmer–Lemeshow test, and predictive power was expressed via the Nagelkerke coefficient of determination. The overall significance of the model was evaluated using the Wald chi-square test. A p-value of <0.05 was considered statistically significant for all tests.

STUDY RESULTS

A comparative analysis of the clinical characteristics of kidney transplant recipients included in the study was conducted (Table 1).

Patients in group 1 were statistically significantly older than those in group 2 (p = 0.007). Gender distribution between the groups was comparable (p = 0.633). Body mass index (BMI) was also significantly higher in group 1 compared to group 2 (p = 0.043). A comparative analysis of underlying diagnoses, types and durations of renal replacement therapy (RRT), and types of transplantation revealed no statistically significant differences between the groups (p > 0.05 for all variables). However, there was a trend toward more frequent use of flowmetry in patients undergoing peritoneal dialysis (14% in group 1 *vs.* 6% in group 2; p = 0.058).

A comparative analysis of donor characteristics showed that donors in group 1 (where flowmetry was performed) were significantly older than those in group 2 (median age 54 [IQR 44–62] *vs.* 48 [IQR 38–57]; p = 0.011). Other donor characteristics, including BMI, gender, and laboratory results, were comparable between groups (p > 0.05 for all).

A comparative analysis of surgical characteristics based on the use of intraoperative TTFM was conducted. Parameters such as surgery duration, intraoperative blood loss, ischemic time, graft type, and frequency of vascular reconstructions were evaluated. No statistically

Table 1

Comparison of clinical characteristics of recipient groups

Indicator	Flowmetry, n = 49	Non-flowmetry, n = 236	P-value
Age, years, Me (IQR)	46.4 (32.4–59)	37.9 (23.1–51.5)	**0.007**
Sex, n (%)			
Men	26 (53%)	134 (57%)	0.633
Women	23 (47%)	102 (43%)	
BMI, kg/m^2, Me (IQR)	25.8 (20.1–27.9)	22.4 (19.5–26)	**0.043**
Diagnosis, n, %			
Chronic glomerulonephritis	9 (18%)	59 (25%)	0.322
Diabetic nephropathy	10 (20%)	29 (12%)	0.132
CAKUT	8 (16%)	54 (23%)	0.312
Nephropathy of unknown etiology	5 (10%)	37 (16%)	0.325
Polycystic disease	7 (14%)	19 (8%)	0.168
Other	10 (20%)	38 (16%)	0.464
RRT (HD), n, %	34 (69%)	171 (72%)	0.663
RRT (PD), n, %	7 (14%)	15 (6%)	0.058
RRT time to KT, months, Me (IQR)	18 (9–55)	27 (12–58)	0.469
RRT (HD) time to KT, months, Me (IQR)	20.1 (8.7–55.4)	29.3 (12.8–58.5)	0.437
RRT (PD) time to KT, months, Me (IQR)	16.8 (8.9–84.2)	14.5 (9.2–29.1)	0.671
Type of transplantation, n, %			
Living donor	17 (35%)	85 (37%)	0.792
Deceased donor	31 (65%)	142 (63%)	

Note: BMI, body mass index; CAKUT, congenital anomalies of the kidney and urinary tract; RRT, renal replacement therapy; HD, hemodialysis; PD, peritoneal dialysis; KT, kidney transplantation.

significant differences were observed between the groups for any of these characteristics ($p > 0.05$ for all).

Additionally, a subgroup analysis was performed on 49 patients who underwent intraoperative TTFM, comparing renal arterial VBF rate (Q) and PI at two time points: after graft reperfusion and after completion of ureteroneocystostomy. Patients were categorized based on the presence or absence of intra- or postoperative vascular complications. Among these, 6 patients (12.2%) developed vascular complications, while 43 patients (87.8%) did not.

In patients with vascular complications, the VBF rate was significantly lower both after graft reperfusion ($p = 0.002$) and after ureteroneocystostomy ($p = 0.006$) compared to patients without complications. Conversely, PI values measured after graft reperfusion were significantly higher in the complication group ($p = 0.037$). However, PI values following ureteroneocystostomy did not differ significantly between the groups ($p = 0.079$).

ROC analysis was performed to assess the prognostic significance of renal arterial VBF rate and PI in relation to the development of vascular complications (Fig. 2).

Renal arterial VBF rates measured both after graft reperfusion and following ureteroneocystostomy were found to be statistically significant predictors of vascular complications ($p < 0.001$). These parameters demonstrated high predictive accuracy, with VBF rates providing 87.2% and 85.7% accuracy at the respective time points.

Table 2

Results of comparative analysis of flowmetric indicators

Indicator	Vascular complications, n = 6	No vascular complications, n = 43	P-value
Volumetric blood flow rate through the renal artery after graft reperfusion (ml/min), Mean ± SD	94 ± 93	291 ± 147	**0.002**
PI after graft reperfusion, Me (IQR)	2 (1.7–2.1)	1.3 (0.8–2)	**0.037**
Renal arterial VBF after ureteroneocystostomy (mL/min), Mean ± SD	160 ± 88	349 ± 157	**0.006**
PI after ureteroneocystostomy, Me (IQR)	1.7 (1.5–2)	1.2 (0.7–1.6)	0.079

Note: VBF, volumetric blood flow; PI, pulsatility index; SD, standard deviation; Me, mean; IQR, interquartile range.

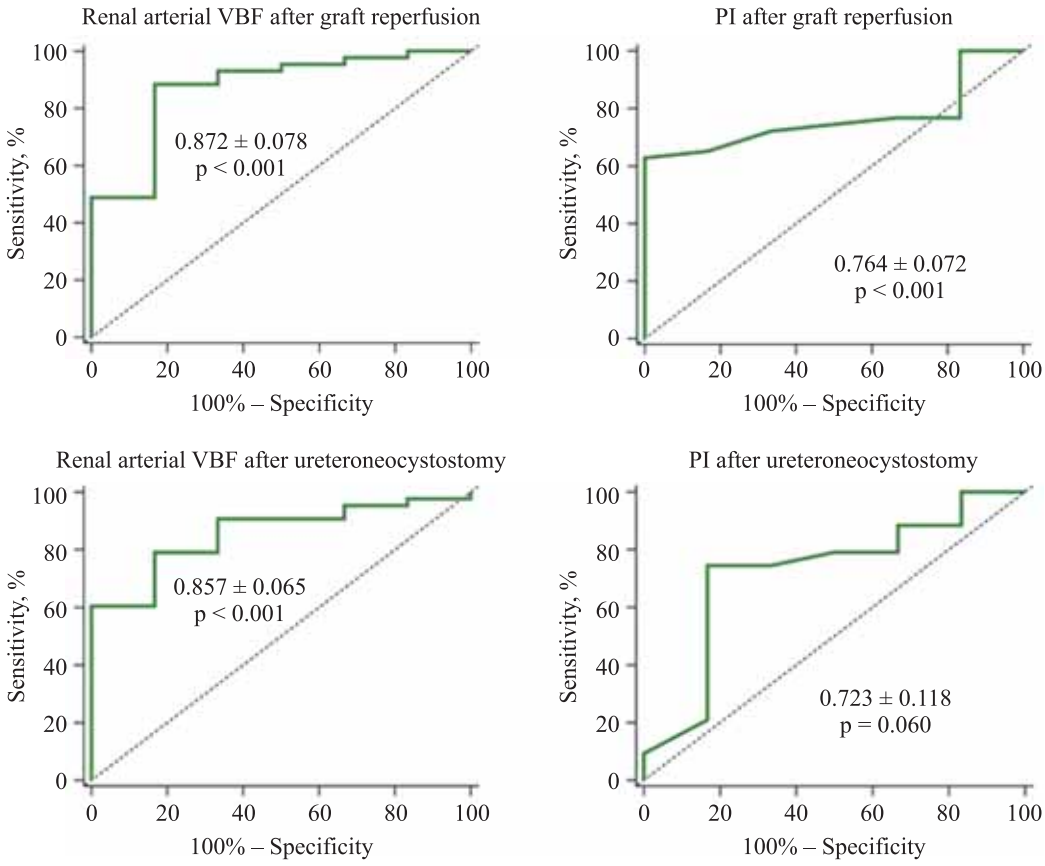

Fig. 2. Assessment of the prognostic significance of indicators of vascular complications (ROC analysis results)

A post-reperfusion VBF rate ≤120 mL/min was associated with an increased risk of vascular complications, demonstrating a sensitivity of 83.3% and a specificity of 88.4%. Similarly, a post-ureteroneocystostomy VBF rate ≤230 mL/min predicted complications with 83.3% sensitivity and 79.1% specificity.

Similarly, a post-reperfusion PI was also significantly associated with vascular complications ($p < 0.001$), with a predictive accuracy of 76.4%. A post-reperfusion PI ≥1.65 yielded a sensitivity of 83.3% and specificity of 65.1% for predicting complications. However, the PI value obtained after ureteroneocystostomy did not demonstrate statistically significant predictive value ($p = 0.060$).

Results of comparative analysis of flowmetric indicators by donor type and vascular reconstruction

Among the 49 kidney transplant recipients who underwent intraoperative TTFM, 18 patients (36.7%) received grafts from living related donors, while 31 patients (63.3%) received grafts from deceased donors. A comparative analysis was performed to evaluate renal arterial VBF rate and PI both after graft reperfusion and following ureteroneocystostomy, stratified by donor type (Table 3).

The post-ureteroneocystostomy PI was significantly lower in patients who received a renal graft from a living related donor compared to those who received a graft from a deceased donor ($p = 0.011$). However, other parameters – renal arterial VBF rate after reperfusion and after ureteroneocystostomy, as well as post-reperfusion PI – did not show statistically significant differences between the two donor groups ($p > 0.05$ for all indicators).

A comparative analysis of renal arterial VBF rate and PI was performed based on whether vascular reconstruction was required (Table 4). Among the 49 patients, vascular reconstruction was performed in 16 cases (32.7%), while 33 patients (67.3%) did not undergo any vascular reconstruction.

Our comparative analysis revealed that following vascular reconstruction, there was a statistically significant decrease in renal arterial VBF rate ($p = 0.007$) and PI ($p = 0.022$) after graft reperfusion. In contrast, VBF rate and PI measured after ureteroneocystostomy did not differ significantly between the groups. However, the VBF rate after ureteroneocystostomy in patients who underwent vascular reconstruction was slightly lower than in those without reconstruction, with a difference approaching statistical significance ($p = 0.058$).

Regression analysis confirmed that vascular complications were significantly associated with renal arterial VBF rate both after graft reperfusion ($p = 0.011$) and following ureteroneocystostomy ($p = 0.018$) (Table 5). In contrast, PI did not demonstrate a statistically significant predictive value for vascular complications.

The regression coefficients for renal arterial VBF rate were negative, indicating that higher flow rates are associated with a lower risk of vascular complications. Specifically, the likelihood of complications decreases by approximately 1% for each unit increase in VBF rate. The probability of complications was explained by 40.8% of the variance in VBF rate after graft reperfusion and by 32.6% of the variance in VBF rate after ureteroneocystostomy, suggesting that post-reperfusion

Table 3

Comparative analysis of flowmetric indicators depending on donor type

Indicator	Living related donor, n = 18	Deceased donor, n = 31	P-value
Renal arterial VBF after graft reperfusion (mL/min), Mean ± SD	298 ± 170	249 ± 146	0.288
PI after graft reperfusion, Me (IQR)	1.15 (0.8–1.9)	1.6 (1–2.3)	0.209
Renal arterial VBF after ureteroneocystostomy (mL/min), Mean ± SD	351 ± 168	312 ± 159	0.422
PI after ureteroneocystostomy, Me (IQR)	0.85 (0.6–1.2)	1.4 (0.8–1.8)	**0.011**

Note: VBF, volumetric blood flow; PI, pulsatility index; SD, standard deviation; Me, mean; IQR, interquartile range.

Table 4

Comparative analysis of flowmetric indicators by donor type

Indicator	Vascular reconstruction, n = 16	No vascular reconstruction, n = 33	P-value
Renal arterial VBF after graft reperfusion (mL/min), Mean ± SD	184 ± 135	308 ± 149	**0.007**
PI after graft reperfusion, Me (IQR)	1.8 (1.5–2.05)	1.2 (0.7–1.7)	**0.022**
Renal arterial VBF after ureteroneocystostomy (mL/min), Mean ± SD	264 ± 153	357 ± 160	**0.058**
PI after ureteroneocystostomy, Me (IQR)	1.4 (0.9–1.7)	1 (0.6–1.6)	0.152

Note: VBF, volumetric blood flow; PI, pulsatility index; SD, standard deviation; Me, mean; IQR, interquartile range.

Table 5

Regression analysis results

Factor	Regressor, B ± SE	Constant, B ± SE	HL test	R^2	P-value
Renal arterial VBF after graft reperfusion (mL/min)	–0.015 ± 0.006	0.627 ± 0.864	0.553	0.408	**0.011**
PI after graft reperfusion	0.242 ± 0.148	–2.583 ± 0.596	0.164	0.142	0.101
Renal arterial VBF after ureteroneocystostomy (mL/min)	–0.011 ± 0.005	0.758 ± 1.002	0.868	0.326	**0.018**
PI after ureteroneocystostomy	0.274 ± 0.17	–2.5 ± 0.587	0.214	0.091	0.108

Note: VBF, volumetric blood flow; B, regression coefficient; SE, standard error; HL test, Hosmer–Lemeshow test; R^2, Nagelkerke's coefficient of determination.

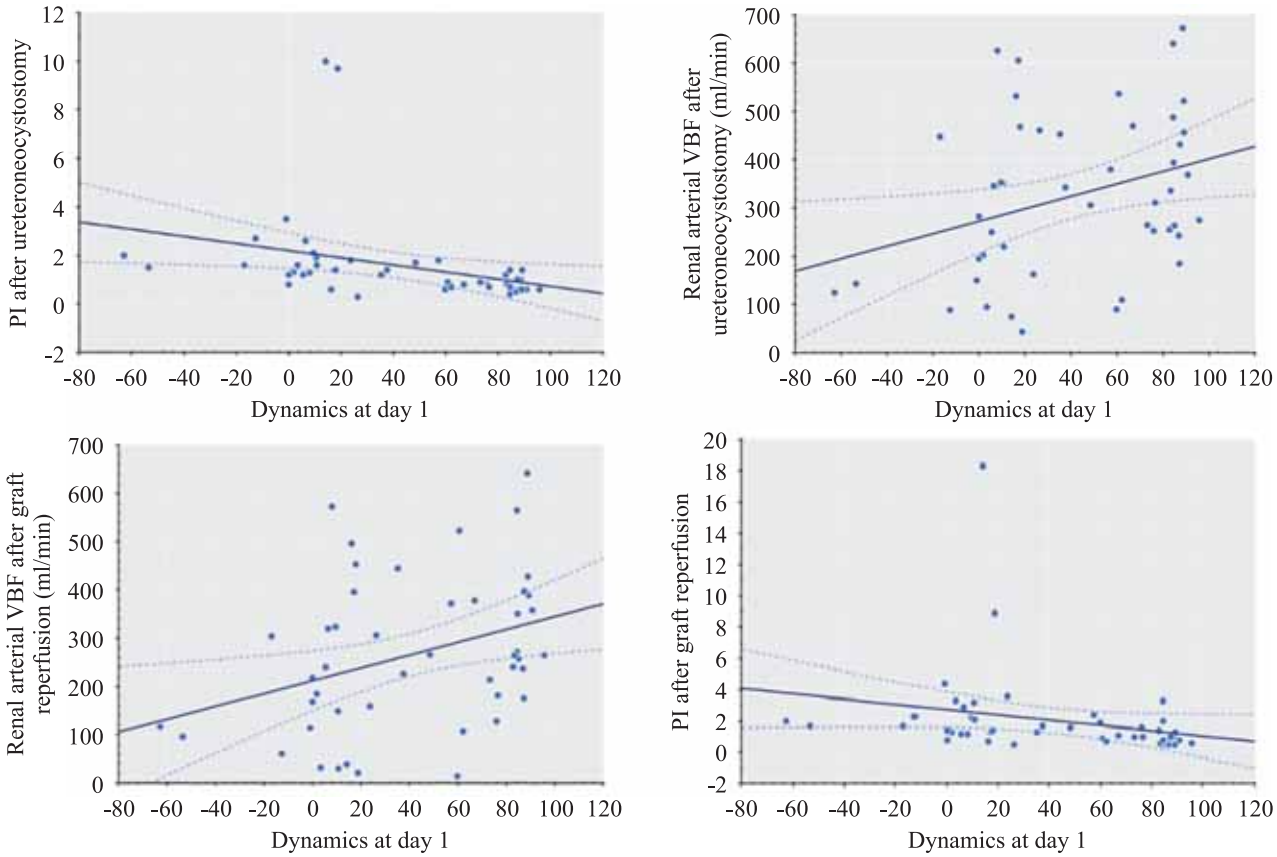

Fig. 3. Calculation of complication probabilities. PI, pulsatility index

measurements are a more robust predictor than post-ureteroneocystostomy values.

Based on these findings, we calculated the estimated probabilities of vascular complications using the VBF rates obtained after graft reperfusion and after ureteroneocystostomy (Fig. 3).

The assessment of the predictive significance of these indicators revealed that they do not play a statistically significant role in predicting vascular complications.

DISCUSSION

Despite being widely practiced and successfully performed by many surgeons globally, KT poses challenges in predicting vascular complications and graft dysfunction, even with extensive experience. Transplant surgeons often rely on careful intraoperative visual and ultrasound evaluation, yet these measures do not always predict the development of complications [10–11].

The occurrence of vascular complications in the perioperative period significantly impacts graft function and survival, underscoring the importance of preventing such complications. Analysis of the causes of these complications reveals three key areas that require special attention: donor organ characteristics (such as angioarchitecture and potential vascular damage during procurement), recipient risk factors (including vascular abnormalities, blood coagulation disorders, and atherosclerotic lesions of major arteries), and the technical aspects of the surgical procedure [12–14]. However, there is currently no unified approach for the intraoperative prevention of vascular complications. The use of flowmetric parameters in solid organ transplantation remains a novel and

insufficiently explored method of prophylaxis, offering both research and practical significance.

Bhatt et al. were among the first to apply this technique in KT. The authors assessed blood flow through the renal artery of the graft, which was found to be 114–120 mL/min. They also temporarily occluded the external iliac artery distal to the renal graft arterial anastomosis, resulting in a near doubling of blood flow to 205 mL/min. Following this, the renal artery anastomoses were revised twice, after which blood flow rates returned to normal. In one case, a high PI (>5) indicated a technical imperfection in the anastomosis. In another case, an accidental entrapment of the graft in the suture of the opposite side of the arterial anastomosis was observed [6].

In our study, 6 patients (12.2%) in the group where intraoperative TTFM was used experienced intraoperative vascular complications, while the remaining 43 patients (87.8%) did not. In the group with vascular complications, intraoperative TTFM revealed statistically significantly lower renal arterial VBF rates immediately after reperfusion (94 ± 93 *vs.* 291 ± 147; p = 0.002) and after re-evaluation at the end of ureteroneocystostomy (160 ± 88 *vs.* 349 ± 157; p = 0.006). A VBF rate of less than 120 mL/min contributed to the intraoperative decision to immediately revise the anastomosis. After revision and repeated anastomosis of the arterial bed, VBF rates and PI values did not differ significantly between recipients with and without complications. In the postoperative period, no further vascular complications were observed in patients after correction of the arterial anastomosis.

In addition to the efficacy of intraoperative blood flow measurement using flowmetry for monitoring the patency of vascular anastomoses and assessing the technical challenges of renal arterial reconstruction, intraoperative flowmetry data have also been shown to correlate with graft function [15–16].

Król et al. conducted intraoperative TTFM in 72 kidney transplant patients with a single renal artery. They excluded cases of acute rejection, early graft loss, and primary non-function from their analysis, then categorized the remaining patients into groups with primary and delayed graft function. A high perioperative resistive index (RI) was identified as a predictor of delayed graft function (52.6% *vs.* 15% for patients with an RI >0.70) and poorer long-term kidney graft function, extending up to 2 years post-transplant [17].

Hoff et al. demonstrated the successful use of intraoperative Doppler ultrasound in surgical decision-making for KT involving two graft veins. The Doppler ultrasound revealed the presence of retrograde diastolic flow, enabling the surgeons to perform an anastomosis of the inferior polar renal vein with the external iliac vein without compromising renal perfusion [18].

CONCLUSION

The prophylactic use of intraoperative flowmetry during KT provides objective data on the quality of vascular anastomoses, allowing for timely intervention to prevent irreversible vascular complications and thereby preserving kidney graft function post-transplant.

The authors declare no conflict of interest.

REFERENCES

1. *Dimitroulis D, Bokos J, Zavos G, Nikiteas N, Karidis NP, Katsaronis P et al.* Vascular complications in renal transplantation: a single-center experience in 1367 renal transplantations and review of the literature. *Transplant Proc*. 2009; 41: 1609–1614.
2. *Natour AK, Al Adas Z, Nypaver T, Shepard A, Weaver M, Malinzak L et al.* Rate of Ipsilateral Chronic Limb-Threatening Ischemia (CLTI) After Kidney Transplantation: A Retrospective Single-Center Study. *Cureus*. 2022; 14: e25455.
3. *Verloh N, Doppler M, Hagar MT, Kulka C, von Kruchten R, Neubauer J et al.* Interventional Management of Vascular Complications after Renal Transplantation. *Rofo.* 2023; 195: 495–504.
4. *Parajuli S, Lockridge JB, Langewisch ED, Norman DJ, Kujovich JL.* Hypercoagulability in Kidney Transplant Recipients. *Transplantation*. 2016; 100: 719–726.
5. *Lundell A, Persson NH, Källen R, Ekberg H.* Impaired renal artery blood flow at transplantation is correlated to delayed onset of graft function. *Transpl Int.* 1996; 9 (1): 57–61.
6. *Bhatt KA, Karamanoukian HL, Bergsland J, D'Ancona G, Stephan R.* Intraoperative graft verification in renal transplants. *Vasc Endovascular Surg*. 2002; 36 (2): 93–96.
7. *Shevchenko YuL, Zaichuk R, Borschev GG, Zemlyanov AV, Ulbashev DS.* The use of ultrasound flowmetry for intraoperative assessment of coronary bypass efficiency. *Bulletin of the N.I. Pirogov National Medical and Surgical Center*. 2019; 14: 98–103.
8. *Akchurin RS, Shiryaev AA, Vasiliev VP, Galyautdinov DM, Zaikovsky VYu, Mukimov ShD.* Intraoperative ultrasound flowmetry in patients with diffuse coronary artery disease in prevention of aortocoronary shunt failure. *Cardiovascular Therapy and Prevention*. 2022; 21: 23–30.
9. *Gaudino M, Sandner S, Di Giammarco G, Di Franco A, Arai H, Asai T et al.* The Use of Intraoperative Transit Time Flow Measurement for Coronary Artery Bypass Surgery: Systematic Review of the Evidence and Expert Opinion Statements. *Circulation*. 2021; 144: 1160–1171.
10. *Baboolal HA, Lane J, Westreich KD.* Intraoperative management of pediatric renal transplant recipients: An opportunity for improvement. *Pediatr Transplant.* 2023; 27 (6): e14545.

11. *Franke D.* The diagnostic value of Doppler ultrasonography after pediatric kidney transplantation. *Pediatr Nephrol.* 2022; 37: 1511–1522.
12. *Mehrabi A, Wiesel M, Zeier M, Kashfi A, Schemmer P, Kraus T et al.* Results of renal transplantation using kidneys harvested from living donors at the University of Heidelberg. *Nephrol Dial Transpl*. 2004; 19: iv48e54.
13. *Sagban TA, Baur B, Schelzig H, Grabitz K, Duran M.* Vascular challenges in renal transplantation. *Ann Transpl*. 2014; 19: 464e71.
14. *Audard V, Matignon M, Hemery F, Snanoudj R, Desgranges P, Anglade MC et al.* Risk factors and long-term outcome of transplant renal artery stenosis in adult recipients after treatment by percutaneous transluminal angioplasty. *Am J Transpl*. 2006; 6: 95e9.
15. *Gerken ALH, Keese M, Weiss C, Krucken HS, Pecher KAP, Ministro A et al.* Investigation of Different Methods of Intraoperative Graft Perfusion Assessment during Kidney Transplantation for the Prediction of Delayed Graft Function: A Prospective Pilot Trial. *J Pers Med*. 2022; 12 (10): 1749. doi: 10.3390/jpm12101749.
16. *Budhiraja P, Reddy KS, Butterfield RJ, Jadlowiec CC, Moss AA, Khamash HA et al.* Duration of delayed graft function and its impact on graft outcomes in deceased donor kidney transplantation. *BMC Nephrol.* 2022; 23: 154.
17. *Krol R, Chudek J, Kolonko A, Ziaja J, Pawlicki J, Wiecek A et al.* Intraoperative resistance index measured with transsonic flowmeter on kidney graft artery can predict early and long-term graft function. *Transplant Proc*. 2011; 43: 2926–2929.
18. *Hoff M, Leighton P, Hosgood SA, Nicholson ML.* Anastomosis of dual renal transplant veins. *J Surg Case Rep.* 2020; 2020 (9): rjaa310.

The article was submitted to the journal on 21.06.2024

DOI: 10.15825/1995-1191-2024-4-24-32

EARLY OUTCOMES OF KIDNEY TRANSPLANTATION IN RECIPIENTS WITH TYPE 1 DIABETES MELLITUS AND END-STAGE KIDNEY DISEASE RESULTING FROM DIABETIC NEPHROPATHY

K.E. Lazareva[1, 2], I.V. Dmitriev[1, 3], A.G. Balkarov[1, 3, 4], N.V. Shmarina[1, 3], N.S. Zhuravel[1, 2], Yu.A. Anisimov[1, 2], V.O. Alexandrova[1]

[1] Sklifosovsky Research Institute for Emergency Medicine, Moscow, Russian Federation
[2] Moscow State University of Medicine and Dentistry, Moscow, Russian Federation
[3] Pirogov Russian National Research Medical University, Moscow, Russian Federation
[4] Research Institute for Healthcare Organization and Medical Management, Moscow, Russian Federation

Objective: to analyze early outcomes of kidney transplantation (KT) in patients with type 1 diabetes mellitus (T1D) and stage 5 chronic kidney disease resulting from diabetic nephropathy. **Materials and methods.** The study group included 145 T1D patients who underwent KT at the kidney and pancreas transplant department of Sklifosovsky Research Institute for Emergency Medicine between January 1, 2007 and December 31, 2023. Among them were 57 men (39.3%) and 88 women (60.7%), the median age was 41.5 [35–47] years. The median age at disease onset was 14.6 [9–17] years. Organ donors consisted of 100 (69%) men, 40 (27.6%) women, and there was no information on the sex of 5 donors (3.4%). Donor median age was 46 [35.5–53] years. **Results.** Ninety-nine recipients (68.3%) had primary renal allograft function (PRAF), whereas 46 recipients (31.7%) had delayed function. The median time for azotemia to normalize was 6 [3; 6] days in PRAF patients and 20.5 [14; 27] days in those with delayed function. Overall, there were 9.7% (n = 14) surgical complications, 12.4% (n = 18) acute rejection crisis, and 9.7% (n = 14) infectious complications. Median serum creatinine and urea levels at discharge were 123 [99–164] μmol/L and 10 [7.4–14] mmol/L, respectively; median fasting blood glucose levels before transplantation and at discharge were 9.8 [7.8; 12] mmol/L and 8.1 [6.5; 10] mmol/L, respectively. A total of 125 patients (86.2%) were discharged with adequately functioning kidney graft, while 13 patients (9%) were discharged with graft dysfunction that did not require renal replacement therapy; one patient (0.7%) was transferred to the outpatient stage of treatment to continue dialysis therapy; however, renal allograft function was restored within 2 months post-transplant. **Conclusion.** Although T1D patients remain the most severe category of dialysis patients, our findings suggest that KT is an effective treatment option for them with high graft and recipient survival rates.

Keywords: kidney transplantation, diabetic nephropathy, chronic kidney disease, type 1 diabetes mellitus.

INTRODUCTION

Diabetes mellitus (DM) is a heterogeneous group of metabolic disorders characterized by chronic hyperglycemia resulting from impaired insulin secretion, insulin action, or both. It is classified as a chronic disease with significant socioeconomic impact due to early disability and high mortality rates. According to the International Diabetes Federation, the global prevalence of DM among individuals aged 20–79 is estimated at 537 million [1]. The growth rate of DM cases is concerning, far exceeding earlier predictions, with the number of affected individuals expected to nearly double by 2045, reaching 783 million [1, 2].

In the Russian Federation, the National Diabetes Registry reports that as of January 1, 2023, over 4.9 million people were registered with diabetes, accounting for 3.3% of the population. Among them, more than 277,000 individuals were diagnosed with type 1 diabetes (T1D), representing 5.6% of the diabetic population. Over a 13-year period (2010–2022), the prevalence of T1D increased from 146 to 191 cases per 100,000 population [3]. A one-time cross-sectional analysis of diabetic complications in T1D on January 1, 2023, revealed the following frequency of microvascular complications: diabetic neuropathy (41.3%), diabetic nephropathy (DN)/chronic kidney disease (CKD) (22.8%), and diabetic retinopathy (DR) (28.9%) [4].

Individuals with diabetes represent the fastest-growing group among those receiving renal replacement therapy (RRT). In 1985, when the first edition of Diabetes in America was published, 20,961 people with diabetes were receiving RRT, comprising 29% of all

Corresponding author: Nikita Zhuravel. Address: 207/30, Olimpyiskiy prospekt, Moscow, 129272, Russian Federation. Phone: (906) 703-05-42. E-mail: zhuravelns@gmail.com

new chronic kidney disease (CKD) cases. By 2012, this number had surged to 239,837, accounting for 44% of all new CKD cases [5]. The prevalence of diabetes-related CKD varies globally, with the condition representing 10–15% of CKD cases in Europe, but rising to 45% in the United States [6, 7].

Patients with diabetic CKD on dialysis face lower survival rates compared to those with non-diabetic CKD. Although dialysis techniques have improved survival, diabetic dialysis patients often have a median survival of less than three years. Cardiovascular disease (58%) and infections (13%) were the leading causes of death among diabetic dialysis patients between 1995 and 2009. In contrast, diabetic patients who undergo kidney transplantation (KT) tend to have significantly better long-term survival outcomes compared to those on RRT [8].

The 5-year survival rate for KT recipients with T1D is significantly lower compared to recipients with non-diabetic CKD, primarily due to the higher incidence of mortality related to cardiovascular complications [9, 10]. Despite advancements in RRT, diabetic CKD remains a major risk factor for poor posttransplant outcomes and continues to be an independent predictor of posttransplant mortality [11].

Reports suggest that simultaneous pancreas-kidney transplants (SPKTs) are associated with better survival rates for patients with diabetic nephropathy than other transplant options. SPKTs reduce mortality by decreasing the incidence of cardiovascular complications and secondary diabetic complications [12, 13]. However, this approach is linked to a higher incidence and severity of complications during the first year after surgery compared to isolated KT. These complications include prolonged hospitalization, higher re-hospitalization rates within the first 30 days post-surgery, more severe infectious complications, and increased perioperative mortality [14–16].

Meanwhile, in the long term, SPKTs offer improved patient survival, especially for recipients with a long-functioning pancreas graft. For example, the 10-year survival for SPKT recipients is 50% higher than for those undergoing a KT alone [15, 16]. Unfortunately, organ shortages mean that not all T1D recipients can receive SPKTs. Consequently, KT remains the most viable treatment for diabetic CKD, offering improved quality of life and lower mortality rates in this patient population [8, 17].

Objective: to analyze early KT outcomes in patients with T1D and stage 5 CKD resulting from DN.

MATERIALS AND METHODS

Recipient characteristics

The study group comprised 145 recipients with T1D who underwent KT between January 1, 2007, and December 31, 2023, at the Kidney and Pancreas Transplant Department of Sklifosovsky Research Institute for Emergency Medicine in Moscow. Among these recipients, 57 (39.3%) were men, and 88 (60.7%) were women. The median age was 41.5 years [range: 35–47], with a median body mass index (BMI) of 22.3 kg/m^2 [range: 19.8–25]. The median age at disease onset was 14.6 years [range: 9–17].

Of the recipients, 17 (11.7%) underwent pre-dialysis KT, while 128 (88.3%) had received RRT prior to transplantation. Of those on RRT, 86 patients (67.2%) were on long-term hemodialysis (HD), and 42 (32.8%) were on peritoneal dialysis (PD). The duration of RRT ranged from a few months to 15 years, with a median duration of 2 years [range: 1–4]. Among the recipients, 17 (13.3%) had been on RRT for less than one year, 86 (67.2%) had been on RRT for 1–5 years, 22 (17.2%) had been on RRT for more than 5 years, and 3 (2.3%) had been on RRT for over 10 years.

The majority of patients (93.1%) underwent primary KT, while only 6 (2.8%) underwent repeat KT. Before transplantation, 67 recipients (46.2%) had preserved residual urine output of more than one liter per day. In addition to DN, recipients had other secondary diabetic complications of varying severity, including diabetic polyneuropathy.

Pre-transplant macroangiopathy, particularly coronary heart disease, was present in 31 recipients (21.4%). Of these, 7 (22.6%) had a history of myocardial infarction, and 9 (29%) underwent coronary artery stenting as part of the KT preparation process. Nine (6.2%) patients had a history of stroke before transplantation. Nineteen patients (13.1%) had a history of trophic ulcers on the lower limbs, with 14 (73.7%) requiring amputations of one or more toes. Ninety recipients (62%) had chronic urinary tract infections, which required treatment for urosepsis and/or antibacterial therapy.

Donor characteristics

The organ donor pool included 100 males (69%) and 40 females (27.6%); gender information was unavailable for 5 donors (3.4%). The median donor age was 46 years [range: 35.5–53]. Brain death was confirmed in 143 donors. The primary causes were stroke in 99 donors (68.3%) and traumatic brain injury in 41 donors (28.3%). Cause of death could not be determined in 3 donors (2.1%). Two recipients (1.3%) received kidneys from living-related donors.

At the time of organ procurement, median serum creatinine and urea levels in donors were 95.3 μmol/L [range: 72–112] and 6.3 mmol/L [range: 4–7.59], respectively. Microbiological examination of the transplant grafts revealed the presence of microbial flora in 9 donors (6.2%).

Surgical features of kidney transplantation

KT was performed using a standardized surgical approach. Access to the retroperitoneal space was estab-

lished, followed by mobilization of the external iliac vessels. The kidney allograft (KAG) was revascularized by creating arterial and venous anastomoses between the graft and the recipient's external iliac vessels. Urinary drainage was achieved through ureteroneocystostomy, connecting the donor ureter to the recipient's bladder. Median cold ischemia time of KAG was 13.5 hours [range: 11–16].

Immunosuppressive therapy

All patients received baseline triple-drug immunosuppressive therapy (IST), with or without induction. Induction IST using mono- or polyclonal antibodies was administered to 124 recipients (85.5%). Among them, 97 patients received monoclonal antibodies: basiliximab in 88 cases (60.7%) and daclizumab in 9 cases (6.2%). Polyclonal antibody therapy was given to 27 patients, comprising horse-derived antithymocyte globulin in 7 cases (4.8%) and rabbit-derived antithymocyte globulin in 20 cases (13.8%). In the remaining 21 patients (14.5%), methylprednisolone alone was used for induction.

Maintenance IST consisted of a triple-drug regimen including a calcineurin inhibitor, an antimetabolite or proliferative signal inhibitor, and corticosteroids. Tacrolimus was prescribed to 108 recipients (74.5%), while cyclosporine was used in 37 cases (25.5%). As the second drug, mycophenolic acid derivatives were used in 143 patients (98.6%), while everolimus was used in 2 patients (1.4%). Methylprednisolone was included in the regimen of 144 patients (99.3%); only one patient (0.7%) received a steroid-free maintenance IST regimen.

Study design: observational longitudinal retrospective, cohort, single-center study.

Inclusion criteria: technically successful KT in patients with T1D and stage 5 CKD resulting from DN.

Non-inclusion criteria: technically unsuccessful KT; SPKTs.

Graft function assessment criteria

Primary initial graft function was defined as the absence of a need for RRT during the first 7 days post-transplant. Delayed initial graft function was defined as the requirement for at least one session of extracorporeal detoxification within the first postoperative week. Death-uncensored graft loss was defined as return to RRT, death with a functioning graft, or repeat pre-dialysis KT. Death-censored graft loss excluded deaths with a functioning graft from the definition of graft loss.

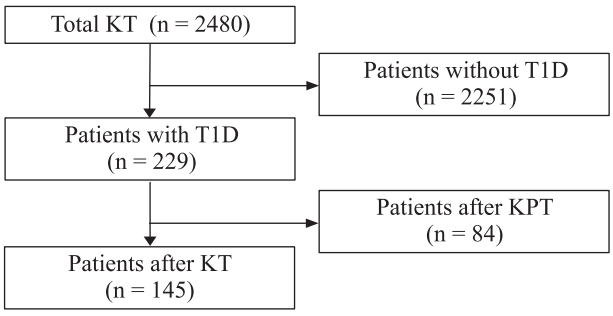

Fig. 1. Patient recruitment scheme for the study

Statistical data processing

Statistical analysis was conducted using Statistica for Windows v. 10.0 (StatSoft Inc., USA) and StatTech v. 2.8.8 (StatTech LLC, Russia). The Shapiro–Wilk test was used to assess the normality of data distribution. Quantitative data were expressed as median (Me) and interquartile range [Q1–Q3]. Qualitative data were compared using Pearson's Chi-square test; for binary variables, Fisher's exact two-tailed test was applied. The Mann–Whitney U test was used for comparisons between two independent groups of non-parametric data. Overall survival and functional graft survival were estimated using the Kaplan–Meier method. A p-value of <0.05 was considered statistically significant in single comparisons.

RESULTS

Initial graft function

Primary initial KAG function was observed in 99 recipients (68.3%), while delayed graft function occurred in 46 recipients (31.7%). In patients with primary initial graft function, median time to azotemia normalization was 6 [3–6] days. In cases of delayed function, median time extended to 20.5 [14–27] days. Median number of hemodialysis sessions required during the recovery phase of graft function was 6.5 [4–9].

Frequency of surgical complications

Early postoperative complications related to urinary tract reconstruction were noted in 7 recipients (4.8%): in six recipients, ureteroneocystostomy failure was attributed to necrosis of the distal ureter. These cases required reoperation with excision of the necrotic ureteral segment and repeat ureteroneocystostomy (Clavien–Dindo grade IIIb). In one case, ureteroneocystostomy failure resulted from an infectious process due to transplantation of a primarily infected KAG. This led to suppuration of the surgical wound and abscess formation in the graft bed, classified as Clavien–Dindo grade IVa. Renal transplantectomy was performed to preserve the patient's life.

Lymphocele formation in the KAG bed was observed in 6 recipients (4.1%) during the early postoperative period. In 5 cases, the condition required only dynamic observation and was classified as Clavien–Dindo grade I. One patient required surgical intervention, corresponding to Clavien–Dindo grade IIIb. Ureteral stricture developed in one recipient (0.7%), leading to hydronephrotic transformation of the KAG. This complication necessita-

ted initial nephrostomy placement, followed by surgical excision of the strictured ureteral segment and repeat ureteroneocystostomy (Clavien–Dindo grade IIIb).

Frequency of acute rejection crisis

The overall incidence of acute rejection was 12.4% (n = 18). All cases presented with unexplained decrease in diuresis, elevated azotemia, and graft enlargement with ultrasound evidence of edema. In 9 patients, acute rejection episodes were successfully managed with methylprednisolone pulse therapy alone (3 injections totaling 1–1.25 g). Three patients received combined therapy consisting of methylprednisolone pulse therapy and infusions of polyclonal antithymocyte antibodies. In 6 patients, triple-modality therapy was administered, including methylprednisolone pulse therapy, polyclonal antithymocyte antibody infusions, and plasmapheresis sessions.

In total, 17 patients (94.4%) demonstrated favorable clinical and laboratory responses to anti-rejection therapy, with normalization of diuresis and azotemia, and restoration of graft function confirmed by instrumental assessments. In one patient (5.6%), therapy proved ineffective; the graft was deemed nonviable and required transplantectomy.

Frequency of infectious complications

The overall incidence of infectious complications was 9.7% (n = 14). Among these, 8 recipients developed graft pyelonephritis in the early postoperative period. Management involved administration of broad-spectrum antibacterial therapy, tailored according to microbiological findings from urine cultures, which identified *Klebsiella pneumoniae* and *Enterobacter spp.* as the predominant pathogens.

Four recipients experienced postoperative wound infections, necessitating surgical revision and sanitation of the graft bed, followed by secondary wound healing.

Two patients developed cytomegalovirus (CMV) pneumonia during the early postoperative phase. Both were successfully treated with ganciclovir-based antiviral therapy, demonstrating favorable clinical responses.

Hospitalization period for recipients ranged from 7 to 83 days, with a median duration of 23 [17–30] days.

Laboratory parameters at discharge: Median creatinine and urea levels at discharge were 123 [99–164] μmol/L and 10 [7.4–14] mmol/L, respectively. Pre-transplant fasting blood glucose levels ranged from 3.5 to 22 mmol/L, with a median of 9.8 [7.8–12] mmol/L. During the first three days post-transplant, blood glucose levels varied between 3.3 and 30 mmol/L, with a median of 15 [12–17] mmol/L. At discharge, glucose levels ranged from 3.9 to 19.5 mmol/L, with a median of 8.1 [6.5–10] mmol/L.

Pre-transplant daily insulin dose ranged from 0.3 to 1.49 U/kg, with a median of 0.7 [0.55–0.9] U/kg. In the early postoperative period (first three days), insulin requirements increased to 0.45–2.37 U/kg, with a median of 0.99 [0.8–1.25] U/kg. By discharge, doses ranged from 0.35 to 1.7 U/kg, with a median of 0.88 [0.7–1.1] U/kg.

Pre-transplant glycated hemoglobin levels ranged from 4.4% to 13.4%, with a median of 7.7 [6.9–8.6]%. Post-transplant values ranged from 5.5% to 11.3%, with a median of 7.3 [6.7–8.3]%.

In-hospital and 90-day death-uncensored renal graft and recipient survival: In-hospital recipient survival was 100% (n = 145), and graft survival was 95.85% (n = 139). A total of 125 patients (86.2%) were discharged with a functioning graft and serum creatinine levels below 200 μmol/L. An additional 13 patients (8.97%) had functioning grafts with creatinine levels above 200 μmol/L, but did not require RRT. One patient (0.69%) was discharged for continuation of RRT in the outpatient setting; graft function was subsequently restored within 2 months post-transplantation.

Morphologically verified primary non-function was observed in 4 patients (2.76%). These patients were discharged for continued outpatient RRT and were re-listed for repeat KT.

Two recipients (1.38%) underwent in-hospital transplantectomy. In one case, persistent graft dysfunction due to an uncontrollable acute rejection crisis led to the graft being deemed nonviable and subsequently removed. In the second case, although the graft was initially functioning, a primary graft infection led to postoperative wound suppuration and abscess formation in the graft bed. To preserve the patient's life, a transplantectomy was performed, IST was discontinued, and targeted antibiotic therapy was initiated based on microbiological sensitivity testing.

The 90-day patient survival rate (post-discharge) was 97.2%. Death-uncensored graft survival was 93%, while death-censored graft survival reached 97.2%.

Among the 139 recipients (95.86%) discharged with functioning grafts, 3 patients developed elevated azotemia in the early post-discharge period. Two of these cases were attributed to immunological complications. In the first patient, graft biopsy revealed borderline changes and signs of calcineurin inhibitor toxicity. The treatment strategy involved pulse glucocorticoid therapy and a reduction in tacrolimus dosage, resulting in clinical improvement and normalization of azotemia. The second patient's biopsy indicated early antibody-mediated rejection and acute tubular necrosis. In addition, CT angiography revealed graft artery stenosis. The patient underwent arterial stenting, combined with pulse glucocorticoid therapy, which led to normalization of graft function. The third patient was diagnosed with ureteroneocystostomy stenosis. Placement of an internal ureteral stent successfully resolved the obstruction, contributing to normalization of renal graft function.

Graft loss occurred in 4 recipients (2.9%). In 3 cases, immunological complications were the cause of graft failure, with diagnoses confirmed post-discharge at another hospital. In the first case, graft rejection led to the development of destructive-necrotic foci, as confirmed morphologically, necessitating transplantectomy. The second patient experienced acute vascular rejection (Banff grade 3), with necrotic foci, requiring transplantectomy. In the third case, acute vascular-cellular rejection (Banff grade 2b–3) did not respond to anti-crisis therapy, and there were no indications for transplantectomy. In the fourth case, transplantectomy was performed due to abscessed graft pyelonephritis. All four patients resumed long-term hemodialysis (HD) following graft loss.

One patient died with an adequately functioning graft due to a septic lesion against the background of fungal

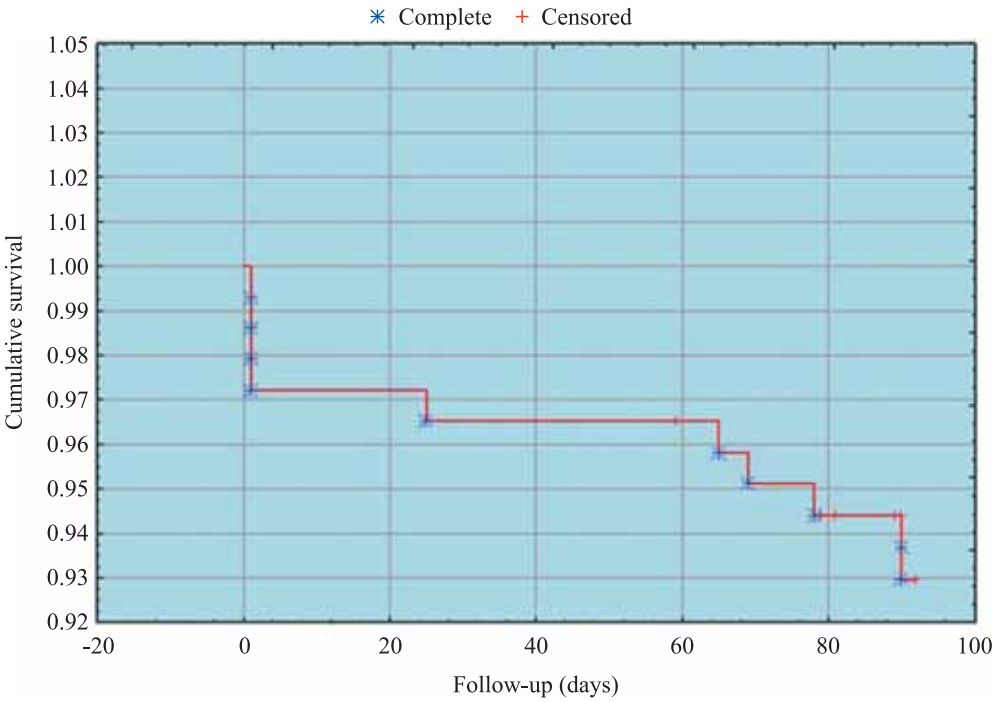

Fig. 2. Kidney graft survival rate in the early postoperative period

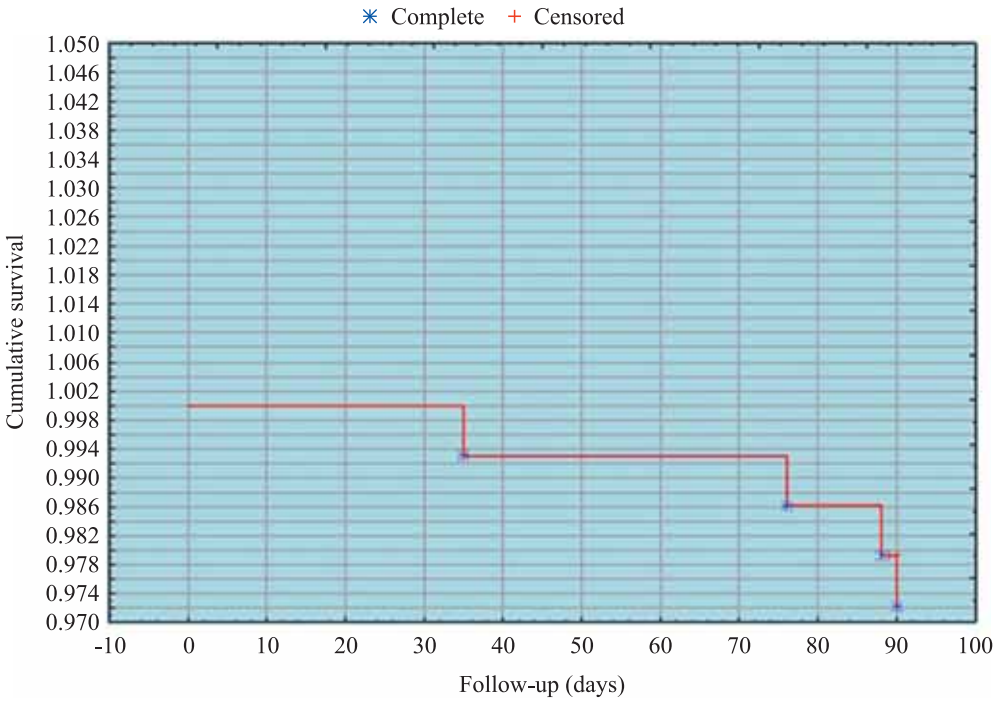

Fig. 3. Survival of recipients with T1D in the early postoperative period

pneumonia. Among those discharged with primary non-function (n = 4, 2.76%), all continued to receive RRT. Of these, 1 had the allograft removed in the early post-transplant period due to abscessed graft pyelonephritis, while 2 patients died from cardiovascular complications.

Two patients were discharged without functioning grafts (n = 2, 1.38%). Of these, one later underwent repeated KT in the long-term period, while the other died in the early post-transplant period due to cardiovascular complications.

DISCUSSION

Diabetes remains a socially significant disease due to the continually rising incidence rates, which remain concerning. Secondary diabetic complications lead to high disability and mortality, significantly reducing the quality of life for these patients. Non-transplant treatment options for stage 5 CKD resulting from DN have limited effectiveness, making KT the preferred treatment. KT has been shown to substantially improve both the duration and quality of life for these patients [18].

Patients with diabetic CKD that has progressed to stage 5 CKD represent the fastest-growing group among those needing renal RRT. Registry data from various countries show that DM is consistently ranked as the second or third most common disease among patients on the kidney transplant waiting lists.

The frequency of post-KT surgical complications in T1D patients varies widely, with reports ranging from 1% to 30% [19–21]. In our study, the overall rate of surgical complications was 9.7%. Notably, 35.7% of complications (n = 5) were classified as Clavien–Dindo grade I, requiring no surgical intervention. The remaining 57.1% of complications were grade IIIb, necessitating surgical intervention under general фтуыеруышф. Only one complication was of grade IVa, which led to graft loss.

The overall frequency of immunological complications of KT ranges from 4.8% to 19% according to existing medical literature [21, 22]. In our study, 12.4% of patients experienced immunological complications. The diagnostic protocols, immunological monitoring, and anti-crisis therapy used in our center were highly effective. Only one patient experienced graft loss due to immunological causes.

According to several studies, the overall incidence of infectious complications in the early postoperative period after KT is estimated at 2%–25% [19, 21, 23], or 9.7% according to data from our center. The selected protocols for prophylactic antibiotic treatment and management of infectious complications were effective in preserving graft function. Only one patient required transplantectomy due to transplantation of a primarily infected kidney graft to preserve the patient's life.

A total of 138 patients (95.2%) were discharged with a functioning kidney graft. One patient, who was discharged to continue RRT, had their graft function restored 2 months after KT. The incidence of primary non-function was 2.8% (n = 4). Two patients (1.4%) had their allografts removed during the hospital stay due to immunological and infectious complications.

In-hospital survival rates for kidney transplants in our study were 95.9%, with a 90-day death-uncensored graft survival of 93% and 90-day recipient survival of 97.2%. In comparison, other transplant centers report 98–99% survival rates [24, 25]. However, such publications are rare, as most studies focus on 1-year and longer post-transplant outcomes. The difference in survival rates may be attributed to factors such as initial condition of recipients, concomitant conditions, and the more stringent selection criteria used by other centers for placing patients on the kidney transplant waiting list.

CONCLUSION

The fatalities recorded in our study highlight the high mortality associated with cardiovascular complications in patients who experience renal graft loss and must return to RRT dialysis. It is clear that patients with T1D and stage 5 CKD present as one of the most complex patient groups. They require more extensive pre-transplant evaluations when being placed on the waiting list, careful preparation for transplantation, and closer management during the early and late postoperative periods.

The authors declare no conflict of interest.

REFERENCES

1. International Diabetes Federation. IDF Diabetes Atlas, 10th edn. Brussels, Belgium; 2021. [cited 11.04.2023]. Available from: https://www.diabetesatlas.org.
2. *Dedov II, Shestakova MV, Vikulova OK*. Epidemiology of diabetes mellitus in Russian Federation: clinical and statistical report according to the federal diabetes registry. *Diabetes Mellitus.* 2017; 20 (1): 13–41. [In Russ., English abstract]. doi: 10.14341/DM8664.
3. *Dedov II, Shestakova MV, Vikulova OK, Zheleznyakova AV, Isakov MA, Sazonova DV et al*. Diabetes mellitus in the Russian Federation: dynamics of epidemiological indicators according to the Federal register of diabetes mellitus for the period 2010–2022. *Diabetes Mellitus*. 2023; 26 (2): 104–123. [In Russ., English abstract]. doi: 10.14341/DM13035.
4. *Dedov II, Shestakova MV, Vikulova OK, Zheleznyakova AV, Isakov MA.* Diabetes mellitus in Russian Federation: prevalence, morbidity, mortality, parameters of glycaemic control and structure of glucose lowering therapy according to the Federal Diabetes Register, status 2017. *Diabetes mellitus*. 2018; 21 (3): 144–159. [In Russ., English abstract]. doi: 10.14341/DM9686.
5. *Pavkov ME, Collins AJ, Coresh J, Nelson RG.* Kidney Disease in Diabetes. In: Cowie CC, Casagrande SS, Menke A, Cissell MA, Eberhardt MS, Meigs JB et al. eds. *Diabetes in America.* 3rd ed. Bethesda (MD): National Institute of Diabetes and Digestive and Kidney

Diseases (US); 2018 Aug. Chapt. 22. [Accessed July 22 2024]. Available from: https://www.ncbi.nlm.nih.gov/books/NBK568002/.
6. *Van Dijk PC, Jager KJ, Stengel B, Gronhagen-Riska C, Feest TG, Briggs JD*. Renal replacement therapy for diabetic end-stage renal disease: data from 10 registries in Europe (1991–2000). *Kidney Int*. 2005; 67 (4): 1489–1499. doi: 10.1111/j.1523-1755.2005.00227.x.
7. *Vonesh EF, Snyder JJ, Foley RN, Collins AJ*. The differential impact of risk factors on mortality in hemodialysis and peritoneal dialysis. *Kidney Int*. 2004; 66 (6): 2389–2401. doi: 10.1111/j.1523-1755.2004.66028.x.
8. *Brunkhorst R, Lufft V, Dannenberg B, Kliem V, Tusch G, Pichlmayr R*. Improved survival in patients with type 1 diabetes mellitus after renal transplantation compared with hemodialysis: a case-control study. *Transplantation.* 2003; 76 (1): 115–119. doi: 10.1097/01.TP.0000070225.38757.81.
9. *Kumar S, Merchant MR, Dyer P, Martin S, Hutchison AJ, Johnson RWG et al.* Increase mortality due to cardiovascular disease in Type I diabetic patients transplanted for end-stage renal failure. *Diabet Med*. 1994; 11 (10): 987–991. doi: 10.1111/j.1464-5491.1994.tb00259.x.
10. *Perez RV, Matas AJ, Gillingham KJ, Payne WD, Canafax DM, Dunn DL et al.* Lessons learned and future hopes: Three thousand renal transplants at the University of Minnesota. *Clin Transpl.* 1990: 217–231.
11. *Ozawa K, Takai M, Taniguchi T, Kawase M, Takeuchi S, Kawase K et al.* Diabetes Mellitus as a Predictive Factor for Urinary Tract Infection for Patients Treated with Kidney Transplantation. *Medicina (Kaunas).* 2022; 58 (10): 1488. doi: 10.3390/medicina58101488.
12. *Medina-Polo J, Domínguez-Esteban M, Morales JM, Pamplona M, Andrés A, Jiménez C et al.* Cardiovascular events after simultaneous pancreas-kidney transplantation. *Transplant Proc.* 2010; 42 (8): 2981–2983. doi: 10.1016/j.transproceed.2010.07.046.
13. *Ziaja J, Chudek J, Kolonko A, Kamińska D, Kujawa-Szewieczek A, Kuriata-Kordek M et al.* Does simultaneously transplanted pancreas improve long-term outcome of kidney transplantation in type 1 diabetic recipients? *Transplant Proc.* 2011; 43 (8): 3097–3101. doi: 10.1016/j.transproceed.2011.08.020.
14. *King EA, Kucirka LM, McAdams-DeMarco MA, Massie AB, Al Ammary F, Ahmed R et al.* Early Hospital Readmission After Simultaneous Pancreas-Kidney Transplantation: Patient and Center-Level Factors. *Am J Transplant*. 2016; 16 (2): 541–549. doi: 10.1111/ajt.13485.
15. *Schreiber PW, Laager M, Boggian K, Neofytos D, van Delden C, Egli A et al.* Swiss Transplant Cohort Study. Surgical site infections after simultaneous pancreas kidney and pancreas transplantation in the Swiss Transplant Cohort Study. *J Hosp Infect*. 2022; 128: 47–53. doi: 10.1016/j.jhin.2022.07.009.
16. *Nagendra L, Fernandez CJ, Pappachan JM.* Simultaneous pancreas-kidney transplantation for end-stage renal failure in type 1 diabetes mellitus: Current perspectives. *World J Transplant.* 2023; 13 (5): 208–220. doi: 10.5500/wjt.v13.i5.208.
17. *Esmeijer K, Hoogeveen EK, van den Boog PJM, Konijn C, Mallat MJK, Baranski AG et al.* Dutch Transplant Centers; Dutch Kidney Transplant Centres. Superior Long-term Survival for Simultaneous Pancreas-Kidney Transplantation as Renal Replacement Therapy: 30-Year Follow-up of a Nationwide Cohort. *Diabetes Care*. 2020; 43 (2): 321–328. doi: 10.2337/dc19-1580.
18. *Shingde R, Calisa V, Craig JC, Chapman JR, Webster AC, Pleass H et al.* Relative survival and quality of life benefits of pancreas-kidney transplantation, deceased kidney transplantation and dialysis in type 1 diabetes mellitus – a probabilistic simulation model. *Transpl Int.* 2020; 33 (11): 1393–1404. doi: 10.1111/tri.13679.
19. *Khadjibaev F, Sultanov P, Ergashev D, Sadikov R, Djuraev J, Iskhakov N et al.* Frequency of Complications After Kidney Transplant in the Early Postoperative Period. *Exp Clin Transplant.* 2024; 22 (Suppl 1): 195–199. doi: 10.6002/ect.MESOT2023.P25.
20. *Timsit MO, Kleinclauss F, Richard V, Thuret R.* Complications chirurgicales de la transplantation rénale [Surgical complications of renal transplantation]. *Prog Urol.* 2016; 26 (15): 1066–1082. [In French, English abstract]. doi: 10.1016/j.purol.2016.09.052.
21. *Gutiérrez P, Marrero D, Hernández D, Vivancos S, Pérez-Tamajón L, Rodríguez de Vera JM et al.* Surgical complications and renal function after kidney alone or simultaneous pancreas-kidney transplantation: a matched comparative study. *Nephrol Dial Transplant*. 2007; 22 (5): 1451–1455. doi: 10.1093/ndt/gfl771.
22. *Treckmann JW, Goldenberg A, Malamutmann E, Witzke O, Fouzas I, Paul A et al.* Kidney Transplantation in Patients with Diabetes Mellitus: Surgical Complications. *Hepatogastroenterol*. 2011; 58 (107–108): 738–739.
23. *Siskind E, Huntoon K, Shah K, Villa M, Blood AJ, Lumerman L et al.* Partial closure of skin wounds after kidney transplantation decreases the incidence of postoperative wound infections. *Int J Angiol.* 2012; 21 (2): 85–88. doi: 10.1055/s-0032-1315797.
24. *Akagun T, Yelken B, Usta M, Turkmen A.* Outcome of Renal Transplantation in Patients with Diabetes Mellitus: A Single-Center Experience. *Transplant Proc*. 2022; 54 (8): 2174–2178. doi: 10.1016/j.transproceed.2022.08.024.
25. *Suzuki T, Nakao T, Harada S, Nakamura T, Koshino K, Sakai K et al.* Results of kidney transplantation for diabetic nephropathy: a single-center experience. *Transplant Proc*. 2014; 46 (2): 464–466. doi: 10.1016/j.transproceed.2013.11.076.

The article was submitted to the journal on 22.07.2024

DOI: 10.15825/1995-1191-2024-4-33-45

RIGHT LOBE LIVING DONOR LIVER TRANSPLANTATION – EXPERIENCE FROM THE DEPARTMENT OF HEPATOBILIARY SURGERY

K.O. Semash[1, 2], T.A. Dzhanbekov[1, 2]

[1] National Children's Medical Center, Tashkent, Uzbekistan
[2] Vakhidov Republican Specialized Surgical Research and Practical Medical Center of Surgery, Tashkent, Uzbekistan

Background. Living-donor liver transplant (LDLT) is a life-saving procedure for patients with end-stage liver diseases. **Objective:** to evaluate the outcomes of the first independent LDLT performed at the Department of Hepatobiliary Surgery, Vakhidov Republican Specialized Surgical Research and Practical Medical Center of Surgery, and to demonstrate that liver transplantation (LT) is a feasible procedure at our institution. **Materials and methods.** From October 2021 to December 2023, 40 right lobe LDLTs were performed in our department. Short-term and long-term outcomes in recipients were assessed. The outcomes of transplant hepatectomy were also evaluated. **Results.** Hepatic artery thrombosis developed in 1 case (2.5%); arterial anastomotic stenosis was detected in 3 cases (7.5%), which were repaired by endovascular balloon dilation; splenic artery steal syndrome was diagnosed in 3 cases (7.5%), which was resolved by endovascular splenic artery embolization. One patient (2.5%) developed portal vein thrombosis. Two patients (5%) had portal vein stenosis 10 months after transplantation; endovascular balloon angioplasty was performed with good clinical effect. Biliary complications accounted for 45%, of which 89% were biliary leaks and 11% were anastomotic biliary stricture. In-hospital mortality was 12.5%. **Conclusion.** The results of our experience and analysis of post-transplant complications are comparable with those of the world literature and are acceptable at the stage of implementation of the LT program. Transplantation is feasible at our center, but it is necessary to improve surgical and conservative treatment techniques in order to minimize early and late postoperative complications.

Keywords: liver transplantation, living-donor liver transplant, cirrhosis.

INTRODUCTION

Since Thomas Starzl performed the first human liver transplant (LT) in 1963 [1], the global transplant community has evolved from isolated clinical attempts to widespread acceptance of LT as a treatment for acute and chronic liver diseases, malignant tumors and other liver conditions. Over the decades, the spectrum of indications for LT has expanded to include numerous nosological entities. As global demand for LT continues to grow, living donor liver transplantation (LDLT) has emerged as a vital alternative for patients who might otherwise die while awaiting a cadaveric organ. In recent years, LDLT has been established as a safe and effective treatment, with outcomes comparable to those of deceased donor liver transplantation (DDLT). Importantly, LDLT also contributes to substantially expanding the limited donor organ pool [2].

The leading etiological factors in this region are chronic viral hepatitis B and C [3, 4]. Until 2018, there was no legal framework to support organ transplantation in the country. This changed in 2018, when the government enacted a decree officially authorizing LDLT. Subsequently, in February of the same year, a pioneering team from the Shumakov National Medical Research Center of Transplantology and Artificial Organs (Moscow, Russian Federation), led by Sergey Gautier – Fellow of the Russian Academy of Sciences – performed the first series of liver transplants in Uzbekistan. However, routine performance of these procedures began only in October 2021 [5].

Objective: the objective of this study was to evaluate the outcomes of the first 40 cases of LDLT performed at the Department of Hepatobiliary Surgery, Vakhidov Republican Specialized Surgical Research and Practical Medical Center of Surgery in Tashkent, in order to demonstrate the feasibility of LT in a hospital-based setting.

MATERIALS AND METHODS

The LDLT program in Uzbekistan commenced on a regular basis in October 2021 at the aforementioned center. Both the donor and recipient surgical procedures, as well as the postoperative management, were conducted

Corresponding author: Konstantin Semash. Address: 10, Kichik Halka Yuli, Tashkent, 100096, Uzbekistan.
Phone: +998 (94) 090-89-05. Email: mail@doctorsemash.com

under the direct supervision of two experienced transplant physicians.

This retrospective review was based on prospectively collected data from transplants performed between October 2021 and December 2023. The median follow-up period was 7 months (range, 1–26 months).

Recipients

During the study period, 40 adult right lobe liver transplants were performed. The cohort included 28 male patients (70%) and 12 female patients (30%), with a median recipient age of 40 years (range, 18–56 years). The mean Model for End-Stage Liver Disease (MELD) score was 18 (range, 10–30). The primary indications for LT were cirrhosis secondary to hepatitis B and D virus co-infection (34 cases), hepatitis C virus-related cirrhosis (3 cases), autoimmune hepatitis (2 cases), and toxic hepatitis (1 case).

All patients presented with portal hypertension and its complications, including esophageal varices (100%), variceal bleeding (7 cases), splenomegaly (100%), and cytopenia (100%). Seven patients underwent pre-transplant endoscopic variceal ligation to prevent bleeding, while three patients underwent splenic artery embolization due to hypersplenism. Two patients presented with stage 3 portal vein thrombosis, classified according to the Yerdel system.

No ABO-incompatible transplantations were performed in this cohort. Perioperative care for all patients was conducted in accordance with the Enhanced Recovery After Surgery (ERAS) protocol [6]. Additionally, all patients with viral hepatitis received antiviral therapy preoperatively, continuing until a sustained virological response was achieved.

The demographic and clinical characteristics of the recipients are summarized in Table 1.

Donors

All recipients in the study underwent right-lobe LDLT. Of the 40 transplants performed, 37 involved living related donors. The donor-recipient relationships were as follows: 11 sons, 10 brothers, 9 sisters, 4 cousins, 1 father, 1 nephew, and 1 aunt. In accordance with national legislation in Uzbekistan, spouses may serve as organ or tissue donors if the marriage has lasted for at least three years. Based on this provision, three wives were approved as donors in this series.

All donors underwent evaluation following a standardized protocol, which was adapted to the specific requirements of our center [7]. This comprehensive assessment included initial screening of medical history, body mass index (BMI), and ABO blood group compatibility, as well as a full blood count, biochemical profile, coagulation tests, and virological screening for hepatitis B and C (HBV and HCV). Cardiopulmonary evaluation included electrocardiography (ECG), echocardiography, and chest radiography.

Imaging studies included abdominal ultrasound, contrast-enhanced computed tomography (CT) with evaluation of hepatic vascular anatomy, and magnetic resonance cholangiopancreatography (MRCP) for biliary tract assessment. Esophagogastroduodenoscopy was also performed. Donor liver steatosis was evaluated using liver elastometry.

In addition to medical testing, all donors underwent psychosocial evaluation and legal counseling to confirm their eligibility and to verify their relationship to the recipient.

Donors with cardiovascular disease, neurological or psychiatric disorders, and hepatic steatosis grade S1 or higher (as assessed by elastometry) were excluded from consideration. Additional exclusion criteria included a low graft-to-recipient weight ratio (GRWR), and variant portal vein anatomy. Only donors with type 1 portal vein anatomy, as defined by the Nakamura classification [8], were accepted.

Liver volumetric analysis was performed to ensure donor safety. Only those with an estimated residual liver volume of at least 35% were deemed eligible. Donors were also excluded if the right hepatic artery diameter was less than 2 mm. Donors with complex venous anatomy in hepatic segments V and VIII – specifically those with multiple segmental branches requiring technically demanding venoplasty – were not considered suitable candidates.

Perioperative donor management adhered to the ERAS Society guidelines [9].

Surgical technique

The graft used in all cases was the right liver lobe. Liver procurement was performed using a conventional surgical technique. Afferent and efferent vessels, along with the bile ducts of the right lobe, were carefully mobilized using precision techniques. The resection plane was identified by temporarily clamping the inflow to the right lobe, marking the demarcation line. In anatomically complex or unclear cases, intraoperative Doppler imaging was employed to assist in defining the resection plane. Parenchymal transection was conducted using a CUSA Excel device (Integra, USA) in combination with bipolar forceps, with continuous irrigation of the coagulation field using saline. Vascular structures supplying the left lobe were preserved. The bile duct was carefully dissected and transected without coagulation.

Histidine-tryptophan-ketoglutarate solution (HTK, Custodiol, Dr. F. Köhler Chemie, GmbH, Germany) was

used in all cases for graft preservation. Venoplasty was performed when segment V and VIII veins measured ≥5 mm in diameter; polytetrafluoroethylene grafts were used. In two cases, a conduit was fashioned using the donor's falciform ligament and the recipient's umbilical vein (Fig. 1). When multiple bile ducts were found in

Table 1

Baseline characteristics of recipients and the surgical features

Data	Values (n = 40)
Age, years	40 (18–56)
Sex, n (%)	
Men	28 (70%)
Women	12 (30%)
Indications for transplantation, n (%)	
Hepatitis B + D virus	34 (85%)
Hepatitis C virus	3 (7.5%)
Autoimmune hepatitis	2 (5%)
Toxic hepatitis	1 (2.5%)
MELD	18 (10–30)
Signs of portal hypertension	40 (100%)
Portal vein thrombosis before transplantation	2 (5%)
Follow-up after transplantation, months	7 (1–26)
Operation time, minutes	570 (410–785)
Blood loss	1200 (600–5000)
Graft weight, grams	720 (515–940)
GRWR, %	1.05 (0.7–2.0)
Graft phleboplasty	
Single RHV, no repair performed	28 (80%)
2 IRHV, no repair performed	3 (7.5%)
3 IRHV, joining the orifices	2 (5%)
Joining of the orifices of veins S8 and RHV	2 (5%)
PTFE graft, S5 vein	1 (2.5%)
PTFE graft, S8 vein	1 (2.5%)
PTFE graft, joining of S5 and S8 veins	1 (2.5%)
Falciform ligament conduit, joining of S5 and S8 veins	1 (2.5%)
Umbilical vein graft, joining of S5 and S8 veins	1 (2.5%)
Number of caval anastomoses	
1	26 (65%)
2	14 (35%)
Arterial anastomosis	
Split suture	17 (42.5%)
Twisted suture	21 (52.5%)
Split suture, anastomosis with splenic artery	2 (5%)
Splenic artery ligation	
HA diameter, mm	4.2 (2.8–6.0)
SA diameter, mm	8.6 (5.2–10.1)
Difference between SA and HA diameters, %	95 (4–239%)
SA ligation, n (%)	35 (87.5%)
Biliary reconstruction	
Bilio-biliary anastomosis (1 duct)	11 (27.5%)
Bilio-biliary + biliodigestive anastomosis	1 (2.5%)
Biliodigestive anastomosis (1 duct)	7 (17.5%)
Biliodigestive anastomosis (2 ducts, 1 anastomosis)	10 (25%)
Biliodigestive anastomosis (2 ducts, 2 anastomoses)	4 (10%)
Biliodigestive anastomosis (3 ducts, 2 anastomoses)	6 (15%)
Biliodigestive anastomosis (3 ducts, 1 anastomosis)	1 (2.5%)

Note: MELD, Model for End Stage Liver Disease; GRWR, graft-to-recipient weight ratio; PTFE, polytetrafluoroethylene; RHV, right hepatic vein; IRHV, inferior right hepatic vein; HA, hepatic artery; SA, splenic artery.

close proximity, ductoplasty was performed by unifying the ducts with a continuous twisted suture using PDS 5/0 polydioxanone suture.

Where technically feasible, caval reconstruction was performed using the piggyback technique with lateral clamping of the hepatic veins, thereby preserving continuous blood flow through the inferior vena cava. In cases where the graft contained multiple right hepatic veins, additional caval anastomoses were performed as required. The recipient's portal vein was anastomosed to the graft portal vein in an end-to-end fashion using 5/0 Prolene suture.

Arterial anastomoses were carried out using various techniques, depending on vessel size and anatomical considerations. For donor right hepatic arteries with diameters less than 2.5 mm or in cases of significant size mismatch between donor and recipient arteries, interrupted sutures were placed using 7/0 Prolene under binocular magnification (3.5×). When the donor artery diameter exceeded 2.5 mm, a continuous twisted suture technique with 7/0 Prolene was employed. All arterial anastomoses were performed with the recipient's common hepatic artery; however, in two cases, the splenic artery was used due to marked intimal atherosclerosis of the common hepatic artery. Intraoperative Doppler ultrasound was routinely used to assess arterial inflow immediately following arterial anastomosis and again after biliary reconstruction and completion of hemostasis.

We also established specific criteria for splenic artery ligation to prevent splenic artery steal syndrome (SASS). In cases where the splenic artery diameter exceeded the hepatic artery diameter by 50% or more – as determined by preoperative contrast-enhanced CT imaging – splenic artery ligation was indicated. This procedure was performed either at the level of the splenic hilum or at the origin from the celiac trunk. To prevent arterial insufficiency and mitigate the risk of portal hyperperfusion [10–11], grafts with a GRWR of more than 0.9% were used.

Biliary reconstruction was performed using either duct-to-duct anastomosis or Roux-en-Y hepaticojejunostomy with external stenting [12]. A duct-to-duct biliary anastomosis was selected when the graft contained a single bile duct with a diameter exceeding 3 mm. In all other cases, a Roux-en-Y hepaticojejunostomy was performed, accompanied by the placement of external biliary stents [26].

Immunosuppressive therapy

Immunosuppression was initiated with basiliximab at 20 mg for induction. This was followed by intraoperative administration of methylprednisolone (10 mg/kg) immediately after portal vein reperfusion. The maintenance immunosuppressive regimen included tacrolimus in combination with low-dose methylprednisolone. Mycophenolate mofetil was added as clinically indicated. Target serum tacrolimus levels were maintained between 6 and 9 ng/mL. Decisions regarding discontinuation or substitution of immunosuppressive agents were guided by the occurrence of adverse effects and patient-specific tolerance.

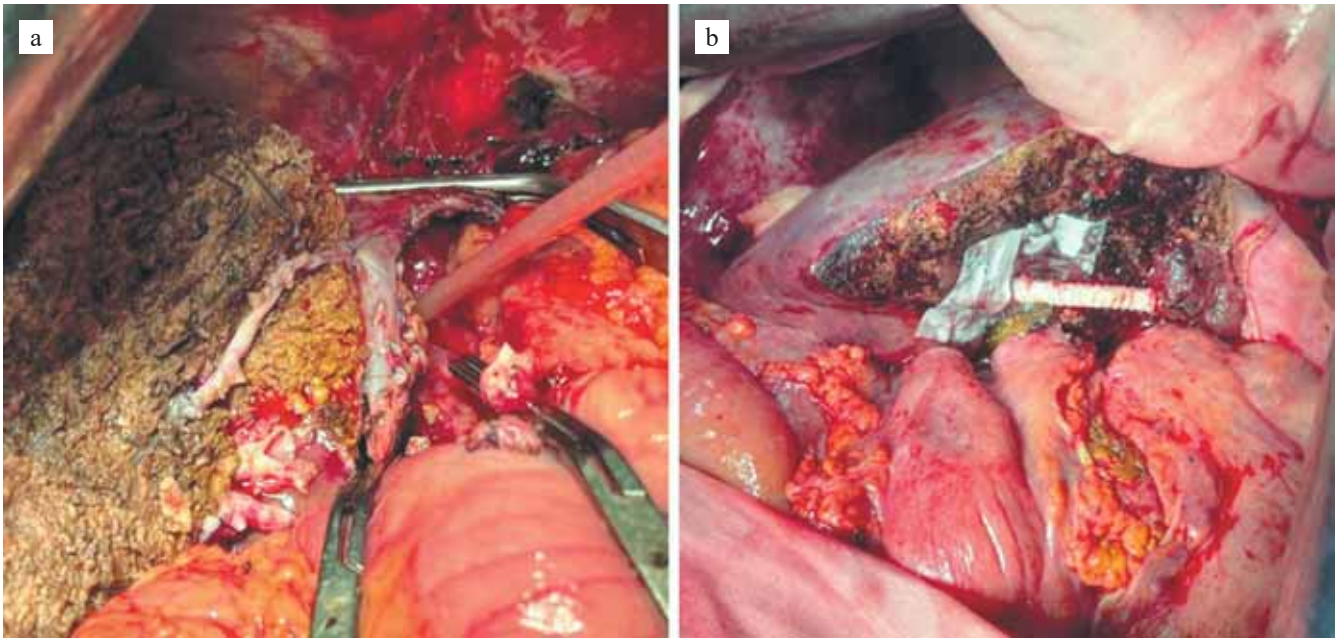

Fig. 1. Venous outflow reconstruction variations: a, vein reconstruction of segments 5 and 8 using the donor's falciform ligament; b, vein reconstruction of segments 5 and 8 using a polytetrafluoroethylene graft

Postoperative vascular monitoring and prophylaxis against vascular complications

All patients received comprehensive thromboprophylaxis to minimize the risk of vascular complications. Prophylaxis against postoperative arterial complications included the administration of alprostadil (prostaglandin E1) immediately following arterial reperfusion. Starting on the first postoperative day, low-molecular-weight heparin (LMWH) was administered, and low-dose aspirin was introduced on postoperative day 4. Alprostadil was discontinued 7 days postoperatively, while LMWH was continued for 2 weeks after transplantation. Aspirin therapy was maintained for 3 months postoperatively. In cases of significant coagulopathy, signs of bleeding, or platelet counts below 50×10^9/L, thromboprophylaxis was modified or temporarily halted until the complications were addressed. Additionally, intravenous fluid support was provided with daily monitoring of fluid balance.

For the first 7 days following transplantation, patients underwent regular ultrasound monitoring using Logiq P6 (General Electric, USA) and DC-40 (Mindray Medical International Limited, China) ultrasound systems, both equipped with standard C6-2 convex sensor units. The initial postoperative ultrasound to assess arterial blood flow was performed after the patient was transferred to the intensive care unit. Subsequent ultrasound exams were conducted every 6 hours during the first week postsurgery. After the first week, monitoring was reduced to once daily. In cases with complications, ultrasound monitoring continued for more than 1 week as needed [11].

The following Doppler ultrasound findings were considered indicative of deteriorating hepatic arterial blood flow: difficulty visualizing the artery, changes in the resistive index (RI) – either an increase above 0.85 or a decrease below 0.5 – and a reduction in arterial peak systolic velocity to less than 15 cm/sec. In such cases, we initiated continuous heparin infusion, beginning with a bolus dose of 80 U/kg followed by a maintenance infusion at 18 U/kg/hr. Activated partial thromboplastin time was monitored every 6 hours [11, 13, 14].

If hepatic arterial flow was not visualized by ultrasound, an emergency contrast-enhanced CT scan was performed, or the patient was urgently transferred to the endovascular suite for diagnostic angiography. Upon confirmation of arterial insufficiency, immediate revascularization was undertaken [15].

To monitor portal vein blood flow, Doppler ultrasound was used to assess both volumetric and linear flow velocities. If signs of occlusive portal vein thrombosis were detected within the first 72 hours post-transplant, the patient underwent relaparotomy with revision of the anastomosis. In other cases, heparin prophylaxis was initiated.

Variables evaluated and statistical processing

Baseline variables including age, sex, body weight, and date of surgery were analyzed for both donors and recipients. Postoperative complications were classified according to the Clavien–Dindo classification system [16]. For patients who experienced complications, the Comprehensive Complication Index (CCI) [17] was additionally calculated. Unlike the Clavien–Dindo system, which records only the highest-grade complication per patient, the CCI accounts for the cumulative burden of all complications, providing a more comprehensive measure of postoperative morbidity and overall patient severity.

Short-term outcomes were defined as events occurring during the initial hospitalization period. Long-term outcomes were assessed over a follow-up period of up to 26 months postoperatively. Continuous variables were reported as medians with corresponding ranges, while categorical variables were expressed as absolute numbers and percentages. Patient survival rates were estimated using the Kaplan–Meier method. A p-value of less than 0.05 was considered statistically significant. Statistical analyses were conducted using Microsoft Excel (USA), Orange3 (Slovenia), and IBM SPSS Statistics version 26 (USA).

RESULTS

Recipients

The median operative time for recipients was 570 minutes (range: 410–785 minutes), with a median intraoperative blood loss of 1,200 mL (range: 600–5,000 mL). In 28 cases (70%), the right lobe grafts had a single right hepatic vein (RHV) without significant accessory veins; these cases required only a single caval anastomosis, and venoplasty was not performed. In 5 cases (12.5%), accessory inferior RHVs (iRHVs) were present: 1 iRHV in three cases (7.5%) and 2 iRHVs in two cases (5%). In patients with two iRHVs, the RHVs were combined into a single venous orifice and two caval anastomoses were performed during reconstruction. In cases with a single iRHV, dual caval anastomoses were performed without additional venoplasty.

In 3 patients, polytetrafluoroethylene grafts were used for venous outflow plasty due to the presence of significant S5 and S8 veins. In one case (2.5%), a conduit fashioned from the donor liver's falciform ligament was used for venoplasty of the S5 and S8 branches. In another case, the recipient's dilated umbilical vein served as a conduit for similar reconstruction. Overall, 14 patients (35%) required 2 caval anastomoses.

All arterial anastomoses were performed using the recipient's common hepatic artery, except in 2 cases where the splenic artery (SA) was used due to severe atherosclerotic changes in the common hepatic artery. In 35 cases (87.5%), the SA diameter exceeded the hepatic artery (HA) diameter by 50% or more. The mean HA diameter was 4.2 mm (range: 2.8–6.0 mm), while the mean SA diameter was 8.8 mm (range: 5.2–10.3 mm). The median difference in diameter between the SA and HA was 95% (range: 4–241%). The median GRWR was 1.1 (range: 0.7–2.0).

In all 35 cases where the SA diameter exceeded the HA diameter by ≥50%, SA ligation was performed to prevent SASS. Among these, the SA was ligated at the splenic hilum in 3 patients, and at the level of the celiac trunk in 27 patients.

Due to anatomical variations in the donor bile ducts, different techniques were employed for biliary reconstruction (see Fig. 2). A duct-to-duct (biliobiliary) anastomosis was performed in 11 patients, while a Roux-en-Y hepaticojejunostomy was used in 28 cases. One patient had an aberrant right hepatic duct, requiring a combined reconstruction approach: a Roux-en-Y hepaticojejunostomy for the main bile duct and a separate biliobiliary anastomosis for the aberrant duct. Perioperative characteristics of all patients are summarized in Table 1.

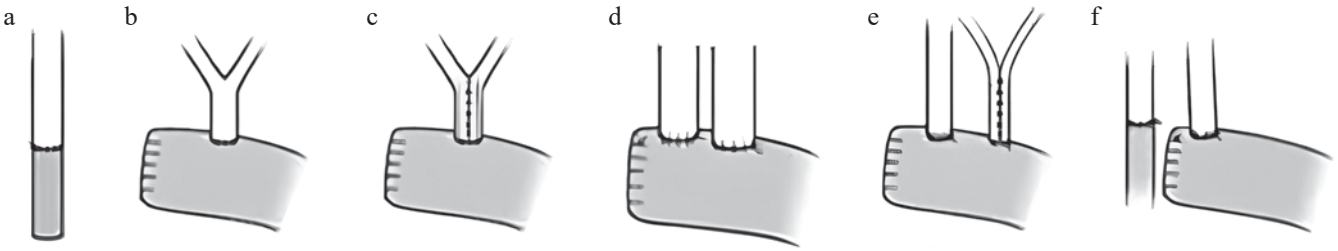

Fig. 2. Biliary reconstruction variations: a, bilio-biliary anastomosis; b, biliodigestive anastomosis on the Roux-en-Y jejunal loop; c, ductoplasty (joining) of two or three ducts and biliodigestive anastomosis on the Roux-en-Y jejunal loop; d, two separate bile duct anastomoses with the Roux-en-Y jejunal loop; e, three bile ducts on the graft – ductoplasty (joining) of two ducts and imposition of two separate bile duct anastomoses with Roux-en-Y jejunal loop; f, common bile duct anastomosis with Roux-en-Y jejunal loop and bilo-biliary anastomosis with aberrant bile duct of the liver right lobe

Table 2

Vascular complications

Total complications, n	8 of 40 (20%)
Arterial complications, n (%)	
HAT	1 (14.4%)
HAS	3 (42.8%)
Steal syndrome	3 (42.8%)
HAS when ligating the SA at the splenic hilum	3 of 3 (100%)
HAS when ligating the SA at the celiac trunk	–
Steal syndrome after SA ligation	–
Steal syndrome without SA ligation	3 of 5 (60%)
Postoperative day of complication (range)	
HAT	7 (7)
HAS	3 (3)
Steal syndrome	4 (0–7)
Portal vein complications, n (%)	
Complication, n	
PVT	1 (2.5%)
PVS	2 (5%)
Postoperative day of complication (range)	
PVT	Postoperative day 2
PVS	Postoperative month 10.5 (9–12)

Note: HAT, hepatic artery thrombosis; HAS, hepatic artery stenosis; SA, splenic artery; PVT, portal vein thrombosis; PVS, portal vein stenosis.

Rejection. Among the patients examined, 10% had an episode of acute rejection, occurring between postoperative days 2 and 14. Pulse methylprednisolone therapy was effective in 50% of these cases. However, two patients succumbed to acute graft dysfunction in the early postoperative period. In all cases of suspected graft rejection, the corticosteroid dose was tapered following pulse therapy, and mycophenolic acid was introduced as a third-line agent in the immunosuppressive regimen.

Vascular complications. Hepatic artery complications occurred in 7 patients, as detailed in Table 2. All episodes of arterial insufficiency developed within the first postoperative week. Hepatic artery thrombosis (HAT) occurred in one patient. Hepatic artery stenosis (HAS) was diagnosed in 3 patients (42.8%), while SASS developed in another three. Notably, all SASS cases occurred in patients whose SA had not been ligated.

Selective celiacography was performed in all cases of arterial insufficiency. The patient diagnosed with HAT was treated with balloon angioplasty followed by stent placement in the HA. All HAS cases were managed with balloon angioplasty alone, without stenting. Patients diagnosed with SASS underwent SA coil embolization.

In one patient with SASS, the arterial anastomosis of the graft was inadvertently damaged during selective angiography, necessitating an emergency relaparotomy to control hemorrhage and subsequent ligation of the SA. No recurrent episodes of arterial insufficiency were observed during the follow-up period.

Portal vein (PV) complications are summarized in Table 2. PV complications occurred in 3 patients. One patient developed acute occlusive portal vein thrombosis (PVT) on postoperative day 2, confirmed by Doppler ultrasound. This was accompanied by a marked elevation in liver transaminases (ALT: 2500 U/L; AST: 1800 U/L) and hyperbilirubinemia (210 μmol/L). The patient underwent emergency laparotomy with revision of the portal vein anastomosis and thrombectomy. Despite restoration of adequate hepatic blood flow and intensive treatment, including extracorporeal detoxification, the patient developed severe liver graft dysfunction and died on postoperative day 9.

Two patients developed portal vein stenosis (PVS) within one year after transplantation. Clinically, PVS presented with signs of graft dysfunction (elevated bilirubin levels and cytolytic syndrome), along with features of portal hypertension (cytopenia, ascites). Both patients were successfully treated with percutaneous balloon angioplasty. They are currently under outpatient follow-up with satisfactory liver graft function [18].

Biliary complications. Biliary complications were observed in 16 patients, with bile leakage being the most common presentation (14 cases). Two patients developed late-onset biliary strictures: one experienced an anastomotic stricture of a bilio-biliary anastomosis 18 months after transplantation, and the other developed a stricture at the site of a biliodigestive anastomosis 12 months post-transplant.

Among patients with arterial complications, biliary complications were also noted in 4 cases (57.1%): one with HAT, two with SASS, and one with HAS. All four experienced bile leakage, but no biliary strictures were detected in this subset.

In one patient with a biliodigestive anastomosis, a biloma was managed by ultrasound-guided percutaneous drainage. Another patient with a bilio-biliary anastomosis underwent endoscopic retrograde cholangiopancreatography (ERCP) with biliary stent placement, which successfully controlled the bile leak. In the remaining patients, bile leakage occurred while intra-abdominal drainage tubes were in place and resolved spontaneously without the need for additional intervention.

By comparison, among patients without arterial complications, bile leakage occurred in 10 cases (30.3%) during the early postoperative period ($P = 0.039$). In this same group, the previously described cases of late-onset anastomotic bile duct strictures also occurred, both of which ultimately required reconstructive surgical intervention.

Other complications. All complications were classified as either early or late and are summarized in Table 2. Among the early complications, two patients developed wound seromas (Clavien–Dindo grade I), seven patients experienced pleural effusions requiring drainage, and one patient had gastrointestinal bleeding (Clavien–Dindo

Table 3

Early and late post-transplant complications

Complication (Clavien–Dindo grade)	Early complications, n	Late complications, n
Stage 1		
Seroma/wound infection	2	
Stage 2		
Biliary leak	6	
Acute rejection	2	
Chronic rejection		1
De novo hepatitis B virus		1
Stage 3a		
Biliary leak	6	
Right-sided pleurisy	5	
Bilateral pleurisy	2	
Gastrointestinal bleeding	1	
Liver transplant abscesses		3
HAT	1	
HAS	3	
SASS	2	
PVS		2
Stage 3b		
Biliary peritonitis	2	
Anastomotic stricture		2
Intra-abdominal hemorrhage	2	
SASS	1	
Stage 4		
Seizure syndrome	1	
Demyelination of the pons	1	
Biliary sepsis		1
Aspiration	1	
Sepsis	3	
Stage 5		
PVT	1	
Sepsis, MOD	2	
Acute rejection	2	
Covid-19 pneumonia		1
Aspiration		1
Chronic rejection (non-compliance)		1
Median CCI (for patients with complications)	42.6 (8.7–100)	80.1 (39.7–100)

Note: HAT, hepatic artery thrombosis, HAS – hepatic artery stenosis, PVS, portal vein stenosis; SASS, splenic artery steal syndrome; PVT, portal vein thrombosis; MOD, multiple organ dysfunction; CCI, comprehensive complication index.

grade IIIa). Severe complications included two cases of biliary peritonitis requiring surgical intervention and two cases of internal bleeding – one due to disseminated intravascular coagulation and the other from arterial bleeding at the remaining coronary ligament of the liver (Clavien–Dindo grade IIIb).

Additionally, three cases of sepsis and one case of severe aspiration (on postoperative day 7) were successfully managed. One patient experienced seizures due to elevated tacrolimus levels, which resolved with dose reduction and administration of valproic acid. Another patient developed central pontine myelinolysis, presenting with neurological deficits, reduced consciousness, and aphasia. This occurred in the context of rapid plasma sodium correction (an increase of 11 μmol/L within 24 hours) on the first postoperative day, with clinical symptoms appearing on day 8. Diagnosis was confirmed by brain MRI. The patient was discharged in improved condition on postoperative day 30 and remains under neurological follow-up.

Among the late complications, one episode of chronic rejection was recorded, as well as one case of *de novo* HBV, which was managed conservatively. Three patients developed liver abscesses, all of which were successfully treated with percutaneous drainage. One patient was urgently admitted to the intensive care unit 35 days post-transplant with acute cholangitis. Management included temporary cessation of immunosuppressive therapy and initiation of broad-spectrum antibiotics. The patient was discharged after 10 days and continues to be followed on an outpatient basis.

Mortality. A total of eight patients died during the follow-up period. In-hospital mortality was 12.5%. The causes of death included sepsis (2 patients), acute rejection (2 patients), and liver failure secondary to PVT (1 patient). Among the long-term deaths, the causes were COVID-19-associated pneumonia, aspiration, and chronic rejection in a non-compliant patient. Overall patient survival is illustrated in Fig. 3.

Donor results

Among the donors, 13 were female and 27 were male. The mean BMI was 23.2 kg/m^2. Based on perioperative data, the median operative time for donors was 342.5 minutes (range: 230–440 minutes), and the median intraoperative blood loss was 250 mL (range: 50–850 mL) (Table 4).

Donor complications are summarized in Table 4. Wound seroma occurred in two donors. One donor developed renal failure during antibacterial prophylaxis with sulperazone, presenting with oliguria, proteinuria, hematuria, edema, and pleural effusion. The condition resolved after sulperazone was discontinued and diuretic therapy was initiated. Two donors experienced wound infections that required prolonged local wound care and antibiotic therapy. Hospital-acquired pneumonia (Clavien–Dindo grade II) was diagnosed in one donor. Pleural effusion developed in two donors, both of whom underwent drainage procedures. Bilomas requiring per-

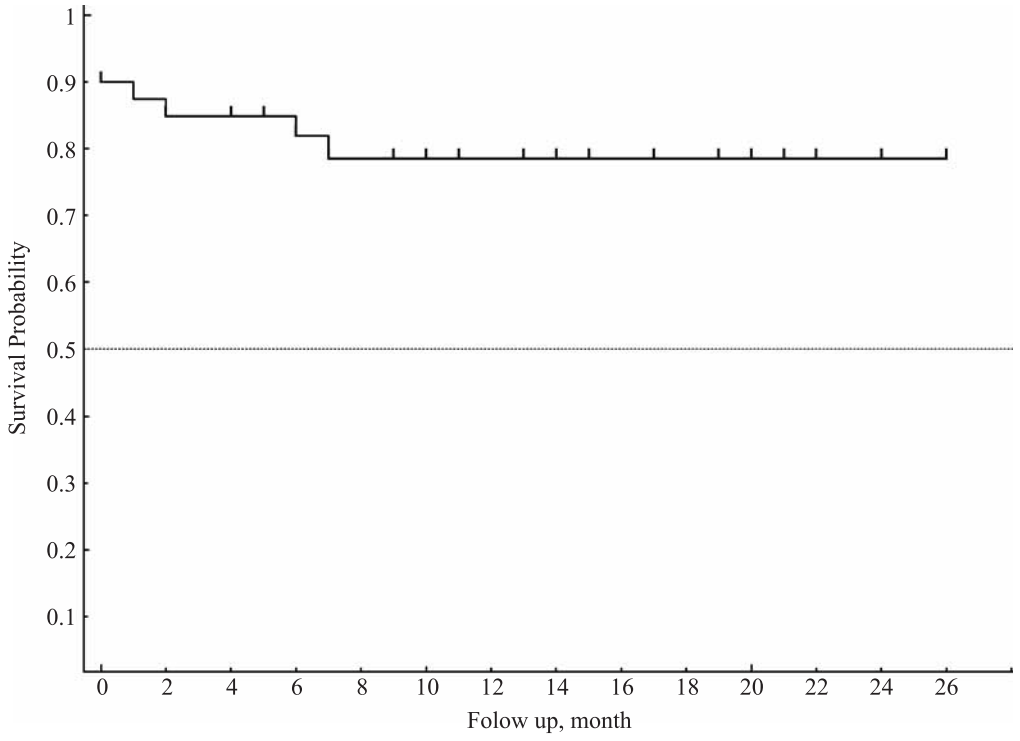

Fig. 3. Survival of right lobe liver recipients

Table 4

Donor characteristics and clinical outcomes

Data	Values (n = 40)
Age, years	40 (18–56)
Sex, n (%)	
Male	27 (67.5%)
Female	13 (32.5%)
BMI	23.2 (18–28.3)
Surgery time	342.5 (230–440)
Blood loss	250 (50–850)
Blood loss (Clavien–Dindo)	
Stage 1	
Seroma	1
Stage 2	
Kidney failure	1
Pneumonia	1
Wound infection	2
Hemorrhagic wound discharge	2
Stage 3a	
Right-sided pleurisy	2
Biliary leak (biloma).	2
Stage 3b	
Inferior vena cava hemorrhage	1
Biliary leak	2
Median CCI (for donors with complications)	33.7
Hospitalization period, days	10 (7–28)

Note: BMI, body mass index; CCI, comprehensive complication index.

cutaneous drainage were observed in two patients, while another two patients with biliary effusion underwent open surgical revision. One donor experienced hemorrhage due to dislodgement of a clip from the inferior vena cava, necessitating emergency surgical intervention. The median postoperative hospital stay was 10 days (range: 7–28 days). No late complications were observed among donors.

DISCUSSION

LDLT has emerged as a life-saving option for adult patients with end-stage liver disease in settings where deceased donor LT is not available [19]. Despite its generally favorable outcomes, LDLT in adult recipients presents significant challenges and risks. Donors are required to undergo major hepatic surgery, which carries the potential for serious complications and necessitates a prolonged recovery period. Ethical concerns are also inherent in the procedure, as the decision to donate a portion of one's liver involves balancing altruistic motivations with the potential impact on the donor's health [20]. In the Republic of Uzbekistan, the absence of a legal framework for DDLT means that LDLT remains the sole viable treatment option for patients in critical need of LT.

Furthermore, LDLT is associated with a higher incidence of post-transplant surgical complications compared to DDLT, with reported in-hospital mortality rates ranging from 3.6% to 18.9% [21–23]. In our study, the complications most frequently associated with mortality included infection, acute graft rejection, and liver graft dysfunction due to PVT. Among the two acute graft rejection cases, both patients exhibited persistent elevation of liver enzymes – alanine aminotransferase and aspartate aminotransferase – alongside rising bilirubin levels, in the absence of clinical or imaging evidence of obstructive jaundice. Infectious causes, including acute cytomegalovirus infection, as well as vascular complications, were ruled out. The primary indications for transplantation in these two patients were autoimmune hepatitis and HBV. Despite the initiation of intensive therapy, including pulse methylprednisolone therapy and extracorporeal detoxification, liver function failed to recover.

Vascular complications in our series were observed at a slightly higher frequency than reported in the literature [11]. We attribute this discrepancy to the learning curve associated with the first 15–20 LDLT procedures performed [24, 25]. Among the patients with arterial complications, three died during the follow-up period. However, the causes of death in these cases were unrelated to the arterial complications themselves. One patient with arterial stenosis succumbed to severe COVID-19-induced pneumonia two months post-transplant. A second patient with SASS died from aspiration at home one month after discharge. The third patient, also with SASS, passed away two months following transplantation due to ovarian apoplexy complicated by sepsis, a diagnosis that had been missed by the local healthcare providers.

Biliary complications continue to be a significant challenge in LT and are more prevalent in LDLT recipients. The incidence of these complications varies across transplant centers, but it can reach as high as 30%, with an associated mortality rate of 10%, making them a serious concern for post-transplant patients [26]. Most biliary complications, primarily biliary leakage, occurred in recipients with complex donor bile duct anatomy and those who had arterial complications.

In-hospital mortality in our study was 12.5%, which is comparable to the data reported in the literature [19, 21]. Survival at 26 months of follow-up was 80%.

Regarding LDLT donors, the reported complication rate in the literature is around 25%, with some studies indicating rates as high as 40% [27, 28]. Mild complications are reported in 17% of cases, while major complications account for approximately 5.5%. In our cohort, donor outcomes aligned with these figures.

CONCLUSION

Our experience with LDLT and the analysis of post-transplant complications are consistent with world literature and align with acceptable standards for the implementation stage of an LT program. Transplantation is feasible at our center, but there is a need to enhance both surgical and conservative therapeutic approaches to minimize the incidence of early and long-term post-operative complications.

The authors declare no conflict of interest.

REFERENCES

1. *Starzl TE, Marchioro Tl, Vonkaulla KN, Hermann G, Brittain RS, Waddell WR.* Homotransplantation of the liver in humans. *Surg Gynecol Obstet*. 1963; 117: 659–676.
2. *Nadalin S, Bockhorn M, Malagó M, Valentin-Gamazo C, Frilling A, Broelsch CE.* Living donor liver transplantation. *HPB (Oxford)*. 2006; 8 (1): 10–21. https://doi.org/10.1080/13651820500465626.
3. *Huang DQ, Terrault NA, Tacke F, Gluud LL, Arrese M, Bugianesi E et al.* Global epidemiology of cirrhosis – aetiology, trends and predictions. *Nat Rev Gastroenterol Hepatol*. 2023; 20 (6): 388–398. https://doi.org/10.1038/s41575-023-00759-2.
4. *Dunn R, Musabaev E, Razavi H, Sadirova S, Bakieva S, Razavi-Shearer K et al.* Progress Toward Hepatitis B and Hepatitis C Elimination Using a Catalytic Funding Model – Tashkent, Uzbekistan, December 6, 2019 – March 15, 2020. *MMWR Morb Mortal Wkly Rep*. 2020; 69 (34): 1161–1165. https://doi.org/10.15585/mmwr.mm6934a3.
5. *Akbarov M, Ismailov S, Nazirov F, Ibadov R, Bahritdinov F, Dzhanbekov T et al.* Transplantology: a requirement of the time or the next evolutionary step of high-tech surgery? *JESM*. 2023; 1: 15–23. https://journals.tma.uz/index.php/jesm/article/view/285.
6. *Katsanos G, Karakasi KE, Antoniadis N, Vasileiadou S, Kofinas A, Morsi-Yeroyannis A et al.* Enhanced recovery after surgery in liver transplantation: Challenges and feasibility. *World J Transplant*. 2022; 12 (7): 195–203. https://doi.org/10.5500/wjt.v12.i7.195.
7. *Semash K, Janbekov T, Akbarov M, Usmonov A, Gaibullaev T.* Stages of preparation and examination of related liver donors and their perioperative management. *Coloproc*. 2023; 15 (1): 41–54. https://doi.org/10.56121/2181-4260-2023-1-41-54.
8. *Radulova-Mauersberger O, Weitz J, Riediger C.* Vascular surgery in liver resection. *Langenbecks Arch Surg*. 2021; 406 (7): 2217–2248. https://doi.org/10.1007/s00423-021-02310-w.
9. *Joliat GR, Kobayashi K, Hasegawa K, Thomson JE, Padbury R, Scott M et al.* Guidelines for Perioperative Care for Liver Surgery: Enhanced Recovery After Surgery (ERAS) Society Recommendations 2022. *World J Surg*. 2023; 47 (1): 11–34. https://doi.org/10.1007/s00268-022-06732-5.
10. *Wong TC, Fung JYY, Cui TYS, Sin SL, Ma KW, She BWH et al.* The Risk of Going Small: Lowering GRWR and Overcoming Small-For-Size Syndrome in Adult Living Donor Liver Transplantation. *Ann Surg*. 2021; 274 (6): e1260–e1268. https://doi.org/10.1097/sla.0000000000003824.
11. *Semash KO, Dzhanbekov TA, Akbarov MM.* Vascular complications after liver transplantation: contemporary approaches to detection and treatment. A literature review. *Russian Journal of Transplantology and Artificial Organs*. 2023; 25 (4): 46–72. https://doi.org/10.15825/1995-1191-2023-4-46-72.
12. *Monakhov AR, Dzhanbekov TA, Mescheryakov SV, Semash KO, Khizroev KM, Voskanov MA.* Frame drainage of the bile ducts in biliary reconstruction during transplantation of the left lateral sector of the liver (In Russ.). *Russian Journal of Transplantology and Artificial Organs*. 2020; 20 (S): 74.
13. *Raschke RA, Reilly BM, Guidry JR, Fontana JR, Srinivas S.* Theweight-based heparin dosing nomogram compared with a "standard care" nomogram: A randomized controlled trial. *Ann Intern Med*. 1993; 119 (9): 874–881. https://doi.org/10.7326/0003-4819-119-9-199311010-00002.
14. *Gautier SV, Voskanov MA, Monakhov AR, Semash KO.* The role of endovascular and endobiliary methods in the treatment of post-liver transplant complications. *Russian Journal of Transplantology and Artificial Organs*. 2020; 22 (4): 140–148. (In Russ.). https://doi.org/10.15825/1995-1191-2020-4-140-148.
15. *Clavien PA, Barkun J, de Oliveira ML, Vauthey JN, Dindo D, Schulick RD et al.* The Clavien–Dindo classification of surgical complications: five-year experience. *Ann Surg*. 2009; 250 (2): 187–196. https://doi.org/10.1097/SLA.0b013e3181b13ca2.
16. *Monakhov A, Mironkov B, Tsiroulnikova O, Voskanov M, Dzhanbekov T, Semash K et al.* Interventional Radiology in Complication Management after Pediatric Liver Transplantation. *Transplantation*. 2018; 102 (S7): S150. https://doi.org/10.1097/01.tp.0000542777.01469.
17. *Lai Q, Melandro F, Nowak G, Nicolini D, Iesari S, Fasolo E et al.* The role of the comprehensive complication index for the prediction of survival after liver transplantation. *Updates Surg*. 2021; 73 (1): 209–221. https://doi.org/10.1007/s13304-020-00878-4.
18. *Semash K, Djanbekov T, Akbarov M, Usmonov A, Shermatov M, Gaybullaev T.* Interventional correction of extrahepatic portal hypertension in patient after liver transplant. The first case report in Uzbekistan. *CAJM*. 2023; 1: 87–96. https://journals.tma.uz/index.php/cajm/article/view/556.
19. *Emiroglu R, Sevmis S, Moray G, Savas N, Haberal M.* Living-donor liver transplantation: results of a single center. *Transplant Proc*. 2007; 39 (4): 1149–1152. https://doi.org/10.1016/j.transproceed.2007.02.052.

20. *Nizamuddin I, Gordon EJ, Levitsky J.* Ethical Issues When Considering Liver Donor Versus Deceased Donor Liver Transplantation. *Clin Liver Dis (Hoboken)*. 2021; 17 (2): 71–74. https://doi.org/10.1002/cld.982.
21. *Yoo S, Jang EJ, Yi NJ, Kim GH, Kim DH, Lee H et al.* Effect of Institutional Case Volume on In-hospital Mortality After Living Donor Liver Transplantation: Analysis of 7073 Cases Between 2007 and 2016 in Korea. *Transplantation*. 2019; 103 (5): 952–958. https://doi.org/10.1097/TP.0000000000002394.
22. *Kim YJ, Yoon JH, Kim SI, Choi HJ, Choi JY, Yoon SK et al.* Impact of Pretransplant Infections on Clinical Course in Liver Transplant Recipients. *Transplant Proc*. 2018; 50 (4): 1153–1156. https://doi.org/10.1016/j.transproceed.2018.01.036.
23. *Kaido T, Egawa H, Tsuji H, Ashihara E, Maekawa T, Uemoto S.* In-hospital mortality in adult recipients of living donor liver transplantation: experience of 576 consecutive cases at a single center. *Liver Transpl*. 2009; 15 (11): 1420–1425. https://doi.org/10.1002/lt.21873.
24. *Miller CM, Quintini C, Dhawan A, Durand F, Heimbach JK, Kim-Schluger HL et al.* The International Liver Transplantation Society Living Donor Liver Transplant Recipient Guideline. *Transplantation*. 2017; 101 (5): 938–944. https://doi.org/10.1097/TP.0000000000001571.
25. *Manas D, Burnapp L, Andrews PA.* Summary of the British Transplantation Society UK Guidelines for Living Donor Liver Transplantation. *Transplantation*. 2016; 100 (6): 1184–1190. https://doi.org/10.1097/TP.0000000000001128.
26. *Daniel K, Said A.* Early Biliary complications after liver transplantation. *Clin Liver Dis (Hoboken)*. 2017 Sep 29; 10 (3): 63–67. https://doi.org/10.1002/cld.654.
27. *Xiao J, Zeng RW, Lim WH, Tan DJH, Yong JN, Fu CE et al.* The incidence of adverse outcome in donors after living donor liver transplantation: A meta-analysis of 60,829 donors. *Liver Transpl*. 2024 May 1; 30 (5): 493–504. https://doi.org/10.1097/LVT.0000000000000303.
28. *Kim PT, Testa G.* Living donor liver transplantation in the USA. *Hepatobiliary Surg Nutr*. 2016; 5 (2): 133–140. https://doi.org/10.3978/j.issn.2304-3881.2015.06.01.

The article was submitted to the journal on 30.04.2024

DOI: 10.15825/1995-1191-2024-4-46-60

PERIOPERATIVE PROPHYLAXIS OF RENAL ISCHEMIA-REPERFUSION INJURY

S.V. Popov, R.G. Guseinov, K.V. Sivak, V.V. Perepelitsa, A. Beshtoev, T.A. Lelyavina
Almazov National Medical Research Centre, St. Petersburg, Russian Federation

This paper reviews the strategies for correcting ischemia-reperfusion injury (IRI) in kidneys during surgeries and transplantation, discussed and proposed in the current literature. The pathophysiological mechanisms of IRI and a wide range of proposed methods for reducing the severity of injury are considered. The use of such techniques as the combination of ischemic, pharmacological pre- and postconditioning is still being studied. It was observed that researchers were very interested in immunological and biological (stem cell) therapeutic strategies as a potential avenue to lessen the severity of IRI.

Keywords: renal ischemia-reperfusion injury, renal IRI, antioxidants, IRI therapeutic strategies.

Ischemia-reperfusion injury (IRI) is currently a critical issue widely discussed across various fields of medicine, particularly in the context of organ transplantation and surgical or vascular interventions. Therapeutic approaches to correcting IRI vary depending on the organ affected.

This paper specifically focuses on renal IRI, which occurs during kidney surgery and transplantation, and explores potential methods to mitigate kidney injury resulting from IRI during these procedures.

The aim of this paper is to review the proposed and emerging strategies for alleviating the severity of IRI in kidney surgery and kidney transplantation (KT), as discussed in current literature.

Before delving into the methods of correction, their efficacy, and the stages at which they are applied, it is essential to first examine the mechanism of IRI in light of current research.

Mechanism of development. IRI is a form of tissue injury that occurs when blood supply is interrupted or depleted (due to blood loss or ischemia), followed by reperfusion. This process triggers the release of a variety of mediators, leading to cellular injury and, eventually, organ dysfunction. Notably, the injury caused during reperfusion is often more severe than during ischemia itself. During ischemia, tissues are deprived of metabolic reserves and oxygen, which leads to the accumulation of metabolic waste products. The absence of oxygen results in the depletion of energy reserves, such as adenosine triphosphate (ATP) and glycogen. Energy-dependent sodium-potassium (Na^+-K^+) exchangers, which help maintain an electrolyte gradient across the cell membrane, become dysfunctional due to energy depletion. As a result, the ion gradient across the cell membrane is disrupted. Sodium ions move into the cells from the extracellular space, while potassium ions shift out of the cells into the extracellular space. In response to the lack of oxygen, metabolic processes switch from aerobic to anaerobic pathways, leading to the accumulation of lactate and intracellular acidosis. This creates a vicious cycle that progressively reduces the efficiency of cellular energy production [1, 2].

Decreased intracellular pH further inhibits glycolysis, while increased intracellular sodium concentration can lead to a secondary rise in intracellular calcium levels. Calcium is also released from the mitochondria through the mitochondrial Na^+-H^+/Ca^{2+} exchanger. The activity of the sarcoplasmic reticulum Ca^{2+} pump, which helps in calcium reuptake, is suppressed, exacerbating the increase in intracellular calcium. As calcium ions accumulate inside the cell, they bind to and activate the regulatory protein calmodulin. This, in turn, activates calcium-calmodulin-dependent protein kinases, phospholipase A2, and proteases, leading to vesicle degranulation. This process releases proinflammatory chemokines and cytokines, such as interleukin-8, von Willebrand factor, and P-selectin, etc. [3].

Intracellular acidosis disrupts the hydrogen ion gradient across the mitochondrial membrane, halting ATP production. This, coupled with the increased levels of reactive oxygen species (ROS) in the mitochondria, exacerbates cellular damage. Increased intracellular calcium and elevated inorganic phosphate levels, resulting from accelerated ATP degradation [4], further influence the state of mitochondrial permeability transition pores (mPTPs). However, during the ischemic phase, low intracellular pH inhibits the opening of these mPTPs [3].

Dephosphorylation of AMP-activated protein kinase exacerbates IRI-induced acute kidney injury (AKI) by

Corresponding author: Tatiana Lelyavina. Address: 2, Akkuratova str., St. Petersburg, 197341, Russian Federation.
Phone: (981) 908-90-18. E-mail: tatianalelyavina@mail.ru

promoting mitochondrial dysfunction [5], accompanied by impaired mitochondrial iron homeostasis [6].

These processes are now collectively referred to as the ischemic sterile tissue injury theory, which suggests that ischemia leads to the release of endogenous molecules known as damage-associated molecular patterns (DAMPs), such as ATP, calcium, uric acid, and DNA. The cells of the innate immune system recognize these molecular signals, triggering a cascade of events. This includes the release of cytokines that promote chemotaxis, the labeling of damaged cells for clearance (opsonization), and direct cell killing. Such disorders activate the complement system, which, in turn, triggers chemotaxis and facilitates cell death through the formation of the terminal complement complex (C5b-9) [7].

IRI triggers a series of local and systemic pathophysiological mechanisms that ultimately result in cell death through necrosis, apoptosis, and autophagy. Necrosis is an uncontrolled process associated with inflammation [8], whereas apoptosis is a regulated, programmed form of cell death that occurs without inflammation. Apoptosis, as a programmed cell death process, is driven by intracellular changes following reperfusion. These changes include increased ATP production and calcium binding in mitochondria via Na^{+}-Ca^{2+} exchangers when intracellular pH returns to normal. ROS, generated during ischemia and reperfusion, play a critical role in the opening of mPTPs. During the ischemic phase, mPTPs remain closed due to low intracellular pH. However, when acidosis is corrected during reperfusion, mPTP opening occurs, leading to cell death by mitoptosis [9, 10]. The opening of mPTPs increases mitochondrial outer membrane permeability and facilitates the release of pro-apoptotic proteins like cytochrome c. Evidence suggests that BNIP3-mediated mitophagy plays a vital role in mitochondrial quality control and cell survival during IRI [11]. The loss of cytochrome c from the mitochondrial membrane triggers a cycle of reduced aerobic respiration, increased ROS production, and consequently, amplified apoptotic activity.

Mitochondria contain several antioxidants, such as Mn-superoxide dismutase (Mn-SOD), glutathione, glutathione peroxidase, thioredoxin-2, and glutaredoxin, which neutralize ROS and aid in cellular repair. However, these antioxidant systems become significantly overexpressed during ischemia and reperfusion. Additionally, mitochondrial ROS production stimulates the secretion of extracellular vesicles by epithelial cells, containing RNA, lipids, and proteins, suggesting their involvement in the pathogenesis of the process [12]. Spatial transcriptome sequencing has revealed mechanisms that drive tissue infiltration by immune cells [13].

At the same time, ischemic injury to endothelial cells reduces the production of nitric oxide (NO), endothelium-dependent hyperpolarizing factor, and prostacyclin, thereby increasing the risk of microthrombosis. The oxygen free radicals generated during reperfusion can further damage the vascular endothelium. For instance, superoxide radicals react directly with NO, which results in the loss of NO's physiological activity and the formation of peroxynitrite, a highly cytotoxic free radical [14].

We report the identification of 8-oxoguanine DNA glycosylase (OGG1) as a key mediator of hypoxia- and reoxygenation-induced apoptosis *in vitro*, as well as renal tissue injury in a renal ischemia-reperfusion injury (IRI) model. OGG1 is recognized for its role in the excision repair of damaged nuclear and mitochondrial DNA during IRI. These findings suggest that OGG1 may represent a novel clinical target with therapeutic potential [15, 16].

The N6-methyladenosine (m6A) mRNA methylase METTL14 has been shown to exacerbate renal IRI by suppressing Yes-associated protein 1 (YAP1). The discovery of the METTL14–YAP1 pathway offers a new perspective on the molecular mechanisms underlying IRI and paves the way for the development of innovative therapeutic strategies and molecular targets [17].

In addition to the mechanisms already discussed in the pathogenesis of IRI, recent studies have reported the expression of transient receptor potential melastatin 7 (TRPM7) in renal IRI, a finding previously documented only in IRI of other organs [18]. This novel evidence expands the potential role of TRPM7 in mediating renal injury during ischemia-reperfusion. Furthermore, various signaling pathways influencing gene regulation, including those involving microRNAs (miRNAs), have been explored. Several miRNAs have been identified as either upregulated or downregulated during IRI, suggesting their potential utility as biomarkers for early detection of IRI or as future therapeutic targets in clinical practice [19].

The involvement of AMP-activated protein kinase (AMPK) in renal IRI has been demonstrated, with several potential mechanisms proposed for its protective effects [20]. The renin-angiotensin system has also been implicated in the development and progression of IRI [21].

The measures employed to manage IRI in KT differ significantly from those used in non-transplant kidney surgeries. In transplantation, the first substantial injury to the allograft often occurs while the organ is still in the donor. Notably, the development of ROS-mediated oxidative stress following brain death (BD) is well-documented in both experimental models and clinical observations involving deceased donors. BD is believed to contribute to the maturation of immunostimulatory dendritic cells, which act as potential sources of DAMPs. These DAMPs activate the innate immune system of the deceased donor, particularly following severe trauma, leading to acute systemic autoimmune syndrome.

DAMPs released from injured graft cells further stimulate the recipient's innate immune response, triggering the secretion of pro-inflammatory cytokines such as tumor necrosis factor (TNF), type I interferons, interleukin (IL)-1, IL-6, and various chemokines. Neutrophils play a pivotal role in mediating microvascular occlusion and local tissue destruction during IRI [7].

Consequently, regulated forms of cell death such as necroptosis, pyroptosis, and ferroptosis have been reported in numerous models of post-ischemic reperfusion injury, including those within transplantation contexts. Among these, necroptosis and ferroptosis have garnered particular attention in the field of organ transplantation due to their emerging relevance in mediating graft injury [2, 22, 23]. Recent findings suggest that ferroptosis may represent an first stage of IRI, preceding the subsequent development of inflammatory responses and necrotic cell death [24].

Following donor organ transplantation, reperfusion-induced oxidative stress results in the release of DAMPs, which in turn reignite the innate immune response, creating a booster effect. Mitoglitazone has demonstrated a protective effect against renal IRI by inhibiting ferroptosis through its action on mitoNEET-regulated ferroptosis, also considered as a promising target for therapeutic intervention [25].

A variety of donor resuscitation and graft perfusion strategies have been explored to mitigate the effects of IRI in transplantation. In humans, prevention of IRI remains a major area of investigation, focusing on donor conditioning, modification of preservation solutions, graft reperfusion techniques, and optimization of recipient-targeted interventions [26]. One promising area of research includes the use of pharmacological additives, such as hydrogen sulfide (H_2S), in renal preservation solutions, as well as the modulation of preservation temperatures to improve graft viability and enhance recipient survival rates [27].

To prevent the excessive accumulation of oxygen-derived free radicals during organ storage and reperfusion, several pharmacological strategies have been proposed. These include the incorporation of xanthine oxidase inhibitors like allopurinol into preservation solutions, along with antioxidant agents such as reduced glutathione, mannitol, superoxide dismutase, desferrioxamine, and 21-aminosteroids [28]. Preconditioning of kidney grafts with H_2S is thought to mitigate IRI.

As previously discussed, intracellular calcium (Ca^{2+}) overload is a critical factor in the pathogenesis of IRI. Several strategies have been proposed to mitigate Ca^{2+} accumulation during reperfusion, including reducing extracellular Ca^{2+} levels in preservation solutions, supplementation with magnesium (Mg^{2+}) – which competes with Ca^{2+} for binding sites on exchangers and pumps – and pharmacological inhibition of Ca^{2+} influx. The latter involves the use of Ca^{2+} channel blockers and Na^+/H^+ exchanger inhibitors. However, some experimental studies have reported limited efficacy of verapamil in reducing renal IRI [29].

GM-CSF-induced MCP-1/CCR2 signaling has been implicated in sustaining cross-reactivity between injured tubular epithelial cells, infiltrating immune cells, and myofibroblasts, which promotes chronic inflammation and progressive interstitial fibrosis in the later stages of IRI [30].

The eIF5A hypusination inhibitor GC7 (N1-guanyl-1,7-diaminoheptane) has been shown to protect against ischemic injury. GC7 treatment has been shown to attenuate BD-induced renal injury, preserve mitochondrial homeostasis, and enhance antioxidant defenses, thereby improving post-transplant outcomes [31, 32].

The addition of sigma-1 receptor (S1R) agonists to preservation solutions improves graft function and minimizes structural damage, ultimately leading to enhanced long-term transplant outcomes. By reducing ischemic injury during cold storage, S1R agonists can potentially increase the pool of viable donor organs available for transplantation [33]. Quantitative assessment of ischemic tubular lesions in donor kidney biopsies – in kidneys retrieved after cardiac death – serves as a valuable predictive tool for post-transplant kidney function and is considered a reliable metric for evaluating graft quality [34].

These findings underscore the critical importance of a comprehensive understanding of IRI pathophysiology and the development of effective strategies for mitigating or reversing its effects in clinical practice. However, it is important to acknowledge that, while significant advances have been made in elucidating the mechanisms underlying IRI, the therapeutic approaches for its correction remain relatively underdeveloped [35].

Currently, IRImitigation strategies are broadly categorized into pharmacological and non-pharmacological approaches. The non-pharmacological methods include ischemic preconditioning (IPC) and ischemic postconditioning (IPostC).

IPC involves subjecting the target organ to brief, controlled periods of ischemia followed by reperfusion prior to a more prolonged ischemic stroke. This technique has been shown in both clinical and experimental studies to effectively reduce tissue damage, particularly in organs such as the liver [36]. While the exact protective mechanisms of IPC are still not fully understood, it is thought to slow ATP depletion, enhance autophagy, and preserve mitochondrial function during ischemic stress. In addition, IPC enhances autophagy and reduces cellular damage and mitochondrial dysfunction during injury. The so-called preischemic renal artery washout, proposed in experimental rat models, suggests that flushing

the renal artery before ischemia may reduce the burden of circulating leukocytes [37].

IPostC, on the other hand, entails a series of brief, intermittent reperfusion periods, each separated by short occlusion phases, followed by continuous reperfusion. Its beneficial effects have been demonstrated in experimental models [38] and further validated in clinical trials, particularly in cardiac patients [39]. The pathophysiological rationale for IPostC was described as early as 1989 by Russian researcher Marianna Bilenko, who found that perfusion of kidneys with blood twice depleted of oxygen and enriched with antioxidants can significantly reduce the severity of reperfusion injury [40]. Unlike donor preconditioning, which is not always feasible, graft postconditioning offers a more practical and adaptable intervention. It can be tailored to the specific risk factors associated with the donor organ and is particularly valuable in complex cases involving prolonged ischemia [41]. IPostC can also be included in complex non-transplant cases requiring prolonged periods of ischemia.

Non-pharmacological strategies also encompass the use of specially designed electric fields, which have demonstrated efficacy in delaying ATP depletion during ischemia and preserving Na^+/K^+-ATPase activity. This technique has been shown to reduce renal injury by approximately 45%, as evidenced by plasma creatinine levels of 1.17 ± 0.04 mg/dL in treated groups versus 1.97 ± 0.06 mg/dL in controls. Allograft function improved by over 50% compared to untreated counterparts [42].

Promising results have also been reported with pharmacological preconditioning and postconditioning using metformin, particularly in *ex vivo* models of normothermic machine perfusion involving rat and pig kidneys. These studies indicate that metformin exhibits renoprotective properties, potentially reducing the extent of IRI when administered prior to transplantation [43].

Contemporary pharmacological strategies to mitigate IRI are remarkably diverse. While early approaches predominantly relied on antihypoxants, the current landscape has expanded to include immunological, enzymatic, and biological interventions. However, much of the supporting evidence remains experimental or indirect, particularly concerning the effectiveness of pharmacological organ protection during procurement, preservation, and the early postoperative phase [35].

A number of medications have the ability to limit or completely inhibit ROS formation. These include urea, ceruloplasmin, nicotinic acid, mannitol, trimetazidine dihydrochloride (Trimetazidine), sodium polyhydroxyphenylene thiosulfonate (Hypoxene), and melatonin.

There is also a class of drugs known as scavengers – also referred to as free radical traps or interceptors. Their antioxidant mechanism involves neutralizing lipid radicals, lipoperoxide radicals, and lipid hydroperoxides, thereby interrupting the lipid peroxidation (LP) chain reaction. Examples include tocopherols, oxypyridine derivatives such as ethylmethylhydroxypyridine succinate (Mexidol) and methyl ethylpyridinol (Emoxipin), ionol, flavonoids, glutathione, acetylcysteine, methionine, as well as derivatives of succinic, fumaric, and other organic acids, ubiquinones, selenites, retinols, and carotenoids.

Recombinant preparations used by Russian authors that either inactivate ROS directly or the enhance endogenous biosynthesis of LP inhibitors have also been developed [44].

Vitamins have been used for decades as a means to reduce IRI, and research into their mechanisms and therapeutic potential continues to generate interest. These vitamins are generally classified into two types: water-soluble (hydrophilic), such as ascorbic acid (vitamin C), and fat-soluble (hydrophobic), such as beta-carotene and alpha-tocopherol (vitamin E). Hydrophilic antioxidants primarily interact with oxidants in blood plasma and the cytosol of cells, while hydrophobic antioxidants function predominantly to protect cellular membranes from lipid peroxidation [45]. Curcumin, which has pronounced antioxidant and anti-inflammatory properties, has been shown to have a positive effect [46].

Melatonin, a potent antioxidant synthesized by the pineal gland, also plays a significant role in combating oxidative stress and inflammation [47]. It not only scavenges reactive oxygen species and reactive nitrogen species (RNS) but also enhances the activity of key antioxidant enzymes such as superoxide dismutase (SOD), glutathione peroxidase (GPx), and glutathione reductase (GR), contributing to membrane stabilization [36]. Due to its endogenous origin and low toxicity profile, melatonin is typically well tolerated [48, 49]. Emerging evidence supports its therapeutic potential, including studies that highlight the efficacy of melatonin alone [49], as well as in combination with mesenchymal stem cells and their exosomes, in reducing renal IRI in experimental rat models [48].

The prognosis of IRI can be improved by targeting the expression of endogenous cytokines. One such pharmacological agent is sevoflurane, a third-generation halogenated inhalational anesthetic known for its influence on the duration of neuromuscular blockade induced by non-depolarizing muscle relaxants. In experimental studies, pre-treatment with sevoflurane significantly reduced concentrations of TNF-alpha, IL-8 and IL-6 [50]. Sevoflurane has been reported to protect rat kidneys from IRI by reducing the expression of transient receptor potential melastatin 7 (TRPM7) [15].

Anesthetics help limit the elevation of extracellular glutamate levels and inhibit the overactivation of excitatory glutamatergic receptors, both of which are associated with increased oxidative stress in ischemic

tissues. In particular, ketamine has been reported to exert beneficial effects in rat models [51].

The use of medical gases in oxidative stress therapy represents an emerging therapeutic approach. These gases can be administered directly to patients via inhalation using a nasal cannula, face mask, or ventilator. IRI has been treated with several therapeutic gases, including hydrogen (H_2), hydrogen sulfide (H_2S), nitric oxide (NO), and carbon monoxide (CO). The therapeutic effects of H_2S have been demonstrated in rodent models of IRI, and it has been shown that H_2S can induce reversible hypothermia and an anabiosis-like state. The antioxidant effects of H_2S may be attributed to its interaction with cytochrome c oxidase and its influence on mitochondrial function. H_2S may modulate gene expression through pathways involving nuclear factor-kappa B (NF-κB) and extracellular signal-regulated kinase (ERK) [52].

In a rat model, evodiamine administration significantly reduced renal injury resulting from IRI, owing to its potent antioxidant, anti-inflammatory, and anti-apoptotic properties [53].

Alkaline phosphatase (ALP) has also emerged as a potential therapeutic agent for attenuating IRI. A double-blind, randomized, placebo-controlled, single-center pilot study investigated the safety and feasibility of peri-procedural ALP administration in living donor KT. Participants in the treatment group received 1000 IU of bRESCAP (bovine RESCue Alkaline Phosphatase, test substance name: bovine intestinal alkaline phosphatase, bIAP; EC 3.1.3.1). The study concluded that bRESCAP administration was safe, feasible, and may help reduce IRI-induced renal inflammation. Notably, this was the first trial to assess the use of bRESCAP in the context of KT, and further studies are currently planned to explore its therapeutic potential [55].

Inhibition of pyruvate dehydrogenase kinase-4 (PDK4) has been demonstrated to improve kidney IRI outcomes by reducing succinate accumulation during ischemia and preserving mitochondrial function during reperfusion [56]. Downregulation of G protein-coupled receptor kinase 4 (GRK4) has been shown to exert a protective effect against kidney IRI [57].

The NFAT inhibitor 11R-VIVIT has been shown to reduce renal fibrosis in mice after IRI. As a peptide inhibitor of nuclear factor of activated T-cells (NFAT), 11R-VIVIT was found to exert a renoprotective effect during a transition to chronic kidney disease after IRI. The study's findings support the hypothesis that NFAT2 inhibition may represent a promising new therapeutic strategy to prevent post-IRI kidney fibrosis [58].

In another mouse study, researchers identified a fucosylated ligand associated with ischemic injury that plays a role in initiating complement activation and AKI. The findings suggest that administration of supraphysiological levels of L-fucose in the renal cortex may exert therapeutic effects, likely through altering the cell-binding properties of collectin-11 (CL-11). These preliminary results warrant further investigation [59].

Propofol has been reported to confer a protective effect against IRI, although its precise mechanism of action remains unclear [60].

The polyoxylate-based copolymer APP-103, which incorporates vanillyl alcohol (VA) into its hydrophobic polymer backbone, has demonstrated high sensitivity and specificity to hydrogen peroxide (H_2O_2). In experimental models, APP-103 was shown to be safe and effective in improving renal function after IRI and enhancing survival following KT [61].

Prostacyclin (PGI_2), a product of prostacyclin synthase (PGIS), has also been identified as a renoprotective agent in IRI-induced AKI cases. The PGIS/PGI_2 axis presents a promising therapeutic target in AKI [62]. Another promising compound is N-(p-Amylcinnamoyl) anthranilic acid, an inhibitor of phospholipase A_2 and a potential melastatin-2 receptor blocker, which has shown protective effects against renal IRI [63].

Semaglutide, a GLP-1 receptor agonist, was found to exert renoprotective effects through modulation of inflammatory and oxidative pathways, particularly via the PI3K/AKT signaling pathway [64].

Disulfiram has demonstrated efficacy in ameliorating IRI-induced AKI by inhibiting the caspase-11–GSDMD pathway. Interestingly, disulfiram selectively blocked this pathway without significantly affecting classical pyroptosis markers such as NLRP3 and ASC, suggesting its targeted action on caspase-11-mediated pyroptosis [65].

Inhibition of NADPH oxidase 1 (NOX1) has also shown protective effects in the context of kidney IRI [66].

Cholecalciferol (vitamin D_3), a clinically available compound, has been reported to protect kidney function in IRI by reducing ROS production, inhibiting NF-κB activation, and suppressing GSDMD-mediated pyroptosis [67].

Gold-platinum nanoparticles (AuPt NPs) – consisting of a gold core and a loosely branched platinum shell – have been proposed as a novel therapeutic strategy for renal IRI) [68]. Mitoglitazone improves kidney IRI by inhibiting ferroptosis [25, 69]. Modulation of NF-κB signaling via exosomal delivery is being explored as a potential therapeutic approach for AKI resulting from IRI [70].

There is also growing evidence suggesting sex hormones influence the susceptibility to renal IRI. Female sex hormones, particularly estradiol, appear to confer protective effects, while male hormones may exacerbate ischemia-induced renal injury [71]. Experimental studies in rats have shown that estradiol administration significantly reduces renal injury and improves outcomes following IRI [72, 73].

Multipotent adult progenitor cells (MAPC®) have potent immunomodulatory properties that may mitigate IRI [74]. This is the first reported series in which cell therapy was successfully delivered directly to human donor kidneys as an isolated *ex vivo* perfusion platform. Kidneys treated with MAPC cells exhibited improved clinically relevant outcomes, along with reduced tissue injury and lower levels of pro-inflammatory biomarkers. These effects may be mediated through alterations in circulating cytokines or secretion of soluble anti-inflammatory mediators. This approach could represent a paradigm shift in transplant medicine, offering a novel opportunity to treat donor organs directly prior to transplantation in order to minimize IRI [75].

Of particular interest is recent work exploring advanced technologies such as 3D renal organoids and kidney-on-a-chip platforms. The review provides information for creating models to study acute renal conditions associated with IRI [76, 77].

In addition, a study identified two distinct IRI clusters based on differentially expressed necroptosis-related genes (DE-NRGs). The researchers developed predictive models for delayed graft function (DGF) and graft survival, providing a framework for early prevention and personalized management of postoperative complications in KT recipients [78].

Russian researchers have also made significant strides in investigating potential solutions to IRI. In recent years, Netrebenkoet et al. have presented several studies examining the effects of various substances on the severity of kidney IRI. Notably, infliximab has shown experimental effectiveness in kidney IRI models, demonstrating a positive impact on IRI severity [79–81]. Similarly, a combination of a peptide mimicking the alpha helix of erythropoietin beta has been found to exert a beneficial effect in kidney IRI [81–83].

Carbamylated darbepoetin [84] and arginase II [85] have been demonstrated in experiments to be effective in preventing kidney IRI. Acyzol, based on zinc bisvinylimidazole diacetate, has been proposed for use as post-ischemic pharmacological conditioning. In preclinical studies, Acyzol showed positive effects when administered starting from the first day after surgery [86].

Goncharov et al. developed a genetically engineered construct encoding the PSH enzyme. In a mouse model, administration of a chimeric recombinant protein (PSH antioxidant enzyme) 15 minutes prior to ischemia was shown to reduce the severity of kidney IRI, offering a form of pharmacological ischemic preconditioning (IPC) [87, 88]. Additionally, Goncharov's team proposed the recombinant protein TAT-Prx2, a modified human peroxiredoxin 2, for intravenous administration to mitigate complications associated with kidney IRI. This protein was shown to enhance cellular resistance to IRI in experimental models [89]. Further research also demonstrated its efficacy in liver IRI [90].

Of significant scientific and practical interest are the works of Russian authors focused on understanding the mechanisms and developing preventive strategies for IRI in various organs. A substantial body of work by Konstantin Popov has provided in-depth and comprehensive analyses of the mechanisms underlying liver IRI and various treatment methods [91–100]. Other studies have also explored approaches to liver IRI treatment, contributing to a growing body of research in this area [101–105].

Several studies by Russian researchers have addressed the challenges posed by myocardial IRI [106–113]. While a detailed review of these studies is beyond the scope of the current discussion, their inclusion highlights the broad scientific interest in IRI-related research.

Furthermore, the development of the biobank model offers promising potential for large-scale studies, aiding in the prediction and prevention of IRI across various organ systems [114].

Based on the analysis of a broad spectrum of studies addressing the treatment of IRI, it is evident that there is currently an active, multidirectional, and pathophysiologically grounded effort to identify effective strategies for mitigating kidney injury associated with IRI. Continued development and refinement of approaches – such as combined ischemic preconditioning and postconditioning, alongside pharmacological and mechanical pre- and post-ischemic interventions – reflect this dynamic field of investigation.

Several of the pharmacological agents presented, including those with novel structures, mechanisms of action, and methods of synthesis, offer considerable promise and highlight important avenues for future research. The search for optimal solutions will persist until a standardized, situation-specific protocol for ischemic conditioning is established.

The authors declare no conflict of interest.

REFERENCES

1. *Naito H, Nojima T, Fujisaki N, Tsukahara K, Yamamoto H, Yamada T et al.* Therapeutic strategies for ischemia reperfusion injury inemergency medicine. Review Article. *Acute Med Surg*. 2020; 7 (1): e501.
2. *Granata S, Votrico V, Spadaccino F, Catalano V, Netti GS, Ranieri E et al.* Oxidative stress and ischemia/reperfusion injury in kidney transplantation: focus on ferroptosis, mitophagy and new antioxidants. *Antioxidants (Basel)*. 2022 Apr 12; 11 (4): 769.
3. *Nieuwenhuijs-Moeke GJ, Pischke SE, Berger SP, Sanders JSF, Pol RA, Struys MMRF et al.* Ischemia and reperfusion injury in kidney transplantation: relevant mechanisms in injury and repair. *J Clin Med*. 2020; 9 (1): 253. doi: 10.3390/jcm9010253.

4. *Giraud S, Thuillier R, Cau J, Hauet T. In vitro/ex vivo* Models for the Study of Ischemia Reperfusion Injury during Kidney Perfusion. *Int J Mol Sci*. 2020 Oct 31; 21 (21): 8156. doi: 10.3390/ijms21218156. PMID: 33142791; PMCID: PMC7662866.
5. *Ma H, Guo X, Cui S, Wu Y, Zhang Y, Shen X et al*. Dephosphorylation of AMP-activated protein kinase exacerbates ischemia/reperfusion-induced acute kidney injury via mitochondrial dysfunction. *Kidney Int*. 2022 Feb; 101 (2): 315–330. doi: 10.1016/j.kint.2021.10.028. Epub 2021 Nov 11. PMID: 34774556.
6. *Qi Y, Hu M, Wang Z, Shang W.* Mitochondrial iron regulation as an emerging target in ischemia/reperfusion injury during kidney transplantation. *Biochem Pharmacol*. 2023 Sep; 215: 115725. doi: 10.1016/j.bcp.2023.115725. Epub 2023 Jul 29. PMID: 37524207.
7. *Johnson RJ, Floege J, Tonelli M.* Comprehensive Clinical Nephrology. Seventh Edition. Elsevier, 2024. 1309 p.
8. *Pefanis A, Bongoni AK, McRae JL, Salvaris EJ, Fisicaro N, Murphy JM et al*. Dynamics of necroptosis in kidney ischemia-reperfusion injury. *Front Immunol*. 2023 Nov 2; 14: 1251452. doi: 10.3389/fimmu.2023.1251452. PMID: 38022500; PMCID: PMC10652410.
9. *Anzell AR, Maizy R, Przyklenk K, Sanderson TH.* Mitochondrial quality control and disease: Insights into ischemia-reperfusion injury. *Mol Neurobiol*. 2018; 55: 2547–64.
10. *Livingston MJ, Wang J, Zhou J, Wu G, Ganley IG, Hill JA et al.* Clearance of damaged mitochondria via mitophagy is important to the protective effect of ischemic preconditioning in kidneys. *Autophagy*. 2019; 15 (12): 2142–2162.
11. *Onishi M, Yamano K, Sato M, Matsuda N, Okamoto K.* Molecular mechanisms and physiological functions of mitophagy. *EMBO J*. 2021; 40 (3): e104705.
12. *Norgård MO, Svenningsen P.* Acute Kidney Injury by Ischemia/Reperfusion and Extracellular Vesicles. *Int J Mol Sci*. 2023 Oct 18; 24 (20): 15312. doi: 10.3390/ijms242015312. PMID: 37894994; PMCID: PMC10607034.
13. *Melo Ferreira R, Sabo AR, Winfree S, Collins KS, Janosevic D, Gulbronson CJ et al*. Integration of spatial and single-cell transcriptomics localizes epithelial cell-immune cross-talk in kidney injury. *JCI Insight*. 2021 Jun 22; 6 (12): e147703. doi: 10.1172/jci.insight.147703. PMID: 34003797; PMCID: PMC8262485.
14. *Dufour L, Ferhat M, Robin A, Inal S, Favreau F, Goujon JM et al*. Ischémie reperfusion en transplantation rénale [Ischemia-reperfusion injury after kidney transplantation]. *Nephrol Ther*. 2020 Nov; 16 (6): 388–399. French. doi: 10.1016/j.nephro.2020.05.001. Epub 2020 Jun 19. PMID: 32571740.
15. *Zhao F, Zhu J, Zhang M, Luo Y, Li Y, Shi L et al.* OGG1 aggravates renal ischemia–reperfusion injury by repressing PINK1-mediated mitophagy. *Cell Prolif*. 2023; 56 (8): e13418. doi: 10.1111/cpr.1341818.
16. *Visnes T, Cázares-Körner A, Hao W, Wallner O, Masuyer G, Loseva O et al.* Small-molecule inhibitor of OGG1 suppresses proinflammatory gene expression and inflammation. *Science*. 2018; 362 (6416): 834–839.
17. *Xu Y, Yuan XD, Wu JJ, Chen RY, Xia L, Zhang M et al*. The N6-methyladenosine mRNA methylase METTL14 promotes renal ischemic reperfusion injury via suppressing YAP1. *J Cell Biochem*. 2020 Jan; 121 (1): 524–533. https://doi.org/10.1002/jcb.29258.
18. *Xu X, Deng R, Zou L, Pan X, Sheng Z, Xu D, Gan T*. Sevoflurane participates in the protection of rat renal ischemia-reperfusion injury by down-regulating the expression of TRPM7. *Immun Inflamm Dis*. 2023 Jan; 11 (1): e753. doi: 10.1002/iid3.753.
19. *Ma M, Li H, Yin S, Lin T, Song T.* Overexpression of miR-92a attenuates kidney ischemia-reperfusion injury and improves kidney preservation by inhibiting MEK4/JNK1-related autophagy. *Cell Mol Biol Lett*. 2023 Mar 8; 28 (1): 20. doi: 10.1186/s11658-023-00430-3. PMID: 36890442; PMCID: PMC9997008.
20. *Cai J, Chen X, Liu X, Li Z, Shi A, Tang X et al*. AMPK: The key to ischemia-reperfusion injury. *J Cell Physiol*. 2022; 237 (11): 4079–4096. https://doi.org/10.1002/jcp.30875.
21. *Karimi F, Maleki M, Nematbakhsh M.* View of the Renin-Angiotensin System in Acute Kidney Injury Induced by Renal Ischemia-Reperfusion Injury. *J Renin Angiotensin Aldosterone Syst*. 2022 Oct 22; 2022: 9800838.
22. *Shi L, Song Z, Li Y, Huang J, Zhao F, Luo Y et al*. MiR-20a-5p alleviates kidney ischemia/reperfusion injury by targeting ACSL4-dependent ferroptosis. *Am J Transplant*. 2023 Jan; 23 (1): 11–25. doi: 10.1016/j.ajt.2022.09.003. Epub 2023 Jan 11. PMID: 36695612.
23. *Sun Z, Wu J, Bi Q, Wang W.* Exosomal lncRNA TUG1 derived from human urine-derived stem cells attenuates renal ischemia/reperfusion injury by interacting with SRSF1 to regulate ASCL4-mediated ferroptosis. *Stem Cell Res Ther*. 2022 Jul 15; 13 (1): 297. doi: 10.1186/s13287-022-02986-x. PMID: 35841017; PMCID: PMC9284726.
24. *Hu Z, Zhang H, Yang SK, Wu X, He D, Cao K, Zhang W*. Emerging role of ferroptosis in acute kidney injury. *Oxid Med Cell Longev*. 2019; 2019: 8010614.
25. *Qi Y, Hu M, Qiu Y, Zhang L, Yan Y, Feng Y et al*. Mitoglitazone ameliorates renal ischemia/reperfusion injury by inhibiting ferroptosis via targeting mitoNEET. *Toxicol Appl Pharmacol*. 2023 Apr 15; 465: 116440. doi: 10.1016/j.taap.2023.116440. Epub 2023 Mar 3. PMID: 36870574.
26. The Kidney Book. A Practical Guide on Renal Medicine. Editors: Terence Kee Yi Shern, Jason Choo Chon Jun, Woo Keng Thye. Tan Chieh Suai. World Scientific Publishing, Singapore, 2024. 869 p.
27. *Abou Taka M, Dugbartey GJ, Sener A.* The Optimization of Renal Graft Preservation Temperature to Mitigate Cold Ischemia-Reperfusion Injury in Kidney Transplantation. *Int J Mol Sci*. 2022 Dec 29; 24 (1): 567. doi: 10.3390/ijms24010567. PMID: 36614006; PMCID: PMC9820138.

28. *McFarlane L, Nelson P, Dugbartey GJ, Sener A.* Pre-Treatment of Transplant Donors with Hydrogen Sulfide to Protect against Warm and Cold Ischemia-Reperfusion Injury in Kidney and Other Transplantable Solid Organs. *Int J Mol Sci*. 2023 Feb 9; 24 (4): 3518. doi: 10.3390/ijms24043518. PMID: 36834928; PMCID: PMC9963309.
29. *Gupta N, Caldas M, Sharma N, Bidnur S, Ghosh S, Todd GT, Moore RB*. Does intra-operative verapamil administration in kidney transplantation improve graft function. *Clin Transplant*. 2019 Aug; 33 (8): e13635. https://doi.org/10.1111/ctr.13635.
30. *Xu L, Sharkey D, Cantley LG*. Tubular GM-CSF Promotes Late MCP-1/CCR2-Mediated Fibrosis and Inflammation after Ischemia/Reperfusion Injury. *J Am Soc Nephrol*. 2019 Oct; 30 (10): 1825–1840. doi: 10.1681/ASN.2019010068. Epub 2019 Jul 17. PMID: 31315923; PMCID: PMC6779361.
31. *Giraud S, Kerforne T, Zely J, Ameteau V, Couturier P, Tauc M, Hauet T*. The inhibition of eIF5A hypusination by GC7, a preconditioning protocol to prevent brain death-induced renal injuries in a preclinical porcine kidney transplantation model. *Am J Transplant*. 2020; 20 (12): 3326–3340. https://doi.org/10.1111/ajt.15994.
32. *Kerforne T, Giraud S, Danion J, Thuillier R, Couturier P, Hebrard W et al.* Rapid or slow time to brain death? impact on kidney graft injuries in an allotransplantation porcine model. *Int J Mol Sci*. 2019; 20 (15): 3671.
33. *Hosszu A, Lakat T, Balogh DB, Lenart L, Rimaszombati F, Saeed A et al*. Sigma-1 Receptor Agonists Are Renoprotective in Experimental Kidney Transplantation. *FASEB J*. 2020; 34 (S1). https://doi.org/10.1096/fasebj.2020.34.s1.09051.
34. *Zagni M, Croci GA, Cannavò A, Passamonti SM, De Feo T, Boggio FL et al*. Histological evaluation of ischemic alterations in donors after cardiac death: A useful tool to predict post-transplant renal function. *Clin Transplant*. 2022 May; 36 (5): e14622. https://doi.org/10.1111/ctr.14622.
35. *Vatazin AV, Artemov DV, Zulkarnaev AB*. Prevention and treatment of ischemia-reperfusion syndrome. *Nephrology (Saint-Petersburg)*. (In Russ). https://doi.org/10.24884/1561-6274-2019-23-2-41-48.
36. Peri-operative Anesthetic Management in Liver Transplantation. Editors: Vijay Vohra, Nikunj Gupta, Annu Sarin Jolly, Seema Bhalotra. Springer, 2023. 617 p. https://doi.org/10.1007/978-981-19-6045-1.
37. *Guo S, Zhang F, Chen Y, Chen Y, Shushakova N, Yao Y et al.* Pre-ischemic renal lavage protects against renal ischemia-reperfusion injury by attenuation of local and systemic inflammatory responses. *FASEB J*. 2020; 34 (12): 16307–16318. https://doi.org/10.1096/fj.201902943R.
38. *Tian Y, Shu J, Huang R, Chu X, Mei X.* Protective effect of renal ischemic postconditioning in renal ischemic-reperfusion injury. *Transl Androl Urol*. 2020; 9 (3): 1356–1365. doi: 10.21037/tau-20-859.
39. *Theodoraki K, Karmaniolou I, Tympa A, Tasoulis MK, Nastos C, Vassiliou I et al*. Beyond preconditioning: postconditioning as an alternative technique in the prevention of liver ischemia-reperfusion injury. *Oxidative Med Cell Longev*. 2016; 2016: 8235921. https://doi.org/10.1155/2016/8235921.
40. *Bilenko MV.* Ischemic and reperfusion injuries of organs (molecular mechanisms, ways of prevention and treatment). M.: Medicine, 1989. 368 s.
41. Transplantation Immunology. Methods and Protocols. Second Edition. Edited by Andrea A. Zachary and Mary S. Leffell. Humana Press is a brand of Springer, 2013. 411 p.
42. *Wang L, Chen W, Liang P, Wei J, Zhang J, Buggs J, Liu R*. A Novel Technique to Reduce Kidney Injury by Maintaining Na/K Pump Functions Using Electric Energy. *FASEB J*. 2022; 36 (S1). https://doi.org/10.1096/fasebj.2022.36.S1.R3905.
43. *Huijink TM, Venema LH, Posma RA, de Vries NJ, Westerkamp AC, Ottens PJ et al*. Metformin Preconditioning and Postconditioning to Reduce Ischemia Reperfusion Injury in an Isolated *Ex Vivo* Rat and Porcine Kidney Normothermic Machine Perfusion Model. *Clin Transl Sci*. 2021; 14 (1): 222–230. doi: 10.1111/cts.12846.
44. *Popov SV, Guseynov RG, Skryabin ON, Sivak KV.* Teplovaya ishemiya pochki M.: GEOTAR-Media, 2021. 272 s.
45. *Spoelstra-de Man AME, Elbers PWG, Oudemans-van Straaten HM.* Making sense of early high-dose intravenous vitamin c in ischemia/reperfusion injury. *Crit Care*. 2018; 22 (1): 70.
46. *Mohamadian M, Parsamanesh N, Chiti H, Sathyapalan T, Sahebkar A.* Protective effects of curcumin on ischemia/reperfusion injury. *Phytother Res*. 2022 Dec; 36 (12): 4299–4324. https://doi.org/10.1002/ptr.7620.
47. *Wang J, Toan S, Li R, Zhou H.* Melatonin fine-tunes intracellular calcium signals and eliminates myocardial damage through the IP3R/MCU pathways in cardiorenal syndrome type 3. *Biochem Pharmacol*. 2020; 174: 113832.
48. *Zahran R, Ghozy A, Elkholy SS, El-Taweel F, El-Magd MA.* Combination therapy with melatonin, stem cells and extracellular vesicles is effective in limiting renal ischemia–reperfusion injury in a rat model. *Int J Urol*. 2020 Nov; 27 (11): 1039–1049. https://doi.org/10.1111/iju.14345.
49. *Ivashin AA, Korobkov DM, Vaganova MA, Pervoikina IS, Kuznetsova MY, Klochkova AA et al*. An evaluation of exogenous melatonin application on functional and histopathological changes in ischaemia reperfusion injury of kidneys. *Int Res J.* 2024; 3 (141): 52. doi: 10.23670/IRJ.2024.141.88. EDN QJNZYV.
50. *Liang TY, Peng SY, Ma M, Li HY, Wang Z, Chen G.* Protective effects of sevoflurane in cerebral ischemia reperfusion injury: a narrative review. *Med Gas Res*. 2021; 11 (4): 152–154. doi: 10.4103/2045-9912.318860.
51. *Zhu L, Zhang Y.* Discovery of novel ketamine-inspired derivatives as a protective agent against renal ischemic/reperfusion injury in Wistar rats. *Chem Biol Drug*

Des. 2022 Jul; 100 (1): 13–24. https://doi.org/10.1111/cbdd.14011.

52. *Hashmi SF, Rathore HA, Sattar MA, Johns EJ, Gan CY, Chia TY, Ahmad A*. Hydrogen sulphide treatment prevents renal ischemia-reperfusion injury by inhibiting the expression of ICAM-1 and NF-kB concentration in normotensive and hypertensive rats. *Biomolecules*. 2021; 11 (10): 1549. doi: 10.3390/biom11101549.
53. *Eraslan E, Tanyeli A, Polat E, Yetim Z.* Evodiamine alleviates kidney ischemia reperfusion injury in rats: A biochemical and histopathological study. *J Cell Biochem*. 2019 Oct; 120 (10): 17159–17166. https://doi.org/10.1002/jcb.28976.
54. *Rosin DL, Hall JP, Zheng S, Huang L, Campos-Bilderback S, Sandoval R et al.* Human recombinant alkaline phosphatase (Ilofotase alfa) protects against kidney ischemia-reperfusion injury in mice and rats through adenosine receptors. *Front Med (Lausanne)*. 2022; 9: 931293. doi: 10.3389/fmed.2022.931293.
55. *Steenvoorden TS, van Duin RE, Rood JAJ, Peters-Sengers H, Nurmohamed AS, Bemelman FJ et al.* Alkaline phosphatase to treat ischaemia–reperfusion injury in living-donor kidney transplantation: APhIRI I feasibility pilot study. *Br J Clin Pharmacol*. 2023; 89 (12): 3629–3636. doi: 10.1111/bcp.15871.
56. *Kim M, Lee JY, Pagire HS, Pagire SH, Bae MA, Chanda D et al*. Inhibition of pyruvate dehydrogenase kinase 4 ameliorates kidney ischemia-reperfusion injury by reducing succinate accumulation during ischemia and preserving mitochondrial function during reperfusion. *Kidney Int*. 2023 Oct; 104 (4): 724–739. doi: 10.1016/j.kint.2023.06.022. Epub 2023 Jul 1. PMID: 37399974.
57. *Yang D, Tang M, Zhang M, Ren H, Li X, Zhang Z et al*. Downregulation of G protein-coupled receptor kinase 4 protects against kidney ischemia-reperfusion injury. *Kidney Int*. 2023 Apr; 103 (4): 719–734. doi: 10.1016/j.kint.2022.12.023. Epub 2023 Jan 18. PMID: 36669643.
58. *Xie ZY, Dong W, Zhang L, Wang MJ, Xiao ZM, Zhang YH et al*. NFAT inhibitor 11R-VIVIT ameliorates mouse renal fibrosis after ischemia-reperfusion-induced acute kidney injury. *Acta Pharmacol Sin*. 2022 Aug; 43 (8): 2081–2093. doi: 10.1038/s41401-021-00833-y. Epub 2021 Dec 22. PMID: 34937917; PMCID: PMC9343462.
59. *Howard MC, Nauser CL, Farrar CA, Wallis R, Sacks SH.* l-Fucose prevention of renal ischaemia/reperfusion injury in mice. *FASEB J*. 2020; 34: 822–834. https://doi.org/10.1096/fj.20190 1582R.
60. *Xuyang Li, Zhan Zhang, Aipeng Li, Yubo Hu.* Propofol attenuates renal ischemia/reperfusion injury by regulating the MALAT1/miR-126-5p axis. *J Gene Med*. 2021 Aug; 23 (8): e3349. https://doi.org/10.1002/jgm.3349.
61. *Minami K, Bae S, Uehara H, Zhao C, Lee D, Iske J et al.* Targeting of intragraft reactive oxygen species by APP-103, a novel polymer product, mitigates ischemia/reperfusion injury and promotes the survival of renal transplants. *Am J Transplant*. 2020; 20 (6): 1527–1537. https://doi.org/10.1111/ajt.15794.
62. *Cao Y, Guan Y, Xu YY, Hao CM.* Endothelial prostacyclin protects the kidney from ischemia-reperfusion injury. *Pflugers Arch*. 2019 Apr; 471 (4): 543–555. doi: 10.1007/s00424-018-2229-6. Epub 2018 Nov 9. PMID: 30413885; PMCID: PMC6435627.
63. *Çakır M, Tekin S, Taşlıdere A, Çakan P, Düzova H, Gül CC*. Protective effect of N-(p-amylcinnamoyl) anthranilic acid, phospholipase A_2 enzyme inhibitor, and transient receptor potential melastatin-2 channel blocker against renal ischemia-reperfusion injury. *J Cell Biochem*. 2019 Mar; 120 (3): 3822–3832. https://doi.org/10.1002/jcb.27664.
64. *Tiba AT, Qassam H, Hadi NR.* Semaglutide in renal ischemia-reperfusion injury in mice. *J Med Life*. 2023 Feb; 16 (2): 317–324. doi: 10.25122/jml-2022-0291. PMID: 36937464; PMCID: PMC10015556.
65. *Cai Q, Sun Z, Xu S, Jiao X, Guo S, Li Y et al*. Disulfiram ameliorates ischemia/reperfusion-induced acute kidney injury by suppressing the caspase-11-GSDMD pathway. *Ren Fail*. 2022 Dec; 44 (1): 1169–1181. doi: 10.1080/0886022X.2022.2098764. PMID: 35837696; PMCID: PMC9291718.
66. *Jung HY, Oh SH, Ahn JS, Oh EJ, Kim YJ, Kim CD et al*. NOX1 Inhibition Attenuates Kidney Ischemia-Reperfusion Injury via Inhibition of ROS-Mediated ERK Signaling. *Int J Mol Sci*. 2020 Sep 21; 21 (18): 6911. doi: 10.3390/ijms21186911. PMID: 32967113; PMCID: PMC7554761.
67. *Wu W, Liu D, Zhao Y, Zhang T, Ma J, Wang D et al*. Cholecalciferol pretreatment ameliorates ischemia/reperfusion-induced acute kidney injury through inhibiting ROS production, NF-κB pathway and pyroptosis. *Acta Histochem*. 2022 May; 124 (4): 151875. doi: 10.1016/j.acthis.2022.151875. Epub 2022 Mar 22. PMID: 35334282.
68. *Feng S, Qu Y, Chu B, Chen X, Yang Z, Li P et al*. Novel gold-platinum nanoparticles serve as broad-spectrum antioxidants for attenuating ischemia reperfusion injury of the kidney. *Kidney Int*. 2022 Nov; 102 (5): 1057–1072. doi: 10.1016/j.kint.2022.07.004. Epub 2022 Jul 21. PMID: 35870640.
69. *Thapa K, Singh TG, Kaur A.* Targeting ferroptosis in ischemia/reperfusion renal injury. *Naunyn Schmiedebergs Arch Pharmacol*. 2022 Nov; 395 (11): 1331–1341. doi: 10.1007/s00210-022-02277-5.
70. *Kim S, Lee SA, Yoon H, Kim MY, Yoo JK, Ahn SH et al*. Exosome-based delivery of super-repressor IκBα ameliorates kidney ischemia-reperfusion injury. *Kidney Int*. 2021 Sep; 100 (3): 570–584. doi: 10.1016/j.kint.2021.04.039. Epub 2021 May 27. PMID: 34051264.
71. *Hosszu A, Fekete A, Szabo AJ.* Sex differences in renal ischemia-reperfusion injury. *Am J Physiol Renal Physiol*. 2020 Aug 1; 319 (2): F149–F154. doi: 10.1152/ajprenal.00099.2020. Epub 2020 Jun 22. PMID: 32567347.
72. *Zhou D, Leung J, Xu W, Ye S, Dong C, Huang W et al*. Protective effect of estradiol copreservation against kidney ischemia-reperfusion injury. *Artif Organs*. 2022 Feb; 46 (2): 219–228. https://doi.org/10.1111/aor.14038.
73. *Ren L, Li F, Di Z, Xiong Y, Zhang S, Ma Q et al*. Estradiol Ameliorates Acute Kidney Ischemia-Reperfusion Injury by Inhibiting the TGF-βRI-SMAD Pathway.

Front Immunol. 2022 Feb 24; 13: 822604. doi: 10.3389/fimmu.2022.822604. PMID: 35281024; PMCID: PMC8907449.

74. *Pool M, Eertman T, Sierra Parraga J, 't Hart N, Roemeling-van Rhijn M, Eijken M et al.* Infusing Mesenchymal Stromal Cells into Porcine Kidneys during Normothermic Machine Perfusion: Intact MSCs Can Be Traced and Localised to Glomeruli. *Int J Mol Sci*. 2019; 20 (14): 3607.
75. *Thompson ER, Bates L, Ibrahim IK, Sewpaul A, Stenberg B, McNeill A et al.* Novel delivery of cellular therapy to reduce ischemia reperfusion injury in kidney transplantation. *Am J Transplant*. 2021; 21 (4): 1402–1414. https://doi.org/10.1111/ajt.16100.
76. *Shiva N, Sharma N, Kulkarni YA, Mulay SR, Gaikwad AB.* Renal ischemia/reperfusion injury: An insight on *in vitro* and *in vivo* models. *Life Sci*. 2020 Sep 1; 256: 117860. doi: 10.1016/j.lfs.2020.117860. Epub 2020 Jun 11. PMID: 32534037.
77. *Li S, Chen Y, Cao X, Yang C, Li W, Shen B.* The application of nanotechnology in kidney transplantation. *Nanomedicine (Lond)*. 2024 Feb; 19 (5): 413–429. doi: 10.2217/nnm-2023-0286. Epub 2024 Jan 26. PMID: 38275168.
78. *Wu J, Zhang F, Zheng X, Zhang J, Cao P, Sun Z, Wang W.* Identification of renal ischemia reperfusion injury subtypes and predictive strategies for delayed graft function and graft survival based on neutrophil extracellular trap-related genes. *Front Immunol*. 2022 Dec 1; 13: 1047367. doi: 10.3389/fimmu.2022.1047367. PMID: 36532016; PMCID: PMC9752097.
79. *Netrebenko AS, Gureev VV, Pokrovskiy MV.* Investigation of nephroprotective properties of infliximab in modeling of acute ischemia-reperfusion kidney injury in experiment. *Clinical and experimental pharmacology: advances in science, practice, education: Proceedings of the All-Russian scientific and practical conference with international participation, dedicated to the 86th anniversary of Kursk State Medical University, 80th anniversary of the birth of Professor N.G. Filippenko, 80th anniversary of the birth of Professor V.V. Pichugin, Kursk, September 29, 2021* / Edited by G.S. Mal, S.V. Povetkin. Kursk: Kursk State Medical University, 2021: 55–58. EDN STFZIA.
80. *Netrebenko AS, Gureev VV, Korokin MV, Pokrovskij MV, Soldatov VO, Pokrovskaya TG et al.* Patent № 2753247 C1 RF, MPK A61K 39/395, A61P 13/12. Method for correcting microcirculation disorders in kidney with infliximab in ischemia-reperfusion injury: № 2021106133: applied. 10.03.2021: publ. 12.08.2021; applicant FGAOU VO "Belgorod State National Research University". EDN BPTPIM.
81. *Netrebenko AS, Gureev VV, Pokrovskiy MV, Yakushev VI, Saprykina EG, Zatolokina MA.* Protective effect of a combination of the peptide mimicking the α-spatial structure of the β erythropoietin chain and infliximab on the epithelium of the nephron tubules in renal ischemia-reperfusion injury. *Journal of Volgograd State Medical University*. 2023; 20 (2): 168–171. doi: 10.19163/1994-9480-2023-20-2-168-171. EDN NIRSLX.
82. *Netrebenko AS, Elagin VV, Kostina DA, Gureev VV, Pokrovsky MV, Yakushev VI et al.* Nephroprotective effect of a combination of the peptide mimicking the α-spatial structure of the β erythropoietin chain and infliximab in renal ischemia-reperfusion injury. *Journal of Volgograd State Medical University*. 2022; 19 (3): 121–127. doi: 10.19163/1994-9480-2022-19-3-121-127. EDN KFXWUC.
83. *Netrebenko AS, Gureev VV, Korokin MV, Pokrovskij MV, Soldatov VO, Pokrovskaya TG et al.* Patent № 2751413 C1 RF, MPK A61K 38/08, A61P 13/12. Method for correcting microcirculation disorders in kidney with peptide that mimics alpha-helix β of erythropoietin in ischemia-reperfusion injury: № 2021106163: applied. 10.03.2021: publ. 13.07.2021; applicant FGAOU VO "Belgorod State National Research University". EDN XYVRJJ.
84. *Kostina DA, Pokrovskaya TG, Pokrovskij MV, Gureev VV, Yakushev VI, Peresypkina AA, Kolesnichenko PD.* Patent № 2678768 C1 RF, MPK A61K 38/16, A61K 38/18, C07K 14/505. Method for preventing renal ischemia reperfusion injury by carbamylated darbepoetin in experiment: № 2018133675: applied. 25.09.2018: publ. 01.02.2019; applicant FGAOU VO "Belgorod State National Research University". EDN NVYUFM.
85. *Elagin VV, Bratchikov OI, Pokrovskij MV, Pokrovskaya TG, Kostina DA, Gureev VV et al.* Patent № 2695333 C1 RF, MPK A61K 38/43, A61P 13/12. Method for preventing ischemia-reperfusion renal injuries with an inhibitor of arginase II in experiment: № 2018133652: applied. 24.09.2018: publ. 23.07.2019; applicant FGAOU VO "Belgorod State National Research University". EDN UQHAEP.
86. *Islaev AA, Brin VB*. Prevention of ischemic-reperfusion injury of kidneys by acyzol. *Journal of New Medical Technologies*. 2020; 27 (1): 100–104. doi: 10.24411/1609-2163-2020-16604. EDN LLVQAY.
87. *Goncharov RG, Filkov GI, Trofimenko AV, Boyarintsev VV, Novoselov VI, Sharapov MG*. The protective effect of a chimeric psh antioxidant enzyme in renal ischemia–reperfusion injury. *Biophysics*. 2020; 65 (2): 303–312. doi: 10.31857/S0006302920020180. EDN OTFVBM.
88. *Goncharov RG, Novoselov VI, Sharapov MG.* Protective effect of chimeric enzyme-antioxidant PSH in ischemia-reperfusion kidney injury. *Collection of scientific papers of the VI Congress of Biophysicists of Russia, Sochi, September 16–21, 2019. T. 2*. Sochi: Plekhanovets, 2019: 184. EDN NTGBKJ.
89. *Goncharov RG, Novoselov VI, Sharapov MG.* Patent № 2747121 C1 RF, MPK A61P 39/06, C12N 15/11, C12N 15/64. Method of agent application based on human modified peroxyredoxin 2 for correcting consequences of ischemic-reperfusive kidney damage: № 2020121240: applied. 26.06.2020: publ. 28.04.2021; applicant Federal Research Center "Pushchino Scientific Center for Biological Research of the Russian Academy of Sciences". EDN HXPFKH.

90. *Gordeeva AE, Kurganova EA, Novoselov VI.* The hepatoprotective effect of peroxiredoxin 6 in ischemia–reperfusion kidney injury. *Biophysics*. 2021; 66 (5): 840–847. doi: 10.31857/S0006302921050173. EDN SAFNQA.
91. *Popov KA.* Pathobiochemical changes in ischemic-reperfusion liver damage. *Biochemistry of the XXI Century: Proceedings of Scientific and Practical Conference with International Participation, Krasnodar, November 26, 2021.* Krasnodar: Kachestvo, 2021: 207–210. EDN MEZFHH.
92. *Popov KA, Bykov IM, Tsymbalyuk IYu, Azimov EA, Bykov MI, Denisova YaE et al.* Prooxidant preconditioning of ischemic-reperfusion liver damage in experiment. *Medical News of North Caucasus*. 2022; 17 (1): 56–59. doi: 10.14300/mnnc.2022.17015. EDN SNWJWQ.
93. *Popov KA, Denisova YaE, Bykov IM, Tsymbalyuk IYu, Ermakova GA, Zavgorodnyaya AG, Shevchenko AS*. The Role of the Pyruvate Dehydrogenase Complex in the Development of Ischemic-Reperfusion Syndrome. *Kuban Scientific Medical Bulletin*. 2022; 29 (4): 75–93. (In Russ.). doi: 10.25207/1608-6228-2022-29-4-75-93. EDN IANYFF.
94. *Popov KA, Stolyarova AN, Ermakova GA, Esaulenko EE, Bykov IM, Tutarisheva SM et al*. Pharmacological preconditioning of ischemic-reperfusion damage to the liver of rats by pharmaceutical means of energotropic action. *Crimean Journal of Experimental and Clinical Medicine*. 2022; 12 (3): 50–56. doi: 10.29039/2224-6444-2022-12-3-50-56. EDN IKXDBO.
95. *Popov KA, Bykov IM, Ustinova ES, Tsymbaliuk IY, Tutarisheva SM.* Modern approaches to metabolic prophylaxis of postoperative ischemia-reperfusion complications. *Health-saving technologies: experience of the present and prospects for the future: Proceedings of the I interregional scientific-practical conference of young scientists with international participation, Krasnodar, December 16, 2022*. Krasnodar: KubGMU, 2022: 308–311. EDN IGZIVY.
96. *Popov KA, Bykov IM, Tsymbaliuk IY, Bykov MI, Azimov EA, Stolyarova AN, Timoshenko YaE*. Pathobiochemistry of ischemia-reperfusion injuries. Krasnodar: Kachestvo, 2023. 213 s. EDN HTSNDO.
97. *Popov KA, Bykov IM, Stolyarova AN, Denisova YA, Goncharova AA, Vladimirov AS.* Mechanisms of protective effect of sodium dichloroacetate in ischemia-reperfusion syndrome. *III United Scientific Forum of Physiologists, Biochemists and Molecular Biologists. Proceedings: III United Scientific Forum of Physiologists, Biochemists and Molecular Biologists; VII Congress of Physiologists of the CIS; VII Congress of Biochemists of Russia; X Russian Symposium, Sochi-Dagomys, October 3–8, 2021. T. 3*. M.: Pero, 2022: 71–72. EDN TSNQBV.
98. *Popov KA, Bykov IM, Ustinova ES, Tsymbaliuk IY, Stolyarova AN, Denisova YA, Azimov EA*. Preconditioning of ischemia-reperfusion liver injury using pro-oxidant agents. *III United Scientific Forum of Physiologists, Biochemists and Molecular Biologists: Proceedings: VII Congress of Biochemists of Russia. X Russian Symposium "Proteins and Peptides". VII Congress of Physiologists of the CIS, Sochi, Dagomys, October 3–8, 2021. T. 2.* M.: Pero, 2021: 241–242. EDN ANXODF.
99. *Popov KA, Bykov IM, Tsymbaliuk IY, Dyakov OV.* The role of the functional state of mitochondria in ischemia-reperfusion injury of the liver. *II United Scientific Forum. VI Congress of CIS physiologists. VI Congress of Biochemists of Russia. IX Russian symposium "Proteins and peptides": scientific proceedings, Sochi-Dagomys, October 1-6, 2019. Union of Physiological Societies of the CIS countries; Russian Society of Biochemists and Molecular Biologists. T. 2.* M.: Pero, 2019: 214. EDN BLJXXZ.
100. *Popov KA, Bykov IM, Ermakova GA, Tsymbalyuk IY*. Active dynamics of the enzymes of the antiradical protection and the general antioxidative activity by the development of the experimental ischemic reperfusion of liver. *RUDN Journal of Medicine*. 2018; 22 (2): 171–182. doi: 10.22363/2313-0245-2018-22-2-171-182. EDN XTRIWD.
101. *Stolyarova AN, Esaulenko EE, Bykov IM, Dyakov OV*. Effect of tret-butyl hydroperoxide on the development of ischemic-reperfusion liver in experiment. *Biochemistry of XXI century: Proceedings of scientific and practical conference with international participation, Krasnodar, November 26, 2021*. Krasnodar: Kachestvo, 2021: 219–223. EDN RQSBGA.
102. *Azimov EA, Bykov IM, Tutarisheva SM, Tsymbalyuk IYu*. Effect of thiol-containing antioxidants on the severity of ischemic-reperfusion liver injury in the experiment. *Biochemistry of XXI century: Proceedings of scientific and practical conference with international participation, Krasnodar, November 26, 2021*. Krasnodar: Kachestvo, 2021: 29–32. EDN EANAZH.
103. *Dyakov OV, Zavgorodnyaya AG.* Preconditioning of ischemia-reperfusion liver injury using tert-butyl hydroperoxide. *Collection of abstracts of the 83rd interregional scientific-practical conference with international participation of student scientific society named after Professor N.P. Pyatnitsky, Krasnodar, April 27–28, 2022.* Krasnodar: Kuban State Medical University, 2022: 1229–1232. EDN MMRLAQ.
104. *Yaremin BI, Novruzbekov MS, Lutsyk KN, Olisov OD, Gulyaev VA, Magomedov KM, Akhmedov AR.* New factors of predicting the severity of ischemia-reperfusion injury of liver transplant. *Russian Journal of Transplantology and Artificial Organs.* 2022; 24 (S): 75. (In Russ.). EDN TVGCLO.
105. *Stolyarova AN, Esaulenko EE.* Influence of preconditioning with pro-/antioxidants on the development of ischemia-reperfusion liver damage in experimental conditions. *MCU Journal of Natural Sciences*. 2023; 4 (52): 38–49. doi: 10.25688/2076-9091.2023.52.4.03. EDN VTULQE.
106. *Paremsky EV, Kharsak AV.* Reduction of ischemia-reperfusion injury of rat myocardium at restoration of blood flow on the background of intravenous administration of quinacrine. *Forcipe*. 2019; 2 (S1): 807. EDN MTIMSD.

107. *Papayan GV, Petrishchev NN, Galagudza MM, Sonin DL, Minasyan SM.* Patent № 2622983 C RF, MPK A61B 5/00, B82B 1/00. Method of intraoperative visualization of myocardial ischemia-reperfusion injury: № 2016130494: applied. 25.07.2016: publ. 21.06.2017; applicant FGBOU VO "First St. Petersburg State Medical University named after Academician I.P. Pavlov" of the Ministry of Health of Russia, FGBU "North-West Federal Medical Research Center named after V.A. Almazov" of the Ministry of Health of Russia. EDN XWNEVP.
108. *Tarasova AP, Pokrovsky MV, Danilenko LM.* Incretin peptides: new targets in correction of ischemic-reperfusion myocardial damages. Kursk Scientific and Practical Bulletin "Man and His Health". 2020; 1: 29–36. doi: 10.21626/vestnik/2020-1/04. EDN ZGBEKG.
109. *Shibeko NA, Gelis LG, Rusak TV, Semenova NV, Grinchuk II, Tarasik ES, Aliyeva FR.* Risk factors of ischemic-reperfusion dysfunction of the myocardium. *Cardiology in Belarus*. 2019; 11 (5): 658–667. EDN QGTDBB.
110. *Sonin DL, Pochkaeva EI, Papayan GV, Minasian SM, Mukhametdinova DV, Zaytseva EA et al.* Cardio- and vasoprotective effect of quinacrine in an *in vivo* rat model of myocardial ischemic reperfusion injury. *Bulletin of Experimental Biology and Medicine*. 2024; 177 (2): 152–159. doi: 10.47056/0365-9615-2024-177-2-152-159. EDN ANVJAD.
111. *Sonin DL, Pochkaeva EI, Papayan GV, Petrishchev NN, Zajtseva EA, Novruzova KK et al*. Patent № 2716596 C1 RF, MPK A61K 31/44, A61P 9/10. Method for reducing the size of ischemic-reperfusion myocardial injury with the use of quinacrine: № 2019128217: applied. 06.09.2019: publ. 13.03.2020; applicant FGBU "North-West Federal Medical Research Center named after V.A. Almazov" of the Ministry of Health of Russia. EDN LBSHGN.
112. *Rusak TV, Gelis LG, Miadzvedzeva AA, Shibeko NA, Kurganovich SA, Haidzel IK, Gevorkyan TT.* Cardiac structural and functional changes in ischemia-reperfusion injury of myocardium. *Eurasian Heart Journal*. 2022; 3 (40): 74–82. doi: 10.38109/2225-1685-2022-3-74-82. EDN IJJSLA.
113. *Stepanov AV, Dobretsov MG, Novikova EV, Filippov YuA, Panov AA, Kubasov IV.* Remodeling of extracellularly recorded action potentialsof rat heart subepicardial cardiomyocytes after ischemia reperfusion injurya. *Journal of Evolutionary Biochemistry and Physiology*. 2023; 59 (5): 378–388. doi: 10.31857/S004445292305008X. EDN KQFEOG.
114. *Kuzmin DO, Skvortsov AE, Kutenkov AA, Reznik ON.* Biobank for studying the issues of ischemia-reperfusion injury. *Russian Journal of Transplantology and Artificial Organs*. 2019; 21 (S): 199. (In Russ.). EDN URCBDQ.

The article was submitted to the journal on 08.04.2024

DOI: 10.15825/1995-1191-2024-4-61-68

FEATURES OF THE ETIOLOGY, PATHOGENESIS AND EPIDEMIOLOGY OF RENAL CELL CARCINOMA IN KIDNEY TRANSPLANT RECIPIENTS

R.N. Trushkin[1], *T.K. Isaev*[1], *A.A. Sokolov*[2]

[1] Municipal Clinical Hospital No. 52, Moscow, Russian Federation
[2] Central Clinical Hospital with Clinic, Moscow, Russian Federation

Renal cell carcinoma (RCC) in a kidney transplant is a rare condition as it occurs in the donor kidney of a recipient undergoing immunosuppressive therapy and differs exceptionally from a similar cancer that develops in the native kidney. Given the relative rarity, characteristic specificity of RCC in transplant recipients, and the difficulty in diagnosis and treatment, this type of tumor is less thoroughly studied than the "standard" RCC. However, as more transplants are performed and recipients are being detected with this pathology more frequently, the study of this tumor becomes significantly relevant.

Keywords: kidney graft, renal cell carcinoma, etiology, pathogenesis, epidemiology.

INTRODUCTION

Kidney transplantation (KT) is widely recognized as the most effective treatment for end-stage chronic kidney disease (CKD). Compared to dialysis, KT significantly improves overall survival and enhances quality of life for patients [1]. In the Russian Federation, according to the most recent report from the Nationwide Registry of Renal Replacement Therapy by the Russian Dialysis Society, there are 9,984 kidney transplant recipients, representing 16.5% of all patients requiring renal replacement therapy (RRT) [2]. Annually, over 1,000 kidney transplants are performed in Russia, and this number continues to rise [3].

Despite the clear benefits of KT, a major ongoing challenge remains even with advances in surgical techniques and immunosuppressive therapies, graft longevity remains a critical issue in the field of transplantation [4].

Graft and recipient survival rates after KT vary significantly – not only between countries, but also among transplant centers within the same country. For instance, a single-center cohort study conducted by E. Van Loon et al. (2020), which examined long-term graft and recipient survival, reported that 42.2% of recipients had graft failure within ten years, necessitating either a return to dialysis or a re-transplantation [5].

Similarly, a 2013 report by the American Society of Transplant Surgeons, based on data from the Scientific Registry of Transplant Recipients (SRTR), noted marked improvements in graft survival rates over time. According to this review, the 10-year overall survival rate for kidney transplants from both living and deceased donors had increased from 35–40% to 55–60% compared to the previous decade. Five-year graft survival was highest in living donor recipients under the age of 11 (89%) and lowest in deceased donor recipients aged 11–17 years (68%) [6].

Taken together, a synthesis of global literature suggests that, on average, approximately 40–42% of kidney grafts fail within ten years of transplantation, regardless of donor type or recipient characteristics [4].

One of the contributing factors to graft loss in KT recipients is the development of malignant tumors, particularly renal cell carcinoma (RCC) within the graft. This paper focuses on the etiology, pathogenesis, and epidemiology of RCC in the context of KT.

Multiple studies have demonstrated that KT recipients face a significantly increased risk of RCC compared to the general, non-transplanted population [7–9]. For instance, according to the 2023 Clinical Guidelines – Renal Parenchyma Cancer, RCC incidence in Russia was reported to be 16.9 cases per 100,000 population (0.016%) in 2017 [10].

Various single-center studies suggest a much higher incidence of RCC among KT recipients. For example, a study by Guillaume Ploussard et al. (2012) estimated the incidence at approximately 0.5% [7]. However, the statistical robustness of such studies is limited due to small sample sizes, typically encompassing only a few dozen RCC cases.

More comprehensive data comes from a large meta-analysis conducted by Griffith et al. (2017), which reviewed 56 studies published between 1988 and 2015.

Corresponding author: Alexander Sokolov. Address: 26/38, Barvikha settlement, Odintsovo district, 143083, Moscow Oblast, Russian Federation.
Phone: (985) 492-35-77. E-mail: salexdoc@gmail.com

This analysis found the incidence of RCC in transplant recipients to range from 0.19% to 0.5%, representing a more than 10-fold increase compared to the general population (0.017%) [11]. In total, the analysis documented 174 cases of solid renal tumors among 163 KT recipients worldwide as of 2017.

Over time, as the number of kidney transplants and the duration of recipient follow-up have increased, a growing body of research has emerged investigating variations in RCC incidence among transplant recipients, with studies now examining differences across geographic regions and racial populations.

Thus, Chun-Chieh Yeh, et al. in 2020 published a large study based on the Taiwan's National Health Institute Research Database for the period from 1997 to 2011, which included 5038 kidney transplant recipients (50% living related-donor, 50% deceased-donor transplants). This study found that in the Taiwanese population, the likelihood of developing RCC occurring in a recipient was 37.3 times higher than in the general world population. Based on this, the authors concluded that "regional endemic epidemiologic factors play significant roles in the development of RCC in kidney transplant recipients and that each regional organ transplant program should tailor and establish its surveillance protocol based on epidemiologic data [12].

It should be noted that about 90% of RCC cases in transplant recipients are found in the native kidneys, and only about 10% are detected in the transplanted organ itself [13].

It is reasonable to anticipate that the rising number of transplants, combined with the increasing average age of both donors and recipients, may contribute to a future increase in RCC incidence within graft kidneys [14].

This trend is supported by comparative meta-analyses: the number of RCC cases in kidney transplant recipients reported worldwide has increased significantly – from 163 cases as of 2017 (according to a meta-analysis by Griffith et al.) to 357 cases by 2023 (as reported in a more recent meta-analysis by Fabio et al.) [11, 13]. This reflects a more than twofold increase in detected cases over a six-year period [11, 13].

CURRENT TRENDS IN THE SELECTION OF DONOR ORGANS FOR KIDNEY TRANSPLANTATION

In response to the growing global shortage of donor organs, there is a discernible shift in transplant practices toward relaxing the selection criteria for donor kidneys. A notable trend involves the increased use of extended criteria donor kidneys, including those from elderly individuals and even reconstituted kidneys with previously undiagnosed or historical RCC [15–16].

The aforementioned risks, combined with the growing number of kidney transplants and prolonged survival of transplant recipients, are likely to result in a progressive increase in the detection of RCC within graft kidneys – both in absolute numbers and as a percentage relative to RCC in native kidneys. It is important to note that the previously cited estimate – where only 10% of RCC cases in transplant recipients occurred in graft kidneys – was reported during a period when strict donor selection criteria were consistently applied [17–18].

Supporting this trend, Hendrik Eggers et al. (2019) published the results of a retrospective study involving 5,250 KT recipients at Hannover Medical School (Germany), revealing a significantly higher incidence of RCC in graft kidneys – 2.36%, compared to the previously estimated 0.5% [19].

In line with these findings, several authors, including Warren H. and Olsburgh J., emphasize that with the growing use of organs from elderly donors and the increasing longevity of graft survival, the development of neoplasia within the renal graft is likely to become a more prevalent clinical challenge for both urologists and transplant surgeons [20].

ETIOLOGY AND PATHOGENESIS

RCC in a transplanted kidney presents a unique pathological entity. On one hand, the tumor originates in the donor kidney, whose tissues are genetically distinct from the recipient. On the other hand, the graft functions long-term within the recipient's physiological environment, becoming integrated into the homeostatic system, yet remains subject to ongoing immune surveillance due to its allogeneic nature. Importantly, tumor development and progression occur under the influence of chronic immunosuppressive therapy [21–22].

Immunosuppression is a risk factor for malignant tumors in transplant recipients. It compromises the immune system's ability to recognize and destroy emerging cancer cells [23]. This increased risk is largely attributed to prolonged viral infections with oncogenic potential and a partial loss of immune surveillance mechanisms [24–25].

A number of studies have investigated the impact of specific immunosuppressants on the risk of cancer development in KT recipients. These studies emphasize the crucial role of natural killer (NK) cells, CD4+, and CD8+ T-cells in virus-specific immunity and the elimination of tumor cells [26]. Notably, lymphocyte-depleting agents such as polyclonal anti-T-lymphocyte antibodies (e.g., ATG-Fresenius S) [27], monoclonal anti-CD52 antibody alemtuzumab [28], and calcineurin inhibitors (CNIs) like cyclosporine and tacrolimus [29] have been shown to modulate these immune responses. In particular, calcineurin inhibitors (CNIs) act by inhibiting T-

cell activation and proliferation through suppression of interleukin-2 (IL-2) production. In addition, CNIs have been associated with a direct upregulation of vascular endothelial growth factor (VEGF) and transforming growth factor beta-1 (TGF-β1) [29]. A study by Engels et al. demonstrated that CNIs significantly increase circulating levels of VEGF and TGF-β1, potentially promoting the proliferation and survival of malignant cells in transplant recipients [30]. A dose-dependent elevation of TGF-β1 levels has been documented both *in vitro* and *in vivo* [29].

This creates a clinical dilemma: while low-dose CNI regimens are linked to reduced risk of malignancy, they simultaneously increase the risk of acute rejection [31]. As research progresses, a growing body of evidence supports the antitumor potential of proliferation signal inhibitors, particularly sirolimus and everolimus, which belong to the class of mammalian target of rapamycin (mTOR) inhibitors (mTOR-I) [23, 32–33].

The primary immunosuppressive mechanism of mTOR-Is involves the inhibition of T-cell activation and proliferation, achieved through suppression of IL-2 signaling and cell cycle arrest [25, 27, 34]. Beyond their immunosuppressive role, mTOR pathways also regulate amino acid metabolism, ribosome biosynthesis, transcriptional programming, cell growth, proliferation, senescence, and lifespan in virtually all human cells. Consequently, mTOR signaling is involved in angiogenesis, tumor progression, and metastasis [35–38].

The use of mTOR inhibitors as part of immunosuppressive regimens can reduce the incidence of *de novo* malignancies in transplant recipients. However, this benefit must be weighed against their side effect profile, which can lead to treatment discontinuation in some cases.

In addition to immunosuppressive therapy, other established risk factors for RCC in the graft include prolonged end-stage CKD, extended dialysis duration, advanced recipient age, and a personal history of RCC in the native kidneys [39–40].

FEATURES OF MORPHOLOGICAL FORMS OF RCC IN KIDNEY TRANSPLANT RECIPIENTS

In terms of morphological characteristics, the largest meta-analysis to date – encompassing 129 studies conducted between 1980 and 2020 and published by Fabio et al. in 2023 – revealed that the most frequent histological subtype of RCC arising in graft kidneys is the papillary type, accounting for 42.5% of all cases. This is followed by clear cell carcinoma at 40.2%, and chromophobe carcinoma at 3.5% of cases [13].

By contrast, in the general population of patients without a history of KT or dialysis, the predominant histological subtype is clear cell carcinoma, comprising up to 90% of cases, as documented in earlier epidemiological studies [41–42].

The higher prevalence of papillary RCC over clear forms in a kidney graft may be attributed to the factors described above [39–40, 43].

Further insight into the morphological spectrum of RCC in renal transplant recipients is provided by a large retrospective study by Billis et al., which analyzed RCC cases in patients undergoing dialysis or KT between 2003 and 2016 [44]. This study revealed an increased incidence of rare histological subtypes, specifically acquired cystic disease-associated RCC (11.8%) and clear cell papillary RCC (5.9%), which are exceedingly uncommon in patients not receiving dialysis or transplantation. Notably, both of these subtypes were only recently recognized and were officially included in the World Health Organization (WHO) Classification of Renal Tumors in 2016 [45–46].

Of particular significance, papillary RCC was the most frequently identified subtype in this patient group, accounting for 64.7% of all tumors [44]. It has been proposed that papillary RCC in transplant or dialysis patients may be associated with c-MET oncogene activation, trisomy of chromosomes 7 or 17, and loss of the Y chromosome, although these genetic mechanisms remain under investigation [11].

In addition, current research is examining the potential role of ischemic injury – both warm and cold ischemia – during donor kidney procurement and transplantation as a contributing factor to the increased risk of developing papillary RCC in the graft [11].

The third most common histological subtype of RCC identified in renal grafts is chromophobe carcinoma (3.5%) [13, 47–48]. One particularly noteworthy case involved the detection of chromophobe RCC in a transplanted kidney following the onset of macrohematuria nearly three decades post-transplant in a patient with a history of three prior kidney transplants [49].

Among other histological forms of tumor in a transplanted kidney, it is worth mentioning the single, at this time of observation, cases of mucinous tubular and spindle cell variant of RCC [50], oncocytoma [51], and benign anastomosing hemangioma that mimicked RCC [52].

In summary, the predominance of papillary RCC over clear cell RCC in kidney grafts represents a distinctive histopathological profile that differentiates transplant-associated renal tumors from those typically arising in the native kidneys of patients without a history of transplantation or dialysis.

ORIGIN OF RENAL TRANSPLANT TUMORS

For a long time, the origin of tumors developing in transplanted kidneys remained a subject of uncertainty. It was traditionally believed that RCC in the graft origi-

nated exclusively from donor-derived cells, a view supported by several genetic analyses of newly diagnosed cases [53].

However, a pivotal study published in 2009 by Boix et al. challenged this notion. Using microsatellite analysis, the authors provided the first evidence of RCC in a renal transplant arising from recipient-derived cells [54–55].

The accumulation of renal cancer cases in KT recipients enabled a landmark scientific study in 2023 at Municipal Clinical Hospital No. 52 in Moscow, aimed at elucidating the etiology of RCC in graft kidneys. The researchers analyzed chromosomal DNA from both tumor and surrounding normal tissue of the transplanted kidneys. Using short tandem repeat (STR) markers, they confirmed that in 100% of cases, the tumor originated from donor-derived tissue.

Notably, this study was the first in the world to assess Von Hippel–Lindau (VHL) gene expression in a cohort of KT recipients. The findings provided compelling evidence of genetic determinism in the development of clear cell RCC in graft kidneys. The authors concluded that this tumor type most likely arises from an inherent genetic predisposition in the donor renal parenchyma, which is exacerbated by long-term immunosuppressive therapy in the recipient [56].

FEATURES OF RENAL TUMORS IN KIDNEY RECIPIENTS

In a comprehensive study by Fabio et al. examining the quantitative characteristics of renal tumors in kidney grafts, it was found that the majority of RCC cases (84.5%) presented as solitary tumors, with most falling into the cT1a stage category (83.6%). In contrast, among patients with multifocal lesions, the proportion of cT1a tumors was notably lower at 67.9%.

Histologically, clear cell RCC was more prevalent in multifocal tumors (39.6%), whereas papillary RCC predominated in solitary lesions (42.7%), with clear cell tumors accounting for 40.2% in this group.

When classified by Fuhrman nuclear grading, the majority of solitary tumors were grade 2 (60.1%), while multifocal tumors were more frequently high-grade, with 41.7% classified as grade 3 [13].

It is important to note that, in contrast to the extensively studied "classical" RCC observed in non-transplanted patients, RCC in KT recipients remains poorly understood and is currently the subject of active investigation [57–58].

For instance, the aforementioned comprehensive meta-analysis by Fabio et al., published in 2023, emphasized the limited volume of literature on this topic. According to their findings, the majority of publications (73%) were clinical case reports, 21% were retrospective single-center studies, and only 4% comprised retrospective multicenter analyses. Notably, as of 2023, only 357 cases of RCC in transplanted kidneys had been documented worldwide [13].

This relative scarcity of data can be attributed to the narrow scope and highly specialized nature of the subject, as well as the limited number of transplant centers with the capacity and expertise to study such cases in detail – typically no more than one or two per country.

CONCLUSION

RCCs arising in the native kidneys of renal transplant recipients differ from those occurring in the native kidneys of individuals without transplantation or dialysis in several key aspects. These tumors exhibit a complex interplay of genetic factors, a tendency for multifocal growth, and a potential connection to chronic immunosuppressive therapy. Furthermore, there is a potential for increased incidence of this tumor in the future, as transplant numbers rise and recipient follow-up periods continue to lengthen under current clinical conditions.

The authors declare no conflict of interest.

REFERENCES

1. *Tonelli M, Wiebe N, Knoll G, Bello A, Browne S, Jadhav D et al.* Systematic review: kidney transplantation compared with dialysis in clinically relevant outcomes. *Am J Transplant.* 2011 Oct; 11 (10): 2093–2109. doi: 10.1111/j.1600-6143.2011.03686.x. Epub 2011 Aug 30. PMID: 21883901.
2. *Andrusev AM, Peregudova NG, Shinkarev MB, Tomilina NA.* Kidney replacement therapy for end Stage Kidney disease in Russian Federation, 2016–2020. Russian National Kidney Replacement Therapy Registry Report of Russian Public Organization of Nephrologists "Russian Dialysis Society". *Nephrology and Dialysis.* 2022; 24 (4): 555–565. [In Russ.]. doi: 10.28996/2618-9801-2022-4-555-565.
3. *Gautier SV, Khomyakov SM.* Organ donation and transplantation in Russian Federation in 2019. 12th report of National Registry. *Russian Journal of Transplantology and Artificial Organs.* 2020; 22 (2): 8–34. [In Russ, English abstract]. doi: 10.15825/1995-1191-2020-2-8-34.
4. *Lai X, Zheng X, Mathew JM, Gallon L, Leventhal JR, Zhang ZJ.* Tackling Chronic Kidney Transplant Rejection: Challenges and Promises. *Front Immunol.* 2021 May 20; 12: 661643. doi: 10.3389/fimmu.2021.661643. eCollection 2021. PMID: 34093552.
5. *Van Loon E, Senev A, Lerut E, Coemans M, Callemeyn J, Van Keer JM et al.* Assessing the Complex Causes of Kidney. *Transplantation.* 2020 Dec; 104 (12): 2557–2566. doi: 10.1097/TP.0000000000003192. PMID: 32091487.
6. *Matas AJ, Smith JM, Skeans MA, Thompson B, Gustafson SK, Stewart DE et al.* OPTN/SRTR 2013 Annual

data report: Kidney. *Am J Transplant.* 2015 Jan; 2: 1–34. doi: 10.1111/ajt.13195.

7. *Ploussard G, Chambade D, Meria P, Gaudez F, Tariel E, Verine J et al.* Biopsy-confirmed *de novo* renal cell carcinoma (RCC) in renal grafts: a single-centre management experience in a 2396 recipient cohort. *BJU Int.* 2012 Jan; 109 (2): 195–199. doi: 10.1111/j.1464-410X.2011.10315.x. Epub 2011 Aug 2. PMID: 21810160.
8. *Chewcharat A, Thongprayoon C, Bathini T, Aeddula NR, Boonpheng B, Kaewput W et al.* Incidence and Mortality of Renal Cell Carcinoma after Kidney Transplantation: A Meta-Analysis. *J Clin Med.* 2019 Apr 17; 8 (4): 530. doi: 10.3390/jcm8040530. PMID: 30999706.
9. *Favi E, Raison N, Ambrogi F, Delbue S, Clementi MC, Lamperti L et al.* Systematic review of ablative therapy for the treatment of renal allograft neoplasms. *World J Clin Cases.* 2019 Sep 6; 7 (17): 2487–2504. doi: 10.12998/wjcc.v7.i17.2487. PMID: 31559284.
10. Clinical recommendations. Cancer of the kidney parenchyma – 2021–2022–2023. Ministry of Health of the Russian Federation. Available from: https://oncology-association.ru/wp-content/uploads/2023/11/rak-pochki_23.pdf?ysclid=lwuz3mnez3384504166.
11. *Griffith JJ, Amin KA, Waingankar N, Lerner SM, Delaney V, Ames SA et al.* Solid Renal Masses in Transplanted Allograft Kidneys: A Closer Look at the Epidemiology and Management. *Am J Transplant.* 2017 Nov; 17 (11): 2775–2781. doi: 10.1111/ajt.14366. Epub 2017 Jun 27. PMID: 28544435.
12. *Yeh CC, Khan A, Muo CH, Yang HR, Li PC, Chang CH et al. De Novo* Malignancy After Heart, Kidney, and Liver Transplant: A Nationwide Study in Taiwan. *Exp Clin Transplant.* 2020 Apr; 18 (2): 224–233. doi: 10.6002/ect.2019.0210. Epub 2020 Mar 4. PMID: 32133940.
13. *Crocerossa F, Autorino R, Derweesh I, Carbonara U, Cantiello F, Damiano R et al.* Management of renal cell carcinoma in transplant kidney: a systematic review and meta-analysis. *Minerva Urol Nephrol.* 2023 Feb; 75 (1): 1–16. doi: 10.23736/S2724-6051.22.04881-9. Epub 2022 Sep 12. PMID: 36094386.
14. *Lentine KL, Smith JM, Hart A, Miller J, Skeans MA, Larkin L et al.* OPTN/SRTR 2020 Annual Data Report: Kidney. *Am J Transplant.* 2022 Mar; 22 (2): 21–136. doi: 10.1111/ajt.16982. PMID: 35266618.
15. *Ogawa Y, Kojima K, Mannami R, Mannami M, Kitajima K, Nishi M et al.* Transplantation of Restored Kidneys From Unrelated Donors After Resection of Renal Cell Carcinoma: Results From 10 Patients. *Transplant Proc.* 2015 Jul-Aug; 47 (6): 1711–1719. doi: 10.1016/j.transproceed.2015.06.030. PMID: 26293039.
16. *Sultan S, Finn C, Craig-Schapiro R, Aull M, Watkins A, Kapur S et al.* Simultaneous Living Donor Kidney Transplant and Laparoscopic Native Nephrectomy: An Approach to Kidney Transplant Candidates with Suspected Renal-Cell Carcinoma. *J Endourol.* 2021 Jul; 35 (7): 1001–1005. doi: 10.1089/end.2020.0841. Epub 2020 Dec 31. PMID: 33238756.
17. *Ambrosi F, Ricci C, Malvi D, De Cillia C, Ravaioli M, Fiorentino M et al.* Pathological features and outcomes of incidental renal cell carcinoma in candidate solid organ donors. *Kidney Res Clin Pract.* 2020 Dec 31; 39 (4): 487–494. doi: 10.23876/j.krcp.20.050. PMID: 32855366.
18. *Musquera M, Sierra A, Diekmann F, Perez M, Mercader C, Peri L et al*. Increasing kidney grafts for transplantation. *World J Urol.* 2021 Jul; 39 (7): 2795–2800. doi: 10.1007/s00345-020-03463-x. Epub 2020 Sep 30. PMID: 33000340.
19. *Eggers H, Güler F, Ehlers U, Ivanyi P, Peters I, Grünwald V.* Renal cell carcinoma in kidney transplant recipients: descriptive analysis and overview of a major German transplant center. *Future Oncol.* 2019 Nov; 15 (32): 3739–3750. doi: 10.2217/fon-2019-0397. Epub 2019 Oct 30. PMID: 31664864.
20. *Warren H, Olsburgh J.* Management of Renal Cell Carcinoma and Other Renal Masses in the Kidney Graft. *Curr Urol Rep.* 2020 Feb 11; 21 (1): 8. doi: 10.1007/s11934-020-0959-4. PMID: 32048068.
21. *Frohlich FA, Halleck F, Lehner L, Schrezenmeier EV, Naik M, Schmidt D et al.* De-novo malignancies after kidney transplantation: A long-term observational study. *PLoS One.* 2020 Nov 30; 15 (11): e0242805. doi: 10.1371/journal.pone.0242805. PMID: 33253202.
22. *Nabi Z, Zahid T, Nabi R.* Post Renal Transplant Malignancies: A Basic Concept. *J Ayub Med Coll Abbottabad.* 2023 Oct-Dec; 35 (4): 664–668. doi: 10.55519/JAMC-04-12230. PMID: 38406957.
23. *Crespo E, Fernandez L, Lucia M, Melilli E, Lauzurica R, Penin RM et al.* Effector Antitumor and Regulatory T Cell Responses Influence the Development of Nonmelanoma Skin Cancer in Kidney Transplant Patients. *Transplantation.* 2017 Sep; 101 (9): 2102–2110. doi: 10.1097/TP.0000000000001759. PMID: 28403126.
24. *Buell JF, Gross TG, Woodle ES.* Malignancy after transplantation. *Transplantation.* 2005 Oct 15; 80 (2): 254–264. doi: 10.1097/01.tp.0000186382.81130.ba. PMID: 16251858.
25. *Krisl JC, Doan VP.* Chemotherapy and Transplantation: The Role of Immunosuppression in Malignancy and a Review of Antineoplastic Agents in Solid Organ Transplant Recipients. *Am J Transplant.* 2017 Aug; 17 (8): 1974–1991. doi: 10.1111/ajt.14238. Epub 2017 Apr 10. PMID: 28394486.
26. *Morvan MG, Lanier LL.* NK cells and cancer: you can teach innate cells new tricks. *Nat Rev Cancer.* 2016 Jan; 16 (1): 7–19. doi: 10.1038/nrc.2015.5. PMID: 26694935.
27. *Billups K, Neal J, Salyer J.* Immunosuppressant-driven *de novo* malignant neoplasms after solid-organ transplant. *Prog Transplant.* 2015 Jun; 25 (2): 182–188. doi: 10.7182/pit2015826. PMID: 26107280.
28. *Wang K, Xu X, Fan M.* Induction therapy of basiliximab versus antithymocyte globulin in renal allograft: a systematic review and meta-analysis. *Clin Exp Nephrol.* 2018 Jun; 22 (3): 684–693. doi: 10.1007/s10157-017-1480-z. Epub 2017 Oct 6. PMID: 28986715.

29. *Maluccio M, Sharma V, Lagman M, Vyas S, Yang H, Li B et al.* Tacrolimus enhances transforming growth factor-beta1 expression and promotes tumor progression. *Transplantation.* 2003 Aug 15; 76 (3): 597–602. doi: 10.1097/01.TP.0000081399.75231.3B. PMID: 12923450.
30. *Engels EA, Jennings L, Kemp TJ, Chaturvedi AK, Pinto LA, Pfeiffer RM et al.* Circulating TGF-β1 and VEGF and risk of cancer among liver transplant recipients. *Cancer Med.* 2015 Aug; 4 (8): 1252–1257. doi: 10.1002/cam4.455. Epub 2015 Apr 27. PMID: 25919050.
31. *Dantal J, Hourmant M, Cantarovich D, Giral M, Blancho G, Dreno B et al.* Effect of long-term immunosuppression in kidney-graft recipients on cancer incidence: Randomized comparison of two cyclosporin regimens. *Lancet.* 1998 Feb 28; 351 (9103): 623–628. doi: 10.1016/S0140-6736(97)08496-1. PMID: 9500317.
32. *Ghidini M, Petrelli F, Ghidini A, Tomasello G, Hahne JC, Passalacqua R et al.* Clinical development of mTor inhibitors for renal cancer. *Expert Opin Investig Drugs.* 2017 Nov; 26 (11): 1229–1237. doi: 10.1080/13543784.2017.1384813. Epub 2017 Oct 3. PMID: 28952411.
33. *Hall EC, Engels EA, Pfeiffer RM, Segev DL.* Association of antibody induction immunosuppression with cancer after kidney transplantation. *Transplantation.* 2015 May; 99 (5): 1051–1057. doi: 10.1097/TP.0000000000000449. PMID: 25340595.
34. *Stucker F, Marti HP, Hunger RE.* Immunosuppressive drugs in organ transplant recipients-rationale for critical selection. *Curr Probl Dermatol.* 2012; 43: 36–48. doi: 10.1159/000335148. Epub 2012 Feb 17. PMID: 22377918.
35. *Campistol JM, Cuervas-Mons V, Manito N, Almenar L, Arias M, Casafont F et al.* New concepts and best practices for management of pre- and post-transplantation cancer. *Transplant Rev (Orlando).* 2012 Oct; 26 (4): 261–279. doi: 10.1016/j.trre.2012.07.001. Epub 2012 Aug 15. PMID: 22902168.
36. *Nguyen LS, Vautier M, Allenbach Y, Zahr N, Benveniste O, Funck-Brentano C et al.* Sirolimus and mTOR Inhibitors: A Review of Side Effects and Specific Management in Solid Organ Transplantation. *Drug Saf.* 2019 Jul; 42 (7): 813–825. doi: 10.1007/s40264-019-00810-9. PMID: 30868436.
37. *Populo H, Lopes JM, Soares P.* The mTOR signalling pathway in human cancer. *Int J Mol Sci.* 2012; 13 (2): 1886–1918. doi: 10.3390/ijms13021886. Epub 2012 Feb 10. PMID: 22408430.
38. *Lamberti G, Brighi N, Maggio I, Manuzzi L, Peterle C, Ambrosini V et al.* The Role of mTOR in Neuroendocrine Tumors: Future Cornerstone of a Winning Strategy? *Int J Mol Sci.* 2018 Mar 6; 19 (3): 747. doi: 10.3390/ijms19030747. PMID: 29509701.
39. *Au EH, Chapman JR, Craig JC, Lim WH, Teixeira-Pinto A, Ullah S et al.* Overall and site-specific cancer mortality in patients on dialysis and after kidney transplant. *J Am Soc Nephrol.* 2019 Mar; 30 (3): 471–480. doi: 10.1681/ASN.2018090906. Epub 2019 Feb 14. PMID: 30765426.
40. *Cognard N, Anglicheau D, Gatault P, Girerd S, Essig M, Hurault de Ligny B et al.* Recurrence of Renal Cell Cancer After Renal Transplantation in a Multicenter French Cohort. *Transplantation.* 2018 May; 102 (5): 860–867. doi: 10.1097/TP.0000000000002009. PMID: 29215458.
41. *Hsieh JJ, Purdue MP, Signoretti S, Swanton C, Albiges L, Schmidinger M et al.* Renal cell carcinoma. *Nat Rev Dis Primers.* 2017 Mar 9; 3: 17009. doi: 10.1038/nrdp.2017.9. PMID: 28276433.
42. *Bahadoram S, Davoodi M, Hassanzadeh S, Bahadoram M, Barahman M, Mafakher L.* Renal cell carcinoma: an overview of the epidemiology, diagnosis, and treatment. *G Ital Nefrol.* 2022 Jun 20; 39 (3): 20–22. PMID: 35819037.
43. *Tillou X, Doerfler A, Collon S, Kleinclauss F, Patard JJ, Badet L et al. De novo* kidney graft tumors: results from a multicentric retrospective national study. *Am J Transplant.* 2012 Dec; 12 (12): 3308–3315. doi: 10.1111/j.1600-6143.2012.04248.x. Epub 2012 Sep 7. PMID: 22959020.
44. *Billis A, Freitas LL, Costa LB, Barreto IS, Asato MA, Araujo KS et al.* Genitourinary Malignancies in Transplant or Dialysis Patients: The Frequency of Two Newly Described 2016 World Health Organization Histopathologic Types. *Transplant Proc.* 2017 Oct; 49 (8): 1783–1785. doi: 10.1016/j.transproceed.2017.06.035. PMID: 28923625.
45. *Hubatsch M, Peters R, Maxeiner A, El-Bandar N, Weinberger S, Friedersdorff F.* Nephron Sparing Surgery in Renal Allograft in Recipients with *de novo* Renal Cell Carcinoma: Two Case Reports and Review of the Literature. *Urol Int.* 2020; 104 (11–12): 997–999. doi: 10.1159/000509292. Epub 2020 Sep 23. PMID: 32966984.
46. *Song Y, Zheng J, Guo S, Fan L.* An intracapsular nephrectomy for the acquired cystic disease-associated renal cell carcinoma in renal transplant allograft: A clinical case report. *Medicine (Baltimore).* 2021 May 14; 100 (19): 258. doi: 10.1097/MD.0000000000025858. PMID: 34106631.
47. *Saparbay J, Assykbayev M, Abdugafarov S.* Chromophobe Renal Cell Carcinoma of a Renal Allograft. *Am J Case Rep.* 2021 Oct 8; 22: 933168. doi: 10.12659/AJCR.933168. PMID: 34620815.
48. *Casuscelli J, Weinhold N, Gundem G, Wang L, Zabor EC, Drill E et al.* Genomic landscape and evolution of metastatic chromophobe renal cell carcinoma. *JCI Insight.* 2017 Jun 15; 2 (12): e92688. doi: 10.1172/jci.insight.92688. PMID: 28614790.
49. *Zahran MH, Soltan MA, Kamal AI, Abdelrahim M, Fakhreldin I, Osman Y et al. De novo* chromophobe renal cell carcinoma in the graft three decades after renal transplantation in a patient with a history of three renal transplants. *Saudi J Kidney Dis Transpl.* 2020 Jan-Feb; 31 (1): 271–275. doi: 10.4103/1319-2442.279952. PMID: 32129224.

50. *Dincer E, Ipek OM, Kayipmaz SS, Akca O.* Solid Renal Mass in a Transplanted Allograft Kidney: Mucinous Tubular and Spindle Cell Renal Cell Carcinoma. *J Coll Physicians Surg Pak.* 2022 Aug; 32 (8): 192–194. doi: 10.29271/jcpsp.2022.Supp2.S192. PMID: 36210692.
51. *Pagano D, Francesco F, Rosa L, Nwaiwu CA, Petri SL, Gruttadauria S.* Oncocytoma managed by active surveillance in a transplant allograft kidney: a case report. *World J Surg Oncol.* 2018 Jul 2; 16 (1): 123. doi: 10.1186/s12957-018-1426-2. PMID: 29966524.
52. *Kim CS, Choi SJ, Kim SS, Suh SH, Bae EH, Ma SK et al.* An anastomosing hemangioma mimicking a renal cell carcinoma in a kidney transplant recipient: a case report. *BMC Nephrol.* 2021 Jul 13; 22 (1): 262. doi: 10.1186/s12882-021-02467-y. PMID: 34256731.
53. *Rotman S, Deruaz C, Venetz JP, Chaubert P, Benhattar J, Meuwly JY et al. De novo* concurrent papillary renal cell carcinoma and angiomyolipoma in a kidney allograft: evidence of donor origin. *Hum Pathol.* 2006 Apr; 37 (4): 481–487. doi: 10.1016/j.humpath.2005.11.024. PMID: 16564925.
54. *Boix R, Sanz C, Mora M, Quer A, Beyer K, Musulen E et al.* Primary renal cell carcinoma in a transplanted kidney: genetic evidence of recipient origin. *Transplantation.* 2009 Apr 15; 87 (7): 1057–1061. doi: 10.1097/TP.0b013e31819d1e5f. PMID: 19352128.
55. *Paradis V, Dargere D, Bonvoust F, Rubbia-Brandt L, Ba N, Bioulac-Sage P et al.* Clonal analysis of micronodules in virus C-induced liver cirrhosis using laser capture microdissection (LCM) and HUMARA assay. *Lab Invest.* 2000 Oct; 80 (10): 1553–1559. doi: 10.1038/labinvest.3780165. PMID: 11045572.
56. *Isaev TK.* Renal cell carcinoma of the transplanted kidney. [Dissertation]. M., 2023; 162.
57. *Tillou X, Guleryuz K, Collon S, Doerfler A.* Renal cell carcinoma in functional renal graft: Toward ablative treatments. *Transplant Rev (Orlando).* 2016 Jan; 30 (1): 20–26. doi: 10.1016/j.trre.2015.07.001. PMID: 26318289.
58. *Vasisth G, Kapoor A, Piercey K, Lambe S.* Renal cell carcinoma in renal allograft: Case series and review of literature. *Urol Ann.* 2018 Apr-Jun; 10 (2): 229–232. doi: 10.4103/UA.UA_66_17. PMID: 29719341.

The article was submitted to the journal on 08.04.2024

DOI: 10.15825/1995-1191-2024-4-69-76

A RARE CASE OF TRANSPLANT HEPATECTOMY FOR METACHRONOUS COLORECTAL CANCER METASTASIS (*DE NOVO*)

V.E. Zagainov[1, 3], N.M. Kiselev[1, 3], D.V. Komarov[2], S.A. Vasenin[2], E.A. Ashimov[1, 3], D.S. Myalik[3], S.V. Gamayunov[1, 3], S.V. Romanov[2], E.N. Ryabova[1, 2]

[1] Privolzhsky Research Medical University, Nizhniy Novgorod, Russian Federation
[2] Privolzhsky District Medical Center, Nizhny Novgorod, Russian Federation
[3] Nizhny Novgorod Regional Clinical Oncology Center, Nizhny Novgorod, Russian Federation

In the presented case, a patient who underwent liver transplant procedure for cirrhosis resulting from chronic hepatitis C was diagnosed with colorectal cancer 12 years after the operation. A combined treatment plan consisting of right hemicolectomy followed by nine cycles of adjuvant polychemotherapy using the FOLFOX6 regimen was performed. Seven months following the conclusion of treatment, 22×35 mm foci in segment 8 was detected as a sign of metastatic liver disease. The patient had a transplant hepatectomy. At present, the relapse-free survival is 22 months.

Keywords: liver transplantation, transplant hepatectomy, cirrhosis, colorectal cancer, liver metastasis.

INTRODUCTION

The number of organ transplant recipients continues to grow, reflecting significant advancements in transplant care within our country. According to the 15th Report from the Registry of the Russian Transplant Society, approximately 21,969 organ recipients were under medical follow-up in Russia by the end of 2022 – equivalent to 151.0 per 1 million population [1]. As clinical experience in managing these patients increases, so does the length of their post-transplant follow-up. However, the use of immunosuppressive therapy, an essential component of post-transplant care, remains a known risk factor for the development of malignancies at various time points after surgery [2].

Immunosuppressive therapy following organ transplantation compromises the recipient's ability to control viral infections, thereby increasing the risk of infection-associated malignancies such as non-Hodgkin's lymphoma, Kaposi's sarcoma, liver cancer, and cervical cancer. Certain immunosuppressive agents, particularly calcineurin inhibitors and azathioprine, have been shown to promote *de novo* carcinogenesis through mechanisms that extend beyond their immunosuppressive effects. The rising average age of transplant recipients further contributes to the overall increased risk of malignancy. In liver transplantation (LT) for hepatocellular carcinoma (HCC), tumor recurrence remains a significant concern. It is essential to differentiate between post-transplant recurrence of the primary tumor and the emergence of *de novo* malignancies. Less frequently, cancer may arise from latent malignancies in the donor that went undetected prior to organ procurement. However, current evidence suggests that the risk of donor-derived cancer transmission is extremely low – estimated at no more than 0.05% [3].

In Russian literature, studies addressing the risk of malignant neoplasms in transplant recipients are extremely limited [4]. In contrast, the international literature contains a substantially greater number of studies exploring the risk factors, incidence, and types of malignancies that occur following organ transplantation. Malignant tumors diagnosed in transplant recipients are more aggressive. Median survival rates for cancers such as colorectal, lung, breast, prostate, and bladder cancer are significantly lower in transplant patients compared to the general population [5–8].

A 2021 Mayo Clinic study examined the risk and timing of the most common gastrointestinal (GI) malignancies – particularly colorectal cancer (CRC) and pancreatic cancer – in liver transplant recipients, with the aim of optimizing screening strategies for this population. The study analyzed data from the United Network for Organ Sharing (UNOS) on the incidence of malignancies over a 20-year period (1997–2017) in post-transplant patients compared to the general population. A total of 866 *de novo* GI malignancies were identified, including 405 cases of CRC. The highest incidence of CRC was observed among recipients with primary sclerosing cholangitis, as well as in recipients over the age of 50 with cirrhosis due to nonalcoholic steatohepatitis, HCC, or cholangiocarcinoma. These findings help define a high-risk group of liver transplant recipients who may benefit

Corresponding author: Elena Ryabova. Address: 20a, Marshal Voronov str., Nizhny Novgorod, 603074, Russian Federation. Phone: (951) 919-78-25. E-mail: ryabova__elena@mail.ru

from more intensive and individualized CRC screening protocols [9].

A 2021 study from South Korea analyzed 8,734 liver and kidney recipients, 66 of whom were diagnosed with *de novo* CRC. The incidence of *de novo* CRC in liver recipients was 3.1-fold higher in males and 2.25-fold higher in females. *De novo* CRC was diagnosed in 13.6% of patients within the first year after surgery, in 31.8% between 1 and 5 years, and in 54.6% more than 5 years after surgery [10].

An emerging area of particular clinical interest is the occurrence of CRC metastases in transplanted livers. The management and treatment strategies for such cases continue to be a subject of active research.

The world's first documented case of CRC metastasis in a transplanted liver was reported by Spanish authors in 2017. The patient was diagnosed with a well-differentiated colon adenocarcinoma 12 years after undergoing LT. Following colon resection, the patient's immunosuppressive regimen was modified to include an mTOR proliferative signaling inhibitor (everolimus). Six months later, follow-up imaging revealed metastatic lesions in segments IV and VII of the liver graft. The patient subsequently underwent a left hemihepatectomy combined with radiofrequency ablation of the lesion in segment VII [11].

In light of such occurrences, a 15-year follow-up case of a liver transplant recipient from our own clinical practice presents particular interest and is worthy of detailed discussion.

CASE DESCRIPTION

A 67-year-old male patient (52 years old at the time of LT) underwent orthotopic LT from a deceased donor on August 8, 2009, due to hepatitis C virus (HCV)-induced liver cirrhosis, classified as Child-Pugh class C. The indication for transplantation included decompensated cirrhosis with portal hypertension, grade 1–2 esophageal varices, splenomegaly with hypersplenism, and ascites. The postoperative period was uneventful.

The patient was initiated on standard immunosuppressive therapy with cyclosporine at a dose of 75 mg twice daily. In October 2009, routine biochemical testing revealed elevated liver enzyme levels. A liver biopsy was performed, confirming acute graft rejection. Glucocorticoid pulse therapy was administered, with a total dose of 2000 mg.

A month later, under the influence of glucocorticoid therapy, an increase in the patient's HCV viral load was observed. As a result, antiviral therapy with pegylated interferons combined with ribavirin was initiated in December 2009. A delayed virologic response was achieved by June 2010.

In August 2010, a protocol biopsy of the liver graft revealed moderate fibrosis, corresponding to F2 on the Knodell, METAVIR, and Ishak scoring systems. However, six months after completing antiviral therapy, in December 2010, HCV reappeared in the bloodstream.

From May 27 to July 21, 2016, the patient was hospitalized due to graft dysfunction caused by severe acute rejection, confirmed by histological examination. Two courses of intravenous methylprednisolone pulse therapy were administered. In response to ongoing graft dysfunction, immunosuppressive therapy was modified – cyclosporine was discontinued and replaced with tacrolimus at a dose of 2.5 mg twice daily. Following clinical improvement, the patient was discharged for continued outpatient follow-up.

In the autumn of 2016, the patient underwent antiviral therapy for hepatitis C using a regimen of direct-acting antivirals (DAAs), specifically sofosbuvir and ledipasvir, administered over a 6-month course. Since the initiation of DAA therapy, hepatitis C RNA has remained undetectable in the blood by polymerase chain reaction (PCR).

In September 2017, the patient presented with severe generalized weakness, jaundice, and itching. Diagnostic evaluation revealed an anastomotic biliary stricture causing obstructive jaundice. Management was staged: initially, percutaneous transhepatic cholecystostomy was performed under ultrasound guidance for external biliary drainage, aiming to decompress the biliary system and reduce bilirubin levels. Following stabilization, a Roux-en-Y hepaticojejunostomy was performed on September 17, 2017.

The postoperative period was complicated by intra-abdominal bleeding and the formation of an abdominal hematoma, necessitating multiple relaparotomies and abdominal cavity sanitation procedures. The patient developed sepsis, which was managed successfully with intensive antibacterial therapy. After stabilization, the patient was discharged and has since been monitored on an outpatient basis.

In January 2021, following a COVID-19 infection, a routine follow-up examination revealed a decrease in the patient's hemoglobin level to 89 g/L for the first time. In accordance with the diagnostic protocol for anemia of unclear etiology, standard tests were initiated. Video-guided esophagogastroduodenoscopy showed no abnormalities. However, video-guided colonoscopy identified a tumor in the hepatic flexure of the colon (Fig. 1). A biopsy was performed, and histological analysis confirmed a moderately differentiated adenocarcinoma of the colon.

A computed tomography (CT) scan of the abdomen and pelvis revealed thickening of the colonic wall in the region of the hepatic flexure, with no evidence of additional focal pathology in the abdomen. A chest CT scan showed no signs of pulmonary lesions. Tumor marker levels were as follows: carbohydrate antigen (CA) 19-9 at 15.4 U/mL and carcinoembryonic antigen (CEA) at 2.28 ng/mL. Based on clinical and histological findings, the patient was diagnosed with colon cancer of the hepatic flexure: cT4aN0M0 G2 (moderately differentiated

adenocarcinoma), corresponding to stage IIB, clinical group 2. Immunosuppressive therapy was modified by reducing the dose of tacrolimus and introducing everolimus.

On December 02, 2021, the patient underwent radical surgical treatment – extended right hemicolectomy, D3 lymphadenectomy. Histological examination of the tumor: moderately differentiated adenocarcinoma pT4aN1c.

After surgical treatment, the patient underwent 9 cycles of adjuvant polychemotherapy (PCT) using the FOLFOX6 regimen. This included oxaliplatin (85 mg/m^2 administered intravenously over 2 hours on day 1), calcium folinate (400 mg/m^2 intravenously over 2 hours), followed by an intravenous bolus of fluorouracil (400 mg/m^2), and a continuous 46-hour infusion of fluorouracil (total dose 2400 mg/m^2, 1200 mg/m^2 per day). All PCT cycles were completed without dose reduction by August 2021.

During a routine follow-up examination on March 22, 2022 – seven months after completing chemotherapy – an abdominal CT scan revealed a mass in the right lobe of the liver graft, measuring 22×35 mm (Fig. 2).

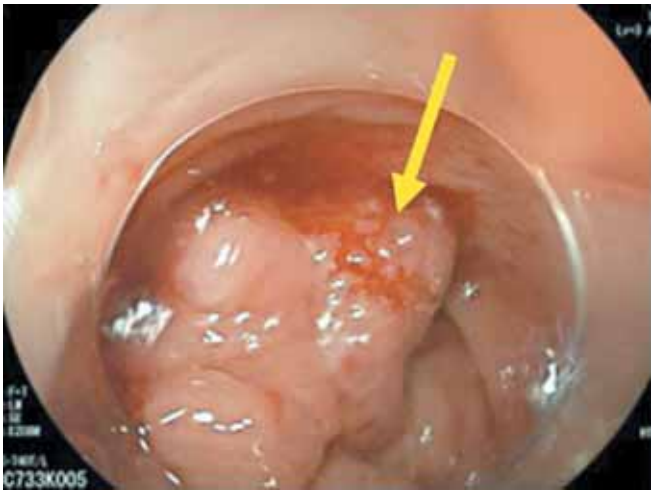

Fig. 1. Video colonoscopy. Hepatic flexure colon cancer in a patient (arrow)

A PET-CT scan performed on April 7, 2022 (Fig. 3) revealed a secondary lesion in the liver graft, demonstrating increased metabolic activity with a maximum standardized uptake value (SUVmax) of 5.61. No other hypermetabolic foci were detected.

As part of the diagnostic protocol, the patient underwent video colonoscopy on April 11, 2022. The findings were consistent with status post right hemicolectomy, and no focal pathology was observed. Blood tumor marker levels were as follows: CA 19-9 at 20.1 U/mL and CEA at 4.55 ng/mL. The Fong Clinical Risk Score for colorectal cancer recurrence was 2, indicating an estimated one-year survival of 89% and a 5-year survival of 40% following metastasectomy.

On May 16, 2022, the patient underwent atypical resection of liver segment 8. Intraoperatively, the liver appeared steatotic. A focal lesion measuring 25×35 mm was identified on the diaphragmatic surface of segment 8. Intraoperative ultrasound of the liver graft confirmed the absence of additional focal lesions (Fig. 4).

Histopathological examination of the resected liver specimen confirmed the diagnosis of metastatic colorectal adenocarcinoma. The demarcated edge located in non-tumorous liver tissue (R0) (Fig. 5).

Molecular genetic analysis of the extracted DNA revealed an activating G13D mutation in exon 2 (codon 12) of the KRAS gene (NM_033360.3), which is known to confer resistance to anti-epidermal growth factor receptor (EGFR) therapy.

In light of these findings, immunosuppressive therapy was adjusted to monotherapy with everolimus, a proliferation signal inhibitor in the mammalian target of rapamycin (mTOR) drug class.

The patient was discharged from the hospital on postoperative day 7 in satisfactory condition. However, on day 14, his condition deteriorated with the onset of tachyarrhythmia. He was urgently admitted to a city cardiology on-call hospital with an episode of paroxysmal atrial fibrillation, which was managed conservatively.

During further evaluation, right-sided hydrothorax was identified. Repeated pleural punctures were perfor-

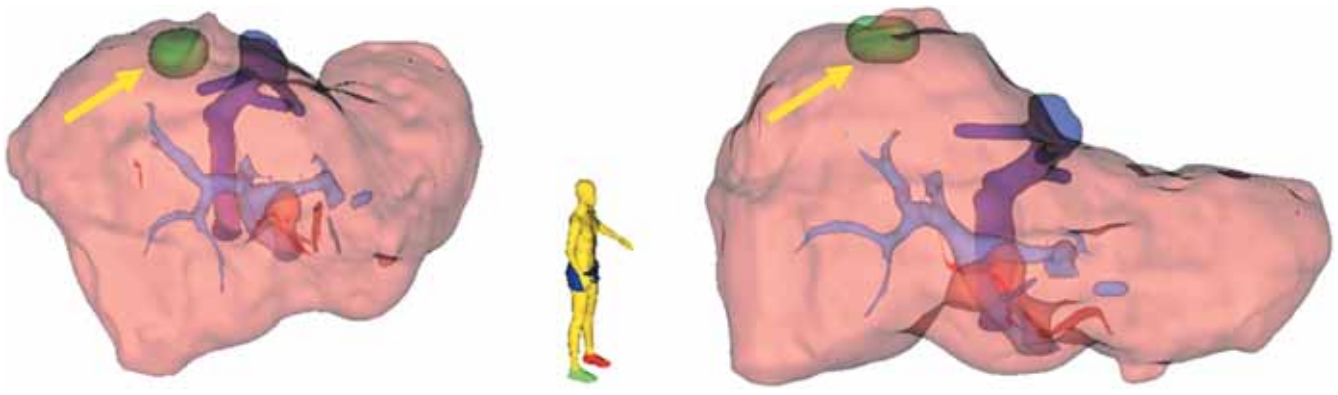

Fig. 2. CT modeling of a focal liver graft mass in a patient. Metastasis is indicated by an arrow

med, and serous fluid was evacuated. Subsequently, the patient developed pleural empyema accompanied by signs of sepsis. In this connection, he was transferred to an oncologic dispensary for inpatient management.

From June 23 to August 1, 2022, he underwent treatment for pleural empyema and hemothorax, which included drainage and sanitation of the right pleural cavity, along with antibacterial therapy. He experienced

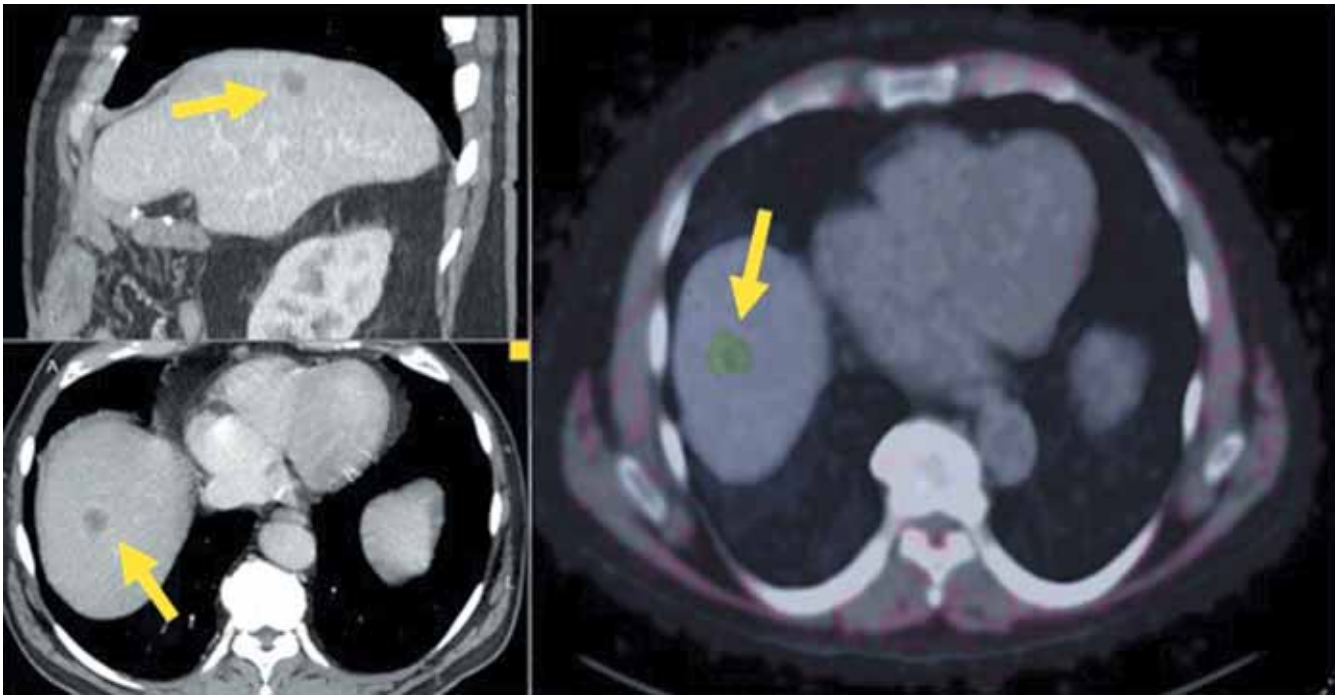

Fig. 3. Computed tomography and positron emission tomography images in a patient. Metastasis is indicated by an arrow

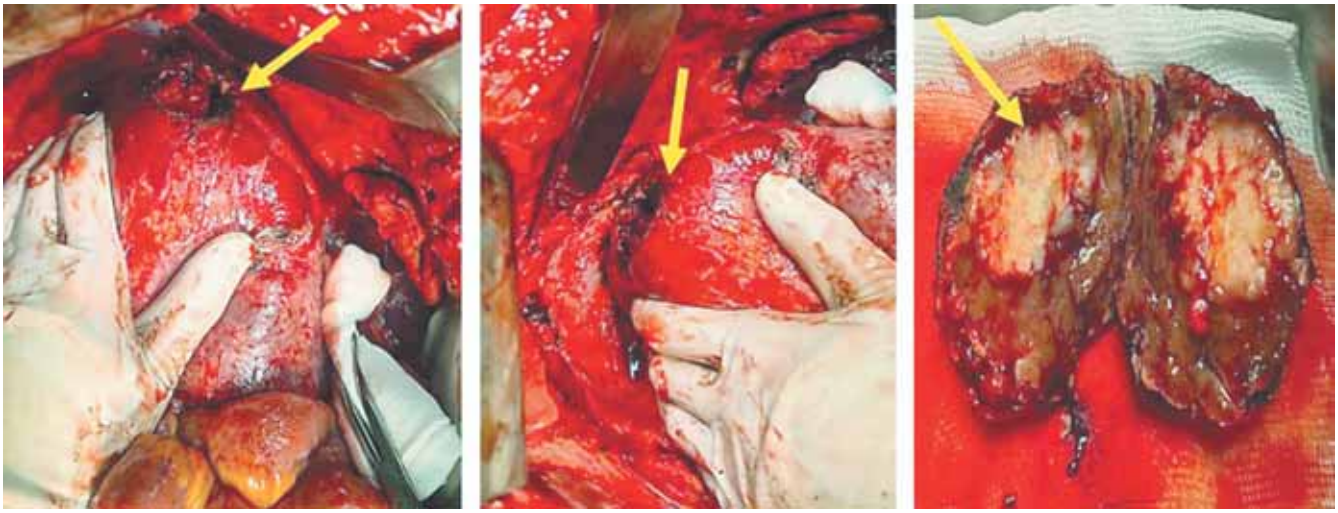

Fig. 4. Intraoperative photo (arrows indicate liver graft metastasis)

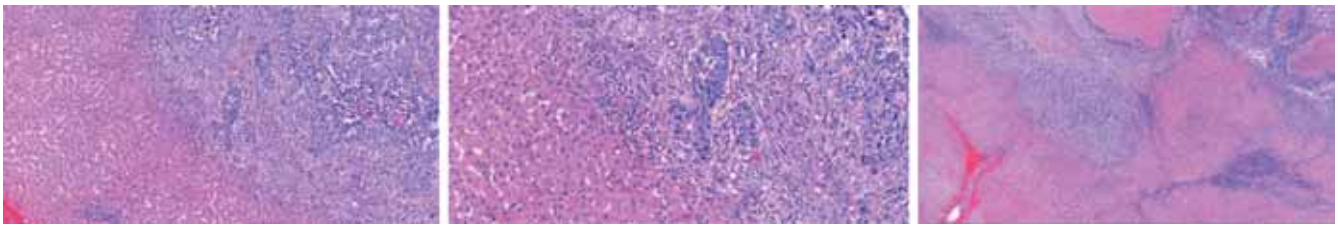

Fig. 5. Morphological examination of the removed liver graft metastasis

a prolonged febrile period with body temperatures reaching 38–39 °C. Once his condition stabilized, he was discharged for outpatient follow-up.

At the end of August 2022, the patient again developed a fever reaching 38.9 °C. From September 5 to October 11, 2022, he underwent inpatient treatment in the surgical organ transplant department, Privolzhsky District Medical Center, presenting with right-sided hydropneumothorax and pneumonia of the upper lobe of the left lung. Despite antibacterial therapy with Thienam (2 g/day), the fever persisted. Microbiological culture of the right pleural cavity revealed Acinetobacter baumannii at a concentration of 10^5 CFU/mL. Following a change in antibiotic therapy to Baccefort (4 g/day), the patient's fever subsided, and he was discharged in satisfactory condition.

At present, the patient remains under regular outpatient follow-up. Colonoscopy, as well as abdominal and chest CT scans, are conducted according to established surveillance protocols. As of the time of writing this paper, there is no evidence of recurrence of the oncologic process, and liver graft function remains satisfactory. The duration of follow-up since the transplant hepatectomy is 22 months.

DISCUSSION

Liver transplant recipients face an elevated risk of developing *de novo* malignancies due to prolonged immunosuppressive therapy required to prevent acute and chronic graft rejection. The overall incidence of CRC in this population is higher compared to the general population. Although current strategies aimed at reducing immunosuppressive load have helped mitigate the risk of *de novo* cancers, they do not fully eliminate the potential for graft fibrosis and rejection.

A French national study found that 13.45% (1,480) of 11,004 adult patients who received a liver transplant between 2000 and 2013 developed a *de novo* malignancy. The most common types of *de novo* malignancy were: hematological malignancy (22.36%), non-melanoma skin cancer (19.53%), and lung cancer (12.36%); CRC (4.9%) ranked 6th [12]. According to a systematic review and meta-analysis including 29 studies, the risk of developing CRC in patients who have had a liver transplant is 2.6 times (95% CI 1.7–4.1) higher than in the general population, and the risk of *de novo* cancer gradually increases starting from the first year after transplantation and peaks after 6–10 years of follow-up [13, 14]. In this regard, the International Liver Transplantation Society (ILTS) at the ILTS-SETH conference (2022) adopted a consensus on prevention and early detection of *de novo* malignancies after liver transplantation with recommendations to perform colonoscopy 1 year after transplantation and then 3–5 years later. Earlier and more frequent screening is indicated for high-risk patients (liver transplantation for hepatocellular carcinoma, primary sclerosing cholangitis, over 50 years of age, with a history of colon polyps) [15].

CRC is still the third most commonly diagnosed malignancy in the general population, accounting for 7.2% [16].

Long-term survival of liver recipients and the increasing trend for patients to receive a donor organ at an older age have added additional risks of developing CRC. CRC after LT is more often a right-sided lesion, is aggressive, and is associated with a higher rate of metastasis and poor survival [17].

Specialized treatment for relapsed or *de novo* cancer in transplant recipients should adhere to general oncologic principles as outlined in current clinical guidelines [18].

In the presented clinical case, the patient underwent definitive surgical intervention as the initial step, which remains the optimal treatment approach for a primary localized colorectal malignancy. Based on histopathological analysis of the resected specimen, the disease was restaged as pT4aN1c, warranting the initiation of adjuvant chemotherapy using the FOLFOX regimen to reduce the risk of disease progression [19].

Large-scale studies have demonstrated that adjuvant chemotherapy significantly improves both overall survival and progression-free survival in patients with stage $N \geq 1$ or stage T3N0M0 colorectal cancer [20, 21]. Notably, adjuvant chemotherapy can be administered effectively alongside standard immunosuppressive therapy without the need for dose reduction [22].

In the general population, 30–50% of CRC patients develop liver metastases [23]. In the present clinical case, dynamic follow-up revealed metastatic lesions within the liver graft. Transplant hepatectomy, at this stage of surgical advancement, remains a relatively rare procedure. A significant contribution to the understanding of liver resections in transplant recipients was provided by the Charité Clinic in 2020. Between 2004 and 2017, the clinic performed 4,100 liver resections, of which 14 were in patients who had previously undergone LT (0.34%). The primary indications for liver resection after transplantation included recurrent combined hepatocellular-cholangiocarcinoma and post-LT biliary and vascular complications leading to liver abscesses. However, metastatic lesions developing in a transplanted liver in the context of a *de novo* cancer are extremely rare.

According to European, American, and Asian guidelines, surgical resection is the recommended first-line treatment for resectable colorectal liver metastases, given its high efficacy compared to other methods [24–27]. Following these clinical guidelines, the patient underwent surgical treatment, specifically an R0 liver resection. Early diagnosis and radical treatment in accordance with established standards have resulted in a favorable long-term outcome, with the patient remaining recurrence-free for 22 months.

CONCLUSION

As the number of organ recipients increases, along with the age of recipients and the duration since transplantation, the risks of malignancies also rise. These trends are becoming more prominent in contemporary medical practice.

To detect *de novo* cancers early in solid organ recipients, regular follow-ups with both transplant surgeons and oncologists are essential. Upon the detection of cancer, immunosuppressive therapy should be switched to mTOR proliferation signal inhibitors. The treatment of malignancies in organ transplant recipients should adhere to general oncological principles as outlined in clinical guidelines. While a history of solid organ transplantation in cancer patients necessitates adjustments to immunosuppression, it does not limit the use of systemic polychemotherapy.

This clinical case highlights the need for a multidisciplinary approach in managing patients after organ transplantation, emphasizing the collaborative efforts of transplant specialists, hepatologists, infectious disease experts, oncologists, chemotherapy specialists, and other healthcare professionals.

The authors declare no conflict of interest.

REFERENCES

1. *Gautier SV, Khomyakov SM*. Organ donation and transplantation in the Russian Federation in 2022. 15th Report from the Registry of the Russian Transplant Society. *Russian Journal of Transplantology and Artificial Organs*. 2023; 25 (3): 8–30. https://doi.org/10.15825/1995-1191-2023-3-8-30.
2. *D'Arcy M, Coghill A, Lynch C, Koch L, Li J, Pawlish K et al*. Survival after a cancer diagnosis among solid organ transplant recipients in the United States. *Cancer*. 2019 Mar 15; 125 (6): 933–942. doi: 10.1002/cncr.31782.
3. *Lapointe M, Kerbaul F, Meckert F, Cognard N, Mathelin C, Lodi M*. Breast cancer and organ transplantation: Systematic review and meta-analysis. *Gynecol Obstet Fertil Senol*. 2023 Jan; 51 (1): 60–72. doi: 10.1016/j.gofs.2022.11.002.
4. *Babkina AV, Khubutiya MSh*. Development of oncological diseases after organ transplantation. *Transplantologiya. The Russian Journal of Transplantation*. 2022; 14 (4): 476–487. https://doi.org/10.23873/2074-0506-2022-14-4-476-487.
5. *Engels EA, Pfeiffer RM, Fraumeni JF Jr, Kasiske BL, Israni AK, Snyder JJ et al.* Spectrum of cancer risk among US solid organ transplant recipients. *JAMA*. 2011; 306 (17): 1891–1901. doi: 10.1001/jama.2011.1592.
6. *Collett D, Mumford L, Banner NR, Neuberger J, Watson C.* Comparison of the incidence of malignancy in recipients of different types of organ: A UK Registry audit. *Am J Transplant.* 2010; 10: 1889–1896. doi: 10.1111/j.1600-6143.2010.03181.x.
7. *Vajdic CM, van Leeuwen MT.* Cancer incidence and risk factors after solid organ transplantation. *Int J Cancer*. 2009; 125: 1747–1754. doi: 10.1002/ijc.24439.
8. *Dameworth JL, Colburn L, Corrigan D, Driessen R, Chapple K, Gagliano RA et al*. Colorectal Cancer Prevention in Lung Transplant Recipients: The Need for an Enhanced Surveillance Protocol. *J Am Coll Surg*. 2021 May; 232 (5): 717–725. doi: 10.1016/j.jamcollsurg.2020.12.053.
9. *Nasser-Ghodsi N, Mara K, Watt KD*. *De novo* Colorectal and Pancreatic Cancer in Liver-Transplant Recipients: Identifying the Higher-Risk Populations. *Hepatology*. 2021 Aug; 74 (2): 1003–1013. doi: 10.1002/hep.31731. Epub 2021 Jun 21.
10. *Kim M, Kim CW, Hwang S, Kim YH, Lee JL, Yoon YS et al*. Characteristics and Prognosis of Colorectal Cancer after Liver or Kidney Transplantation. *World J Surg*. 2021 Oct; 45 (10): 3206–3213. doi: 10.1007/s00268-021-06219-9.
11. *Villegas Herrera MT, Becerra Massare A, Muffak Granero K*. Liver metastasis from colorectal cancer 12 years after liver transplantation. *Rev Esp Enferm Dig*. 2017 Mar; 109 (3): 236. doi: 10.17235/reed.2017.4507/2016.
12. *Altieri M, Sérée O, Lobbedez T, Segol P, Abergel A, Blaizot X et al.* Risk factors of *de novo* malignancies after liver transplantation: a French national study on 11004 adult patients. *Clin Res Hepatol Gastroenterol*. 2021 Jul; 45 (4): 101514. doi: 10.1016/j.clinre.2020.07.019. Epub 2021 Mar 11.
13. *Nicolaas JS, De Jonge V, Steyerberg EW, Kuipers EJ, Van Leerdam ME, Veldhuyzen-van Zanten SJO.* Risk of colorectal carcinoma in post-liver transplant patients: a systematic review and meta-analysis. *Am J Transplant*. 2010 Apr; 10 (4): 868–876. doi: 10.1111/j.1600-6143.2010.03049.x. PMID: 20420641.
14. *Taborelli M, Piselli P, Ettorre GM, Baccarani U, Burra P, Lauro A et al.* Survival after the diagnosis of *de novo* malignancy in liver transplant recipients. *Int J Cancer*. 2019 Jan 15; 144 (2): 232–239. doi: 10.1002/ijc.31782. Epub 2018 Oct 26.
15. *Colmenero J, Tabrizian P, Bhangui P, Pinato DJ, Rodríguez-Perálvarez ML, Sapisochin G et al*. *De novo* Malignancy After Liver Transplantation: Risk Assessment, Prevention, and Management-Guidelines From the ILTS-SETH Consensus Conference. *Transplantation*. 2022 Jan 1; 106 (1): e30–e45. doi: 10.1097/TP.0000000000003998. PMID: 34905760.
16. *Kaprin AD, Starinsky VV, Petrova GV*. Malignant neoplasms in Russia in 2022 (morbidity and mortality). M.: MNIOI im. P.A. Herzen – branch of the Federal State Budgetary Institution "National Medical Research Center of Radiology" of the Russian Ministry of Health, 2023.
17. *Sung H, Ferlay J, Siegel RL, Laversanne M, Soerjomataram I, Jemal A, Bray F.* Global cancer statistics 2020: GLOBOCAN estimates of incidence and mortality worldwide for 36 cancers in 185 countries. *CA Cancer J Clin*. 2021 May; 71 (3): 209–249. https://doi.org/10.3322/caac.21660. Epub 2021 Feb 4.

18. *Fedyanin MYu, Achkasov SI, Bolotina LV, Gladkov OA, Glebovskaya VV, Gordeev SS et al*. Practical recommendations for drug treatment of colon and rectosigmoid cancer. *Malignant tumors*. 2021; 11 (3s2-1): 330–372. https://doi.org/10.18027/2224-5057-2021-11-3s2-22.
19. *Argilés G, Tabernero J, Labianca R, Hochhauser D, Salazar R, Iveson T et al*. ESMO Guidelines Committee. Electronic address: clinicalguidelines@esmo.org. Localised colon cancer: ESMO Clinical Practice Guidelines for diagnosis, treatment and follow-up. *Ann Oncol*. 2020 Oct; 31 (10): 1291–1305. doi: 10.1016/j.annonc.2020.06.022.
20. *Grothey A, Sobrero AF, Shields AF, Yoshino T, Paul J, Taieb J et al*. Duration of Adjuvant Chemotherapy for Stage III Colon Cancer. *N Engl J Med*. 2018 Mar 29; 378 (13): 1177–1188. doi: 10.1056/NEJMoa1713709.
21. *Gray R, Barnwell J, McConkey C, Hills RK, Williams NS, Kerr DJ; Quasar Collaborative Group*. Adjuvant chemotherapy versus observation in patients with colorectal cancer: a randomised study. *Lancet*. 2007 Dec 15; 370 (9604): 2020–2029. doi: 10.1016/S0140-6736(07)61866-2.
22. *Chen J, Zhang C, Wu Y*. Does adjuvant chemotherapy improve outcomes in elderly patients with colorectal cancer? A systematic review and meta-analysis of real-world studies. *Expert Rev Gastroenterol Hepatol*. 2022 Apr; 16 (4): 383–391. doi: 10.1080/17474124.2022.2056014.
23. *Lin HS, Wan RH, Gao LH, Li JF, Shan RF, Shi J*. Adjuvant chemotherapy after liver transplantation for hepatocellular carcinoma: a systematic review and a meta-analysis. *Hepatobiliary Pancreat Dis Int*. 2015 Jun; 14 (3): 236–245. doi: 10.1016/s1499-3872(15)60373-3.
24. *Wang SH, Song L, Tang JY, Sun WP, Li Z*. Safety and long-term prognosis of simultaneous versus staged resection in synchronous colorectal cancer with liver metastasis: a systematic review and meta-analysis. *Eur J Med Res*. 2022 Dec 19; 27 (1): 297. doi: 10.1186/s40001-022-00937-z.
25. *Cervantes A, Adam R, Roselló S, Arnold D, Normanno N, Taïeb J et al*. ESMO Guidelines Committee. Electronic address: clinicalguidelines@esmo.org. Metastatic colorectal cancer: ESMO Clinical Practice Guideline for diagnosis, treatment and follow-up. *Ann Oncol*. 2023 Jan; 34 (1): 10–32. doi: 10.1016/j.annonc.2022.10.003.
26. *Bridgewater JA, Pugh SA, Maishman T, Eminton Z, Mellor J, Whitehead A et al.* New EPOC investigators. Systemic chemotherapy with or without cetuximab in patients with resectable colorectal liver metastasis (New EPOC): long-term results of a multicentre, randomised, controlled, phase 3 trial. *Lancet Oncol*. 2020 Mar; 21 (3): 398–411. doi: 10.1016/S1470-2045(19)30798-3. Epub 2020 Jan 31. PMID: 32014119; PMCID: PMC7052737.
27. *Morris VK, Kennedy EB, Baxter NN, Benson AB 3rd, Cercek A, Cho M et al*. Treatment of Metastatic Colorectal Cancer: ASCO Guideline. *J Clin Oncol*. 2023 Jan 20; 41 (3): 678–700. doi: 10.1200/JCO.22.01690.

The article was submitted to the journal on 18.03.2024

DOI: 10.15825/1995-1191-2024-4-77-89

FULMINANT EMPHYSEMATOUS PYELONEPHRITIS IN A TRANSPLANT KIDNEY (CLINICAL OBSERVATION AND LITERATURE REVIEW)

R.N. Trushkin[1, 2], S.S. Andreev[1], N.I. Belavina[1], T.K. Isaev[1], D.E. Okonskaya[1, 3], E.S. Stolyarevich[1, 4, 5], N.N. Klochkova[1, 6], M.A. Lysenko[1, 6]

[1] Municipal Clinical Hospital No. 52, Moscow, Russian Federation
[2] Peoples' Friendship University of Russia, Moscow, Russian Federation
[3] National Medical Research Center of Surgery, Moscow, Russian Federation
[4] Moscow State University of Medicine and Dentistry, Moscow, Russian Federation
[5] Shumakov National Medical Research Center of Transplantology and Artificial Organs, Moscow, Russian Federation
[6] Pirogov Russian National Research Medical University, Moscow, Russian Federation

Emphysematous pyelonephritis (EPN) is a necrotizing infection of the renal parenchyma and its surrounding areas that causes gas accumulation around the renal parenchyma, collecting system and surrounding tissues in the process of vital activity of several microorganisms. EPN occurs nearly exclusively in people with diabetes. Treatment strategies for EPN have evolved over the past 20 years, with minimally invasive procedures replacing nephrectomy, which has resulted in lower mortality rates (12.5–13%). EPN is rare in kidney transplant (KT) recipients and is characterized by a severe, often fulminant course with a high rate of adverse outcomes, which is determined primarily by background immunosuppressive therapy. There is no universally accepted consensus on the radiographic classification of EPN in KT recipients and its management. We present the first description of EPN in transplanted kidney in a 45-year-old woman with post-transplant diabetes, obesity and recurrent urinary tract infections. Massive antibiotic therapy (ABT), percutaneous nephrostomy, transplantectomy, renal replacement therapy, selective cytokine adsorption, and ventilatory support were all administered on the patient after she was admitted to the hospital with increasing clinical symptoms of sepsis and multiple organ failure. Death occurred on the fourth day after disease onset. The article examines 38 clinical cases from the English-language segment of the medical literature from the late 1970s to the present. EPN in KT recipients is characterized by the predominance of male gender, including among the deceased, rapid development of sepsis and acute kidney injury. There was no statistically significant difference in the frequency of emergency transplantectomies among surviving and deceased patients. Mortality was 28%. The issue of EPN in transplanted kidney requires more research and the development of optimal therapeutic plans, including surgical strategies.

Keywords: emphysematous pyelonephritis, renal graft, diabetes mellitus, transplantectomy, clinical case.

INTRODUCTION

Emphysematous pyelonephritis (EPN) is a rare, severe infection of the kidney that causes gas to accumulate in the tissues. It's characterized by a necrotizing inflammation of the renal parenchyma, collecting ducts, and surrounding tissues [1, 2]. Gas formation results from the metabolic activity of certain bacteria, including *Escherichia coli*, *Klebsiella pneumoniae* and some others, which primarily generate gas through glucose fermentation. Consequently, EPN predominantly occurs in patients with diabetes mellitus (DM). The current mortality rates for EPN in patients with native kidneys range from 12.5% to 13% [3, 4].

EPN in kidney transplant (KT) recipients is extremely rare, with only a few dozen cases reported worldwide to date. When it does occur, EPN in KT recipients is typically severe and fast-developing, leading to a high rate of unfavorable outcomes, including graft loss. Due to the limited number of reported cases, there is no established consensus on its diagnosis and management in KT recipients. We present the first documented case of EPN in a KT recipient in the Russian Federation.

Objective of the study: the aim of this study is to explore the clinical features and progression of EPN in KT recipients based on our case report and existing literature. We also seek to compare the radiologic classification approaches for EPN in native kidneys versus KT recipients and discuss modern strategies for patient management, including surgical interventions.

Corresponding author: Sergey Andreev. Address: 3/2, Pekhotnaya str., Moscow, 123182, Russian Federation.
Phone: (968) 075-89-39. E-mail: nerowolf@mail.ru

MATERIALS AND METHODS

This study presents a clinical case of EPN in a KT recipient with post-transplant diabetes mellitus (PTDM), obesity, and recurrent urinary tract infections (UTIs). The analysis includes initial clinical and laboratory data, the course of the disease, radiologic diagnostics, conservative and surgical treatments, and pathomorphological findings about the KT. Thirty-eight cases of EPN in KT recipients, reported from the late 1970s to the present, were reviewed and summarized from English-language medical literature.

CLINICAL CASE

A 46-year-old female patient was evaluated at a consultative and diagnostic nephrology center starting in 2017, following allogeneic kidney transplantation from a deceased donor. Her medical history includes end-stage renal failure due to chronic glomerulonephritis in 2016, which required treatment with hemodialysis. KT function was immediate, and she was placed on a triple-drug immunosuppressive therapy (IST) regimen (tacrolimus, mycophenolic acid, and methylprednisolone).

In the post-transplant period, the patient developed insulin-dependent diabetes mellitus with difficult-to-control hyperglycemia, as well as recurrent UTIs. The patient was hospitalized on three separate occasions and received multiple courses of antimicrobial therapy. Her baseline serum creatinine level remained stable, not exceeding 130 μmol/L. However, a sudden deterioration occurred on February 9, 2024, marked by a fever of up to 38.5 °C, pain localized to the KT area, worsening general weakness, nausea, repeated vomiting, and the onset of anuria.

She was initially admitted to a local hospital and, on February 10, 2024, was transferred to our clinic with a preliminary diagnosis of renal graft dysfunction. Upon admission, the above symptoms persisted, though her mental status remained unchanged.

Physical examination: height 155 cm, weight: 100 kg, body mass index (BMI): 41.6 kg/m^2, and stable hemodynamics.

Local findings: Marked palpation tenderness in the left iliac region (transplant zone), with edema of the surrounding soft tissues of the anterior abdominal wall.

Laboratory screening in the emergency unit revealed metabolic acidosis and hyperlactatemia. Additional findings included leukocytosis (14.86 × 10^9/L), hemoglobin 128 g/L, C-reactive protein (CRP) 37.5 mg/L, elevated serum creatinine at 256.4 μmol/L, plasma glucose 10.35 mmol/L, and glycated hemoglobin (HbA1c) at 9.9%. In light of acute kidney injury (AKI) and associated metabolic disorders, the patient was admitted to the intensive care unit (ICU). A contrast-enhanced multislice computed tomography (MSCT) scan was subsequently performed (Fig. 1).

Contrast-enhanced abdominal and pelvic MSCT (Fig. 1) revealed edema of the peritransplant and periureteral soft tissues. Gas bubbles were identified within the lumen of the renal pelvis and calyces of the allograft

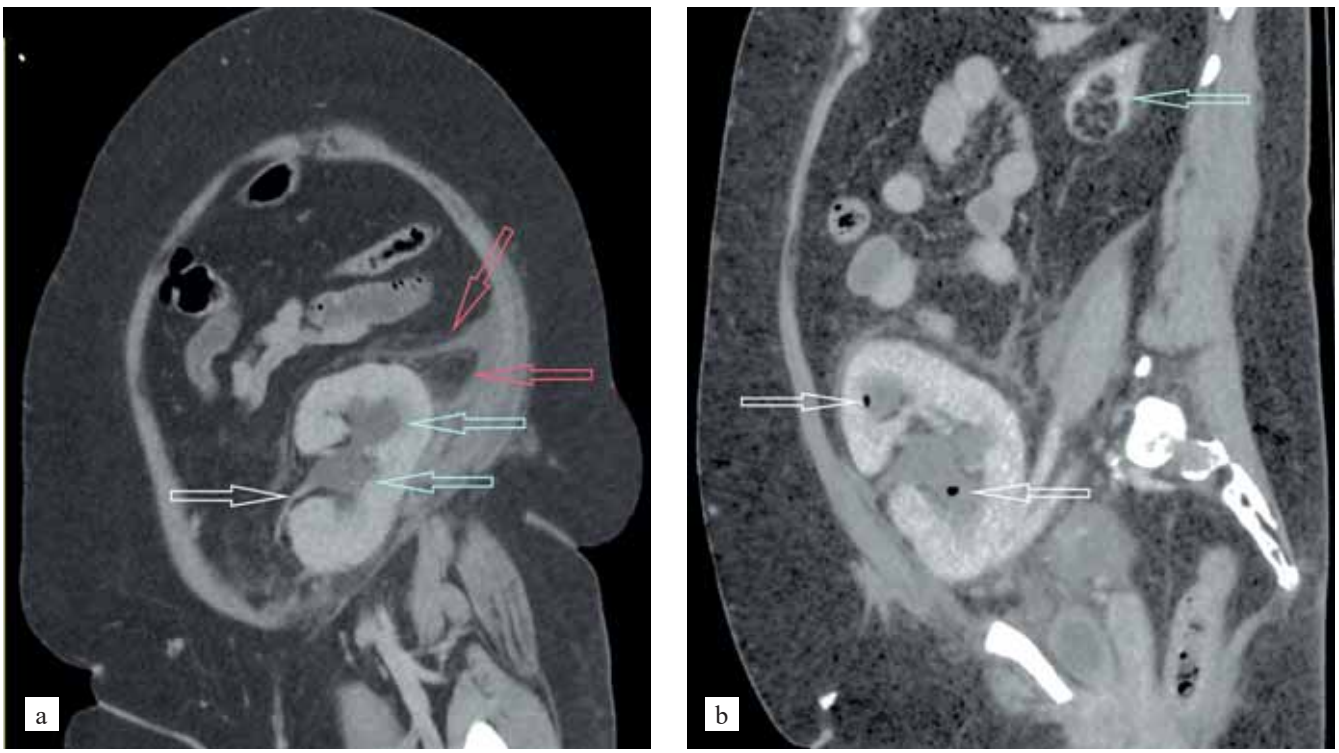

Fig. 1. Contrast-enhanced MSCT of abdominal and pelvic organs, venous phase: a, sagittal plane: gas bubbles in the kidney transplant calyxes (arrow), shriveled kidney (blue arrow); b, oblique plane: narrowing in the area of the ureteropelvic junction obstruction in kidney allograft (arrow), dilated calyces (blue arrow), perigraft tissue edema (red arrow)

(Fig. 1, a). A pronounced narrowing of the pelviureteric junction was observed, with high-density material within its lumen (Fig. 1, b), accompanied by dilatation of the pelvicalyceal system and a non-dilated ureter. The transplant parenchyma showed homogeneous contrast enhancement, with no signs of structural destruction. No excretion of contrast agent was observed during examination.

An emergency percutaneous nephrostomy (PCN) was performed, yielding urine mixed with mucous-purulent material. Given the high initial risk factors for multidrug-resistant flora – including decompensated diabetes mellitus, obesity, ongoing IST, prior antimicrobial treatment, recurrent UTIs, and recent hospitalization – empirical antibiotic therapy with piperacillin/tazobactam was initiated.

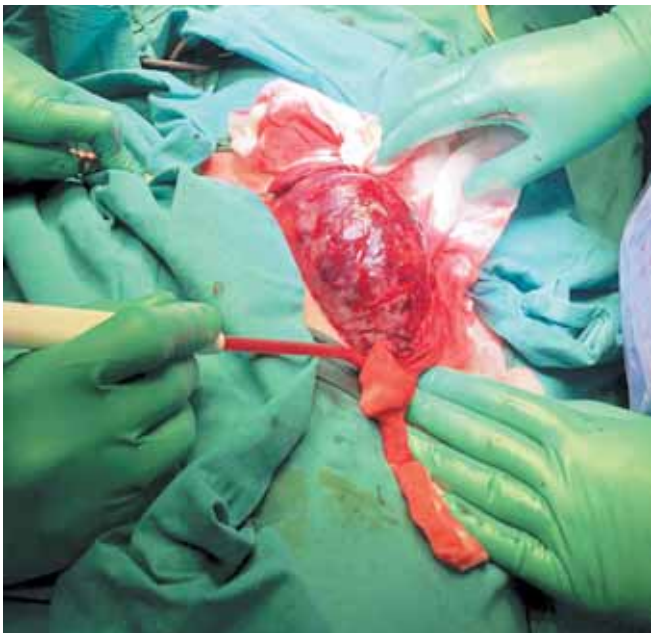

Fig. 2. Renal allograft during transplantectomy. Purulent debris areas are visible through the graft capsule

Renal replacement therapy was started in the form of prolonged venovenous hemodiafiltration. However, within the first 24 hours of observation, the patient experienced a rapid and profound deterioration of vital functions, progressing to distributive shock and multiple organ failure. This necessitated mechanical ventilation and vasopressor therapy.

Laboratory findings revealed a dramatic escalation in systemic inflammatory markers: leukocytosis (47.8 × 10^9/L), C-reactive protein (CRP) 447.6 mg/L, interleukin-6 (IL-6) >1000 pg/mL (reference: 0.00–6.40), interleukin-2 (IL-2) 5054 GE/mL (reference: 158–623), procalcitonin (PCT) >13 ng/mL, total protein 33.4 g/L, albumin 17 g/L, and platelets 34 × 10^9/L.

Considering the fulminant course of EPN in the KT recipient, complicated by systemic inflammatory response syndrome (SIRS) and multiple organ failure, a multidisciplinary team concluded that emergency transplantectomy was indicated for life-saving purposes. Surgical intervention was performed on February 12, 2024 (Fig. 2).

Following the isolation of Escherichia coli producing extended-spectrum beta-lactamases from both urine and blood cultures, antimicrobial therapy was escalated to meropenem in combination with amikacin. Intensive care measures included a multimodal extracorporeal detoxification strategy, comprising selective hemoperfusion, cytokine adsorption, and therapeutic plasma exchange.

Despite comprehensive treatment, the patient's condition continued to deteriorate rapidly. One day after the transplantectomy and on day 4 from disease onset, she died due to progressive multiple organ failure and refractory distributive shock. Findings from pathomorphological examination of the explanted kidney transplant are presented in Fig. 3.

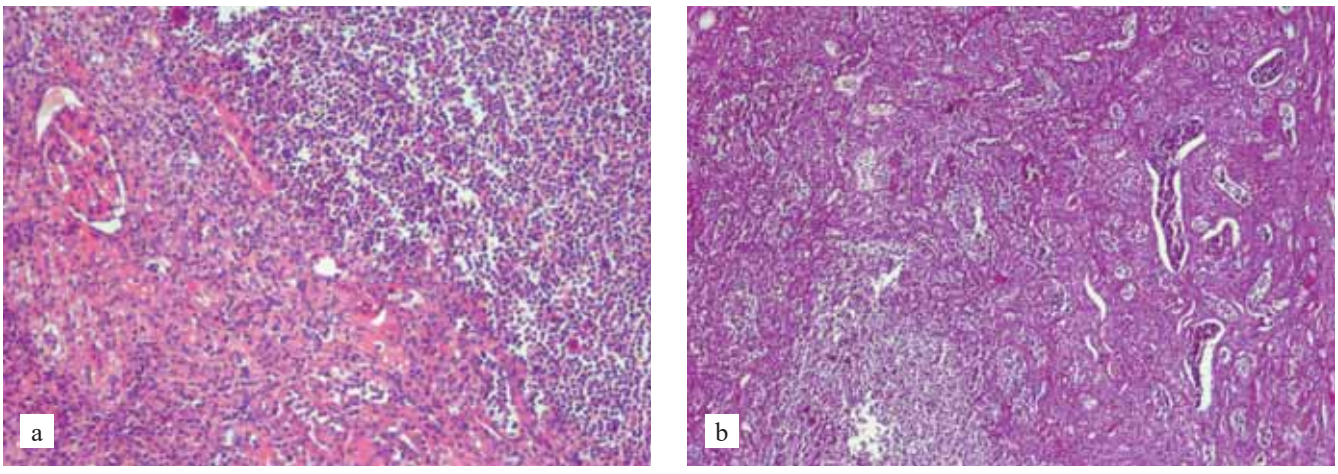

Fig. 3. Cortical layer of the kidney with diffuse, predominantly neutrophilic infiltration of the interstitium and abscess formation. Leukocytic cylinders are detected in the tubule lumen. Interstitial fibrosis and tubular atrophy. The glomerulus appears ischemic: a, H&E stain, magnification 40×; b, PAS, magnification 40×

DISCUSSION

By the end of the 19th century, several reports had described the presence of gas within the kidneys and urinary tract. In 1898, Kelly and MacCallum presented their clinical observations and summarized the data available at that time. They identified three primary causes of "pneumaturia": gas formation within the urinary tract due to invasive interventions or trauma (e.g., urological procedures or masturbation); the presence of fistulous connections between the bladder and bowel (congenital, acquired, or iatrogenic); and UTIs caused by gas-forming microorganisms [5].

The term emphysematous pyelonephritis (EPN) was introduced later, following the 1962 publication by Schultz and Klorfein, who analyzed 13 cases of renal and upper urinary tract gas accumulation due to infection [6]. In true EPN, the presence of gas is directly attributable to microbial activity, primarily from gas-producing pathogens.

It is important to recognize some historical terminological ambiguity: while "emphysematous pyelonephritis" technically describes infections involving both the kidney parenchyma and upper urinary tract, the term is sometimes used in the literature to include isolated "emphysematous pyelitis," which is limited to the collecting system.

Features of pathogens in emphysematous pyelonephritis

In approximately 70% of EPN cases, *Escherichia coli* is identified as the primary causative agent. Other members of the *Enterobacterales* order, most notably *Klebsiella pneumoniae* and *Proteus spp.*, as well as non-fermenting Gram-negative bacteria such as *Pseudomonas aeruginosa*, serve as less common etiologic agents [3, 7]. Up to 33% of the isolated pathogens are producers of extended-spectrum beta-lactamases [1, 2]. These bacteria are characterized by a high degree of structural heterogeneity and a frequent association with multidrug resistance [2, 8, 9].

Considerable attention has been directed toward identifying bacterial virulence factors that contribute to the onset and fulminant progression of EPN. In a comparative study, Tseng and Wu evaluated a broad spectrum of pathogenicity determinants expressed by E. coli strains isolated from EPN cases and contrasted them with strains obtained from patients with acute kidney infections not associated with gas formation.

The virulence genes of E. coli strains isolated from both groups were remarkably similar. However, a notable distinction was the significantly higher prevalence of the urovirulence-specific protein (usp) gene in EPN-associated strains – detected in 94% of patients with EPN versus only 67% in those with non-EPN. Additionally, there was a trend toward a lower frequency of the papG allele II gene among EPN pathogens [10]. Interestingly, epidemiological studies in both adult and pediatric populations have consistently demonstrated a predominant presence of the papG gene in strains responsible for acute pyelonephritis and recurrent UTIs in women [11].

EPN pathogens exhibit high biochemical activity, with the ability to shift to mixed acid and alcohol fermentation of glucose – processes that result in the production of hydrogen and carbon dioxide. In DM patients, elevated glucose levels in renal tissues create an ideal environment for the proliferation of gas-forming bacteria and promote high metabolic rates that lead to massive gas accumulation. In addition, uropathogenic strains of *E. coli* are known to produce a cytotoxic necrotizing factor, which induces tissue necrosis. The breakdown of necrotic tissue further contributes to additional release of methane and ammonia through the catabolism of amino acids [12].

Clinical presentation and risk factors for adverse outcomes in emphysematous pyelonephritis

The clinical presentation of EPN largely mirrors that of acute purulent pyelonephritis [1, 2]. Patients typically present with fever and chills, flank pain (often in the lumbar or subcostal regions), nausea, and vomiting. In cases of a fulminant course, there may be extensive manifestations of distributive shock and SIRS. Mental status disturbances, ranging from mild confusion to coma, are possible. The underlying causes of altered mental status in EPN patients should be evaluated individually, considering factors such as systemic intoxication, uncontrolled hypotension, DM decompensation (e.g., hyperglycemia or ketoacidosis), and, air embolism affecting the cerebral venous system. Altered mental status is a critical symptom that influences diagnostic and therapeutic tactics. There are isolated reports of the so-called "gas embolism" phenomenon in EPN cases, with gas being observed in the pulmonary artery, pelvic vessels, and even the upper sagittal and cavernous sinuses in patients with EPN of native kidneys [13, 14].

For a time, it was believed that the development of EPN required the presence of three conditions: DM (particularly poorly controlled diabetes), urinary tract obstruction, and an infectious agent capable of producing gas. However, as more data became available, it became evident that not all these factors need to be present for EPN to develop [15]. Huang et al. identified four key factors that play a determining role in the pathogenesis of EPN: presence of gas-producing bacteria, high tissue glucose levels, impaired tissue perfusion, and an altered immune response [12]. According to a meta-analysis by Desai et al. (2022), more than 80% of patients with EPN have DM, 16% have urolithiasis, and 20.5% suffer from obstructive uropathy [3]. In contrast, in the 1980s, it was believed that urinary tract obstruction accompanied EPN in at least 40% of cases, particularly in bilateral lesions or in cases where the only kidney was affected by EPN [7].

EPN involving native kidneys is more common in women, with a prevalence 1.8 to 6 times higher according to different studies. This is thought to be due to the anatomical characteristics of the female urogenital system. The left kidney is considered to be more vulnerable [5, 7, 12]. Interestingly, despite the higher incidence of EPN in women, men tend to experience a more unfavorable outcome (as highlighted in a meta-analysis by Ngo et al., 2022) [4]. Other risk factors for an unfavorable outcome in EPN include: signs of developing distributive shock (such as hemodynamic instability on admission, confusion, and the need for pressor therapy), confusion despite stable hemodynamic indices, laboratory parameters indicating the intensity of systemic inflammatory response, and secondary disorders of hemostasis and acid-base balance (initial thrombocytopenia, hypoalbuminemia, hyponatremia, hyperlactatemia, metabolic acidosis), AKI, and the extent of gas expansion as seen on CT imaging [1, 4, 12, 16, 17].

Approaches to diagnosis

In the 1930s and 1940s, early reports suggested the possibility of visualizing renal gas through radiography [15]. Currently, the primary method for diagnosing EPN is native computed tomography (CT). This method not only helps to identify the presence of gas but also allows for the assessment of its extent. The radiological classification proposed by Huang and Tseng in 2000 [12] is widely recognized as the best method for classifying EPN. According to this classification, EPN is divided into four classes based on the presence of gas in the collecting system, renal parenchyma, peri- and paranephric spaces, and whether one or both kidneys are involved (Table 1).

It is important to note that the renal fascia, with its anterior leaflet known as Gerota's fascia, encircles the kidney along with the surrounding fatty tissue, dividing the retroperitoneal space into two areas: the perinephric space (located within the renal fascia) and the perinephric space (located outside it).

Ultrasound (US) imaging has limited sensitivity for visualizing renal gas in patients with EPN. The primary ultrasound indicator of gas within the renal parenchyma and collecting system is the presence of linear hyperechogenic foci of varying sizes, often accompanied by distal reverberations. The characteristic "dirty shadow", which is a type of distal acoustic shadow, helps differentiate gas accumulation from a renal nodule. In some cases, the movement of these hyperechogenic gas foci within the collecting system, as the patient changes body position, can assist in distinguishing them from nodules [18].

An important indirect sign of gas presence in the perirenal space is the disappearance of renal visualization, which is particularly noticeable during KT ultrasound. However, it is crucial to note that ultrasound has a low sensitivity for diagnosing EPN, meaning that the absence of ultrasound signs does not exclude the diagnosis of EPN.

Table 1

Radiological classification of EPN (Huang-Tseng, 2000 [12])

Class	Gas detection zone
Class 1	Gas in the collecting system only
Class 2	Gas in the renal parenchyma with no extension beyond the organ
Class 3A	Extension of gas or abscess to perirenal space
Class 3B	Extension of gas or abscess to pararenal space
Class 4	Bilateral EPN or solitary kidney with EPN

Treatment approaches for emphysematous pyelonephritis

Over the past two decades, treatment approaches for EPN have evolved significantly. Nephrectomy as the first-choice strategy has given way to minimally invasive interventions, such as percutaneous nephrostomy (PCN), ureteral stenting, and abscess drainage, all in conjunction with aggressive antibiotic therapy (ABT) [1].

This shift toward less invasive tactics is largely driven by the high mortality rates associated with emergency nephrectomy. According to a meta-analysis by Desai et al. (2022), which included data from 1146 patients (1980–2020), the cumulative mortality rate for EPN was 12.5%. However, the mortality rate specifically for those undergoing emergency nephrectomy was significantly higher at 27% [3].

The choice of empirical ABT for EPN is a complex process that requires careful consideration of several factors. These include the risk of infection with multidrug-resistant bacteria, the patient's specific prognosis, and changes in drug pharmacokinetics, especially in cases of hypoalbuminemia or critical conditions. Previously recommended third- and fourth-generation cephalosporins, as well as fluoroquinolones, are no longer as effective due to the widespread resistance of Enterobacterales bacteria producing extended-spectrum beta-lactamases, which are common pathogens in UTIs, including EPN [8, 9]. Therefore, carbapenems from Group 2 and "new" inhibitor-protected cephalosporins remain the most appropriate choices for initiating therapy [19–21].

An attempt to algorithmize the management of EPN patients was made by Huang and Tseng in 2000. They analyzed the course and outcomes of EPN in 48 patients and identified thrombocytopenia, AKI, shock, and impaired consciousness as key risk factors. According to their algorithm, patients in grade 1 or 2 should receive ABT and PCN. For grade 3 or 4 patients with one risk factor, ABT and PCN are still indicated, but if two or more risk factors are present, nephrectomy should be considered [12]. This algorithm has been widely adopted in clinical practice; however, in light of modern resuscitation strategies that have evolved over the last 25 years, we believe that the approach, especially regarding risk

factors, may need to be updated. To this day, determining the optimal therapeutic strategy for EPN remains a subject of ongoing debate.

Emphysematous pyelonephritis involving the renal graft

We identified 38 cases of EPN in KT recipients published in the English-language medical literature from the late 1970s to the present day [22–58]. The characteristics and course of EPN in KT recipients, based on this literature analysis and our current observation, are summarized in Table 2.

An analysis of the data in the table shows a cumulative mortality rate of 28%. Among KT recipients, males were predominant (59%), and the age range was from 12 to 76 years, with a mean age of 51 ± 14 years. In the fatal cases, there was a clear male predominance (n = 9, 82%), compared to male representation (n = 14, 50%) in the surviving group. The mean age of surviving versus dead patients was not significantly different, at 49 ± 15 *vs.* 56 ± 12 years (p = 0.17). DM was present in 82% of cases, and PTDM developed in 9 patients (23%).

Failure to achieve glycemic and glycated hemoglobin targets was a common finding among KT recipients who developed EPN. A notable anamnestic risk factor was the presence of recurrent UTIs, observed in 35% of cases. Unlike the general population with EPN in native kidneys, obstructive uropathy was rarely reported among KT recipients.

Several isolated reports have linked the onset of EPN in KT recipients with urologic or angiographic procedures performed shortly before the disease debut, particularly among DM-free patients. For example, Althaf et al. [47] described a case of EPN following transurethral resection of the prostate. Boltan et al. [38] attributed the development of EPN to bladder catheterization, identifying it as an iatrogenic trigger. Salehipour et al. [41] reported the rapid onset of EPN and graft loss in a patient who underwent renal artery stenting while febrile. A notable case was also presented by Spanish researchers, who diagnosed EPN three weeks after renal artery embolization in a non-functioning KT [35].

The most common presenting symptoms were fever (76%) and abdominal pain (58%), typically localized to the graft area, though in some cases the pain was diffuse or associated with palpable tension over the transplant site. Confusion was reported in 30% of patients, while oliguria or anuria occurred in 28%. Gastrointestinal symptoms such as nausea or vomiting were present in 20%, whereas diarrhea or constipation were documented only sporadically.

A rare but notable case involved the simultaneous occurrence of EPN in the kidney transplant and both native kidneys [58]. Additionally, EPNs affecting non-functioning grafts have been reported in three observations [35, 51, 53], highlighting the diagnostic challenge of distinguishing between non-functioning kidney graft intolerance syndrome and infectious complications, as both may present with similar clinical features [59]. Although comprehensive laboratory data were often lacking, leukocytosis with a neutrophilic shift was commonly observed, suggesting a significant systemic inflammatory response in many cases.

Data on the causative pathogen were available for 33 out of 39 patients. *E. coli* was the most frequently detected organism, isolated in 20 cases (60.6%) from urine and/or blood cultures. In two of these cases, *E. coli* was found in combination with *Klebsiella pneumoniae* and *Staphylococcus epidermidis*. *K. pneumoniae* alone was detected in 7 patients (21.2%). Less commonly reported pathogens included *Bacteroides* species (2 cases), *Enterobacter* (1), *Salmonella* in combination with *Enterobacter* (1), *Proteus* species (1), and *Candida glabrata* (1).

IST is a clear predisposing factor for EPN in KT recipients. The time interval from transplantation to onset of EPN – effectively the duration of IST – ranged widely from 2 weeks to 11 years. However, the influence of specific IST regimens or the duration of immunosuppression on the risk of developing EPN remains uncertain. Interestingly, a recent case reported the development of severe fungal EPN necessitating transplantectomy just one week after initiation of empagliflozin, likely triggered by drug-induced glycosuria [55].

AKI was reported in 26 patients (67%), including the present case. The development of oligo/anuria due to AKI at the onset of EPN is characteristic in KT recipients, as the infection typically involves the only functioning kidney. In contrast, AKI in EPN affecting native kidneys is less common and usually occurs in cases of bilateral involvement or in patients with a solitary native kidney.

Due to the lack of consistent reporting in the reviewed cases, it is not possible to reliably assess the impact of body mass index (BMI) on the clinical course and prognosis of EPN in KT recipients. However, our patient was morbidly obese, which likely contributed to challenges in maintaining adequate personal hygiene.

Instrumental diagnosis of EPN in KT recipients requires specific consideration. It should be emphasized that in seven cases, KT ultrasound either revealed or suggested the presence of gas in the parenchyma or collecting system. Despite this, ultrasound remains the primary method for diagnosing EPN in KT recipients.

As the number of documented cases of EPN in KT recipients increased, it became clear that the radiological classification system proposed by Huang and Tseng had limitations. First, this classification automatically categorizes EPN in KT as grade 4, since the infection typically affects only a single kidney. Second, the classification's division of the disease into peri- and paranephric spaces is only applicable in native kidneys, where Gerota's fascia is present.

Table 2

Publications on clinical cases of EPN in renal allografts (1977–2024)

Author, publication year	Age, sex	DM	Uncontrolled DM	RUTIs	Clinical presentation on admission	Causative agent	Gas distribution on admission	Treatment	Outcome
Parameswaran et Feest 1977 [22]	53, f	Yes (PTDM)	N/A	No	Low-grade fever, pain around the KT, AKI, confusion	*Proteus spp.*	KT	TE + ABT	Alive
Brenbridge et al. 1979 [23]	33, m	Yes (PTDM)	N/A	No	Low-grade fever, pain around the KT, AKI	*E. coli*	KT + perirenal space	TE + ABT	Alive
Balsara et al. 1985 [18]	32, m	No	-	No	Fever, confusion	*E. coli*	KT + RCS	PD + ABT	Alive
Potter et al. 1985 [24]	31, f	Yes	N/A	Yes	Fever, pain around the KT, AKI	*E. coli*	KT + perirenal space	TE + ABT	Alive
O'Donnell et al. 1985 [25]	27, m	Yes	N/A	N/A	Fever, tension in the KT area	*Enterobacter spp*	KT + perirenal space	ABT	Alive
Glen et al. 1989 [26]	66, f	Yes	N/A	N/A	Fever, confusion	*E. coli*	N/A	PD + ABT	Alive
Kalra et al. 1993 [27]	35, m	No	-	N/A	Painful urination	*K. pneumoniae*	N/A	TE + ABT	Dead
Akalin et al. 1996 [28]	62, m	Yes	N/A	N/A	Painful urination, confusion	*K. pneumoniae*	RCS	ABT	Alive
Cheng et al. 2001 [29]	55, m	Yes (PTDM)	No	No	Fever, pain around the KT	*E. coli*	KT	PD + ABT	Alive
Iqubal et al. 2004 [30]	39, f	Yes (PTDM)	No	Yes	Fever, abdominal pain, AKI, confusion	*E. coli*	KT + perirenal space	PD + ABT	Alive
Ishigami et al. 2004 [31]	67, f	Yes (PTDM)	No	No	Low-grade fever, pain around the KT	Not detected	RCS	TE + ABT	Alive
Al-Makadma et Al-Akash 2005 [32]	12, m	No	-	Yes	Fever, vomiting, abdominal pain, tension in the KT area, AKI	*E. coli*	RCS	ABT	Alive
Fujita et al. 2005 [33]	49, f	Yes	Yes	No	Fever, pain around the KT, blood in urine, AKI, confusion	*Salmonela spp.* + *Enterobacter spp.*	KT + perirenal space	TE + ABT	Alive
Arai et al. 2006 [34]	61, m	Yes	N/A	N/A	Abdominal pain, AKI, confusion	*E. coli*	KT + perirenal space	TE + ABT	Dead
Ortiz et al. 2007 [35]	40, m	No	-	No	Fever, abdominal pain	*Bacteroides capillosus*	KT + RCS	TE + ABT	Alive
Chuang et al. 2007 [36]	51, m	Yes (PTDM)	Yes	No	Fever, abdominal pain	*E. coli*	RCS	PD + ABT	Alive
Baliga et al. 2007 [37]	52, f	Yes	No	Yes	Fever, pain around the KT, vomiting, AKI, confusion	*E. coli*	KT	ABT	Alive
Boltan et al. 2008 [38]	76, m	Yes	Yes	No	Fever, AKI	*K. pneumoniae*	KT + perirenal space	PD + TE + ABT	Alive
Debnath et al. 2009 [39]	52, f	Yes	N/A	Yes	Fever, abdominal pain, AKI	N/A	KT	ABT	Alive
Schmidt et al. 2009 [40]	55, m	Yes	N/A	No	Fever, abdominal pain, AKI	*E. coli*	KT + perirenal space	TE + ABT	Alive

End of table 2

Author, publication year	Age, sex	DM	Uncontrolled DM	RUTIs	Clinical presentation on admission	Causative agent	Gas distribution on admission	Treatment	Outcome
Salehipour et al. 2010 [41]	23, f	No	-	No	Fever, nausea, vomiting, blood in urine, pain around the KT, AKI	N/A	KT + perirenal space	TE + ABT	Alive
Al-Geizawi et al. 2010 [42]	58, f	Yes	Yes	No	Fever, nausea, vomiting, AKI, confusion	*K. pneumoniae*	KT	PD + ABT	Alive
Alexander et al. 2012 [43]	51, f	Yes (PTDM)	No	Yes	Fever, abdominal pain, vomiting, AKI, confusion	*K. pneumoniae*	KT + perirenal space	PD + ABT	Alive
Tsai et al. 2012 [44]	46, m	Yes	N/A	No	Fever, pain on palpation of KT	*E. coli*	KT	ABT	Dead
Agreda Castaneda et al. 2014 [45]	74, f	Yes	Yes	No	Fever, AKI	*E. coli*	KT	TE + ABT	Alive
Tienza et al. 2014 [46]	53, m	Yes	Yes	Yes	Low-grade fever, weakness, AKI	*S. epidermidis* + *E. coli*	KT + RCS	PD + ABT	Alive
Althaf et al. 2014 [47]	71, m	No	-	Yes	Fever, abdominal pain, vomiting, AKI, confusion	*E. coli*	KT + perirenal space	ABT	Dead
Narcisse et al. 2016 [48]	62, f	Yes (PTDM)	No	No	Fever, abdominal pain, diarrhea, AKI	*K. pneumoniae*	KT	TE + ABT	Alive
Alhajjaj et Pasha 2016 [49]	71, m	Yes	N/A	N/A	Shortness of breath, constipation, vomiting, tension in the KT area, AKI	N/A	KT + perirenal space	ABT	Dead
Oliveira et al. 2016 [50]	58, m	Yes	N/A	Yes	Fever, weakness	*E. coli* + *K. pneumoniae*	KT + perirenal space	PD + TE + ABT	Dead
Bansal et al. 2016 [51]	60, m	Yes	Yes	No	Fever, abdominal pain	*Bacteroides*	KT	TE + ABT	Dead
Crouter et al. 2017 [52]	61, m	Yes	Yes	No	Fever, shortness of breath, AKI, confusion	N/A	KT	ABT	Alive
Rajaian et al. 2019 [53]	44, m	Yes	Yes	Yes	Fever, tension in the KT area	*E. coli*	2 KT + perirenal space	TE + ABT	Alive
Ambinder et al. 2021 [54]	51, m	No	-	No	Fever, weakness, AKI	N/A	KT	PD + TE + ABT	Dead
Cases-Corona et al. 2022 [55]	53, m	Yes	No	Yes	N/a	*Candida glabata*	N/A	TE + ABT	Alive
Abu Jawdeh et al. 2022 [56]	49, f	Yes	Yes	Yes	Normothermia, abdominal pain, AKI, confusion	*E. coli*	KT + perirenal space	TE + ABT	Alive
Hassanein et al. 2022 [57]	51, f	Yes	N/A	No	Worn out	*K. pneumoniae*	KT	TE + ABT	Dead
Chippa et al. 2022 [58]	71, m	Yes	Yes	Yes	On a ventilator from another facility	*E. coli*	KT + perirenal space	ABT	Dead
Trushkin et al. 2024	46, f	Yes (PTDM)	Yes	Yes	Fever, pain around the KT, AKI	*E. coli*	RCS	PD + TE + ABT	Dead

Note: DM, diabetes mellitus; PTDM, post-transplant diabetes mellitus; RUTIs, recurrent urinary tract infections; AKI, acute kidney injury; KT, kidney transplant; RCS, renal collecting system; PD, percutaneous drain; ABT, antibiotic therapy; TE, transplantectomy.

Table 3

EPN stages in renal allografts (Al-Geizawi, 2010 [42])

Stage 1	Gas in the collecting system
Stage 2	Gas in <50% of the renal parenchyma, with minimum extension to perirenal space, quickly controlled sepsis
Stage 3	Gas in >50% of the renal parenchyma or extensive spread to perirenal space or evidence of organ failure, or uncontrolled sepsis, or refractory shock

The absence of Gerota's fascia at the transplant site results in a more rapid spread of the purulent destructive process within the abdominal cavity in KT recipients.

In 2010, Al-Geizawi et al. proposed a revised classification system that accounts for the unique characteristics of KT, including an assessment of gas distribution in the allograft based on CT findings, as well as some clinical features of patients [42] (Table 3).

According to the authors, CT imaging plays a crucial role in the early detection and ongoing monitoring of EPN. Stages 1 and 2, as identified on CT, justify the use of minimally invasive, nephron-preserving surgical interventions, which serve as an alternative to emergency nephrectomy. Stage 3, however, necessitates more aggressive surgical management. Schmidt et al. recommend using the "pulmonary window" mode on CT to better visualize the true distribution of gas within the allograft parenchyma and surrounding tissues, [40].

However, an analysis of EPN outcomes in KT recipients, including both published cases and our own clinical experience, suggests that the patient's classification stage according to the Al-Geizawi et al. system does not necessarily correlate with the disease outcome. In our case, radiological findings indicated stage 1, which is typically associated with a favorable prognosis. Additionally, several studies have highlighted the presence of severe comorbidities in patients who experienced fatal outcomes. These included acute myocardial infarction in a patient with severe mitral valve disease [51], sudden cardiac death [49], fulminant hepatitis [34], and EPN in a patient with COVID-19 complicated by cryptococcal infection [58]. The exacerbation of underlying comorbidities in the context of EPN in KT recipients likely plays a key role in the onset of a fatal outcome, regardless of the radiological stage of the disease.

CONCLUSION

The analysis of literature data and our own clinical experience leads to several practical considerations for the structured management of patients with EPN in KT recipients.

1. An optimal management algorithm for patients with EPN in KT recipients has yet to be developed due to the limited number of published cases and data.
2. The presence of initial DM and ongoing IST significantly increases the likelihood of infection dissemination, leading to SIRS, multiple organ failure, and distributive shock.
3. The presence of gas in the allograft, regardless of its spread according to the Al-Geizawi et al. classification, represents a poor prognostic indicator. It negatively affects both graft survival and the overall clinical course of the disease.
4. Patients with EPN in KT recipients should be promptly transferred to the ICU, regardless of baseline hemodynamic status, renal function, or acid-base balance, to initiate comprehensive intensive therapy, considering the patient's comorbid background.
5. The decision regarding the volume and sequence of surgical interventions (PCN and transplantectomy) should be carefully individualized, guided by a multidisciplinary team approach.

The authors declare no conflict of interest.

REFERENCES

1. *Wu SY, Yang SS, Chang SJ, Hsu CK.* Emphysematous pyelonephritis: classification, management, and prognosis. *Tzu Chi Med J*. 2022; 34 (3): 297–302. doi: 10.4103/tcmj.tcmj_257_21. PMID: 35912050; PMCID: PMC9333110.
2. *Novinsky AA, Zinukhov AF.* Emphysematous pyelonephritis: epidemiology, modern approaches to diagnosis and treatment. *Experimentaland Clinical Urology*. 2020; 13 (5): 100–105. [In Russ, English abstract]. doi: 10.29188/2222-8543-2020-13-5-100-105.
3. *Desai R, Batura D.* A systematic review and meta-analysis of risk factors and treatment choices in emphysematous pyelonephritis. *Int Urol Nephrol*. 2022; 54 (4): 717–736. doi: 10.1007/s11255-022-03131-6. PMID: 35103928.
4. *Ngo XT, Nguyen TT, Dobbs RW, Thai MS, Vu DH, Dinh LQV et al.* Prevalence and Risk Factors of Mortality in Emphysematous Pyelonephritis Patients: A Meta-Analysis. *World J Surg*. 2022; 46 (10): 2377–2388. doi: 10.1007/s00268-022-06647-1.
5. *Kelly HA, MacCallum WG.* Pneumaturia. *JAMA*. 1898; XXXI (8); 375–381. doi:10.1001/jama.1898.92450080001001.
6. *Schultz EH Jr, Klorfein EH.* Emphysematous pyelonephritis. *J Urol*. 1962; 87: 762–766. doi: 10.1016/S0022-5347(17)65043-2. PMID: 13909504.
7. *Michaeli J, Mogle P, Perlberg S, Heiman S, Caine M.* Emphysematous pyelonephritis. *J Urol*. 1984; 131 (2): 203–208. doi: 10.1016/s0022-5347(17)50309-2.
8. *Palagin IS, Sukhorukova MV, Dekhnich AV, Edelstein MV, Perepanova TS, Kozlov RS et al.* Antimicrobial resistance of pathogens causing community-acquired urinary tract infections in Russia: results of the multicenter study "DARMIS-2018". *Clinical Microbiology and Antimicrobial Chemotherapy*. 2019; 21 (2): 134–146. [In Russ, English abstract]. doi: 10.36488/cmac.2019.2.134-146.
9. *Kuzmenkov AYu, Vinogradova AG, Trushin IV, Edelstein MV, Avramenko AA, Dekhnich AV, Kozlov RS et al.* AM-

Rmap – antibiotic resistance surveillance system in Russia. *Clinical Microbiology and Antimicrobial Chemotherapy*. 2021; 23 (2): 198–204. [In Russ, English abstract]. doi: 10.36488/cmac.2021.2.198-204.
10. *Tseng CC, Wu JJ, Wang MC, Hor LI, Ko YH, Huang JJ.* Host and bacterial virulence factors predisposing to emphysematous pyelonephritis. *Am J Kidney Dis*. 2005; 46 (3): 432–439. doi: 10.1053/j.ajkd.2005.05.019. PMID: 16129204.
11. *Norinder BS, Lüthje P, Yadav M, Kadas L, Fang H, Nord CE, Brauner A.* Cellulose and PapG are important for Escherichia coli causing recurrent urinary tract infection in women. *Infection*. 2011; 39 (6): 571–74. doi: 10.1007/s15010-011-0199-0. PMID: 22002732.
12. *Huang JJ, Tseng CC.* Emphysematous pyelonephritis: clinicoradiological classification, management, prognosis, and pathogenesis. *Arch Intern Med*. 2000; 160 (6): 797–805. doi: 10.1001/archinte.160.6.797. PMID: 10737279.
13. *Darsan SL, Pillai BS, Krishnamoorthy H.* A rare neurological presentation of emphysematous pyelonephritis. *Indian J Urol*. 2022; 38 (4): 315–316. doi: 10.4103/iju.iju_145_22. PMID: 36568452.
14. *Razazi K, Luciani A, de Prost N, Mekontso Dessap A*. Multiple gas emboli complicating an emphysematous pyelonephritis. *IDCases*. 2018; 12: 64–65. doi: 10.1016/j.idcr.2018.03.005. PMID: 29942752.
15. *Gillies CL, Flocks R.* Spontaneous renal and perirenal emphysema. Report of a case in a diabetic from Escherichia coli infection. *Amer J Roentgen*. 1941; 46 (2): 173–174.
16. *Arrambide-Herrera JG, Robles-Torres JI, Ocaña-Munguía MA, Romero-Mata R, Gutiérrez-González A, Gómez-Guerra LS.* Predictive factors for mortality and intensive care unit admission in patients with emphysematous pyelonephritis: 5-year experience in a tertiary care hospital. *Actas Urol Esp (Engl Ed)*. 2022; 46 (2): 98–105. English, Spanish. doi: 10.1016/j.acuroe.2021.01.010. PMID: 35120854.
17. *Lu YC, Chiang BJ, Pong YH, Huang KH, Hsueh PR, Huang CY et al.* Predictors of failure of conservative treatment among patients with emphysematous pyelonephritis. *BMC Infect Dis*. 2014; 14: 418. doi: 10.1186/1471-2334-14-418. PMID: 25074590.
18. *Balsara VJ, Raval B, Maklad NF.* Emphysematous pyelonephritis in a renal transplant: sonographic and computed tomographic features. *J Ultrasound Med*. 1985; 4 (2): 97–99. doi: 10.7863/jum.1985.4.2.97. PMID: 3882994.
19. *Harris PNA, Tambyah PA, Lye DC, Mo Y, Lee TH, Yilmaz M et al.* MERINO Trial Investigators and the Australasian Society for Infectious Disease Clinical Research Network (ASID-CRN). Effect of Piperacillin-Tazobactam *vs.* Meropenem on 30-Day Mortality for Patients With E coli or Klebsiella pneumoniae Bloodstream Infection and Ceftriaxone Resistance: A Randomized Clinical Trial. *JAMA*. 2018; 320 (10): 984–994. doi: 10.1001/jama.2018.12163. doi: 10.1001/jama.2019.6706. PMID: 30208454.
20. *Lu YC, Hong JH, Chiang BJ, Pong YH, Hsueh PR, Huang CY et al.* Recommended Initial Antimicrobial Therapy for Emphysematous Pyelonephritis: 51 Cases and 14-Year-Experience of a Tertiary Referral Center. *Medicine (Baltimore)*. 2016; 95 (21): e3573. doi: 10.1097/MD.0000000000003573. PMID: 27227920.
21. *Hsueh PR, Lau YJ, Ko WC, Liu CY, Huang CT, Yen MY et al.* Consensus statement on the role of fluoroquinolones in the management of urinary tract infections. *J Microbiol Immunol Infect*. 2011; 44 (2): 79–82. doi: 10.1016/j.jmii.2011.01.015. PMID: 21439507.
22. *Parameswaran R, Feest T.* Gas nephrogram: an unusual complication of renal transplantation. *Br J Radiol*. 1977; 50 (594): 438–440. doi: 10.1259/0007-1285-50-594-438. PMID: 326327.
23. *Brenbridge AN, Buschi AJ, Cochrane JA, Lees RF.* Renal emphysema of the tranplanted kidney: sonographic appearance. *AJR Am J Roentgenol*. 1979; 132 (4): 656–658. doi: 10.2214/ajr.132.4.656. PMID: 106703.
24. *Potter JL, Sullivan BM, Flournoy JG, Gerza C.* Emphysema in the renal allograft. *Radiology*. 1985; 155 (1): 51–52. doi: 10.1148/radiology.155.1.3883423. PMID: 3883423.
25. *O'Donnell D, Rumbak M, Anderson J.* Emphysematous pyelonephritis in a transplanted kidney. *Clin Nephrol*. 1986; 25 (1): 52–53. PMID: 3514013.
26. *Glen D, Bayliss AP, Robertson EM.* Percutaneous drainage in emphysematous pyelonephritis. *Clin Radiol*. 1989; 40 (4): 434. doi: 10.1016/s0009-9260(89)80155-2. PMID: 2667850.
27. *Kalra OP, Malik N, Minz M, Gupta KL, Sakhuja V, Chugh KS.* Emphysematous pyelonephritis and cystitis in a renal transplant recipient – computed tomographic appearance. *Int J Artif Organs*. 1993; 16 (1): 41–44. PMID: 8458671.
28. *Akalin E, Hyde C, Schmitt G, Kaufman J, Hamburger RJ.* Emphysematous cystitis and pyelitis in a diabetic renal transplant recipient. *Transplantation*. 1996; 62 (7): 1024–1026. doi: 10.1097/00007890-199610150-00023. PMID: 8878399.
29. *Cheng YT, Wang HP, Hsieh HH.* Emphysematous pyelonephritis in a renal allograft: successful treatment with percutaneous drainage and nephrostomy. *Clin Transplant*. 2001; 15 (5): 364–367. doi: 10.1034/j.1399-0012.2001.150511.x. PMID: 11678965.
30. *Iqubal M, John GT, Gopalakrishnan G, Jacob CK.* Abdominal gas is not always bowel associated: lessons from an allograft recipient. *Nephrol Dial Transplant*. 2004; 19 (2): 503–504. doi: 10.1093/ndt/gfg465. PMID: 14736985.
31. *Ishigami K, Olsen KM, Hammet BK, Katz DA, Wu YM.* Intravascular gas in the transplanted kidney: a sign of extensive graft necrosis. *Emerg Radiol*. 2004; 10 (5): 279–281. doi: 10.1007/s10140-004-0334-7. PMID: 15290479.
32. *Al-Makadma AS, Al-Akash SI*. An unusual case of pyelonephritis in a pediatric renal transplant recipient. *Pediatr Transplant*. 2005; 9 (2): 258–560. doi: 10.1111/j.1399-3046.2004.00276.x. PMID: 15787804.
33. *Fujita S, Watanabe J, Reed AI, Hemming AW, Solis D, Netzel TC et al.* Case of emphysematous pyelonephritis in a renal allograft. *Clin Transplant*. 2005; 19 (4): 559–562. doi: 10.1111/j.1399-0012.2005.00264.x.
34. *Arai S, Makino T, Okugi H, Hasumi M, Shibata Y, Hatori M et al.* A case of emphysematous pyelonephritis in a renal allograft. *Transplantation*. 2006; 81 (2): 296–

297. doi: 10.1097/01.tp.0000191623.83885.ee. PMID: 16436977.
35. *Ortiz A, Petkov V, Urbano J, Contreras J, Alexandru S, Garcia-Pérez A et al.* Emphysematous pyelonephritis in dialysis patient after embolization of failed allograft. *Urology*. 2007; 70 (2): 372.e17–372.e19. doi: 10.1016/j.urology.2007.04.044. PMID: 17826516.
36. *Chuang YW, Chen CH, Cheng CH, Hung SW, Yu TM, Wu MJ et al.* Severe emphysematous pyelonephritis in a renal allograft: successful treatment with percutaneous drainage and antibiotics. *Clin Nephrol*. 2007; 68 (1): 42–46. doi: 10.5414/cnp68042. PMID: 17703835.
37. *Baliga KV, Narula AS, Sharma A, Khanduja R, Manrai M, Debnath J et al.* Successful medical treatment of emphysematous pyelonephritis in a renal allograft recipient. *Ren Fail*. 2007; 29 (6): 755–658. doi: 10.1080/08860220701460434. PMID: 17763174.
38. *Boltan LE, Randall H, Barri YM.* Iatrogenic emphysematous pyelonephritis in a renal transplant patient. *Transpl Infect Dis*. 2008; 10 (6): 409–412. doi: 10.1111/j.1399-3062.2008.00319.x. PMID: 18507751.
39. *Debnath J, Baliga KV, George RA, Satija L, Khanduja R, Vaidya A et al.* Temporal evolution of emphysematous pyelonephritis in a renal allograft: imaging findings. *Emerg Radiol*. 2009; 16 (3): 231–233. doi: 10.1007/s10140-008-0728-z. PMID: 18473150.
40. *Schmidt S, Foert E, Zidek W, van der Giet M, Westhoff TH.* Emphysematous pyelonephritis in a kidney allograft. *Am J Kidney Dis*. 2009; 53 (5): 895–897. doi: 10.1053/j.ajkd.2008.12.032. PMID: 19344987.
41. *Salehipour M, Roozbeh J, Rasekhi AR, Afrasiabi MA, Rezaee H, Izadpanah K et al.* Emphysematous pyelonephritis in a transplant kidney. *Int J Organ Transplant Med*. 2010; 1 (1): 49–51. PMID: 25013564.
42. *Al-Geizawi SM, Farney AC, Rogers J, Assimos D, Requarth JA, Doares W et al.* Renal allograft failure due to emphysematous pyelonephritis: successful non-operative management and proposed new classification scheme based on literature review. *Transpl Infect Dis*. 2010; 12 (6): 543–250. doi: 10.1111/j.1399-3062.2010.00538.x. PMID: 20825591
43. *Alexander S, Varughese S, David VG, Kodgire SV, Mukha RP, Kekre NS et al.* Extensive emphysematous pyelonephritis in a renal allograft treated conservatively: case report and review of the literature. *Transpl Infect Dis*. 2012; 14 (6): E150–E155. doi: 10.1111/tid.12016. PMID: 23025565.
44. *Tsai YF, Wu CC, Lin AC.* Emphysematous pyelonephritis in a renal allograft. *J Emerg Med*. 2012; 43 (6): e485–e486. doi: 10.1016/j.jemermed.2011.06.048. PMID: 22070875.
45. *Agreda Castañeda F, Lorente D, Trilla Herrera E, Gasanz Serrano C, Servian Vives P, Iztueta Saavedra I et al.* Extensive emphysematous pyelonephritis in a renal allograft: case report and review of literature. *Transpl Infect Dis*. 2014; 16 (4): 642–647. doi: 10.1111/tid.12246. PMID: 24984587.
46. *Tienza A, Hevia M, Merino I, Velis JM, Algarra R, Pascual JI et al.* Case of emphysematous pyelonephritis in kidney allograft: Conservative treatment. *Can Urol Assoc J*. 2014; 8 (3–4): E256–E259. doi: 10.5489/cuaj.1555. PMID: 24839494.
47. *Althaf MM, Abdelsalam MS, Rashwan M, Nadri Q.* Emphysematous pyelonephritis and cystitis in a renal transplant recipient. *BMJ Case Rep*. 2014; 2014: bcr2014205589. doi: 10.1136/bcr-2014-205589. PMID: 25320257.
48. *Narcisse D, Agarwal M, Hancock M, Wells D, Sands C.* A rare case of emphysematous pyelonephritis in a renal transplant patient. *Ther Adv Infect Dis*. 2016; 3 (6): 141–144. doi: 10.1177/2049936116678122. PMID: 28386406.
49. *Alhajjaj FS, Pasha F.* Emphysematous Pyelonephritis in Renal Allograft – a case report. *Int J Health Sci (Qassim)*. 2016; 10 (2): 311–313. PMID: 27103911.
50. *Oliveira CC, Garcia PD, Viero RM*. Emphysematous pyelonephritis in a transplanted kidney. *Autops Case Rep*. 2016; 6 (4): 41–47. doi: 10.4322/acr.2016.051. PMID: 28210573.
51. *Bansal RK, Lambe S, Kapoor A*. Emphysematous pyelonephritis in failed renal allograft: Case report and review of literature. *Urol Ann*. 2016; 8 (1): 111–113. doi: 10.4103/0974-7796.171500. PMID: 26834417.
52. *Crouter AJ, Abraham MK, Wilkerson RG*. Emphysematous pyelonephritis in a renal allograft. *Am J Emerg Med*. 2017; 35 (3): 520.e1–520.e2. doi: 10.1016/j.ajem.2016.09.043. PMID: 27717721.
53. *Rajaian S, Pragatheeswarane M, Krishnamurthy K, Murugasen L.* Bilateral graft emphysematous pyelonephritis. *BMJ Case Rep*. 2019; 12 (6): e231051. doi: 10.1136/bcr-2019-231051. PMID: 31227572.
54. *Ambinder D, Saji A, Bassily D, Wong V, John D, Wong NC.* Evolving case of emphysematous pyelonephritis in a second renal allograft. *Urol Case Rep*. 2021; 38: 101663. doi: 10.1016/j.eucr.2021.101663. PMID: 33981584.
55. *Cases-Corona C, Shabaka A, Gonzalez-Lopez A, Martin-Segarra O, Moreno de la Higuera MA, Lucena R et al.* Fulminant Emphysematous Pyelonephritis by Candida glabrata in a Kidney Allograft. *Nephron*. 2020; 144 (6): 304–309. doi: 10.1159/000507259. PMID: 32344404.
56. *Abu Jawdeh BG, Nguyen MC, Ryan MS, Vikram HR.* Case report: Emphysematous pyelonephritis associated with kidney allograft abscess formation. *Front Med (Lausanne)*. 2022; 9: 1066512. doi: 10.3389/fmed.2022.1066512. PMID: 36619614.
57. *Hassanein M, Aleter O, Stephany BR, Eltemamy M, Augustine JJ.* Emphysematous pyelonephritis in a kidney transplant recipient. *Transpl Infect Dis*. 2022; 24 (2): e13807. doi: 10.1111/tid.13807. PMID: 35148025.
58. *Chippa V, Chenna S, Gujarathi R.* Emphysematous Pyelonephritis Involving Native Kidneys and a Transplanted Kidney. *Cureus*. 2022; 14 (9): e29024. doi: 10.7759/cureus.29024. PMID: 36237790.
59. *Belavina NI, Trushkin RN, Artyukhina LYu, Ivanova ES, Stolyarevich ES, Manchenko OV et al.* Ultrasound examination of failed renal transplant in patients with graft intolerance syndrome. Case series. *Nephrology and Dialysis*. 2023; 25 (3): 401–412. [In Russ, English abstract]. doi: 10.28996/2618-9801-2023-3-401-412.

The article was submitted to the journal on 16.08.2024

DOI: 10.15825/1995-1191-2024-4-90-99

SINGLE-CENTER EXPERIENCE IN KIDNEY TRANSPLANTATION: OUTCOMES, CONCLUSIONS, AND PERSPECTIVES

M.Sh. Khubutia[1–3], I.V. Dmitriev[1, 4], A.G. Balkarov[1, 3, 4], Yu.A. Anisimov[1, 2], N.V. Shmarina[1, 4], N.V. Zagorodnikova[1], N.V. Borovkova[1, 4], M.G. Minina[5], D.V. Lonshakov[1], V.O. Aleksandrova[1], V.V. Smirnova[1], A.U. Rustambek[1]

[1] Sklifosovsky Research Institute for Emergency Medicine, Moscow, Russian Federation
[2] Moscow State University of Medicine and Dentistry, Moscow, Russian Federation
[3] Research Institute for Healthcare Organization and Medical Management, Moscow, Russian Federation
[4] Pirogov Russian National Research Medical University, Moscow, Russian Federation
[5] Botkin Hospital, Moscow, Russian Federation

Kidney transplantation (KT) remains the best treatment for patients with chronic kidney disease (CKD) stage 4–5. It helps patients live longer, have better quality of life, and undergo improved medical and social rehabilitation. This paper examines the outcomes of KT performed between 2019 and 2023. **Materials and methods.** There were 1,106 KTs deceased donor KTs performed between January 1, 2029, and December 31, 2023. The recipients had a median age of 45 (37–54) years, with 664 (60%) males and 442 (40%) females. Donors were mainly males (n = 706, 63.8%), with the median donor age being 50 (43–57) years. Induction immunosuppressive therapy (IST) with monoclonal antibodies was administered to 859 (77.7%) recipients, with polyclonal antibodies to 122 recipients (11%), and induction without antibodies to 125 recipients (11.3%). Triple-drug baseline IST consisted of a combination of calcineurin inhibitors, antimetabolites and glucocorticoids. Tacrolimus was the most often utilized calcineurin inhibitor (n = 961, 86.9%), while cyclosporine was used less often (n = 145, 13.1%). Mycophenolic acid (n = 1041, 94.1%) was used as the second medication in most recipients, while everolimus (n = 54, 4.9%) and azathioprine (n = 11, 1%) were used less often. **Results.** Primary initial renal graft function was noted in 714 patients (64.6%) and delayed in 392 recipients (35.4%). Overall incidence of surgical complications was 11.6% (n = 130), and immunological complications 9.9% (n = 109). At hospital discharge, 768 recipients (69.4%) had satisfactory kidney allograft (KAG) function, while 276 recipients (25%) were discharged with graft dysfunction; median serum creatinine and blood urea levels were 158 (120–204) μmol/L and 11 (8–16) mmol/L, respectively. Twenty-six recipients (2.4%) were discharged to continue renal replacement therapy; 28 recipients (2.6%) underwent in-hospital graft nephrectomy. Twelve individuals passed away during the hospitalization phase. The cumulative uncensored in-hospital graft and recipient survival rates were 97.5% (n = 1078) and 98.9% (n = 1094), respectively. **Conclusion.** KT is an effective and safe transplant modality for stage 4–5 CKD. Our KT outcomes are consistent with those of reputable transplant centers around the globe.

Keywords: kidney transplantation, post-kidney transplant complications, immunological complications, acute kidney transplant rejection, kidney transplant survival, recipient survival.

INTRODUCTION

Chronic kidney disease (CKD) remains a significant financial burden worldwide and a major challenge for modern medicine. According to international data, kidney disease affects over 10% of the global population [1]. Approximately 850 million individuals worldwide are living with various stages of CKD, and about 3.9 million progressing to kidney failure [2]. A study by Vivekanand Jha et al. estimates that the average annual cost of treating CKD at stages IIIa, IIIb, IV, and V are approximately $3,060, $3,544, $5,332, and $8,736 per patient, respectively [3].

As of December 31, 2020, a total of 60,547 patients with stage 5 CKD in our country were on renal replacement therapy (RRT). Of these, 83.5% (n = 50,563) were undergoing dialysis-based treatment [4]. Non-transplant treatment options for this condition are limited, serving primarily as a "bridge to transplantation", which remains the most effective surgical intervention [5]. Kidney transplantation (KT) offers significantly improved quality and duration of life compared to dialysis-based RRT, offering superior outcomes in terms of medical and social rehabilitation. More than 100,000 kidney transplants are performed globally each year. In 2022 alone, 102,090 kidney transplant procedures were carried out [6], the majority

Corresponding author: Ilya Dmitriev. Address: 3, Bolshaya Sukharevskaya Ploshad, Moscow, 129090, Russian Federation. Phone: (495) 625-08-53. E-mail: dmitrieviv@sklif.mos.ru

involving deceased donors. Despite the reasonable expansion of donor eligibility criteria and advancements in organ preservation technologies, critical organ shortage persists, leading to a significant gap between the demand for and availability of transplant care [7–9].

One of the pressing challenges in clinical KT remains the prevention and management of delayed graft function (DGF), which leads to prolonged hospitalization and increased treatment costs. Currently, the incidence of DGF ranges widely from 20% to 62.2% [10–21]. Despite advances over the past two to three decades in protocols for the prevention, diagnosis, and treatment of immunological complications, these issues remain the leading cause of renal graft loss. Surgical complications, occurring in 16% to 46% of cases, also contribute significantly to increased morbidity and extended hospital stays [22–27]. Infectious complications continue to have a profound negative impact on both graft and recipient survival rates [28–36]. The development and implementation of modern, evidence-based protocols for patient management and the treatment of post-transplant complications are therefore crucial for improving outcomes.

Globally, it is common practice within the transplant community to publish KT outcomes from both individual transplant centers and national registries. Unfortunately, in the Russian literature, such comprehensive reports remain unreasonably scarce [37]. With this article, we aim to initiate and encourage the regular publication of transplant outcomes by other transplant centers in our country.

Objective: to analyze KT outcomes performed at the transplant center with the highest annual volume of deceased-donor KTs in the Russian Federation during the period 2019–2023.

MATERIALS AND METHODS

From January 1, 2019, to December 31, 2023, a total of 1,106 deceased-donor KTs were performed at the Kidney and Pancreas Transplant Department, Sklifosovsky Research Institute for Emergency Medicine. This Institute currently holds the highest annual volume of deceased-donor KTs in the Russian Federation. The annual distribution of transplant procedures performed during this five-year period is illustrated in Fig. 1.

Recipients

The study included 1,106 KT recipients, comprising 664 men (60%) and 442 women (40%). Recipient ages ranged from 18 to 75 years, with a median age of 45 years (interquartile range: 37–54). The age distribution based on WHO classification is shown in Fig. 2.

Body mass index (BMI) ranged from 14 to 39, with a median of 25 (IQR: 21–28). Among the patients, 83 (7.5%) were underweight, 469 (42.4%) had normal weight, 355 (32.1%) were overweight, 169 (15.3%) had obesity class I, and 30 (2.7%) had obesity class II.

Blood group distribution among recipients was as follows: 0(I) – 398 patients (36%), A(II) – 417 (37.7%), B(III) – 210 (19%), and AB(IV) – 81 (7.3%).

The underlying conditions leading to stage 4–5 CKD included: chronic glomerulonephritis in 461 patients (41.7%), polycystic kidney disease – 142 (12.8%), diabetes mellitus – 127 (11.5%), tubulointerstitial diseases – 101 (9.1%), hypertensive nephroangiosclerosis – 80 (7.2%), nephropathy of unknown origin – 59 (5.3%), congenital anomalies of the urinary system – 55 (5.0%), and other less common conditions – 81 patients (7.3%) (Fig. 3).

The majority of recipients (n = 1000; 90.4%) received RRT prior to transplantation. Of these, 772 patients (69.8%) underwent maintenance hemodialysis, and 228 (20.6%) were on out-patient peritoneal dialysis. The remaining 106 recipients (9.6%) were in the predialysis stage IV CKD at the time of transplantation.

Elevated levels of pre-existing anti-HLA antibodies were observed in 103 patients (9.3%). Among them, 75 had antibodies targeting HLA class I antigens, with mean fluorescence intensity (MFI) values ranging from

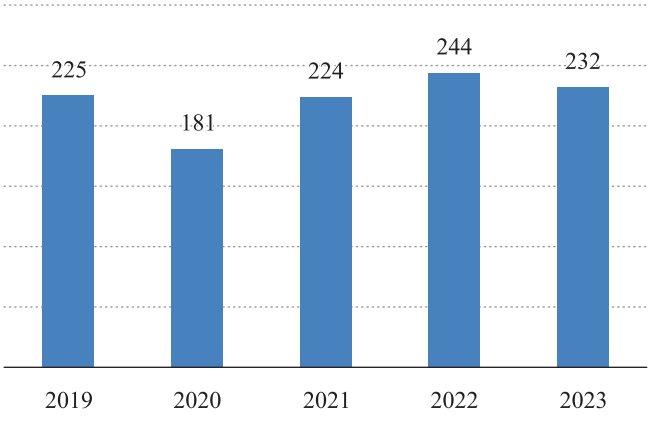

Fig. 1. Number of deceased donor kidney transplants by year for the period 2019–2023

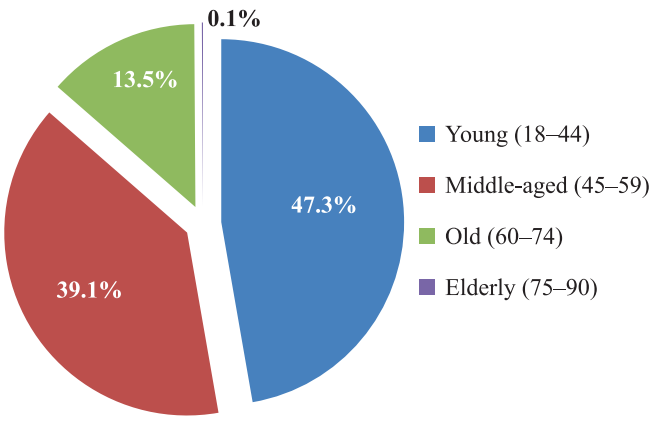

Fig. 2. Distribution of patients by age group according to the World Health Association classification for the period 2019–2023

505 to 14,444 (median 1567; IQR: 681.5–4188.5). Anti-HLA class II antibodies were present in 66 patients, with MFI ranging from 503 to 14,116 (median 1887; IQR: 788.8–7539). Both Anti-HLA class I and class II antibodies were detected in 43 patients (41.7%).

Kidney transplantation

Most recipients underwent primary KT (n = 990; 89.5%), while the remaining patients (n = 116; 10.5%) received repeat kidney transplants (second or third procedures). Cold ischemia time ranged from 7 to 27 hours, with a median of 15 hours (IQR: 12.5–17.5 hours).

Donor characteristics

The donor cohort was predominantly male (n = 706; 63.8%). Donor age ranged from 18 to 73 years, with a median age of 50 years (IQR: 43–57 years). According to the WHO age classification, 627 donors (56.7%) were middle-aged, 317 (28.7%) were young adults, and 160 (14.5%) were classified as elderly. Two donors (0.2%) had undocumented age.

The majority of donors (n = 861; 77.8%) were diagnosed with brain death after a stroke. The distribution of donor types is shown in Fig. 4.

Of the total donor pool, 671 donors (60.7%) met standard criteria, while 433 (39.2%) were classified as expanded criteria donors. Information was unavailable for two donors (0.2%). The median duration of donor hospitalization prior to organ retrieval was 2 days (IQR: 1–3.25 days).

Table 1 presents the immunological HLA compatibility and incompatibility characteristics of donor-recipient pairs.

Immunosuppressive therapy

All patients received induction and triple-drug baseline immunosuppressive therapy (IST). Induction IST with monoclonal antibodies was administered to 859 recipients (77.7%), while polyclonal antithymocyte globu-

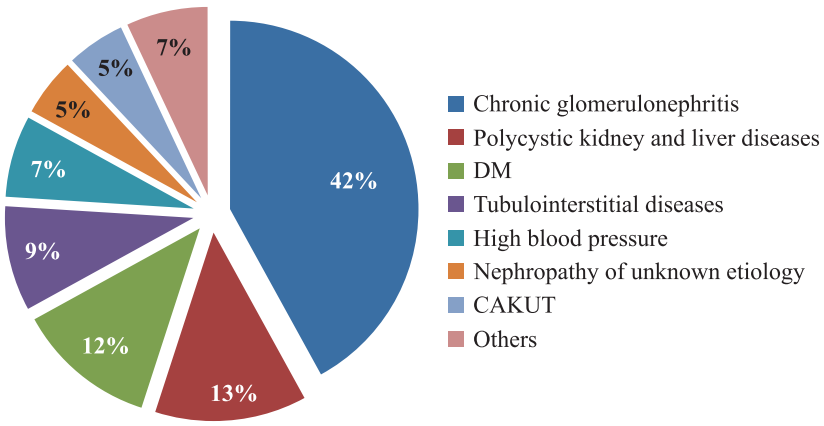

Fig. 3. Structure of the main diseases that led to chronic kidney disease stage 4–5 in patients of the study group. DM, diabetes mellitus; CAKUT, congenital anomalies of kidney and urinary tract

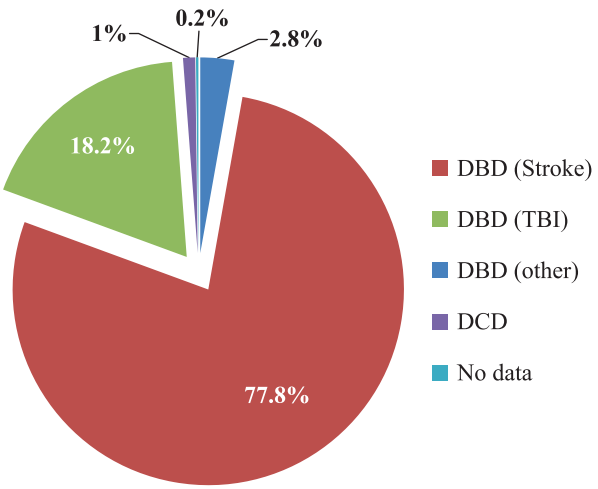

Fig. 4. Structure of donor types. DBD, donation after brain death; TBI, traumatic brain injury; DCD, donation after circulatory death

Table 1

Immunological HLA match/mismatch between donor and recipient

Indicator	Me	Q1–Q3
Number of HLA class I antigen mismatches (n, %)	2.00. 50.00	1.00–2.00. 25.00–50.00
Number of HLA class II antigen mismatches (n, %)	1.00. 50.00	1.00–2.00. 50.00–100.00
Total number of mismatches (n, %)	3.00. 50.00	2.00–4.00. 33.40–66.80
Number of class I antigen matches (n, %)	1.00. 25.00	0.00–1.00 0.00–25.00
Number of class II antigen matches (n, %)	1.00. 50.00	0.00–1.00. 0.00–50.00
Total number of matches (n, %)	1.00. 16.70	1.00–2.00. 16.70–33.40

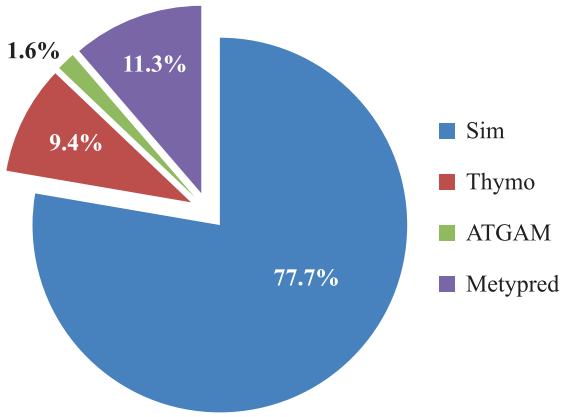

Fig. 5. Structure of induction immunosuppressive therapy. Sim, basiliximab (simulect); Thymo, polyclonal antithymocyte antibodies – human immunoglobulin (rabbit); ATGAM – polyclonal antithymocyte antibodies – human immunoglobulin (equine); Methypred, methylprednisolone

lin was used in 122 recipients (11%). In 125 recipients (11.3%), induction therapy was carried out without the use of antibodies (Fig. 5).

The triple-drug baseline IST regimen consisted of a combination of calcineurin inhibitors, antimetabolites, and glucocorticosteroids. Among calcineurin inhibitors, tacrolimus was predominantly used (n = 961, 86.9%), with cyclosporine being less commonly administered (n = 145, 13.1%).

As the antimetabolite component, mycophenolic acid was used in the majority of recipients (n = 1041, 94.1%). Everolimus was used in 54 patients (4.9%), and azathioprine in 11 patients (1%). No steroid-free IST regimens were used during this period.

Statistical data processing

Statistical analysis was performed using StatTech v. 4.0.6 (StatTech, Russia). The distribution of quantitative variables was assessed using the Shapiro–Wilk test (for sample sizes <50) or the Kolmogorov–Smirnov test (for sample sizes >50).

For variables with a normal distribution, results were presented as the arithmetic mean (M) and standard deviation (SD), along with 95% confidence intervals (95% CI). In cases where data did not follow a normal distribution, results were expressed as the median (Me) and interquartile range (Q1–Q3). Categorical variables were described using absolute counts and percentages (%).

Comparison of two groups by a quantitative variable with a non-normal distribution was performed using the Mann–Whitney U test. For comparisons among three or more groups, the Kruskal–Wallis test was applied, followed by Dunn's post hoc test with Holm's correction for multiple comparisons.

Analysis of categorical variables in 2×2 contingency tables was carried out using Pearson's chi-square test (when the expected frequencies were >10) or Fisher's exact test (when the expected frequencies were <10). For multi-field contingency tables, Pearson's chi-square test was used to compare proportions.

RESULTS

Renal graft function

Immediate graft function was observed in 714 recipients (64.6%), while delayed graft function (DGF) occurred in 392 patients (35.4%). The time to azotemia normalization ranged from 1 to 66 days, with a median of 8 days (IQR: 4–14 days). In DGF cases, the median number of extracorporeal detoxification procedures required was 4 (IQR: 2–8).

Surgical complications

The overall incidence of surgical complications was 11.6%, with 130 complications recorded in 128 patients. The distribution of surgical complications according to the Clavien–Dindo classification is presented in Table 2.

A classification of surgical complications is presented in Table 3.

Immunologic complications

The incidence of immunologic complications was 9.9%, with 109 episodes of acute rejection occurring in 107 patients. The onset of acute renal graft rejection ranged from 1 to 58 days post-transplant, with a median onset of 10 days (IQR: 6–17 days). The patients with rejection episodes received pulse corticosteroid (methyl-

Table 2

Structure of surgical complications according to the Clavien–Dindo Classification

Category of surgical complications	n, abs	%
I	4	3.1
II	6	4.6
IIIa	25	19.2
IIIb	70	53.8
IVa	21	16.2
IVb	4	3.1

Table 3

Types of surgical complications

Type of complication	n, abs	%
Occlusive arterial thrombosis	2	1.5
Non-occlusive venous thrombosis	17	13.1
Subcapsular renal transplant hematoma	22	16.9
Transplant renal artery kinking	1	0.8
Post-renal transplant lymphoceles	37	28.5
Urinary leakage	44	33.8
Ureteral stricture	4	3.1
Urethral stricture	1	0.8
Bleeding	2	1.5

prednisolone) therapy as follows: 31 patients received polyclonal antithymocyte antibody infusions, including 22 with rabbit antithymocyte globulin, 9 with equine antithymocyte globulin, 21 patients underwent plasmapheresis (1–6 sessions; mean: 3.48 ± 1.25 sessions), followed by intravenous immunoglobulin administration.

Outcomes

At the time of hospital discharge, 768 recipients (69.4%) demonstrated satisfactory kidney allograft (KAG) function, with serum creatinine levels below 200 μmol/L. An additional 276 recipients (25%) were discharged with KAG dysfunction, defined as serum creatinine levels exceeding 200 μmol/L, but without the need for RRT. The median serum creatinine among these two groups was 158 μmol/L (IQR: 120–204 μmol/L), and the median blood urea level was 11 mmol/L (IQR: 8–16 mmol/L).

Twenty-six recipients (2.4%) with adequately perfused grafts were transferred to the outpatient stage of care for RRT continuation. Twenty-eight recipients (2.6%) underwent graft nephrectomy during hospitalization for various clinical indications (see Table 4).

A total of 12 recipients (1.1%) died during the hospitalization period: 8 patients with a functioning renal graft and 4 patients following graft removal. The causes of death are presented in Table 5.

The cumulative uncensored graft survival rate during hospitalization was 97.5% (n = 1078), while the recipient survival rate for the same period was 98.9% (n = 1094).

Table 4

Causes of in-hospital renal graft loss

Reason for KAG nephrectomy	n, abs	%
Acute rejection crisis	12	42.9
Venous thrombosis	6	21.4
Sepsis	5	17.9
Donor pathology	1	3.6
Cortical necrosis	1	3.6
Bleeding from KAG	1	3.6
Bleeding from biopsy site	1	3.6
Necrosis of the lower pole of KAG	1	3.6

Table 5

Causes of in-hospital recipient mortality

Cause of death	n, abs.	%
Sepsis	5	41.7
Acute heart failure	3	25.0
COVID-19	2	16.7
Hypoxic brain injury	1	8.3
Acute stroke	1	8.3

DISCUSSION

According to registry data, the global incidence of CKD has been increasing steadily in recent years [38]. Dialysis-based RRTs are crucial for supporting patients with end-stage renal disease while they await KT, significantly extending their lifespan and improving their quality of life [5, 39]. However, there remains a critical gap between the demand for and the availability of kidney transplants, primarily due to a severe shortage of donor organs. Even with the expansion of criteria for graft suitability, this issue persists. Worldwide, the annual number of KTs performed exceeds 100,000, with the United States leading – a record of 25,487 KTs in 2021 [40]. In the Russian Federation, 1,562 KTs were carried out in 2022, with 1,334 from deceased donors and 228 from living-related donors [41]. Over the last decade, the Kidney and Pancreas Transplant Department, Sklifosovsky Research Institute for Emergency Medicine, has performed the highest number of deceased-donor KTs in the country.

Delayed graft function (DGF) remains one of the most common complications following kidney transplantation, negatively impacting early outcomes. It is associated with increased rejection rates, prolonged hospitalization, and consequently higher treatment costs [42–45]. A large study by Kim et al. found that DGF led to an average increase in costs of approximately $18,000 (10%) ($130,492 versus $112,598, $P < 0.0001$), 6 additional days of hospitalization (14.7 versus 8.7 days, $P < 0.0001$), and 2 extra days in the ICU (4.3 versus 2.1 days, $P < 0.0001$). Furthermore, multiple dialysis sessions were associated with an additional cost of $10,000 compared to patients who only required one session [46]. The reported incidence of DGF varies between 24% and 62% [21, 40, 47–50]. In our study, DGF incidence was 35.4%.

While not the primary cause of renal graft failure, surgical complications in kidney transplantation significantly increase patient morbidity and prolong hospitalization. The overall incidence of surgical complications following KT can range from 12% to 25%, with vascular complications occurring in 0.8% to 6% of cases [22, 24, 26]. The most common non-vascular surgical complications are urologic issues, affecting 2.5% to 30% of patients, and nephrotransplant bed lymphocele, which can range from 0.6% to 40% [22, 24]. In our center, the incidence of surgical complications was 11.6%. The incidence of acute graft rejection in the early postoperative period varies between 10% and 30% according to the available literature [51–53]. In our study, the incidence of immunological complications was 9.9%.

We evaluated in-hospital survival rates for both kidney transplants and recipients, which were 97.5% and 98.9%, respectively, aligning with the survival rates seen in leading transplant centers worldwide.

CONCLUSION

KT remains an effective and safe treatment option for stage 4–5 CKD patients. The outcomes achieved in our center – including the incidence of surgical and immunological complications, as well as in-hospital survival rates for both grafts and recipients – are comparable to those reported by leading international transplant centers.

The authors declare no conflict of interest.

REFERENCES

1. *Kovesdy CP.* Epidemiology of chronic kidney disease: an update 2022. *Kidney Int Suppl (2011)*. 2022; 12 (1): 7–11. PMID: 35529086. doi: 10.1016/j.kisu.2021.11.003.
2. *Jager KJ, Kovesdy C, Langham R, Rosenberg M, Jha V, Zoccali C*. A single number for advocacy and communication-worldwide more than 850 million individuals have kidney diseases. *Nephrol Dial Transplant*. 2019; 34 (11): 1803–1805. PMID: 31566230. doi: 10.1093/ndt/gfz174.
3. *Jha V, Al-Ghamdi SMG, Li G, Wu MS, Stafylas P, Retat L et al.* Global Economic Burden Associated with Chronic Kidney Disease: A Pragmatic Review of Medical Costs for the Inside CKD Research Programme. *Adv Ther*. 2023; 40 (10): 4405–4420. PMID: 37493856. doi: 10.1007/s12325-023-02608-9.
4. *Andrusev AM, Peregudova NG, Shinkarev MB, Tomilina NA*. Kidney replacement therapy for end Stage Kidney disease in Russian Federation, 2016–2020. Russian National Kidney Replacement Therapy Registry Report of Russian Public Organization of Nephrologists "Russian Dialysis Society". *Nephrology and Dialysis*. 2022; 24 (4): 555–565. [In Russ, English abstract]. doi: 10.28996/2618-9801-2022-4-555-565.
5. *Данович ГМ.* Трансплантация почки: руководство / Пер. с англ. М.: ГЭОТАР-Медиа; 2013. *Danovich GM*. Transplantatsiya pochki: rukovodstvo / Per. s angl. M.: GEOTAR-Media; 2013. [In Russ].
6. Available from: https://www.statista.com/statistics/398645/global-estimation-of-organ-transplantations/ [Accessed 22/08/2024].
7. *Tingle SJ, Figueiredo RS, Moir JA, Goodfellow M, Talbot D, Wilson CH.* Machine perfusion preservation versus static cold storage for deceased donor kidney transplantation. *Cochrane Database Syst Rev*. 2019; 3 (3): CD011671. PMID: 30875082. doi: 10.1002/14651858.CD011671.pub2.
8. *Hosgood SA, Callaghan CJ, Wilson CH, Smith L, Mullings J, Mehew J et al.* Normothermic machine perfusion versus static cold storage in donation after circulatory death kidney transplantation: a randomized controlled trial. *Nat Med*. 2023; 29 (6): 1511–1519. PMID: 37231075. doi: 10.1038/s41591-023-02376-7.
9. *Malinoski D, Saunders C, Swain S, Groat T, Wood PR, Reese J et al.* Hypothermia or Machine Perfusion in Kidney Donors. *N Engl J Med*. 2023; 388 (5): 418–426. PMID: 36724328. doi: 10.1056/NEJMoa2118265.
10. *Kernig K, Albrecht V, Dräger DL, Führer A, Mitzner S, Kundt G et al.* Predictors of Delayed Graft Function in Renal Transplantation. *Urol Int.* 2022; 106 (5): 512–517. PMID: 34915519. doi: 10.1159/000520055.
11. *Huaman MA, Vilchez V, Mei X, Davenport D, Gedaly R.* Donor positive blood culture is associated with delayed graft function in kidney transplant recipients: a propensity score analysis of the UNOS data-base. *Clin Transpl*. 2016; 30 (4): 415–420. PMID: 26840885. doi: 10.1111/ctr.12703.
12. *Potluri VS, Parikh CR, Hall IE, Ficek J, Doshi MD, Butrymowicz I et al.* Validating early post-transplant outcomes reported for recipients of deceased donor kidney transplants. *Clin J Am Soc Nephrol*. 2016; 11 (2): 324–331. PMID: 26668026. doi: 10.2215/CJN.06950615.
13. *Yao Z, Kuang M, Li Z.* Global trends of delayed graft function in kidney transplantation from 2013 to 2023: a bibliometric analysis. *Ren Fail.* 2024; 46 (1): 2316277. PMID: 38357764. doi: 10.1080/0886022X.2024.2316277.
14. *Schrezenmeier E, Müller M, Friedersdorff F, Khadzhynov D, Halleck F, Staeck O et al.* Evaluation of severity of delayed graft function in kidney transplant recipients. *Nephrol Dial Transplant.* 2022; 37 (5): 973–981. PMID: 34665258. doi: 10.1093/ndt/gfab304.
15. *Mannon RB*. Delayed Graft Function: The AKI of Kidney Transplantation. *Nephron.* 2018; 140 (2): 94–98. PMID: 30007955. doi: 10.1159/000491558.
16. *Tapiawala SN, Tinckam KJ, Cardella CJ, Schiff J, Cattran DC, Cole EH et al.* Delayed graft function and the risk for death with a functioning graft. *J Am Soc Nephrol*. 2010; 21 (1): 153–161. PMID: 19875806. doi: 10.1681/ASN.2009040412.
17. *Wang CJ, Wetmore JB, Israni AK*. Old versus new: progress in reaching the goals of the new kidney allocation system. *Hum Immunol*. 2017; 78 (1): 9–15. PMID: 27527922. doi: 10.1016/j.humimm.2016.08.007.
18. *Zens TJ, Danobeitia JS, Leverson G, Chlebeck PJ, Zitur LJ, Redfield RR et al.* The impact of kidney donor profile index on delayed graft function and transplant outcomes: a single-center analysis. *Clin Transplant*. 2018; 32 (3): e13190. PMID: 29314286. doi: 10.1111/ctr.13190.
19. *Bahl D, Haddad Z, Datoo A, Qazi YA*. Delayed graft function in kidney transplantation. *Curr Opin Organ Transplant*. 2019; 24 (1): 82–86. PMID: 30540574. doi: 10.1097/MOT.0000000000000604.
20. *Leão-Reis FC, De Carvalho Silva BDP, De Morais JDP, Santos JFG, Dias-Sanches M.* Delayed Graft Function Duration in Deceased Donor Kidney Transplants. *Transplant Proc.* 2022; 54 (5): 1247–1252. PMID: 35768295. doi: 10.1016/j.transproceed.2022.02.062.
21. *Shabunin AV, Drozdov PA, Nesterenko IV, Makeev DA, Astapovich SA, Zhuravel OS et al.* Effect of delayed graft function on immediate and long-term kidney transplant outcomes. *Russian Journal of Transplantology and Artificial Organs*. 2024; 26 (1): 20–25. [In Russ, English abstract]. https://doi.org/10.15825/1995-1191-2024-1-20-25.

22. *Haberal M, Boyvat F, Akdur A, Kırnap M, Özçelik Ü, Yarbuğ Karakayalı F*. Surgical Complications After Kidney Transplantation. *Exp Clin Transplant*. 2016; 14 (6): 587–595. PMID: 27934557.
23. *Kim PY, Shoghi A, Fananapazir G.* Renal Transplantation: Immediate and Late Complications. *Radiol Clin North Am*. 2023; 61 (5): 809–820. PMID: 37495289. doi: 10.1016/j.rcl.2023.04.004.
24. *Carvalho JA, Nunes P, Antunes H, Parada B, Tavares da Silva E, Rodrigues L et al.* Surgical Complications in Kidney Transplantation: An Overview of a Portuguese Reference Center. *Transplant Proc*. 2019; 51 (5): 1590–1596. PMID: 31155198. doi: 10.1016/j.transproceed.2019.05.001.
25. *Salamin P, Deslarzes-Dubuis C, Longchamp A, Petitprez S, Venetz JP, Corpataux JM et al.* Predictive Factors of Surgical Complications in the First Year Following Kidney Transplantation. *Ann Vasc Surg*. 2022; 83: 142–151. PMID: 34687888. doi: 10.1016/j.avsg.2021.08.031.
26. *Wolff T, Schumacher M, Dell-Kuster S, Rosenthal R, Dickenmann M, Steiger J et al.* Surgical complications in kidney transplantation: no evidence for a learning curve. *J Surg Educ*. 2014; 71 (5): 748–755. PMID: 24913427. doi: 10.1016/j.jsurg.2014.03.007.
27. *Choffel L, Kleinclauss F, Balssa L, Barkatz J, Lecheneaut M, Guichard G et al.* Surgical complications and graft survival in kidney transplant recipients according to CT-scans evaluation. *Fr J Urol*. 2024; 34 (1): 102543. PMID: 37858380. doi: 10.1016/j.purol.2023.09.030.
28. *Agrawal A, Ison MG, Danziger-Isakov L.* Long-Term Infectious Complications of Kidney Transplantation. *Clin J Am Soc Nephrol*. 2022; 17 (2): 286–295. PMID: 33879502. doi: 10.2215/CJN.15971020.
29. *Fishman JA.* Infection in Organ Transplantation. *Am J Transplant*. 2017; 17 (4): 856–879. PMID: 28117944. doi: 10.1111/ajt.14208.
30. *Vnucak M, Granak K, Beliancinova M, Miklusica J, Dedinska I.* Age and sex disparity in infectious complications after kidney transplantation. *Bratisl Lek Listy.* 2022; 123 (7): 463–469. PMID: 35907050. doi: 10.4149/BLL_2022_074.
31. *Warzyszyńska K, Zawistowski M, Karpeta E, Ostaszewska A, Jonas M, Kosieradzki M.* Early Postoperative Complications and Outcomes of Kidney Transplantation in Moderately Obese Patients. *Transplant Proc*. 2020; 52 (8): 2318–2323. PMID: 32252995. doi: 10.1016/j.transproceed.2020.02.110.
32. *Mourad G, Serre JE, Alméras C, Basel O, Garrigue V, Pernin V et al.* Complications infectieuses et néoplasiques après transplantation rénale [Infectious and neoplasic complications after kidney transplantation]. *Nephrol Ther*. 2016; 12 (6): 468–487. French. PMID: 27686031. doi: 10.1016/j.nephro.2016.06.003.
33. *Bharati J, Anandh U, Kotton CN, Mueller T, Shingada AK, Ramachandran R.* Diagnosis, Prevention, and Treatment of Infections in Kidney Transplantation. *Semin Nephrol*. 2023; 43 (5): 151486. PMID: 38378396. doi: 10.1016/j.semnephrol.2023.151486.
34. *De Castro Rodrigues Ferreira F, Cristelli MP, Paula MI, Proença H, Felipe CR, Tedesco-Silva H et al.* Infectious complications as the leading cause of death after kidney transplantation: analysis of more than 10,000 transplants from a single center. *J Nephrol.* 2017; 30 (4): 601–606. PMID: 28211034. doi: 10.1007/s40620-017-0379-9.
35. *Alangaden GJ, Thyagarajan R, Gruber SA, Morawski K, Garnick J, El-Amm JM et al.* Infectious complications after kidney transplantation: current epidemiology and associated risk factors. *Clin Transplant*. 2006; 20 (4): 401–409. PMID: 16842513. doi: 10.1111/j.1399-0012.2006.00519.x.
36. *Guimarães-Souza NK, Dalboni MA, Câmara NC, Medina-Pestana JO, Paheco-Silva A, Cendoroglo M.* Infectious complications after deceased kidney donor transplantation. *Transplant Proc*. 2010; 42 (4): 1137–1141. PMID: 20534244. doi: 10.1016/j.transproceed.2010.03.074.
37. *Shabunin AV, Parfenov IP, Minina MG, Drozdov PA, Nesterenko IV, Makeev DA et al.* Botkin Hospital Transplant Program: 100 solid organ transplantations. *Russian Journal of Transplantology and Artificial Organs*. 2020; 22 (1): 55–58. [In Russ, English abstract]. https://doi.org/10.15825/1995-1191-2020-1-55-58.
38. *Hill NR, Fatoba ST, Oke JL, Hirst JA, O'Callaghan CA, Lasserson DS et al.* Global Prevalence of Chronic Kidney Disease – A Systematic Review and Meta-Analysis. *PLoS One.* 2016; 11 (7): e0158765. PMID: 27383068. doi: 10.1371/journal.pone.0158765 eCollection 2016.
39. *Matesanz R, Mahíllo B.* The Current Situation Regarding Organ Donation and Transplantation in Europe. In: Figueiredo A, Lledó-García E. (eds.) *European Textbook on Kidney Transplantation.* Netherlands: Arnhem, 2017: 59–85.
40. *Lentine KL, Smith JM, Miller JM, Bradbrook K, Larkin L, Weiss S et al.* OPTN/SRTR 2021 Annual Data Report: Kidney. *Am J Transplant*. 2023; 23 (2 Suppl 1): S21–S120. PMID: 37132350. doi: 10.1016/j.ajt.2023.02.004.
41. *Gautier SV, Khomyakov SM*. Organ donation and transplantation in the Russian Federation in 2022. 15th Report from the Registry of the Russian Transplant Society. *Russian Journal of Transplantology and Artificial Organs*. 2023; 25 (3): 8–30. [In Russ, English abstract]. https://doi.org/10.15825/1995-1191-2023-3-8-30.
42. *Mezzolla V, Pontrelli P, Fiorentino M, Stasi A, Pesce F, Franzin R et al.* Emerging biomarkers of delayed graft function in kidney transplantation. *Transplant Rev (Orlando).* 2021; 35 (4): 100629. PMID: 34118742. doi: 10.1016/j.trre.2021.100629.
43. *Yousif EAI, Muth B, Manchala V, Turk J, Blazel J, Bloom M et al.* In kidney recipients from the same deceased donor, discordance in delayed graft function is associated with the worst outcomes. *Clin Transplant*. 2022; 36 (9): e14779. PMID: 35848635. doi: 10.1111/ctr.14779.
44. *Lai C, Yee SY, Ying T, Chadban S*. Biomarkers as diagnostic tests for delayed graft function in kidney transplantation. *Transpl Int*. 2021; 34 (12): 2431–2441. PMID: 34626503. doi: 10.1111/tri.14132.

45. *Shabunin AV, Loran OB, Pushkar DYu, Veliev EI, Minina MG, Drozdov PA et al.* Integrated strategy for preventing delayed renal graft function. *Russian Journal of Transplantology and Artificial Organs*. 2023; 25 (2): 8–14. [In Russ, English abstract]. https://doi.org/10.15825/1995-1191-2023-2-8-14.
46. *Kim DW, Tsapepas D, King KL, Husain SA, Corvino FA, Dillon A et al.* Financial impact of delayed graft function in kidney transplantation. *Clin Transplant.* 2020; 34 (10): e14022. PMID: 32573812. doi: 10.1111/ctr.14022.
47. *Aitken E, Cooper C, Dempster N, McDermott M, Ceresa C, Kingsmore D.* Delayed graft function is a syndrome rather than a diagnosis. *Exp Clin Transplant*. 2015; 13 (1): 19–25. PMID: 25654410.
48. *Shi B, Ying T, Xu J, Wyburn K, Laurence J, Chadban SJ.* Obesity is Associated with Delayed Graft Function in Kidney Transplant Recipients: A Paired Kidney Analysis. *Transpl Int.* 2023; 36: 11107. PMID: 37324221. doi: 10.3389/ti.2023.11107.
49. *Budhiraja P, Reddy KS, Butterfield RJ, Jadlowiec CC, Moss AA, Khamash HA et al.* Duration of delayed graft function and its impact on graft outcomes in deceased donor kidney transplantation. *BMC Nephrol*. 2022; 23 (1): 154. PMID: 35440023. doi: 10.1186/s12882-022-02777-9.
50. *Maia LF, Lasmar MF, Fabreti-Oliveira RA, Nascimento E.* Effect of Delayed Graft Function on the Outcome and Allograft Survival of Kidney Transplanted Patients from a Deceased Donor. *Transplant Proc*. 2021; 53 (5): 1470–1476. PMID: 34006380. doi: 10.1016/j.transproceed.2021.04.002.
51. *Khater N, Khauli R.* Pseudorejection and true rejection after kidney transplantation: classification and clinical significance. *Urol Int.* 2013; 90 (4): 373–380. PMID: 23095211. doi: 10.1159/000342965.
52. *Cippà PE, Schiesser M, Ekberg H, van Gelder T, Mueller NJ, Cao CA et al.* Risk Stratification for Rejection and Infection after Kidney Transplantation. *Clin J Am Soc Nephrol*. 2015; 10 (12): 2213–2220. PMID: 26430088. doi: 10.2215/CJN.01790215.
53. *Dorr CR, Oetting WS, Jacobson PA, Israni AK.* Genetics of acute rejection after kidney transplantation. *Transpl Int.* 2018; 31 (3): 263–277. PMID: 29030886. doi: 10.1111/tri.13084.

The article was submitted to the journal on 09.09.2024

DOI: 10.15825/1995-1191-2024-4-100-109

HEART TRANSPLANTATION IN PATIENTS UNDERGOING EXTRACORPOREAL CARDIOPULMONARY RESUSCITATION IN IN-HOSPITAL CARDIAC ARREST

V.N. Poptsov, E.A. Spirina, A.K. Solodovnikova, A.S. Epremyan, A.A. Kuznetsova, A.S. Ignatkina, G.B. Glinkin, S.A. Budagaev

Shumakov National Medical Research Center of Transplantology and Artificial Organs, Moscow, Russian Federation

Objective: to analyze heart transplant (HT) outcomes in patients who suffered cardiac arrest requiring extracorporeal cardiopulmonary resuscitation (ECPR) by peripheral veno-arterial extracorporeal membrane oxygenation (VA-ECMO). **Materials and methods.** The study included 41 patients (14 (34.1%) women and 27 (65.9%) men, aged 42.6 ± 16.8 (40.0 [30.5; 54.0]) years with in-hospital cardiac arrest. The causes of cardiac arrest were acute decompensated heart failure (n = 19; 46.3%), irreversible graft dysfunction (n = 9; 22.0%), postcardiotomy acute heart failure (n = 5; 12.2%), acute myocardial infarction (n = 4; 9.8%), and acute graft rejection (n = 4; 9.8%). **Results.** Twenty-seven (65.9%) patients had cardiac arrest in the intensive care unit (ICU) and 14 (34.1%) outside ICU. The interval between femoral artery puncture and ECPR initiation was 4-17 (9 ± 5) minutes, while that between cardiopulmonary resuscitation (CPR) initiation and peripheral VA-ECMO was 26 ± 9 minutes. Atonic seizure developed in 11 (26.8%) of 41 patients while receiving VA-ECMO. Of the 41 patients, 30 (73.2%) had irreversible brain damage. Four (9.8%) patients were discharged from the hospital without neurological or multiple organ dysfunction. In 26 (63.4%) patients (10 (38.5%) women and 16 (61.5%) men) aged 14 to 63 (40.7 ± 15.8) years, ECPR and subsequent treatment resulted in survival to HT while receiving VA-ECMO (duration 1-11 (4.0 [1.5; 5.0]) days). The age of the heart donor (6 (23.1%) women and 20 (76.9%) men) was 44.0 ± 9.9 years, the cumulative Eurotransplant Heart Donor Score was 16.9 ± 2.7, the Donor Risk Index was 6.3 ± 1.5, and the estimated incidence of severe primary graft dysfunction (RADIAL scale) was 15.4 ± 3.7%. Graft ischemia lasted for 188 ± 72 (170.0 [141.25; 185.0]) minutes. Five (19.2%) recipients developed severe dysfunction, which required continuation of peripheral VA-ECMO in the postperfusion period. The cause of death (n = 4; 15.3%) in the early post-HT period was irreversible multiple organ dysfunction. **Conclusion.** In-hospital survival after emergency HT in recipients who underwent ECPR before transplantation is 84.7%.

Keywords: cardiac arrest, peripheral veno-arterial extracorporeal membrane oxygenation, heart transplantation.

INTRODUCTION

Patients waiting for a heart transplant (HT) are at higher risk of cardiac arrest (CA), both inside and outside of hospitals, because of the advanced stages of heart failure and the underlying irreversible heart disease they have [1]. Extracorporeal cardiopulmonary resuscitation (ECPR), which uses veno-arterial extracorporeal membrane oxygenation (VA-ECMO) after conventional cardiopulmonary resuscitation (CPR) fails, using manual or mechanical chest compressions, is a growing life-saving intervention for both out-of-hospital and in-hospital CA (IHCA) [2, 3]. ECPR has demonstrated better survival rates in patients who have suffered CA compared to standard CPR [4].

The **objective** of this study was to evaluate HT outcomes in patients who experienced CA necessitating an ECPR.

MATERIALS AND METHODS

The study included 41 patients (14 women [34.1%] and 27 men [65.9%]) with a mean age of 42.6 ± 16.8 years (median 40.0 [IQR: 30.5–54.0] years), who had IHCA requiring ECPR between 2011 and 2023. ECPR was initiated due to no spontaneous recovery of heart rhythm and effective hemodynamics despite conventional CPR. These cases represented 3.4% (n = 41/1217) of all VA-ECMO initiations at our institution during the study period.

Sudden CA occurred in the context of decompensated chronic heart failure (CHF) in 19 patients (46.3%), irreversible cardiac allograft dysfunction in 9 (22.0%), postcardiotomy cardiogenic shock in 5 (12.2%), acute HF due to myocardial infarction in 4 (9.8%), and acute cardiac graft rejection in 4 patients (9.8%).

Corresponding author: Vitaliy Poptsov. Address: 1, Shchukinskaya str., Moscow, 123182, Russian Federation. Phone: (963) 644-96-39. E-mail: poptsov_vit@mail.ru

Among the 41 patients included in the study, the underlying cardiac pathology was dilated cardiomyopathy (DCM) in 18 cases (43.9%), coronary heart disease (CHD) in 10 (24.4%), irreversible cardiac graft dysfunction in 9 (22.0%), and heart graft rejection in 4 patients (9.8%). Fourteen patients (34.1%) were on the heart transplant waiting list (HTWL) and had been admitted for pre-transplant management. An additional 9 patients (22.0%) were hospitalized for assessment within the potential HT candidate program.

All patients initially underwent conventional CPR in accordance with established clinical protocols, using either manual or mechanical chest compressions [5, 6]. ECPR was initiated after 20 minutes of unsuccessful conventional CPR, defined by failure to restore electrical cardiac activity, adequate myocardial contraction, or systemic hemodynamics. The decision to proceed with ECPR was made in line with current international guidelines and protocols [7].

During continued manual or mechanical chest compressions, percutaneous puncture and catheterization of the common femoral artery and vein (on one or both sides) were performed using 14–16 G single-lumen intravascular catheters. In 21 patients with pre-existing femoral artery catheterization for invasive blood pressure monitoring, this access was used to expedite placement of the femoral arterial ECMO cannula. Femoral access was guided either by anatomical landmarks or ultrasound using a portable device.

Following successful vascular access, 5,000 units of unfractionated heparin were administered intravenously for systemic anticoagulation. An Amplatz Super Stiff J-Tip guidewire (0.89 mm in diameter, 260 cm in length), or its equivalent, was introduced through the intravascular catheter placed in the femoral vein. After stepwise dilation of the percutaneous track, the femoral venous ECMO cannula was inserted to a depth of 35–45 cm, depending on the patient's anthropometric characteristics. The arterial cannula was inserted using the same technique. Both cannulas were then connected to the ECMO circuit, and VA-ECMO was initiated with the following initial settings: volumetric blood flow rate of 2.5–4.0 L/min, gas flow rate of 4.0–8.0 L/min, and FiO_2 of 1.0.

Immediately after ECMO initiation, targeted temperature management was implemented for neuroprotection and prevention of irreversible cerebral injury. This included cooling the patient to 35.0–35.5 °C via the ECMO heat exchanger [8], elevating the head of the resuscitation bed to 35–45°, applying ice packs to the head, and administering intravenous mannitol and hypertonic sodium solution. These measures aimed to achieve serum osmolarity of 310 mOsm/L and serum sodium concentration of 145–155 mmol/L [9].

Hearts from brain-dead donors were used for HT. The presence and number of expanded criteria donation factors were documented according to widely accepted definitions for standard and expanded heart donation. Donor heart marginality was quantitatively assessed using the Eurotransplant Heart Donor Score, the Donor Risk Index, and the RADIAL score. The probability of developing severe primary graft dysfunction was estimated using the RADIAL score.

Quantitative data are presented as mean ± standard deviation ($M \pm \sigma$) and as median with interquartile range (Me [Q1; Q3]).

RESULTS

In all cases, CA occurred in the presence of witnesses (medical staff or other patients). Specifically, 27 patients (65.9%) experienced CA in the intensive care unit (ICU), 12 (29.3%) in the ward, and 2 (4.9%) in the X-ray surgical operating room. The time of CA occurrence was distributed as follows: 9:00 AM to 6:00 PM in 22 patients (53.7%), 6:00 PM to 12:00 AM in 11 patients (26.8%), and 12:00 AM to 9:00 AM in 8 patients (19.5%).

The initial cardiac rhythm recorded upon connection to the ECG monitor was ventricular fibrillation in 26 patients (63.4%), ventricular flutter in 4 (9.8%), and bradyarrhythmia or asystole in 11 (26.8%).

In all cases, ECPR was preceded by comprehensive CPR, which included manual chest compressions in 31 patients (75.6%) and/or automatic mechanical compressions in 10 patients (24.4%). In 8 patients (38.1%) with asystole or severe bradycardia, endocardial pacing electrodes were placed.

In 32 patients (78.0%), CPR was initiated or continued in the ICU, where subsequent VA-ECMO preparation and connection were also carried out. Among the 12 patients who experienced CA in the ward, 7 were transferred to the cardiac surgical operating room for ongoing CPR. In 8 cases from this group, to avoid interruption of CPR and minimize time to VA-ECMO initiation, femoral artery puncture and cannulation were performed directly on the transport trolley wheelchair.

The interval between CPR onset and the initiation of femoral artery puncture for subsequent cannulation ranged from 14 to 35 minutes (mean 23 ± 8 minutes) in patients (n = 27) who experienced CA in the ward, and from 4 to 20 minutes (mean 11 ± 7 minutes) in patients (n = 14) who experienced CA in the ICU or X-ray surgical operating room.

In all cases, peripheral VA-ECMO was initiated via cannulation of the femoral vessels, either unilaterally (n = 34; 82.9%) or bilaterally (n = 7; 17.1%). Cannula sizes used for arterial access ranged from 15 F to 19 F, while venous cannulation utilized 21 F to 28 F cannulas.

Initial VA-ECMO settings included a pump speed of 7167 ± 320 rpm, an extracorporeal blood flow rate of 3.91 ± 0.27 L/min (or 2.14 ± 0.19 L/min/m^2), gas flow of 5.7 ± 0.9 L/min, and a fraction of inspired oxygen (FiO_2) of 1.0.

The mean time from CPR onset to VA-ECMO initiation was 26 ± 9 minutes. The time from the start of femoral vascular puncture to the beginning of ECPR ranged from 4 to 17 minutes, with a mean of 9 ± 5 minutes.

The interval between CPR initiation and VA-ECMO connection was significantly shorter in patients who experienced CA in the ICU compared to those in the ward (22 ± 8 minutes *vs.* 38 ± 13 minutes, respectively; p = 0.001).

In 100% of cases, restoration of cardiac rhythm and mechanical heart activity – confirmed by the appearance of an arterial pressure waveform and visible ventricular contractions on transthoracic or transesophageal echocardiography – was achieved within 3 to 20 minutes after VA-ECMO initiation. Ten patients (24.4%) had a spontaneous return of rhythm, while the remaining 30 patients (75.6%) required repeated antiarrhythmic therapy or electrical defibrillation. Indirect cardiac massage was maintained until both rhythm restoration and mechanical ventricular activity were confirmed, ensuring continued upper body perfusion and decompression of the cardiac chambers.

Following successful peripheral VA-ECMO initiation and cessation of active resuscitation, the superficial femoral artery was catheterized in all patients to prevent lower limb ischemia from . This was achieved via percutaneous puncture in 33 cases (80.5%) and open surgical access in 8 cases (19.5%).

In 6 patients (14.6%), progressive deterioration of left ventricular systolic function and clinical/radiological signs of pulmonary edema necessitated percutaneous left atrial drainage. This was performed to relieve volume overload in the left heart chambers using an additional venous drainage cannula (18–21 F), inserted through the interatrial septum via transfemoral venous access.

Eleven (26.8%) out of 41 patients receiving VA-ECMO had irreversible brain damage with the development of atonic coma and subsequent death (Fig.). The other 30 patients (73.2%) did not exhibit signs of irreversible neurological injury. In 4 patients (9.8%) – 3 with cardiac graft rejection and 1 with postcardiotomy acute heart failure – VA-ECMO was successfully discontinued on days 3 to 6. These patients were discharged from the hospital without clinically significant neurological deficits or manifestations of multiple organ dysfunction.

In 26 patients (63.4%) – including 16 males (61.5%) and 10 females (38.5%), aged 14 to 63 years (mean age 40.7 ± 15.8 years) – ECPR followed by intensive care resulted in survival to HT while on VA-ECMO support. The underlying pathology in this subgroup (n = 26) included DCM (n = 12; 46.2%), CHD (n = 7; 26.9%), and irreversible cardiac graft dysfunction (n = 7; 26.9%).

All patients were successfully weaned to spontaneous breathing while continuing VA-ECMO support, with a maintained extracorporeal blood flow of 3.1 ± 0.5 L/min (or 1.78 ± 0.46 L/min/m^2). In addition to extracorporeal circulatory support, all patients (n = 26) received sympathomimetic cardiotonic or vasopressor agents to support systemic hemodynamics and residual left ventricular function. Specifically, dopamine was administered in 23 patients (88.5%) at a mean dose of 5.7 ± 2.1 μg/kg/min (median 6.0 [4.0; 7.0] μg/kg/min), adrenaline in 10 patients (38.5%) at 22.0 ± 12.9 ng/kg/min (median 17.5 [10.0; 37.75] ng/kg/min), dobutamine in 5 patients (19.2%) at 4.0 ± 2.7 μg/kg/min (median 3.0 [2.5; 4.0] μg/kg/min), and noradrenaline in 2 patients at 50 and 80 ng/kg/min, respectively.

The absence of impaired consciousness, severe organ dysfunction, electrolyte or metabolic impairments, and high pulmonary hypertension at the time of donor heart availability served as key criteria for proceeding with HT (Table 1). The duration of VA-ECMO support prior to HT in these patients ranged from 1 to 11 days, with a mean of 4.1 ± 2.9 days and a median of 4.0 [1.5; 5.0] days.

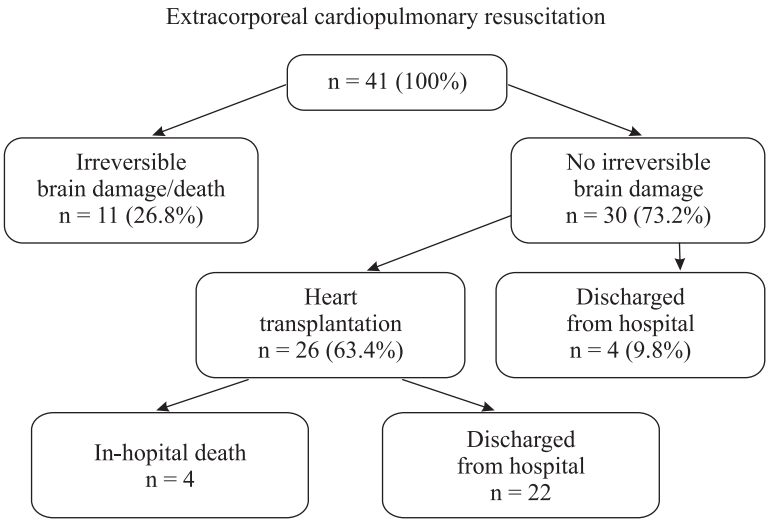

Fig. Study flow diagram

The donors included 20 men (76.9%) and 6 women (23.1%), with a mean age of 44.0 ± 9.9 years (median 45.0 [36.0; 52.0]) and a mean body weight of 86.8 ± 14.9 kg (median 85.0 [75.0; 100.0] kg). The graft-to-recipient weight ratio was 1.20 ± 0.54 (median 1.10 [0.90; 1.30]). Brain death resulted from traumatic brain injury in 9 cases (34.6%) and non-traumatic causes in 17 cases (65.4%). Two donors (7.7%) experienced cardiac arrest and underwent CPR lasting 6 and 11 minutes, respectively. Mechanical ventilation duration averaged 2.4 ± 1.7 days (median 2.0 [1.0; 3.0] days).

During donor management, sympathomimetic support was required in 23 cases (88.5%) with norepinephrine administered at 621 ± 388 ng/kg/min (median 550.0 [300.0; 900.0] ng/kg/min), and dopamine in 8 cases (30.8%). Echocardiographic and laboratory findings for heart donors (n = 26) are summarized in Table 2.

Expanded criteria for heart donation were identified in 16 donors (61.5%), with an average of 1.4 ± 0.4 expanded criteria factors per donor. The mean Eurotransplant Heart Donor Score was 16.9 ± 2.7 (median 16.5 [15.5; 18.0]), the Donor Risk Index was 6.3 ± 1.5 (median 6.0 [5.5; 7.75]), and the predicted incidence of severe primary graft dysfunction based on the RADIAL score was 15.4 ± 3.7% (median 16.25 [12.50; 18.50]%).

Table 1

Data (M ± σ and Me [Q1; Q3]) from preoperative examination of heart recipients who underwent extracorporeal cardiopulmonary resuscitation at the pre-transplant stage (n = 26)

Parameter	Value
Age, sex and anthropometric indicators	
Age, years	40.7 ± 15.8 (39.0 [30.0; 53.0])
Female, n/%	10 (38.5%)
Height, cm	171.6 ± 10.7 (170.0 [166.6; 176.0])
Weight, kg	73.3 ± 15.9 (77.5 [63.5; 84.25])
Body surface area, m^2	1.87 ± 0.24 (1.90 [1.70; 2.04])
BMI, kg/m^2	24.6 ± 4.0 (24.80 [22.87; 27.04])
Invasive central hemodynamic and echocardiographic study	
mAP, mmHg	66.8 ± 12.8 (74.5 [66.5; 80.75])
HR per min	107.7 ± 25.6 (107.5 [86.5; 130.25])
RAP, mmHg	8.6 ± 3.4 (8.0 [5.25; 12.0])
mPAP, mmHg	28.5 ± 10.3 (26.0 (20.0; 27.75)]
PCWP, mmHg	20.8 ± 9.9 (20.0 [12.5; 27.75])
CI, $l/min/m^2$	1.57 ± 0.53 (1.50 [1.30; 1.70])
TPG, mmHg	7.7 ± 3.0 (8.0 [5.0; 10.0])
PAP, Woods units	2.99 ± 1.94 (2.70 [1.70; 3.30])
Laboratory examination	
Hb, g/L	102.6 ± 19.1 (95.0 [90.5; 118.5])
Red blood cell, 10^9/L	3.6 ± 0.7 (3.4 [3.18; 3.76])
Platelets, 10^9/L	139.4 ± 103.0 (102.0 [79.25; 191.25])
White blood cells, 10^9/L	11.7 ± 6.1 (10.1 [7.08; 15.68])
Albumin, g/L	36.1 ± 6.8 (35.0 [32.5; 40.0])
Total protein, g/L	62.4 ± 10.7 (35.0 [32.5; 40.0])
Urea, mmol/L	11.4 ± 5.8 (10.1 [7.43; 14.4])
Creatinine, μmol/L	111.1 ± 49.1 (110.0 [85.58; 131.80])
Total bilirubin, μmol/L	50.7 ± 43.6 (33.4 [17.48; 80.97])
ALT, U/L	66.9 ± 122.4 (36.6 [26.0; 48.28])
AST, U/L	82.0 ± 123.8 (36.0 [33.0; 38.0])
INR	1.47 ± 0.17 (1.40 [1.34; 1.58])
$pH_в$	7.43 ± 0.09 (7.40 [7.40; 7.50])
$BE_в$, mmol/L	1.6 ± 3.7 (2.6 [–0.9; 3.4])
$P_вO_2$, мм рт. ст.	33.6 ± 6.6 (33.8 [28.1; 37.5])
$S_вO_2$, %	60.9 ± 15.8 (58.7 [46.5; 71.5])
Blood lactate, mmol/L	2.1 ± 1.7 (1.4 [1.0; 2.4])
Blood Na^+, mmol/L	138.3 ± 3.1 (138.0 [136.0; 141.0)]

Note: BMI, body mass index; mAP, mean arterial pressure; HR, heart rate, RAP, right atrial pressure; mPAP, mean pulmonary artery pressure; PCWP, pulmonary capillary wedge pressure; CI, cardiac index; TPG, Transpulmonary pressure gradient; PAP, pulmonary artery pressure; ALT, alanine transaminase; AST, aspartate transaminase; INR, international normalized ratio.

Table 2

Data (M ± σ and median with interquartile intervals) obtained from heart donor examination at transplantation to recipients who underwent ECPR at the pre-transplant stage (n = 26)

Parameter	Value
Echocardiographic study parameters	
Aorta, cm	3.1 ± 0.4 (3.0 [2.8; 3.5])
Left atrium, cm	3.9 ± 10.7 (170.0 [166.6; 176.0])
Right ventricle, cm	2.5 ± 0.2 (2.50 [2.40; 84.25])
IVS, cm	1.15 ± 0.16 (1.10 [1.00; 1.20])
LVEDV, ml	96.6 ± 32.1 (88.0 [80.0; 102.0])
SV, ml	60.5 ± 20.2 (58.0 [63.0; 68.0])
LVEF, %	64.4 ± 7.0 (65.0 [63.0; 68.0])
Mitral valve (regurgitation), degree	1.0 ± 0.3 (1.0 [1.0; 1.0])
Tricuspid valve (regurgitation), degree	0.94 ± 0.17 (1.0 [1.0; 1.0])
Laboratory examination	
Hb, g/L	102.6 ± 19.1 (95.0 [90.5; 118.5])
White blood cells, 10^9/L	12.4 ± 3.2 (12.5 [11.0; 13.75])
Total protein, g/L	65.6 ± 7.5 (67.0 [60.0; 72.5])
Urea, mmol/L	6.8 ± 2.9 (5.20 [3.50; 7.40])
Creatinine, μmol/L	97.8 ± 23.9 (87.5 [72.25; 98.5])
Total bilirubin, μmol/L	50.7 ± 43.6 (33.4 [17.48; 80.97])
Blood glucose, mmol/L	10.8 ± 4.7 (8.9 [7.5; 11.5])
Troponin I, pg/mL	0.19 ± 0.08 (0.10 [0.02; 0.45])
$pH_в$	7.44 ± 0.16 (7.40 [7.30; 7.50])
$BE_в$, mmol/L	2.2 ± 1.5 (2.3 [0.55; 3.25])

Note: IVS, interventricular septum; LVEDV, left ventricular end-diastolic volume; VA, stroke volume; LVEF, left ventricular ejection fraction; Hb, hemoglobin.

The average duration of anesthesia was 463 ± 159 minutes (median 435.0 [407.5–482.5] minutes), and the surgical time averaged 307 ± 64 minutes (median 320.0 [262.5–358.5] minutes). Mean heart graft ischemia time was 188 ± 72 minutes (median 170.0 [141.25–185.0] minutes), while the duration of cardiopulmonary bypass averaged 119 ± 39 minutes (median 109.0 [96.25–125.0] minutes).

Maximum doses of sympathomimetic cardiotonic agents administered during surgery included dopamine hydrochloride in all patients (n = 26, 100%) at 6.2 ± 2.0 mcg/kg/min (median 6.0 [6.0–7.5]), adrenaline hydrochloride in 25 patients (96.2%) at 42.7 ± 18.2 (median 40.0 [40.0; 60.0]) ng/kg/min, and dobutamine hydrochloride in 5 patients (19.2%) at 4.0 ± 1.4 mcg/kg/min (median 4.0 [4.0–4.0]).

In the preperfusion period, the VA-ECMO centrifuge pump speed was 6778 ± 358 rpm (median 6600 [6600–6800]), and the extracorporeal blood flow rate was 2.90 ± 0.44 L/min (median 2.80 [2.60–3.23] L/min). At the end of surgery, these parameters were 5274 ± 711 rpm (median 4950 [4725–5975]) and 1.65 ± 0.75 L/min (median 1.50 [1.13–2.23] L/min), respectively.

Early cardiac graft dysfunction with hemodynamic compromise was observed in 5 recipients (19.2%), necessitating continued VA-ECMO in the postperfusion period at blood flow rates exceeding 2.0 L/min (range 2.3–3.7 L/min; mean 3.2 ± 0.4 L/min).

Perioperative blood loss averaged 3499 ± 3679 mL (median 2000 [1550–4400] mL), requiring transfusion of red blood cell mass (1735.0 ± 1173.2 mL; median 1240.0 [1052.25–1798.25]), fresh frozen plasma (2413.2 ± 2012.9 mL; median 1820.0 [1066.25–2495.0]), and platelet mass (276.4 ± 135.9 mL; median 240.0 [157.5–397.5]).

Postoperative mechanical ventilation lasted for 12.6 ± 6.9 hours (median 12.0 [9.5–16.5]). In patients without early cardiac graft dysfunction (n = 21), VA-ECMO support continued postoperatively for 1.8 ± 0.4 days (median 1.8 [1.6–1.9]), while in patients with early graft dysfunction (n = 5), support lasted 4–7 days (mean 5.7 ± 0.7 days).

Seven patients (26.9%) required postoperative renal replacement therapy via continuous veno-venous hemofiltration. Four recipients (15.3%) died in hospital due to multiple organ failure, which developed in two cases with and in two cases without early cardiac graft dysfunction.

DISCUSSION

In recent years, the number of patients on HTWL has increased significantly – by more than 25% – leading to longer waiting times and increased risk of severe adverse cardiovascular events. Both ambulatory and hospitalized patients awaiting HT face an elevated risk of sudden cardiac death due to life-threatening arrhythmias, such as ventricular tachycardia, ventricular fibrillation, and bradyarrhythmias, particularly in the absence of an implantable cardioverter-defibrillator (ICD) [10]. Notably, the underlying etiology – whether dilated or ischemic cardiomyopathy – does not significantly influence the incidence of sudden death in this population.

Sudden CA accounts for approximately 40–70% of all fatalities among patients awaiting HT [10]. Although ICD use can reduce mortality during the waiting period by 13% or more, the overall death rate from sudden CA in this group remains high [11]. One contributing factor is the limited indication for ICD implantation in patients with CHF classified as NYHA functional class IV, given the higher proportion of non-sudden cardiac deaths in this subset [12]. According to international guidelines, ICD implantation is recommended for potential HT recipients managed on an outpatient basis (class IIa, level of evidence C) [13].

ECPR enables not only the rapid restoration of systemic circulation and correction of blood gas abnormalities but also provides a critical window for identifying the underlying causes of sudden CA and implementing targeted therapeutic interventions [2]. The adoption of ECPR has been associated with improved early and long-term survival rates and better neurological outcomes compared to conventional CPR using manual or automated chest compressions [14].

However, the efficacy of ECPR varies considerably across studies, with reported rates of favorable neurological outcomes and survival ranging from 0.33% to 70.4% and 0.24% to 43.1%, respectively [3]. According to the International Extracorporeal Life Support Organization (ELSO) registry, a total of 28,007 ECPR cases involving adults, children, and neonates have been recorded, accounting for 12.6% of all documented extracorporeal life support cases (n = 222,383) [15]. Reported survival rates following ECPR were 30% in adults, 41% in children, and 42% in neonates. The majority of these CA cases occurred in the hospital [15].

Neurological outcomes and survival rates following ECPR for in-hospital cardiac arrest (IHCA) are generally superior to those for out-of-hospital cardiac arrest (OHCA), with reported survival ranging from 20% to 40% [16]. The success of ECPR in IHCA is strongly influenced by the duration and quality of resuscitative efforts [17]. A study by Bartos et al. (2020) demonstrated that ECPR initiated within 60 minutes of CA was associated with significantly better neurological and functional outcomes compared to conventional CPR alone [18]. Moreover, the study indicated that for every additional 10 minutes of CPR beyond the initial 30 minutes, patient survival decreased by approximately 25%.

The effectiveness of ECPR is further modulated by several factors, including the severity of initial metabolic disorders (e.g., blood pH, lactate levels), patient age, adherence to targeted temperature management proto-

cols, and the timeliness of coronary angiography and subsequent interventions (e.g., angioplasty, stenting) in cases of coronary artery-related CA [2]. Advanced age and prolonged periods of hemodynamic instability prior to ECPR initiation are particularly detrimental, often leading to poorer outcomes during both resuscitation and subsequent intensive care management [19].

Given the multifactorial nature of ECPR outcomes in IHCA, the RESCUE-IHCA mortality prediction score was developed to assess prognosis. This score integrates 6 risk factors: (1) age; (2) presence of pre-existing renal failure; (3) patient type (cardiac *vs.* non-cardiac; medical *vs.* surgical); (4) timing of CA (daytime *vs.* nighttime); (5) initial heart rhythm; and (6) total duration of the CA event [21]. The scoring system ranges from –11 to +13 points. A score above 0 indicates a greater than 50% likelihood of mortality, while scores of 20 and 40 are associated with mortality risks exceeding 75% and 85%, respectively.

ELSO has also developed standardized ECPR protocols tailored to various patient age groups, which include recommendations for post-resuscitation management [7].

The annual institutional volume of ECMO procedures has been identified as a key determinant of ECPR program effectiveness. Centers performing more than 30 ECMO procedures annually report improved survival outcomes, likely attributable to greater cannulation proficiency and more experienced multidisciplinary patient management [22]. To enhance ECPR efficacy, it is recommended to establish specialized ECPR teams comprising an anesthesiologist-resuscitator, a physician trained in both percutaneous and surgical femoral vessel cannulation, and a cardiologist with expertise in acute cardiac care and heart failure management [23]. Integration with cardiogenic shock teams is also considered essential.

However, the widespread implementation of ECPR remains limited by its substantial cost, with treatment expenses ranging from €12,000 to €156,000 per patient. This high financial burden restricts access to ECPR in healthcare institutions with constrained budgetary resources [3].

Our study demonstrates the high efficacy of ECPR in both HT candidates and recipients who experience IHCA. At our center, the annual volume of VA-ECMO procedures – including those performed in the context of heart and lung transplantation, post-cardiac acute heart failure, and other emergent conditions – exceeds 80 cases. This extensive experience with percutaneous femoral cannulation for VA-ECMO, used as short-term mechanical circulatory support (MCS) prior to HT, has enabled the rapid initiation of extracorporeal support during ongoing manual or mechanical chest compressions as part of a comprehensive CPR protocol.

Irreversible brain injury and multi-organ dysfunction were both successfully prevented in 73.2% of patients, creating the conditions necessary for urgent primary or repeat heart transplantation in 63.4% of cases. Despite the critical nature of the pre-transplant period, the use of temporary MCS, reliance on donor hearts with one or more expanded criteria in 61.5% of cases, and occurrence of early graft dysfunction in 19.2% of recipients, the in-hospital survival rate following transplantation reached 84.7%. These outcomes are comparable to, and in some cases exceed, the survival rates reported by other leading transplant centers performing emergency HT supported by VA-ECMO [24–26].

CONCLUSION

1. ECPR with peripheral VA-ECMO results in complete cardiac recovery in 100% of cases of IHCA.
2. The incidence of irreversible brain damage in patients who underwent ECPR following witnessed (by medical or nursing staff, patients) IHCA is 26.8%.
3. In 73.2% of patients who experienced witnessed IHCA followed by ECPR, the post-resuscitation period is marked by complete recovery of consciousness and the absence of severe multi-organ complications. This enabled subsequent HT (63.4%) or hospital discharge (9.8%).
4. In-hospital survival after emergency HT in recipients who underwent ECPR prior to transplantation was 84.7%.

The authors declare no conflict of interest.

REFERENCES

1. *Grigioni F, Boriani G, Barbieri A, Russo A, Reggianini L, Bursi F et al.* Relevance of cardioverter defibrillators for the prevention of sudden cardiac death on timing of heart transplantation. *Clin Transplant*. 2006; 20 (6): 684–688.
2. *Abrams D, MacLaren G, Lorusso R, Price S, Yannopoulos D, Vercaemst L et al.* Extracorporeal cardiopulmonary resuscitation in adults: evidence and implications. *Intensive Care Med*. 2022; 48 (1): 1–15.
3. *Holmberg MJ, Granfeldt A, Guerguerian AM, Sandroni C, Hsu CH, Gardner RM et al.* Extracorporeal cardiopulmonary resuscitation for cardiac arrest: an updated systemic review. *Resuscitation*. 2023; 182: 109665.
4. *Kim SJ, Kim HJ, Lee HY, Ahn HS, Lee SW*. Comparing extracorporeal cardiopulmonary resuscitation with conventional cardiopulmonary resuscitation: a meta-analysis. *Resuscitation*. 2016; 103: 106–116.
5. *Cave DM, Gazmuri RJ, Otto CW, Nadkarni VM, Cheng A, Brooks SC et al.* Part 7: CPR techniques and devices: 2010 American Heart Association guidelines for cardiopulmonary resuscitation and emergency cardiovascular care. *Circulation*. 2010; 122 (18 suppl 3): S720–S728.
6. *Monsieurs KG, Nolan JP, Bossaert LL, Greif R, Maconochie IK, Nikolaou NI et al.* European resuscitation council guidelines for resuscitation 2015. Section 1. Executive summary. *Resuscitation*. 2015; 95: 1–80.

7. *Richardson ASC, Tonna JE, Nanjayya V, Nixon P, Abrams DC, Raman L et al.* Extracorporeal Cardiopulmonary Resuscitation in Adults. Interim Guideline Consensus Statement From the Extracorporeal Life Support Organization. *ASAIO J*. 2021; 67 (3): 221–228.
8. *Nielsen N, Wetterslev J, Cronberg T, Erlinge D, Gasche Y, Hassager C et al.* Targeted temperature management at 33 °C versus 36 °C after cardiac arrest. *N Engl J Med*. 2013; 369 (23): 2197–2206.
9. *Cook AM, Morgan Jones G, Hawryluk GWJ, Mailloux P, McLaughlin D, Papangelou A et al.* Guidelines for the Acute Treatment of Cerebral Edema in Neurocritical Care Patients. *Neurocrit Care.* 2020; 32 (3): 647–666.
10. *Nägele H., Rödiger W.* Sudden death and tailored medical therapy in elective candidates for heart transplantation. *J Heart Lung Transplant*. 1999; 18 (9): 869–876.
11. *Vakil K, Duval S, Cogswell R, Eckman P, Levy WC, Anand I et al.* Impact of implantable cardioverter-defibrillators on mortality among patients awaiting heart transplantation: An UNOS/OPTN Analysis. *JACC Clin Electrophysiol*. 2017; 3 (1): 33–40.
12. *Bastante Valiente T, Cano MJ, Delgado JF, Gil ML, Arribas F, Sánchez MA et al.* Defibrillator implantation for the primary prevention of sudden death in patients awaiting cardiac transplantation: one center's experience. *Rev Esp Cardiol*. 2011; 64 (3): 240–242.
13. *Epstein AE, DiMarco JP, Ellenbogen KA, Estes NA 3rd, Freedman RA, Gettes LS et al.* 2012 ACCF/AHA/HRS focused update incorporated into ACCF/AHA/HRS guidelines for device-based therapy of cardiac rhythm abnormalities: a report of the American Colledge of Cardiology Foundation/American Heart Association Task Force on Practice Guidelines and Heart Rhythm Society. *J Am Coll Cardiol*. 2013; 61 (3): e6–e75.
14. *Yannopoulos D, Bartos J, Raveendran G, Walser E, Connett J, Murray TA et al.* Advanced reperfusion strategies for patients without-of-hospital cardiac arrest and refractory ventricular fibrillation (ARREST): a phase 2, single center, open-label, randomized controlled trial. *Lancet*. 2020; 396 (10265): 1807–1816.
15. elso.org/registry/elsoliveregistrydashboard.aspx.
16. *D'Arrigo S, Cacciola S, Dennis M, Jung C, Kagawa E, Antonelli M, Sandroni C.* Predictors of favourable outcome after in-hospital cardiac arrest treated with extracorporeal cardiopulmonary resuscitation: a systemic review and meta-analysis. *Resuscitation*. 2017; 121: 62–70.
17. *Goldberger ZD, Chan PS, Berg RA, Kronick SL, Cooke CR, Lu M et al.* Duration of resuscitation efforts and survival after in-hospital cardiac arrest: an observational study. *Lancet*. 2012; 380 (9852): 1473–1481.
18. *Bartos JA, Grunau B, Carlson C, Duval S, Ripeckyj A, Kalra R et al.* Improved survival with extracorporeal cardiopulmonary resuscitation despite progressive metabolic derangement associated with prolonged resuscitation. *Circulation*. 2020; 141 (11): 877–886.
19. *Matsuyama T, Irisawa T, Yamada T, Hayakawa K, Yoshiya K, Noguchi K et al.* Impact of low-flow duration on favorable neurological outcomes of extracorporeal cardiopulmonary resuscitation after out-of hospital cardiac arrest: a multicenter prospective study. *Circulation*. 2020; 141 (12): 1031–1033.
20. *Djordjevic I, Gaisendrees C, Adler C, Eghbalzadeh K, Braumann S, Ivanov B et al.* Extracorporeal cardiopulmonary resuscitation for out-of-hospital cardiac arrest: first results and outcomes of a new established ECRP program in a large population area. *Perfusion*. 2022; 37 (3): 249–256.
21. *Tonna JE, Selzman CH, Girotra S, Presson AP, Thiagarajan RR, Becker LB et al.* Resuscitation using ECPR during in-hospital cardiac arrest (RESCUE-IHCA) mortality prediction score and external validation. *JACC Cardiovasc Interv.* 2022; 15 (3): 237–247.
22. *Barbaro RP, Odetola FO, Kidwell KM, Paden ML, Bartlett RH, Davis MM, Annich GM.* Association of hospital-level volume of extracorporeal membarane oxygenation cases and mortality. Analysis of the extracorporeal life support organization registry. *Am J Respir Crit Care Med*. 2015; 191 (8): 894–901.
23. *Michalakes PC, DeNino WF, Jara CB, Afari ME, Geller BJ.* Building an extracorporeal cardiopulmonary resuscitation program at high-volume extracorporeal membrane oxygenation center. *J Extra Corpor Technol*. 2023; 55 (4): 185–188.
24. *Coutance G, Jacob N, Demondion P, Nguyen LS, Bouglé A, Bréchot N et al.* Favorable outcomes of a direct heart transplantation strategy in selected patients on extracorporeal membrane oxygenation support. *Crit Care Med*. 2019; 48: 498–506.
25. *Fukuhara S, Takeda K, Kurlansky PA, Naka Y, Takayama H.* Extracorporeal membrane oxygenation as a direct bridge to heart transplantation. *J Thorac Cardiovasc Surg*. 2018; 155 (4): 1607–1618.
26. *López-Vilella R, Sánchez-Lázaro I, Moncho AP, Peregrina MT, Guillén MP, Jáuregui IZ et al.* Analysis of the intrahospital and long-term survival of heart transplant patients with a short-term mechanical assistance device. *Transplant Proc*. 2021; 53 (9): 2728–2730.

The article was submitted to the journal on 15.07.2024

DOI: 10.15825/1995-1191-2024-4-110-121

10-YEAR EXPERIENCE IN ORTHOTOPIC HEART TRANSPLANTATION IN KUZBASS

L.S. Barbarash[1], *O.L. Barbarash*[1, 2], *E.V. Grigoriev*[1, 2], *D.L. Shukevich*[1, 2], *T.B. Pecherina*[1], *M.G. Zinets*[1], *A.V. Sotnikov*[1], *I.K. Halivopulo*[1], *T.S. Golovina*[1], *E.M. Kurguzova*[1], *A.V. Ivanova*[1], *Yu.S. Ignatova*[1], *A.V. Yurkina*[1], *D.P. Golubovskaya*[1], *P.G. Parfenov*[1], *Yu.I. Guselnikova*[1], *E.V. Dren*[1]

[1] Research Institute for Complex Issues of Cardiovascular Diseases, Kemerovo, Russian Federation

[2] Kemerovo State Medical University, Kemerovo, Russian Federation

Background. Orthotopic heart transplantation (OHT) is the gold standard treatment for individuals with end-stage heart failure (HF), providing the best survival and quality of life. In Russia, the number of OHT procedures and transplantation of other organs have significantly increased in recent years. At the same time, there is lower perioperative mortality and higher survival in the post-OHT long-period. **Objective:** to analyze OHT outcomes in Kuzbass over a 10-year period. **Material and methods.** From January 2013 to December 2023, 72 OHTs (36.7% of those included on the heart transplant waiting list (HTWL) over a 10-year period) were performed at the Research Institute for Complex Issues of Cardiovascular Diseases. Recipient median age was 56 [50.5; 61.0] years, which included 61 men and 11 women. Among the etiologic causes of end-stage HF, ischemic cardiomyopathy was predominant in 65.3% (n = 47) of recipients, whereas dilated cardiomyopathy was present in 25% (n = 18) of recipients. Other cardiomyopathies accounted for 9.7% (n = 7). **Results.** A total of 196 patients with end-stage HF were included in the HTWL over a 10-year period; 74 (37.8%) of these did not live to get a transplant. The waitlist time was 173 days (5.77 months) – which is slightly longer than the average waiting time of 3.9 months for OHT according to data from European registries. Waitlist mortality was 19.6%. The 10-year average in-hospital mortality rates among patients after OHT were 16.7% and 1-year mortality was 15.3%. These rates are consistent with worldwide trends for this high-tech medical care. Cumulative survival at the end of 2023 was 51.4% (36 patients after OHT). Median length of stay in the hospital was 28 days, with 14 days spent in the intensive care unit. Donor heart anoxia time was 112 [85.25; 170.5] minutes, and cardiopulmonary bypass time was 145 [124; 169.5] minutes. Ten patients (13.9%) required extracorporeal membrane oxygenation, while 8.3% of cases required extracorporeal homeostasis correction. **Conclusion.** The 10 years of successful experience at the Research Institute for Complex Issues of Cardiovascular Diseases validates the need to develop the OHT program in Kuzbass as a gold standard for treating end-stage HF.

Keywords: heart transplantation, heart failure, organ donation.

Heart failure (HF) is a rapidly escalating global public health concern, currently affecting an estimated 64 million individuals worldwide. It remains associated with high rates of mortality and morbidity, as well as significantly diminished quality of life [1]. The prevalence of HF is expected to continue rising, largely due to the ageing population [1]. In the Russian Federation, data from the ERA-CHF study, a representative sample from the European part of the country, also highlight a marked increase in the prevalence of chronic heart failure (CHF) over the past 16 years, rising from 4.9% to 8.5%. Moreover, the absolute number of individuals diagnosed with CHF more than doubled during this period, increasing from 7.18 million to 12.35 million. The proportion of patients with severe CHF, classified as New York Heart Association (NYHA) functional classes (FC) III–IV, rose from 1.8% to 3.1%, corresponding to an increase from 1.76 million to 4.5 million individuals [2].

Despite advances in therapeutic strategies for HF, the proportion of patients progressing to end-stage heart failure (ESHF) continues to rise. According to large meta-analyses, nearly 10% of patients reach ESHF, defined by NYHA FC III–IV symptoms, despite receiving optimal medical therapy [3]. ESHF is associated with a high 1-year mortality, exceeding 50% following diagnosis [3]. For patients with severe HF, orthotopic heart transplantation (OHT) and left ventricular assist devices (LVADs) remain the most effective and widely recommended treatment options [3].

According to the World Health Organization's Global Observatory on Donation and Transplantation, organ transplantation is performed in 104 countries, encom-

Corresponding author: Julia Ignatova. Address: 6, Barbarash boulevard, Kemerovo, 650002, Russian Federation. Phone: (905) 948-90-15. E-mail: julia-smolina@mail.ru

passing approximately 90% of the global population [4]. Recent data indicate that over 150,000 organ transplants are conducted annually worldwide, representing a 52% increase since 2010[1]. OHT continues to be the gold standard treatment for ESHF, offering the most favorable survival outcomes and quality of life improvements [5]. Over 6,000 heart transplants (HT) are performed globally each year, with a 1-year post-transplant survival rate of about 85% and a current median survival exceeding 12 years [6, 7].

Reports from the International Thoracic Organ Transplant Registry of the International Society for Heart and Lung Transplantation demonstrate both an upward trend in OHT procedures and concurrent improvements in postoperative outcomes over recent decades [8]. However, widespread implementation of HT programs remains constrained by factors such as donor organ shortages and the complexities of waiting list management in real-world clinical settings.

In recent years, Russia has seen a significant increase in the number of heart and other solid organ transplants. This trend has been accompanied by decreased perioperative mortality and higher long-term survival after HT [9, 10]. A notable milestone in the development of transplantology in the Russian Federation was achieved in Kuzbass, where the first HT procedure was successfully performed on January 31, 2013, under the leadership of Professor Leonid Barbarash, Fellow of the Russian Academy of Sciences and founder of the Kemerovo Cardiology Center. With active support from the Shumakov National Medical Research Center of Transplantology and Artificial Organs (Moscow), headed by Professor Sergey Gautier, also a Fellow of the Russian Academy of Sciences, Kemerovo became the first city in Russia with a population under 1 million to establish and implement a HT program.

Objective of the study: to analyze OHT outcomes in Kuzbass over a 10-year period.

MATERIAL AND METHODS

Within the framework of a registry-based study conducted at the Research Institute for Complex Issues of Cardiovascular Diseases (Kemerovo), data were collected and analyzed during both retrospective and prospective phases. The dataset included information from the heart transplant waiting list (HTWL) and the registry of OHT recipients. The study was conducted in accordance with Good Clinical Practice standards and the Declaration of Helsinki Principles. The study protocol was reviewed and approved by the joint local ethics committee of the Institute. The authors declare no conflicts of interest.

Recipients enrolled in the study were diagnosed with end-stage CHF and met the established clinical criteria and indications for OHT, in accordance with the national guidelines of the Russian Federation. These criteria included: refractoriness to optimal pharmacological therapy with a predicted 1-year OHT-free survival <50%; left ventricular ejection fraction (LVEF) <20%; pulmonary artery occlusion pressure >20 mmHg; decreased peak oxygen consumption (VO_2 peak) <12 ml/kg/min in patients not receiving beta-blockers, or <14 ml/kg/min in those receiving the maximum tolerated dose. Additional indications comprised the presence of severe myocardial ischemia in patients with coronary artery disease for whom revascularization (via coronary artery bypass grafting or percutaneous coronary intervention) was not feasible; and recurrent, refractory, life-threatening arrhythmias unresponsive to electrophysiological interventions, including catheter ablation or implantation of an implantable cardioverter-defibrillator (ICD) [9, 11, 12].

The main contraindications to inclusion in the HTWL were [11, 12]:

- Elevated pulmonary vascular resistance >5 Wood units, unresponsive to inhaled vasodilators;
- Body mass index (BMI) greater >35 kg/m^2;
- Age over 80 years amidst comorbidities that increase perioperative risk and compromise long-term prognosis;
- Severe atherosclerosis of the carotid, cerebral, and/or peripheral arteries associated with organ or tissue ischemia for which surgical correction is not feasible;
- Pulmonary hypertension characterized by a transpulmonary gradient >15 mmHg or pulmonary vascular resistance >5 Wood units, refractory to pharmacologic therapy (e.g., nitric oxide, sildenafil) and/or mechanical circulatory support;
- Severe liver and/or kidney dysfunction;
- Autoimmune diseases, including systemic lupus erythematosus, sarcoidosis, or systemic amyloidosis.

Between January 2013 and December 2023, a total of 72 OHTs were performed at the Research Institute for Complex Issues of Cardiovascular Diseases, representing 36.7% of patients included in HTWL over the 10-year period. Recipient median age was 56 years [IQR: 50.5–61.0], with a predominance of males (n = 61, 84.7%) and 11 females (15.3%) (Table 1).

Ischemic cardiomyopathy was the leading etiology of ESHF) present in 47 recipients (65.3%), followed by dilated cardiomyopathy in 18 (25.0%), and other forms of cardiomyopathy in 7 (9.7%). The majority of patients exhibited a traditional cardiovascular risk profile: arterial hypertension (n = 51, 61.3%), hyperlipidemia (n = 40, 55.6%), prior coronary revascularization (n = 38, 52.8%), and cardiac arrhythmias. Among those with

[1] https://apps.who.int/gb/ebwha/pdf_files/WHA75/A75_41-ru.pdf.

arrhythmias, atrial fibrillation or atrial flutter was observed in 28 (38.9%), and ventricular arrhythmias in 43 (59.7%) patients.

ICDs were present in 24 patients (33.3%), and an additional 7 patients (9.7%) had ICDs with cardiac resynchronization therapy (CRT-D). Functional capacity, assessed using the 6-minute walk test, corresponded to NYHA FC III in 56 patients (77.8%) and IV in 16 patients (22.2%). All recipients were classified as United Network for Organ Sharing (UNOS) status 2 (urgency on the HTWL) at the time of transplantation.

Surgical technique was predominantly biatrial (n = 71, 98.6%), with only one case (1.4%) performed using the bicaval technique.

In-hospital and 1-year follow-up endpoints were assessed:

– In-hospital (transplanted heart arrhythmia and conduction disorders; graft rejection and dysfunction; infectious complications; bleeding; multiple organ dysfunction syndrome (MODS); kidney failure; acute stroke/transient ischemic attack (AS/TIA); myocardial infarction (MI); need for extracorporeal membrane oxygenation (ECMO); tacrolimus overdose; death),
– 1-year follow-up (transplanted heart arrhythmia and conduction disorders; graft rejection and dysfunction; infectious complications; bleeding; MODS; kidney failure; AS/TIA; MI; diabetes mellitus; oncologic diseases; chronic/acute kidney failure; need for ECMO; transplant coronary artery disease (TCAD); tacrolimus overdose; rehospitalizations; death).

Statistical processing was carried out using STATISTICA 10.0 software (StatSoft Inc., USA). To assess the conformity of data distribution to normal distribution, the Lilliefors test was employed. A p-value >0.05 indicated normal distribution of the variable. A symmetry test was used to support distributional assumptions.

For variables not meeting the normality criteria, data were presented as median (Me) along with lower and upper quartiles [LQ; UQ]. A p-value <0.05 was considered statistically significant. The Mann–Whitney U test was applied for comparisons between independent groups, while the Wilcoxon signed-rank test was used for dependent samples. Survival analysis was performed using the Kaplan–Meier method to estimate survival functions.

Table 1

Recipient characteristics

Indicator		Result
Age, years Me [LQ;UQ]		56 [50.5; 61.0]
Men, n (%)		61 (84.7)
Women, n (%)		11 (14.3)
HTWL time, days		140 [48.0; 339.8]
UNOS-2, n (%)		72 (100)
Genesis of heart failure		
ICM, n (%)		47 (65.3)
DCM, n (%)		18 (25.0)
Other CMs, n (%)		7 (9.7)
Medical history and risk factors		
CHF FC, n (%)	FC III	56 (77.8)
	FC IV	16 (22.2)
AH, n (%)		51 (61.3)
Afib-AF, n (%)		28 (38.9)
VA, n (%)		43 (59.7)
Heart block, n (%)		21 (29.2)
PM, n (%)		5 (6.9)
ICD, n (%)		24 (33.3)
CRT-D, n (%)		9 (12.5)
PCI, n (%)		27 (37.5)
CABG, n (%)		11 (15.3)
DM/CI, n (%)		13 (18.1)
Hyperlipidemia/dyslipidemia, n (%)		40 (55.6)
CKD C3a/C3b, n (%)		14 (19.4)
AS, n (%)		8 (11.1)
COPD/BA, n (%)		5 (6.9)
Smoking, n (%)		8 (11.1)
BMI, kg/m^2 Me [LQ;UQ]		26.4 [22.7; 29.1]

Note: HTWL, heart transplant waiting list; UNOS, United Network for Organ Sharing; ICM, ischemic cardiomyopathy; DCM, dilated cardiomyopathy; CMs, cardiomyopathies; FC, functional class; CHF, chronic heart failure; AH, arterial hypertension; Afib, atrial fibrillation; AF, atrial flutter; VA, ventricular arrhythmia; PM, pacemaker; ICD, implantable cardioverter-defibrillators; CRT-D, cardiac resynchronization therapy with defibrillator; PCI, percutaneous coronary intervention; CABG, coronary artery bypass grafting; DM, diabetes mellitus; CI, carbohydrate intolerance; CKD, chronic kidney disease; AS, acute stroke; COPD, chronic obstructive pulmonary disease; BA, bronchial asthma; BMI, body mass index.

RESULTS OF THE STUDY

Over the 10-year observation period, there was a consistent increase in the number of OHT performed in Kuzbass. In 2023, a record-high number of procedures was achieved, with 13 OHTs conducted, including 2 performed as single-step interventions (Fig. 1).

HTWL included an average of 29.6 patients per year (range: 21–44 patients) (Fig. 2). Between January 2013 and December 2023, a total of 196 ESHF patients were listed for OHT. Of these, 74 patients (37.8%) died before undergoing transplantation. The average waitlist duration was 173 days (5.77 months), which slightly exceeds the mean waiting time reported in European registries (3.9 months) [13].

Overall HTWL mortality was 19.6%, with the lowest annual mortality observed in 2014 (6.7%) and 2023 (7.5%), and the highest in 2019 (43.3%) and 2020 (37.5%). The elevated mortality rates during 2019–2020 were attributed to the COVID-19 pandemic, particularly among patients with ESHF. Polynomial trend analysis revealed a decline in waitlist mortality from 2021 onward, alongside improved survival to transplantation. This trend is likely associated with introduction of novel

therapeutic agents, such as angiotensin receptor–neprilysin inhibitors (ARNIs) and sodium-glucose cotransporter 2 inhibitors (SGLT2i), in the management of HF patients with reduced ejection fraction (HFrEF).

Over the 10-year period, in-hospital mortality following OHT was 16.7%, and 1-year mortality was 15.3%. These outcomes are consistent with global benchmarks for this type of high-complexity intervention [16, 17]. As of the end of 2023, cumulative survival stood at 51.4%, with 36 OHT recipients still alive.

Median hospital stay post-transplant was 28 days, including a median intensive care unit (ICU) stay of 14 days (Table 2). During the operative and perioperative phases, the median ischemic time of the donor heart (an-

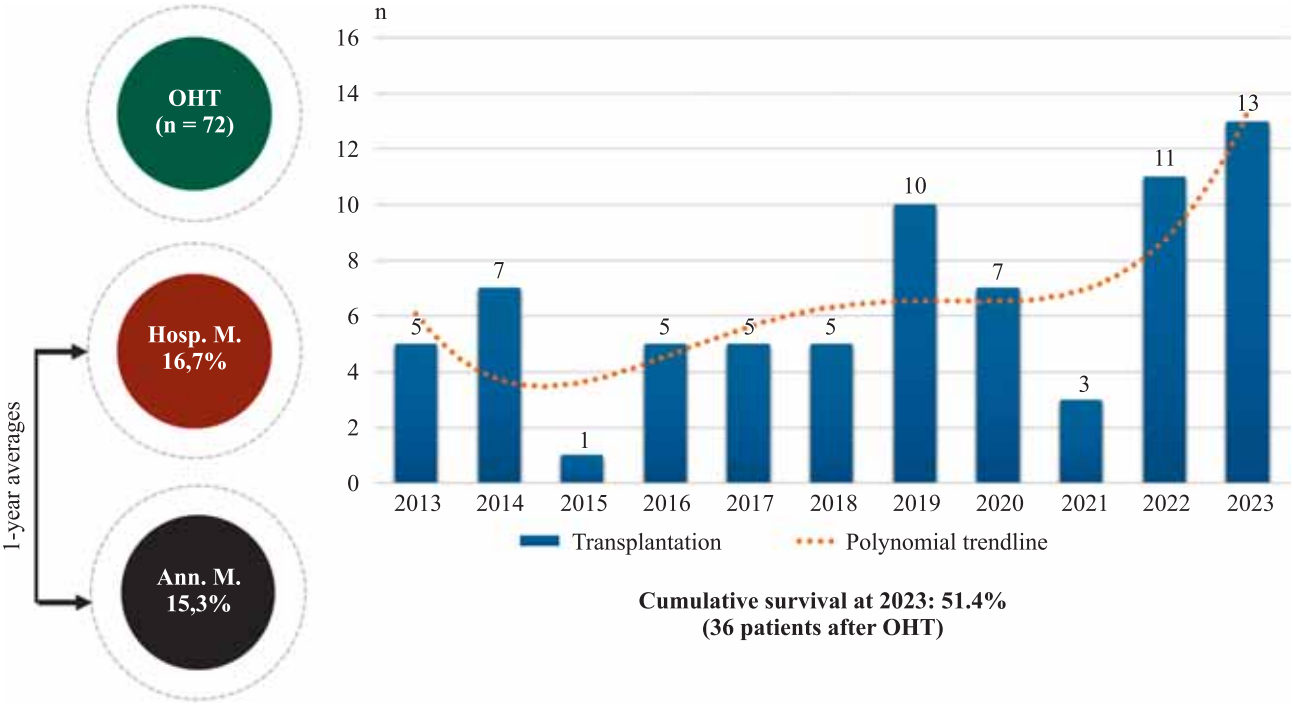

Fig. 1. Average survival between 2013 and 2023. OHT, orthotopic heart transplant; Hosp. M., hospital mortality; Ann. M., annual mortality

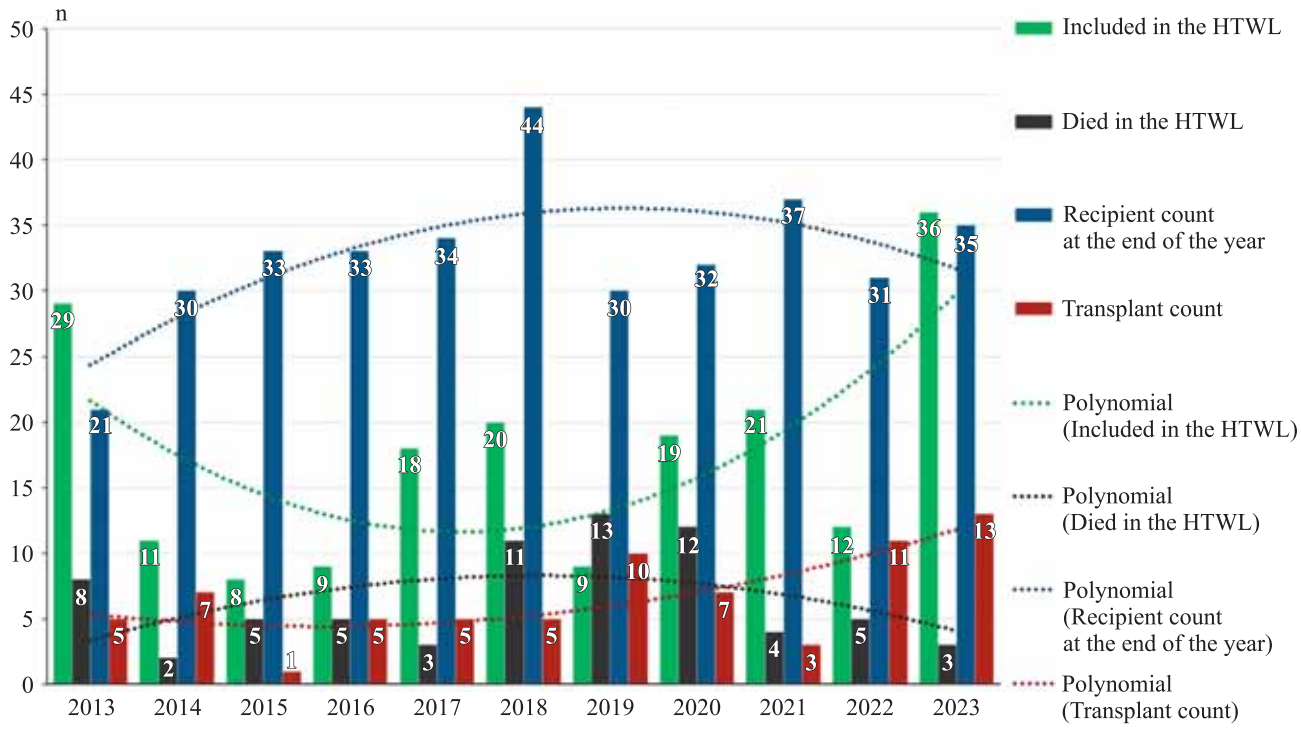

Fig. 2. Trends in the number of HTWL patients between 2013 and 2023

Table 2

Operative and perioperative indicators of heart transplantation

Indicator	Result
CPB time, min	145 [124; 169.5]
Donor heart anoxia time, min	112 [85.25; 170.5]
Surgery time, min	283 [247; 330]
Length of stay in the intensive care unit, day	14 [9; 28]
Hospitalization, day	28 [23; 36]
Need for PM, n (%)	37 (51.4)
ECMO use, n (%)	10 (13.9)
Extracorporeal correction of homeostasis, n (%)	6 (8.3)

Note: CPB, cardiopulmonary bypass; PM, pacemaker; ECMO, extracorporeal membrane oxygenation.

oxia) was 112 minutes [85.25; 170.5], while the median duration of cardiopulmonary bypass was 145 minutes [124; 169.5].

ECMO was required in 10 patients (13.9%), and 8.3% of cases required additional extracorporeal therapies.

Among the non-fatal complications during hospitalization, heart arrhythmias and conduction disorders (such as atrial fibrillation, ventricular extrasystole, and His bundle branch block) were the most prevalent, along with MODS, typically observed in patients experiencing cellular rejection or graft dysfunction (Fig. 3).

At the 1-year follow-up, 48 patients remained under observation, while 24 patients had passed away (including those who died during the hospitalization phase). Consequently, the analysis of therapy at the 1-year stage was based on the 48 surviving patients (Table 3). Notably, all patients showed high adherence to their prescribed specific therapy.

During the hospitalization phase, 100% of patients received specific immunosuppressive therapy. Statins and antiplatelet medications were consistently prescribed to all patients, both during the hospitalization period and at the 1-year follow-up. In the early postoperative period, 50% of patients required vasopressor medications, while 62.5% received inotropic agents. Selective cyclic guanosine monophosphate inhibitors were administered to 29.2% of patients during the hospitalization phase.

The use of loop diuretics decreased by the 1-year follow-up, with only 18.8% of patients requiring them (down from 76.4% during hospitalization). Similarly, the use of amiodarone decreased from 20.8% during hospitalization to 4.2% at the 1-year stage. While sodium-glucose cotransporter-2 (SGLT2) inhibitors were not used during the hospitalization phase, they were prescribed to one patient at the 1-year follow-up.

By 1 year, 5 patients (10.4%) had been switched to everolimus (a selective inhibitor of the mammalian target of rapamycin, mTOR), and 2 patients (4.2%) were receiving corticosteroid therapy.

At 1-year follow-up, the most common non-fatal complications were cellular graft rejection (26.7%) and graft dysfunction (21.7%). In addition, TCAD was identified in 15% of patients, while signs of MI were noted in 5% (Fig. 4). Importantly, the incidence of secondary infectious complications showed a significant decline compared to the hospital phase (8.2% *vs.* 16.5%, p = 0.023).

A detailed analysis of mortality patterns revealed that in 2015 and 2018, both in-hospital and 1-year mortality were zero. In the years 2017, 2019, and 2021, zero mortality was recorded exclusively during the in-hospital phase. Zero 1-year mortality following OHT was observed in 2016 and 2020 (Figs. 5 and 6). The highest in-hospital mortality rates over the 10-year period were recorded in 2016 (60%) and 2020 (43%), which were also associated with increased rates of non-fatal complications during these years (Figs. 3 and 5).

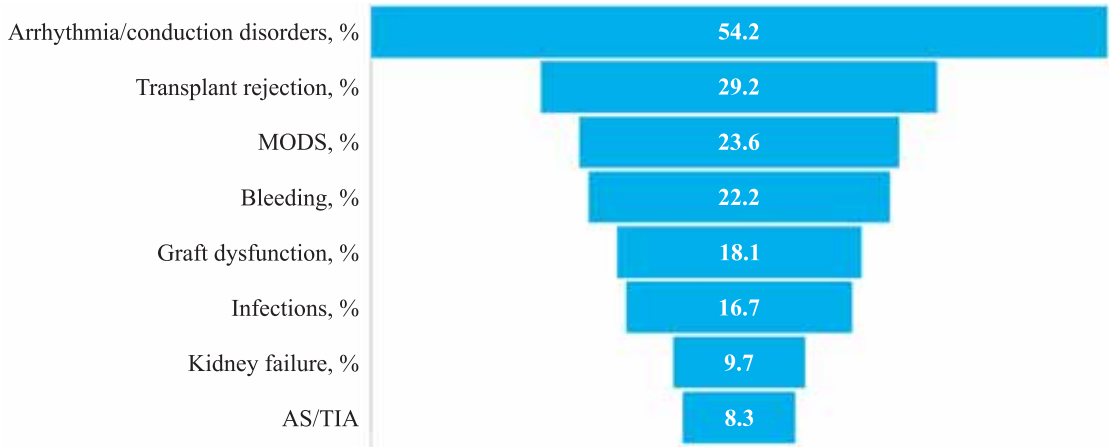

Fig. 3. Non-fatal complications during in-hospital follow-up. MODS, multiple organ dysfunction syndrome; AS, Acute stroke; TIA, transient ischemic attack

Trend analysis showed a consistent annual increase in the number of OHT procedures, accompanied by a rising trend in cumulative mortality (in-hospital + 1-year) (Fig. 6). In-hospital mortality trend remained relatively

Table 3

Therapy after OHT (hospital and 1-year stage)

Therapy (groups/drug)	In hospital (n = 72), n (%)	At 1-year stage (n = 48), n (%)
Specific therapy		
Induction of immunosuppression by an anti-interleukin-2 receptor antibody (basiliximab)	72 (100)	–
Calcineurin inhibitor (tacrolimus)	72 (100)	48 (100)
Mycophenolates	72 (100)	48 (100)
Selective mTOR serine-threonine kinase inhibitor (everolimus)	0 (0)	5 (10.4)
Corticosteroids	72 (100)	2 (4.2)
Antibacterials	72 (100)	27 (56.3)
Antifungals	32 (44.4)	26 (54.2)
Antivirals	72 (100)	26 (54.2)
Acetylsalicylic acid	72 (100)	48 (100)
Statins	72 (100)	48 (100)
RAAS inhibitors	37 (51.4)	26 (54.2)
Other therapy		
Vasopressors	36 (50)	0 (0)
Inotropes	45 (62.5)	
Selective inhibitor of cyclic guanosine monophosphate (cGMP)	21 (29.2)	0 (0)
UFH	34 (47.2)	0 (0)
Loop diuretics	55 (76.4)	9 (18.8)
Calcium channel blockers	7 (9.7)	4 (8.3)
Amiodarone	15 (20.8)	2 (4.2)
OAC	2 (2.8)	2 (4.2)
BB	0 (0)	2 (4.2)
ARNI	0 (0)	1 (2.1)
SGLT2i	0 (0)	1 (2.1)

Note: RAAS, renin-angiotensin-aldosterone system; cGMP, cyclic guanosine monophosphate; UFH, unfractionated heparin; OAC, oral anticoagulant; BB, beta blockers; ARNI, angiotensin receptor neprilysin inhibitor; SGLT2i, sodium-glucose co-transporter 2 inhibitor.

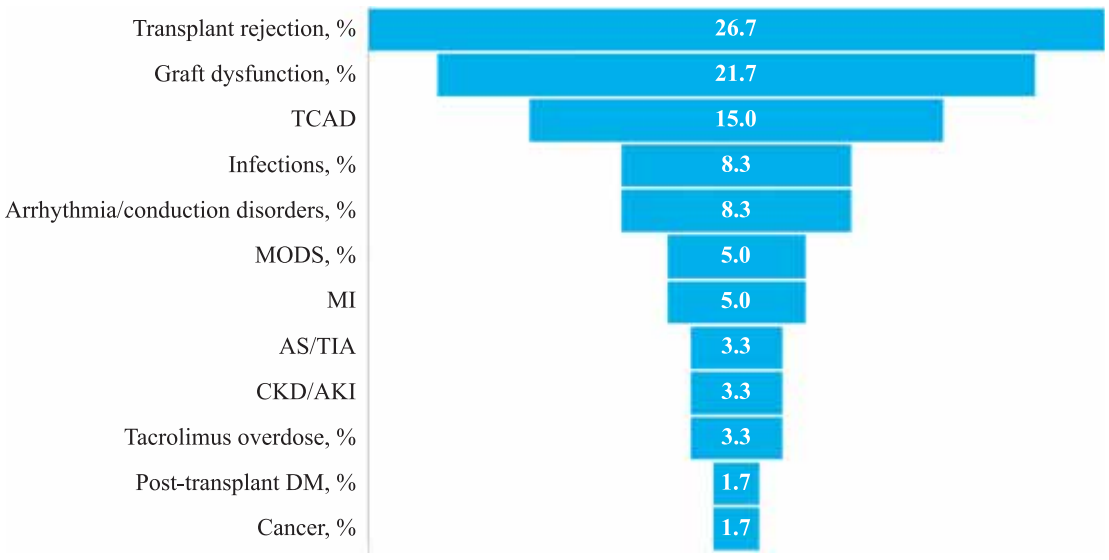

Fig. 4. Non-fatal complications during 1-year follow-up. TCAD, transplant coronary artery disease; MODS, multiple organ dysfunction syndrome; MI, myocardial infarction; AS, acute stroke; TIA, transient ischemic attack; CKD, chronic kidney disease; AKI, acute kidney injury, DM, diabetes mellitus

stable without significant fluctuations. According to Kaplan–Meier survival analysis, the median post-OHT survival among patients with more than 5 years of follow-up was 3.07 years [1.19; 6.09] (Fig. 7).

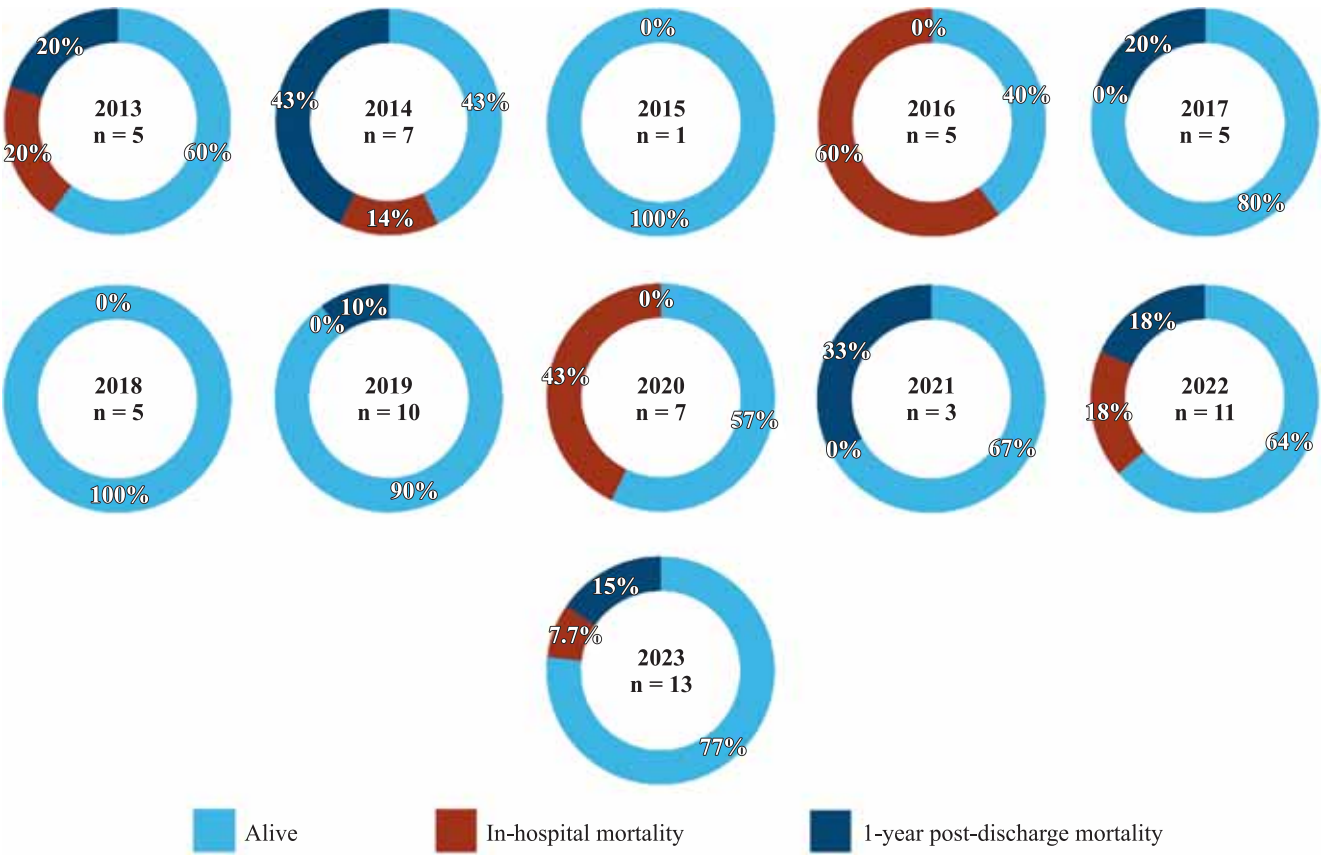

Fig. 5. Trends in 1-year patient mortality after heart transplantation in the period between 2013 and 2023

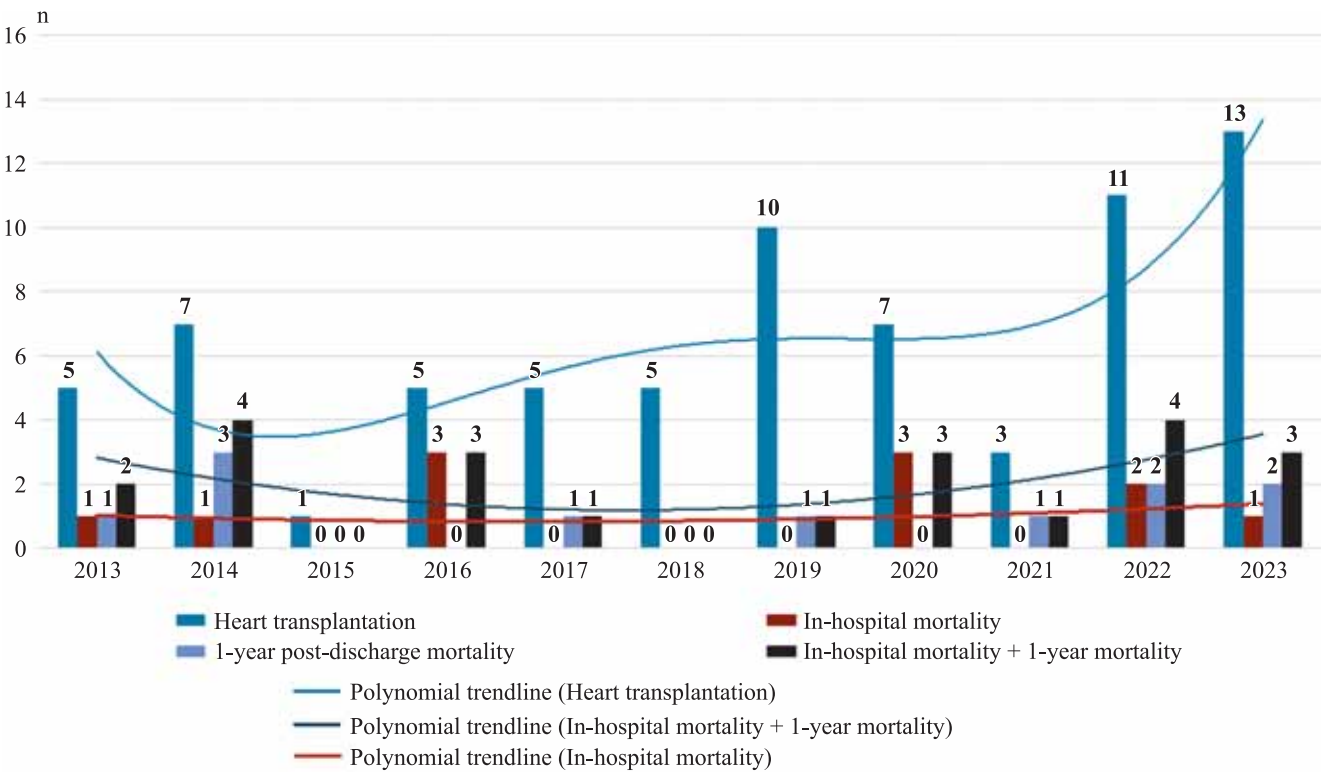

Fig. 6. Polynomial trend analysis of patient mortality after heart transplantation between 2013 and 2023

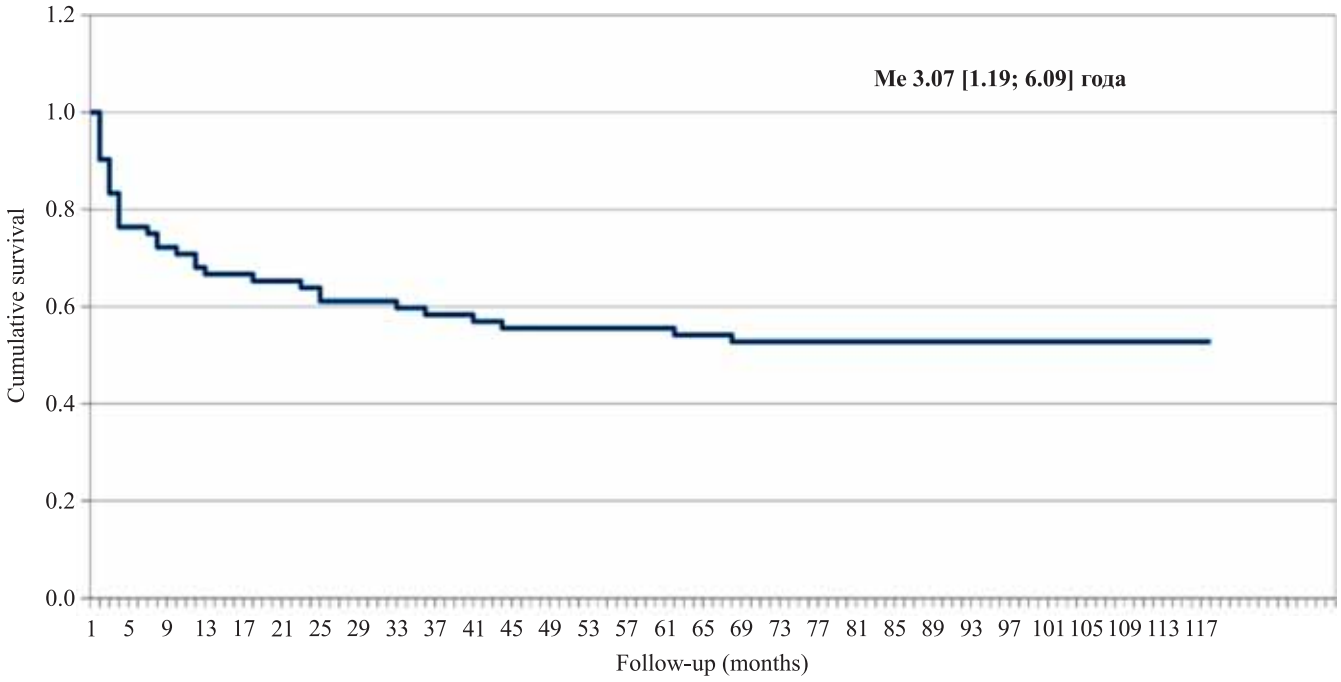

Fig. 7. Kaplan–Meier survival curve

DISCUSSION

Kuzbass is a major industrial region where circulatory system diseases (CSD) consistently rank as the leading cause of morbidity among the adult population, accounting for 20.6% of the total disease burden. According to data from Kemerovostat (a regional branch of the Federal State Statistics Service for Kemerovo Oblast), HF mortality in the region reached 532.7 per 100,000 population in 2023 – representing 38.2% of all deaths. However, this reflects an 18.8% decrease compared to 2022[2]. HF remains a prevalent and significant contributor to the CSD burden in Kuzbass, reaching critical levels in 2023 and highlighting the need for the widespread implementation of modern therapeutic and surgical interventions.

ESHF prevalence among HFrEF patients can reach up to 40%, making the evaluation for inclusion in HTWL a crucial consideration for this patient group [16, 17]. Globally, the HT rate in 2022 was about 1.5 transplants per million population[3], whereas in Russia, this figure stood slightly higher at 1.7 per million. Remarkably, Kuzbass recorded 5 HTs per million population in 2023, over 2.9 times the national average.

In 2023, 16 HT centers were operational across Russia, collectively performing 381 HTs – an increase of 73 procedures (+19.16%) compared to the previous year. From the beginning of 2004 through December 2023, a total of 3,275 OHT have been performed in the Russian Federation.[4]

The estimated need for OHT is typically calculated based on a benchmark of 10 HTs per million population annually. With a population of approximately 2.6 million in 2023, Kuzbass has a projected requirement for 25 OHT procedures per year. Despite a consistent influx of patients into HTWL and its regular updates, a persistent challenge remains the region's low donor activity. This is primarily attributed to factors such as the vast geographical size of Kuzbass and limited transportation accessibility, which in turn restricts the viability of donor organs due to prolonged heart anoxia time. The shortage of donors, coupled with a growing number of eligible candidates, continues to limit access to heart transplantation not only in many regions of the Russian Federation but globally as well [18–22].

According to global statistics, the highest mortality among OHT recipients is observed within the first 6 months post-transplant, with the hospital stay representing the most critical period [23]. In this context, survival outcomes at our center – 83.3% in-hospital survival, 84.7% 1-year survival, and 54.2% 5-year survival – are comparable to those reported by other prominent cardiac surgery centers across Russia. For instance, the Meshalkin National Medical Research Center in Novosibirsk documented an 82% in-hospital survival and 69% 5-year survival over a 10-year period encompassing 66 OHTs

[2] https://rustransplant.com/

[3] https://www.statista.com/

[4] Public Report, Sergey Gautier, December 2023; https://rustransplant.com/

[19]. Similarly, the Sklifosovsky Research Institute for Emergency Medicine in Moscow reported an 82% in-hospital survival from a cohort of 70 OHTs [20]. In Krasnodar, the Ochapovsky Regional Clinical Hospital achieved a 1-year survival of 83.1% based on 230 OHTs performed between 2010 and 2023 [21].

CONCLUSION

Modern pharmacological therapy, guided by current clinical guidelines, has significantly improved symptom control and survival rates in HF patients with preserved ejection fraction. However, the population of patients progressing to ESHF continues to grow. The successful outcomes achieved over a 10-year period at the Research Institute for Complex Issues of Cardiovascular Diseases highlight the necessity of further developing the HT program in Kuzbass, reinforcing its role as the gold standard for the treatment of ESHF. However, long-term success is contingent not only upon surgical expertise and institutional experience but also on comprehensive recipient preparation by a multidisciplinary team, effective organization of the donor network, and implementation of continuous, structured long-term follow-up for transplant recipients.

The authors declare no conflict of interest.

REFERENCES

1. *Shahim B, Kapelios CJ, Savarese G, Lund LH.* Global Public Health Burden of Heart Failure: An Updated Review. *Card Fail Rev*. 2023; 9: e11. doi: 10.15420/cfr.2023.05.
2. *Okunev IM, Kochergina AM, Kashtalap VV*. Chronic and acute decompensated heart failure: topical issues. *Complex Issues of Cardiovascular Diseases*. 2022; 11 (2): 184–195. [In Russ, English abstract]. https://doi.org/10.17802/2306-1278-2022-11-2-184-195.
3. *Aissaoui N, Morshuis M, Maoulida H, Salem JE, Lebreton G, Brunn M et al.* Management of end-stage heart failure patients with or without ventricular assist device: an observational comparison of clinical and economic outcomes. *Eur J Cardiothorac Surg*. 2018; 53 (1): 170–177. doi: 10.1093/ejcts/ezx258.
4. *Poptsov VN.* Heart transplantation: an anesthesiologist-anesthesiologist-animatologist's point of view. M.–Tver': Triada, 2022; 440.
5. *Bounader K, Flécher E.* End-stage heart failure: The future of heart transplant and artificial heart. *Presse Med*. 2023; 53 (1): 104191. doi: 10.1016/j.lpm.2023.104191.
6. *Nesseler N, Mansour A, Bernard C, Coutance G, Bouglé A.* Perioperative management of heart transplantation: a clinical review. *Anesthesiology*. 2023; 139: 493–510. doi: 10.1097/ALN.0000000000004627.
7. *Dren' EV, Sogojan NK, Ljapina IN, Golubovskaja DP, Pecherina TB, Barbarash OL*. Clinical case of a patient with extreme hypertrophic cardiomyopathy and recurrent idiopathic transudative pericardial effusion. *Complex Issues of Cardiovascular Diseases*. 2023; 12 (3): 126–135. [In Russ, English abstract]. doi: 10.17802/2306-1278-2023-12-3-126-135.
8. *Khush KK, Cherikh WS, Chambers DC, Harhay MO, Hayes D, Hsich EM et al.* The International Thoracic Organ Transplant Registry of the International Society for Heart and Lung Transplantation: thirty-sixth adult heart transplantation report – 2019; focus theme: donor and recipient size match. *J Heart Lung Transplant*. 2019; 38: 1056–1066. doi: 10.1016/j.healun.2019.08.004.
9. Order of the Ministry of Health of the Russian Federation from 09.01.2023 № 3n "On approval of the standard of medical care for adults in heart transplantation".
10. *Gautier SV, Khomyakov SM*. Organ donation and transplantation in the Russian Federation in 2022. 15th Report from the Registry of the Russian Transplant Society. *Russian Journal of Transplantology and Artificial Organs*. 2023; 25 (3): 8–30. [In Russ, English abstract]. https://doi.org/10.15825/1995-1191-2023-3-8-30.
11. Heart transplantation, presence of a transplanted heart, heart graft die-off and rejection – Recommendations of the Ministry of Health of the Russian Federation 2020.
12. Heart transplantation, presence of a transplanted heart, heart graft die-off and rejection – Recommendations of the Ministry of Health of the Russian Federation 2023.
13. *Cantrelle C, Legeai C, Latouche A, Tuppin Ph, Jasseron C, Sebbaget L et al.* Access to heart transplantation: a proper analysis of the competing risks of death and transplantation is required to optimize graft allocation. *Transplant Direct*. 2017; 3: e198. doi: 10.1097/TXD.0000000000000711.
14. *Hsich EM, Blackstone EH, Thuita LW, McNamara DM, Rogers JG, Yancy CW et al.* Heart Transplantation: An In-Depth Survival Analysis. *JASS Heart Fail*. 2020; 8 (7): 557–568. doi: 10.1016/j.jchf.2020.03.014.
15. *Cantrelle C, Dorent R, Legeai C, Damy Th, Bastien O, Tuppin Ph et al.* Hospitalisation and life support in the year before and during heart transplantation: a French national study. *Open Heart*. 2018; 5: e000913. doi: 10.1136/openhrt-2018-000913.
16. *Pecherina T, Kutikhin A, Kashtalap V, Karetnikova V, Gruzdeva O, Hryachkova O et al*. Serum and echocardiographic markers may synergistically predict adverse cardiac remodeling after st-segment elevation myocardial infarction in patients with preserved ejection fraction. *Diagnostics*. 2020; 10 (5): 301. doi: 10.3390/diagnostics10050301.
17. *Barbarash OL, Rejtblat OM, Korennova OYu, Efremushkina AA, Ustyugov SA, Hramcova NA et al*. Resolution on the results of the council of experts: "Improving the system of medical care for patients with cardiovascular diseases in the siberian and far eastern federal districts within the framework of the federal project "Combating cardiovascular diseases". Focus on CHF". *Complex Issues of Cardiovascular Diseases*. 2023; 12 (4S): 206–209. (In Russ.). doi: 10.17802/2306-1278-2023-12-4s-206-209.
18. *Zamperetti N, Bellomo R, Piccinni P, Roncoet C.* Reflections on transplantation waiting lists. *Lancet*. 2011; 378: 632–635. doi: 10.1016/S0140-6736(10)62343-4.

19. *Chernyavskiy AM, Doronin DV, Fomichev AV, Osipov DE, Shmyrev VA, Karaskov AM*. 10-year heart transplantation experience in Novosibirsk. *Russian Journal of Transplantology and Artificial Organs*. 2018; 20 (1): 23–31. [In Russ, English abstract]. doi: 10.15825/1995-1191-2018-1-23-31.
20. *Khubutiya MSh, Sokolov VV, Redkoborodyy AV, Kozlov IA, Timerbaev VKh, Khutsishvili LG et al*. The experience of 70 heart transplants in a multidisciplinary medical care facility. *Transplantologiya. The Russian Journal of Transplantation*. 2018; 10 (3): 197–206. [In Russ, English abstract]. doi: 10.23873/2074-0506-2018-10-3-197-206.
21. *Tkhatl LK, Tatarintseva ZG, Kosmacheva ED*. Difficulties in diagnosing and predicting possible complications in patients after heart transplantation: single-center experience in the Krasnodar region. *Russian Journal of Cardiology*. 2024; 29 (2): 55–58. [In Russ, English abstract]. doi: 10.15829/1560-4071-2024-5558.
22. *Trivedi J, Siddharth P, Rabkin D, Gallo M, Guglin M, Slaughter MS et al.* Predictors of Survival After Heart Transplant in the New Allocation System: A UNOS Database Analysis. *ASAIO J*. 2024; 70 (2): 124–130. doi: 10.1097/MAT.0000000000002070.
23. *Tanveer Y, Arif A, Tsenteradze T, Anika NN, Bakht D, Masood QF et al.* Revolutionizing Heart Transplantation: A Multidisciplinary Approach to Xenotransplantation, Immunosuppression, Regenerative Medicine, Artificial Intelligence, and Economic Sustainability. *Cureus*. 2023; 15 (9): e46176. doi: 10.7759/cureus.46176.

The article was submitted to the journal on 24.05.2024

DOI: 10.15825/1995-1191-2024-4-122-132

POLYPHARMACY, THERAPEUTIC INERTIA, AND ADHERENCE OF HEART RECIPIENTS TO DRUG THERAPY

I.I. Muminov[1], A.O. Shevchenko[1–3], V.N. Poptsov[1], N.N. Koloskova[1], A.A. Yusova[1], S.A. Sakhovsky[1], D.D. Uvarova[1]

[1] Shumakov National Medical Research Center of Transplantology and Artificial Organs, Moscow, Russian Federation

[2] Sechenov University, Moscow, Russian Federation

[3] Pirogov Russian National Research Medical University, Moscow, Russian Federation

Heart transplantation remains the gold standard treatment for end-stage heart failure. Lifelong immunosuppressive and adjuvant therapy requires constant medical follow-up in order to optimize treatment regimens and increase the adherence of heart recipients to treatment. **Objective:** to study and adapt a method for systematic assessment of the complexity of treatment regimen using the MRCI index, and its link to long-term prognosis in heart recipients. **Materials and methods.** Results of the study were obtained by analyzing the data of heart recipients observed at the Consultative & Diagnostic Department, Shumakov National Medical Research Center of Transplantology and Artificial Organs (Shumakov Center). The Medication Regimen Complexity Index (MRCI) was used to assess drug therapy. In our study, polypharmacy was defined as taking five or more medications, and high-risk polypharmacy was defined as the use of more than eight medications. The heart recipients were divided into two groups based on how many medications they received daily. **Results.** The study included patients observed at the Consultative & Diagnostic Department, Shumakov Center from January 2008 to December 2017. The number of drugs taken by the patient at year 5 of follow-up was 9.2 ± 4.2. During the conducted data analysis, the mean total MRCI score was 48.72 ± 19.15 (from 32 to 70); medications used to treat comorbidities accounted for 42.9% of the total MRCI score, and immunosuppressive therapy accounted for 28.7%. The total MRCI score in the high-risk polypharmacy group was 58.49 ± 17.41; medications used to treat comorbidities accounted for 50.27% of the total MRCI score. The analysis revealed a correlation between the total MRCI score and the frequency of hospitalizations. **Conclusions.** Patient adherence to prescribed treatment is a predictor of favorable prognosis of event-free long-term survival, but low adherence and therapeutic inertness are associated with decreased quality of life, more frequent hospitalizations and higher risk of adverse events. With proper outpatient follow-up of this patient cohort, there were no significant differences in survival in the polypharmacy and high-risk polypharmacy group.

Keywords: heart transplantation, polypharmacy, comorbidity, immunosuppressive therapy, outpatient follow-up.

INTRODUCTION

In the past decade, the number of heart transplant (HT) recipients requiring dynamic outpatient follow-up has increased, driven by the rise in transplant activity. This follow-up is essential to monitor immunosuppressive therapy, assess graft function, address complications from long-term immunosuppressant use, and manage and prevent concomitant conditions [1].

Currently, the consultative and diagnostic department at the Shumakov National Medical Research Center of Transplantology and Artificial Organs (Shumakov Center) oversees more than 1500 HT recipients from various regions across the Russian Federation [2]. With the extensive experience and personalized care approach developed, long-term survival rates have significantly improved, now exceeding an average of 12 years [3].

Managing HT recipients involves lifelong immunosuppressive therapy combined with medications to prevent the side effects of long-term immunosuppression, as well as adjuvant therapies for treating concomitant conditions [4]. The long-term follow-up of HT recipients is influenced by factors such as interaction between the transplanted organ and the recipient, quality of immunosuppressive therapy and its side effects, and external factors, as well as the patient's genotype and cognitive abilities [5]. In this regard, evaluating both the adequacy of prescriptions and the patient's adherence to medication becomes crucial.

The term "medication regimen complexity" refers to the multiple characteristics of a patient's prescribed medication regimen [6]. Studies have shown that noncompliance with immunosuppressive therapy among HT recipients is as high as 19%, with medication administ-

Corresponding author: Nadezda Koloskova. Address: 1, Shchukinskaya str., Moscow, 123182, Russian Federation. Phone: (926) 651-40-64. E-mail: nkrasotka@mail.ru

ration errors for adjuvant therapy exceeding 43%. These issues are primarily due to the need for daily administration of a large number of medications [7].

A quantitative assessment of medication regimen complexity can be performed using the Medication Regimen Complexity Index (MRCI), based on a specific patient's treatment plan. According to several studies, the MRCI has shown potential as an effective tool for preventing adverse events in HT recipients experiencing polypharmacy [8–10].

The **objective of our study** was to investigate and adapt a systematic approach for assessing treatment regimen complexity using the MRCI, and to explore its relationship with long-term outcomes in HT recipients.

MATERIALS AND METHODS

The results of the study were based on analysis of outcomes in HT recipients under follow-up care at the Shumakov National Medical Research Center of Transplantology and Artificial Organs (Shumakov Center). Outpatient monitoring was conducted by cardiologists from Shumakov Center's consultative and diagnostic department in collaboration with healthcare providers in the patients' place of residence. When necessary, remote consultations were organized through the Shumakov Center's telemedicine system to provide support to local physicians. Adjustments to drug therapy were made on an outpatient basis based on clinical and instrumental examination data. In cases where hospitalization was warranted, patients were admitted to the cardiology ward of Shumakov Center.

All patients underwent routine follow-up examinations, which included clinical evaluations, complete blood counts, biochemical assays, monitoring of blood levels of immunosuppressive drugs, echocardiography, as well as annual coronary angiography and endomyocardial biopsy.

Socio-demographic data – including region of residence, living conditions, marital status, and educational level – along with case histories and outpatient records from patients followed at Shumakov Center, were collected retrospectively. Recipients included in this study were treated in accordance with established clinical guidelines [11].

An adapted and modified version of MRCI was used in this study. To calculate the index, medications prescribed to HT recipients were categorized into three primary groups (Table 1).

Non-pharmacological supplements and herbal preparations were excluded from the analysis and were not recommended for patient use.

All patients received multicomponent immunosuppressive therapy, which typically included a calcineurin inhibitor (tacrolimus) in combination with an antimetabolite (mycophenolic acid or mycophenolate mofetil) or a proliferation signal inhibitor (everolimus), as well as methylprednisolone. The dosage of immunosuppressive drugs was based on the post-transplant period and the assessed risk of graft rejection.

Therapeutic drug monitoring was conducted to maintain target serum levels of immunosuppressive medications. The levels were measured using a Cobas e411 analyzer (Roche, Switzerland) via electrochemiluminescence immunoassay.

According to the literature, polypharmacy is defined as the concurrent use of five or more medications, while high-risk polypharmacy refers to the intake of more than eight medications [12]. Based on the number of medications received daily, HT recipients were divided into two groups: Group 1 included patients receiving 5 to 8 medications per day, and Group 2 included recipients taking 9 or more medications daily [13].

Patients were classified as comorbid if they had two or more coexisting medical conditions, irrespective of their primary diagnosis (ICD-10 code Z94.1, denoting heart transplant status).

MRCI was calculated for all medications self-administered by the patient or taken once daily. The MRCI score represents the cumulative total of points derived from three components evaluated for each individual medication: dosage form, frequency of administration, and any information about the drug. Table 2 summarizes the scoring criteria used to determine the total MRCI score [6].

Table 1

Groups of medications used in recipients after heart transplantation

Group 1 Immunosuppressive drugs	Group 2 Additional drugs (prevention of complications of immunosuppressive therapy)	Group 3 Drugs for the treatment of comorbidities
Cyclosporine/Tacrolimus Everolimus Methylprednisolone Mycophenolate mofetil/ Mycophenolic acid	Calcium/Vitamin D Statins Acetylsalicylic acid Antibacterials Antivirals Antacids Proton pump inhibitors Osteoporosis medications	Antidepressants Antihypertensive drugs Antiarrhythmic drugs Diabetes mellitus medications (oral) Anticoagulants Diuretics Others.

Table 2

MRCI sections

Section A: Dosage form and drug administration route

Administration route	Dosage forms	Score
Oral	Capsules/tablets	1
	Mouthwashes	2
	Chewable lozenges	2
	Powders/pellets	2
	Suspensions	
	Sublingual sprays/tablets	2
Local use products	Cream/gel/ointment	2
	Solutions	2
	Medicated dressings	2
	Medicated pastes	3
	Plasters	2
	Sprays	1
Eye, nose and ear products	Ear drops/creams/ointments	3
	Eye drops	3
	Eye gels/ointments	3
	Nasal sprays	2
	Nasal drops/creams/ointments	3

Administration route	Dosage forms	Score
Inhalation use	Metered-dose inhalers	4
	Nebulizer	5
	Turbuhalers	3
	Accuhalers	3
	Aerosols	3
	Oxygen concentrator	3
	Dry powder inhaler	3
Others	Enemas	2
	Ampoules/vials	4
	Gizzards	3
	Suppositories	2
	Injectable dosage forms	3
	Vaginal creams	2
	Dialysate	5
	Different types of analgesia administered by the patient alone (patient-controlled analgesia)	2

Section B: Dosing frequency

Dosing frequency	Score
Once a day	1
Once a day if required	0.5
Twice a day	2
Twice a day if required	1
Three times a day	3
Three times a day if needed	1.5
Four times a day	4
Four times a day if needed	2
Every 12 hours	2.5
Every 12 hours as needed	1.5
Every 8 hours	3.5

Dosing frequency	Score
Every 8 hours as needed	2
Every 6 hours	4.5
Every 6 hours as needed	2.5
Every 4 hours	6.5
Every 4 hours as needed	3.5
Every 2 hours	12.5
Every 2 hours as needed	6.5
Use of medications as needed	0.5
Use of oxygen concentrator as needed	1
Oxygen use <15 hours per day	2
Oxygen use >15 hours per day	3

Section C: Additional directions

Additional administration directions	Score
Crush	1
Dissolve tablet/powder	1
Administer multiple tablets/inhalations simultaneously	1
Administer within a specified time interval	1

Additional administration directions	Score
Take with food	1
Take with liquids to wash down	1
Take as directed	2
Reduce/increase dose	2
Alternate dose depending on the time of day	2

The minimum possible MRCI score for a patient is 1.5, which corresponds to a single tablet or capsule taken once daily as needed. The maximum MRCI score varies and is individually determined based on the patient's specific medication regimen.

Descriptive statistics are presented as arithmetic mean ± standard deviation (M ± SD). Kaplan–Meier survival analysis was employed to assess event-free survival, with statistical computations performed using IBM SPSS Statistics v23. Comparative analysis between groups was conducted using the log-rank test, Mann–Whitney U test, median test, Kruskal–Wallis test, Kolmogorov–Smirnov test, and Jonckheere–Terpstra test. For all statistical tests, results were considered significant at $p < 0.05$.

RESULTS

Between January 2008 and December 2017, a total of 771 HTs were performed at Shumakov Center. The study excluded cases involving retransplantation, in-

hospital mortality, and recipients under 18 years of age. So, 607 adult HT recipients under outpatient follow-up at Shumakov Center were included in the final analysis.

At the time of the study, recipient mean age was 47.84 ± 11.83 years. The mean follow-up period post-transplant was 8.2 ± 2.8 years, with a range from 2 to 15 years (Table 3).

The distribution of medications taken by HT recipients at different follow-up periods is presented in Table 4.

As shown in Table 4, by the end of the first year of follow-up, the average total number of medications taken by HT recipients had decreased slightly compared to the number prescribed at hospital discharge – 6.8 ± 4.2 versus 8.9 ± 2.7, respectively. However, by year 5 of follow-up, this value had increased to 9.2 ± 4.2 ($p < 0.05$).

When analyzing the average number of medications by drug group, it was observed that in Group 1, the number of immunosuppressive agents used decreased by year 5 ($p = 0.02$).

There was no statistically significant increase in the number of group 2 medications used during the follow-up period of 1 to 5 years ($p = 0.42$). However, a significant increase in the use of group 3 medications was observed by year 5 ($p = 0.001$). The average number of drugs prescribed for the management of comorbid conditions increased from 1.2 ± 1.3 at the end of year 3 to 4.3 ± 2.5 by year 5 of follow-up.

In assessing multicomponent therapy, MRCI was calculated for all recipients included in the study (Table 5).

The mean total MRCI score among the HT recipients was 48.72 ± 19.15, with individual scores ranging from 32 to 70. Medications prescribed for the management of comorbidities accounted for 42.9% of the total MRCI score, while immunosuppressive therapy contributed 28.7%.

To evaluate the prevalence of polypharmacy and high-risk polypharmacy, recipients were stratified into two groups based on the number of self-administered and single-use medications, and the groups were compared as presented in Table 6.

In the high-risk polypharmacy group, there was a significantly higher prevalence of arterial hypertension, diabetes mellitus, lipid metabolism disorders, and varying degrees of obesity compared to the lower-risk group ($p < 0.05$, Fig. 1).

To evaluate the treatment regimen complexity, the MRCI score was calculated for both groups. In the high-risk polypharmacy group, the mean total MRCI score was 58.49 ± 17.41, with 50.27% of the total complexity attributed to medications prescribed for the management of comorbid conditions.

A comparative analysis of recipient hospitalization rates based on the total MRCI score was also conducted (Fig. 2).

Table 3

General characteristics of recipients (n = 607)

Indicators	Values
Age, years	47.84 ± 11.83
Men, n (%)	526 (86.66%)
Women, n (%)	81 (13.34 %)
BMI, kg/m^2	26.87 ± 4.78
Pre-transplant diagnosis	
ICM , n (%)	237 (39.04%)
DCM, n (%)	334 (55.02%)
HCM, n (%)	7 (1.15%)
Others, n (%)	29 (4.77%)
Pre-transplant UNOS status	
1A, n (%)	150 (2.47%)
1B, n (%)	214 (35.26%)
2, n (%)	243 (40.03%)
Donor details	
Age, years	42.25 ± 11.6
Male, n (%)	470 (77.43%)
Female, n (%)	137 (22.57%)

Note: BMI, body mass index; ICM, ischemic cardiomyopathy; DCM, dilated cardiomyopathy; HCM, hypertrophic cardiomyopathy.

Table 4

Number of medications taken by recipients after heart transplantation at different follow-up periods

Value	At the time of discharge after HT (n = 607)	At year 1 post-HT (n = 604)	At year 3 post-HT (n = 595)	At year 5 post-HT (n = 571)
Total number of drugs	8.9 ± 2.7	6.8 ± 4.2	8.8 ± 4.3	9.2 ± 4.2
Group 1 drugs	2.9 ± 0.2	2.5 ± 0.4	2.1 ± 0.2	2.1 ± 0.3
Group 2 drugs	4.8 ± 1.2	3.0 ± 1.3	2.7 ± 1.6	2.8 ± 1.4
Group 3 drugs	1.2 ± 1.3	1.3 ± 2.5	4.0 ± 2.5	4.3 ± 2.5

Table 5

MRCI score of the three drug groups for all recipients included in the study (n = 607)

Drug group	Value
Drug group 1	14.02 ± 2.51
Drug group 2	13.76 ± 4.58
Drug group 3	20.93 ± 10.42

Table 6

General characteristics of recipients, depending on administration of medication

Indicator	Group 1 (use of 5 to 8 drugs), n = 312	Group 2 (use of ≥9 drugs), n = 295	P
Age, years	46.09 ± 12.31	49.68 ± 10.99	0.02
Male, n (%)	270 (86.54%)	256 (86.78%)	0.93
Female, n (%)	42 (13.46%)	39 (13.22%)	
BMI, kg/m²	**23.07 ± 4.51**	**28.12 ± 4.93**	**0.027**
Level of education			
Secondary general education	37 (11.86%)	31 (10.51%)	0.82
Secondary vocational education	143 (45.83%)	145 (49.15%)	
Higher education	132 (42.31%)	119 (40.34%)	
Pre-transplant diagnosis			
ICM, n (%)	103 (33.01%)	134 (45.42%)	0.69
DCM, n (%)	186 (59.62%)	148 (50.17%)	
HCM, n (%)	3 (0.96%)	4 (1.36%)	
Others, n (%)	20 (6.41%)	9 (3.05%)	
Co-existing diseases			
Diabetes mellitus	**57 (18.2%)**	**102 (34.5%)**	**0.002**
Other endocrinological diseases (except diabetes mellitus)	132 (42.3%)	188 (63.7%)	0.415
Cerebrovascular diseases	119 (38.1%)	118 (40.0%)	0.639
Lung diseases	62 (19.8%)	58 (19.6%)	0.948
Gastrointestinal diseases	254 (81.4%)	286 (96.9%)	0.936
Dyslipidemia	**205 (65.7%)**	**265 (89.9%)**	**0.001**
Osteoporosis	113 (36.2%)	197 (66.7%)	0.174
Gout	60 (19.2%)	107 (36.2%)	0.172
Arterial hypertension	**239 (76.6%)**	**274 (92.8%)**	**0.039**
Rheumatic diseases	18 (5.7%)	25 (8.4%)	0.194
Kidney diseases	207 (66.3%)	255 (86.4%)	0.640
Total MRCI score			
Drug group 1	15.2 ± 4.98	13.71 ± 2.05	
Drug group 2	12.48 ± 3.16	15.38 ± 5.42	
Drug group 3	11.45 ± 5.48	29.4 ± 9.94	
Total MRCI score	39.13 ± 13.62	58.49 ± 17.41	

Note: BMI, body mass index; ICM, ischemic cardiomyopathy; DCM, dilated cardiomyopathy; HCM, hypertrophic cardiomyopathy.

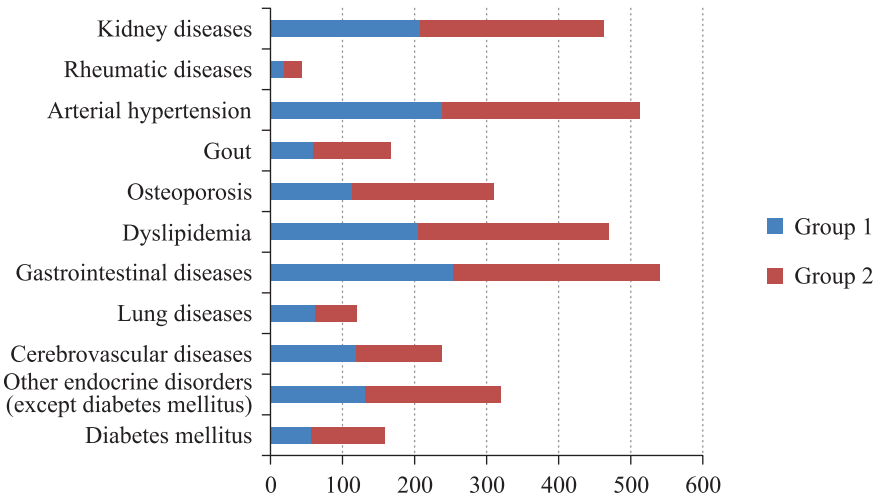

Fig. 1. Concomitant diseases of recipients depending on the number of drugs used

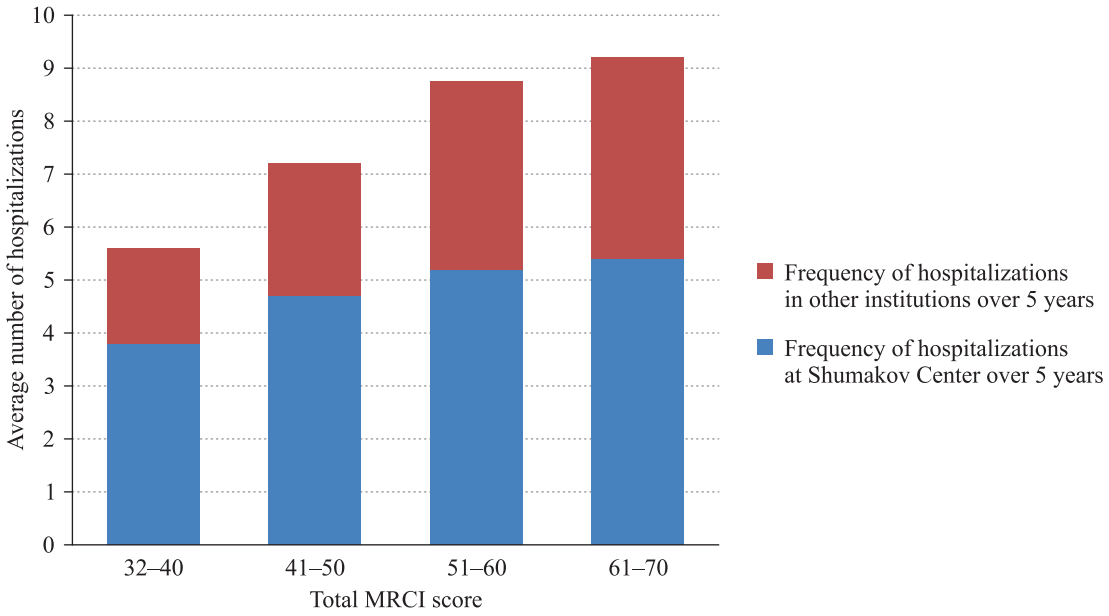

Fig. 2. Frequency of hospitalization of recipients depending on the total MRCI score

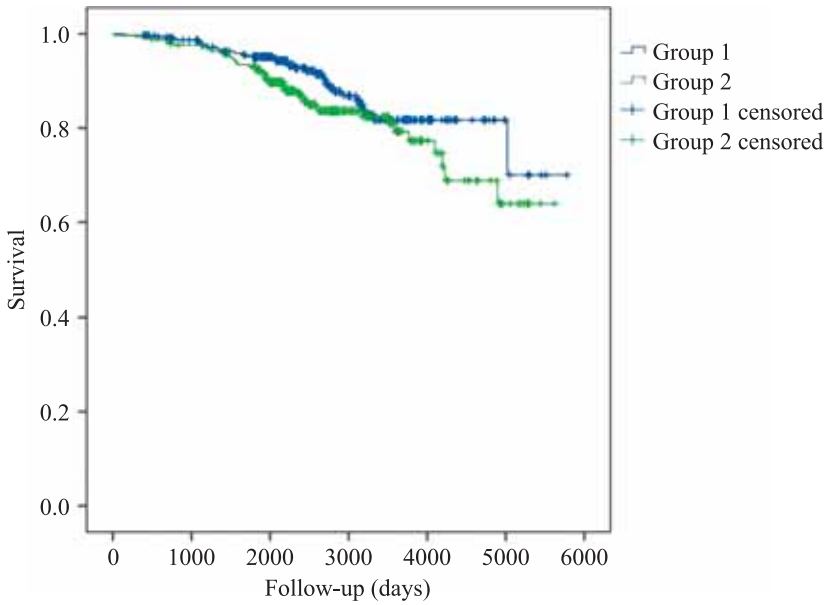

Fig. 3. Survival curves of recipients depending on the number of drugs used

The analysis demonstrated a significant correlation between total MRCI score and hospitalization rate. Patients classified under high-risk polypharmacy required inpatient treatment more frequently, both at Shumakov Center and in other medical facilities ($p < 0.05$).

Despite the observed difference in hospitalization rates, comparative survival analysis using Kaplan–Meier curves revealed no statistically significant difference in overall survival between recipients with polypharmacy and those with high-risk polypharmacy (Fig. 3).

DISCUSSION

The results of this study demonstrated that in the long-term post-HT period, recipients received an average of 5 to 15 medications. The MRCI score showed a clear correlation with the number of comorbidities and the presence of complications associated with immunosuppressive therapy, thereby linking MRCI to hospitalization rate. This is the first study to evaluate the impact of MRCI on long-term follow-up outcomes in HT recipients. To date, only a limited number of international studies have addressed the application of MRCI in this specific patient population. Our findings may become the basis for future research on this topic.

On average, each recipient was diagnosed with four comorbidities (requiring 5 to 15 medications) in the post-transplant period, each necessitating ongoing pharmacologic management. The presence of multiple comorbidi-

ties, coupled with lifelong immunosuppressive therapy, constitutes a significant risk factor for polypharmacy [12]. As the number of comorbid conditions increases, the demand for a broader scope of pharmacotherapy rises.

This study quantitatively analyzed drug therapy in HT recipients using the MRCI score. In a Spanish study, the reported average MRCI score was 42 [14], whereas in our cohort the mean score was 49. This difference may be attributed to a more detailed comparative analysis of the therapeutic components, particularly the contribution of immunosuppressive therapy and medications used to manage comorbid conditions.

When evaluating MRCI components, notably high scores were associated with the frequency of taking medications and additional instructions across the three main drug groups. These findings emphasize the necessity of a deeper examination of therapeutic regimens in HT recipients, particularly to enhance adherence to therapy.

When compared with MRCI scores in non-transplanted populations, the treatment burden in HT recipients is significantly higher. For instance, in a study conducted by Suzanne et al. [9], patients with mental illness undergoing long-term pharmacotherapy exhibited MRCI scores ranging from 6.21 to 25, considerably lower than those observed in our HT cohort.

Kamila et al. [15] also reported elevated MRCI scores in recipients following liver and kidney transplantation. Their study highlighted that MRCI not only quantifies pharmacologic load but also serves as a valuable analytical tool for evaluating the appropriateness and complexity of prescribed regimens in liver and kidney transplant recipients.

In our study, recipients classified within the high-risk polypharmacy group were notably older and had a greater burden of comorbidities, which accounted for the increased MRCI scores, particularly due to the use of medications aimed at managing comorbid conditions. In this group, no significant differences in survival outcomes were observed when compared to recipients with lower MRCI scores. This finding underscores the personalized approach employed by the multidisciplinary team at Shumakov Center, as well as the strong adherence of HT recipients to their therapeutic regimens.

Our results are consistent with those of Colavecchia et al. [16], who demonstrated a positive correlation between higher MRCI scores and increased hospitalization rates across various clinical scenarios. Similarly, our analysis showed that recipients with elevated MRCI scores had higher rates of inpatient treatment.

Evaluating the prescribed drug therapy through calculation of the MRCI score offers physicians an additional tool to identify patients who require more intensive monitoring during prescription and therapy adjustment. This approach can help reduce the risk of complications associated with multi-drug treatment regimens. Given that HT recipients must take a large number of life-saving drugs, cardiologists at the consultative and diagnostic department of Shumakov Center should prioritize regular assessment of pharmacotherapy in order to enhance adherence and minimize complications.

CONCLUSIONS

HT recipients in the long-term postoperative period are required to take a broad spectrum of medications, including immunosuppressive and adjuvant therapies. Consequently, it is essential for specialists overseeing these patients to closely monitor pharmacotherapy in order to evaluate potential drug interactions and promote adherence to prescribed regimens. Regular revision of dosages and treatment plans by the attending physician serves as a predictor of favorable long-term, event-free survival. In contrast, low adherence and therapeutic inertia are associated with reduced quality of life, increased hospitalization rates, and a higher risk of adverse events. Importantly, our study showed that with proper outpatient follow-up, there were no significant differences in survival between patients with polypharmacy and those with high-risk polypharmacy.

The authors declare no conflict of interest.

REFERENCES

1. Transplantology: results and prospects. Vol. XIII. 2021 / Ed. by S.V. Gautier. M.–Tver: Triada, 2022: 416.
2. *Muminov II, Koloskova NN, Poptsov VN, Zakharevich VM, Mozheiko NP, Sakhovsky SA, Shevchenko AO.* Experience of outpatient follow-up of heart transplant recipients at Shumakov center. *Russian Journal of Transplantology and Artificial Organs*. 2023; 25 (3): 68–75. https://doi.org/10.15825/1995-1191-2023-3-68-75.
3. *Gautier SV, Shevchenko AO, Kormer AYa, Poptsov VN, Shevchenko OP.* Prospects to improve long-term outcomes of cardiac transplantation. *Russian Journal of Transplantology and Artificial Organs*. 2014; 16 (3): 23–30. (In Russ.). https://doi.org/10.15825/1995-1191-2014-3-23-30.
4. *Koloskova NN, Nikitina EA, Zakharevich VM, Muminov II, Cvan VS, Poptsov VN et al.* Conversion to everolimus to preserve kidney function in a heart transplant recipient, a personalized approach of immunos uppressive therapy. *Russian Journal of Transplantology and Artificial Organs*. 2018; 20 (3): 70–74. (In Russ.). https://doi.org/10.15825/1995-1191-2018-3-70-74.
5. *Wilkening GL, Brune S, Saenz PF, Vega LM, Kalich BA.* Correlation between medication regimen complexity and quality of life in patients with heart failure. *Res Social Adm Pharm.* 2020 Oct; 16 (10): 1498–1501. doi: 10.1016/j.sapharm.2020.01.003. Epub 2020 Jan 18. PMID: 32001156.
6. *George J, Phun Y-T, Bailey MJ, Kong DC, Stewart K.* Development and Validation of the Medication Regimen Complexity Index. *Ann Pharmacother.* 2004; 38 (9): 1369–1376. doi: 10.1345/aph.1D479.

7. *Hansen R, Seifeldin R, Noe L.* Medication adherence in chronic disease: issues in posttransplant immunosuppression. *Transplant Proc*. 2007; 39: 1287–1300.
8. *Abdelbary A, Kaddoura R, Balushi SA, Ahmed S, Galvez R, Ahmed A et al.* Implications of the medication regimen complexity index score on hospital readmissions in elderly patients with heart failure: a retrospective cohort study. *BMC Geriatr.* 2023 Jun 19; 23 (1): 377. https://doi.org/10.1186/s12877-023-04062-2.
9. *Harris SC, Jean SJ.* Characterization of the medication regimen complexity index in high-utilizer, adult psychiatric patients. *Ment Health Clin.* 2020 Jul 2; 10 (4): 207–214. https://doi.org/10.9740/mhc.2020.07.207.
10. *Masumoto S, Sato M, Momo K, Matsushita A, Suzuki K, Shimamura H et al.* Development of medication regimen complexity index: Japanese version and application in elderly patients. *Int J Clin Pharm.* 2021 Aug; 43 (4): 858–863. doi: 10.1007/s11096-020-01185-z. Epub 2020 Nov 2. PMID: 33136252.
11. Clinical Recommendations “Heart Transplantation, the presence of a transplanted heart, heart graft die-off and rejection”, Russian Transplant Society, approved by the Scientific and Practical Council of the Ministry of Health of the Russian Federation in 2023.
12. *Sychev DA, Otdelenov VA, Krasnova NM, Ilyina ES.* Polypragmasy: A clinical pharmacologist’s view. *Ter Arkh*. 2016; 88 (12): 94–102. (In Russ.). doi: 10.17116/terarkh2016881294-102.
13. *Masnoon N, Shakib S, Kalisch-Ellett L, Caughey GE.* What is polypharmacy? A systematic review of definitions. *BMC Geriatr.* 2017 Oct 10; 17 (1): 230. https://doi.org/10.1186/s12877-017-0621-2.
14. *Gomis-Pastor M, Roig Mingell E, Mirabet Perez S, Brossa Loidi V, Lopez Lopez L, Diaz Bassons A et al.* Multimorbidity and medication complexity: New challenges in heart transplantation. *Clin Transplant.* 2019 Oct; 33 (10): e13682. doi: 10.1111/ctr.13682. Epub 2019 Aug 28. PMID: 31368585.
15. *Kamila P, Smith SG, Patzer R, Wolf MS, Marina S.* Medication regimen complexity in kidney and liver transplant recipients. *Transplantation*. 2014 Oct 15; 98 (7): e73–e74.
16. *Colavecchia AC, Putney DR, Johnson ML, Aparasu RR.* Discharge medication complexity and 30-day heart failure readmissions. *Res Social Adm Pharm*. 2017 Jul-Aug; 13 (4): 857–863. doi: 10.1016/j.sapharm.2016.10.002. Epub 2016 Oct 8. PMID: 27771308.

The article was submitted to the journal on 17.05.2024

DOI: 10.15825/1995-1191-2024-4-133-139

DEVELOPMENT OF AN EXTRACORPOREAL PUMP FOR ECMO SYSTEMS

A.P. Kuleshov, N.V. Grudinin, V.K. Bogdanov, A.S. Buchnev, O.Yu. Esipova

Shumakov National Medical Research Center of Transplantology and Artificial Organs, Moscow, Russian Federation

Objective: today, extracorporeal membrane oxygenation (ECMO) systems remain the main type of short-term circulatory support in various clinical situations. One of the main elements of this system is a blood pump. The objective of this study is to develop the first domestic centrifugal pump for use in ECMO systems. **Materials and methods.** Based on a systematic literature review, the main medical and technical requirements for an extracorporeal centrifugal pump were formulated. To create 3D mathematical models of the outer casing of the pump and all its internal components, calculations were performed in CAD software package SolidWorks (SolidWorks Corp., USA). Hydrodynamic test benches were designed and developed to evaluate the performance of the centrifugal pump mockup. The pump was studied to obtain its head-capacity curve (HCC) and hemolytic characteristics. **Results.** 3D modeling of geometrical parameters of the pump flow impeller was performed. Fluid flow was assessed in the rotor rotation range at speeds from 3000 to 7000 rpm. Hydrodynamic bench tests were performed under conditions simulating the resistance of the oxygenator and connecting cannulas. The HCC was obtained based on the given medical and technical requirements for the operating flow range from 1 to 5 l/min at pressure drops of 200 to 400 mm Hg. **Conclusion.** Based on results from the 3D modeling and bench experiments, a model of extracorporeal centrifugal pump was obtained, which showed its efficiency during the first trials. Further experimental studies will be conducted to obtain the energy and biological characteristics of the developed device.

Keywords: 3D computer model, centrifugal pump, extracorporeal pump, head-capacity curve, hemolysis, ECMO.

INTRODUCTION

Recent advancements in technology have led to significant improvements in extracorporeal membrane oxygenation (ECMO) systems, which have become essential in the management of patients with pulmonary, cardiac, and cardiopulmonary insufficiency. These systems have become more efficient, compact, and even portable [1–2].

The centrifugal pump (CP) is a key component of the extracorporeal circuit in ECMO systems.

It plays a crucial role in maintaining hemodynamic stability by compensating for circulatory failure or partially replacing the heart's pumping function.

Additionally, the CP ensures blood flow through the membrane oxygenator, enabling oxygenation and the removal of carbon dioxide, thus substituting pulmonary function.

The increase in ECMO procedures performed in intensive care units (ICUs) and cardiac resuscitation units over the years has resulted in improved survival rates for critically ill patients.

The development and integration of a Russian-made CP into these systems will further enhance the quality and accessibility of high-tech medical services.

MATERIALS AND METHODS

An analytical review of bibliographic sources on the development of extracorporeal pumps for ECMO systems highlights the following key medical and technical requirements for the CP:

– Body length: up to 80 mm;
– Maximum external diameter: 50 mm;
– Impeller diameter: up to 30 mm;
– Weight: up to 50 g.

The developed pump incorporates a built-in long cylindrical electric motor [3].

The new CP is seated and magnetically coupled, ensuring unobstructed motor operation. The pump head is securely fixed to the motor, with an annular flow section designed to adequately cool the motor under various operating conditions.

The device being developed is a flask-shaped structure that contains an 8-bladed closed impeller mounted on a hinged support. The impeller, with a diameter nearly equal to that of the motor, is positioned between the pump inlet and the motor housing. Centrifugal pumps designed for artificial circulation typically feature impellers with relatively large diameters, around 50 mm

Corresponding author: Arkadiy Kuleshov. Address: 1, Shchukinskaya str., Moscow, 123182, Russian Federation. Phone: (915) 292-47-98. E-mail: ilovemylene@yandex.ru

(e.g., Rotaflow, Maquet, Germany), which allows for pumping blood at low rotational speeds. According to preliminary calculations, the pump head must provide sufficient peripheral speed for an impeller of approximately 30 mm in diameter.

However, this speed could potentially be excessive, increasing shear stress on erythrocytes. The resulting tangential stress in the blood flow layer and the stress proportional to the velocity gradient from erythrocyte momentum exchange may lead to complications [4]. Thus, one of the key areas requiring further development is the detailed calculation of the impeller design, with a focus on minimizing rotor speed.

3D modeling methods

The SolidWorks program (Dassault Systèmes, France) was used to create a 3D model of the CP. Through computer flow simulation, a theoretical head-capacity curve (HCC) was developed to analyze the pump model. A review of literature on computer modeling of pump flow revealed that the key focus lies in constructing an accurate computational mesh and selecting an appropriate turbulence model. Inaccuracies in turbulence modeling can lead to significant errors in calculations [5, 6].

To achieve more accurate characteristics, software methods were employed to calculate flow hydrodynamics within the pump cavities. The primary simulation parameters involved stress analysis and flow velocity estimation, aiming to minimize stagnation and recirculation zones. Theoretical data derived from simulations were then compared with actual results obtained from the pump mock-up on a hydrodynamic bench. This bench simulated the conditions of the ECMO procedure using the LivaNova oxygenator (INSPIRE, USA). The operating characteristics of the RotaFlow centrifugal pump, which is widely used in medical practice [7], were considered when selecting the most appropriate pump operating parameters for the mode.

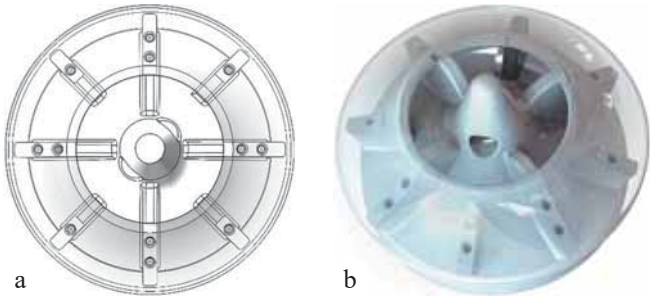

Fig. 1. a, modification of the 8-blade impeller structure; b, 3D model of the impeller

Developed design of the centrifugal pump impeller

The impeller features a configuration of 4 primary radial vanes, with four additional intermediate vanes positioned between them. These intermediate vanes mirror the shape of the primary vanes but are only half their length. Both the inlet and outlet angles of the blades are oriented perpendicular to the axis. Adjustments to the blade twist angles did not yield notable improvements in hydrodynamic performance and introduced unnecessary complexity to the manufacturing process. The final 8-blade impeller configuration is illustrated in Fig. 1, a, with the corresponding 3D computational model shown in Fig. 1, b.

The proposed CP design includes four inlet channels leading to the impeller, each subdivided by short guide blades. The cross-sectional areas at the inlet and outlet of the impeller flow path are proportionate, and the streamlined channel geometry enables unobstructed fluid transfer. The exponential contour of the duct promotes laminar flow within the pump and ensures optimal alignment with the pump casing.

At the swivel support level, the impeller is equipped with perforations that facilitate flushing of the pump. This design feature effectively reduces thrombogenicity without causing any measurable decline in hydraulic performance.

Computational fluid dynamics

In addition to experimental evaluation, the pump design was analyzed using computational fluid dynamics with SolidWorks (Dassault Systèmes, France) and Ansys (ANSYS Inc., USA) software. A computational mesh comprising approximately 220,000 elements was generated to represent the entire flow domain. For the simulations, blood was modeled as a Newtonian fluid with a dynamic viscosity of 5.0 mPa·s and a density of 1055 kg/m^3. Representative results are shown in Fig. 2, illustrating the pressure distribution and flow streamlines within the pump.

The computed HCC was obtained and is presented alongside experimental results to facilitate comparison with bench test data from the pump's operation in a closed-loop circulation circuit.

Computational and mathematical analyses revealed a slight reduction in impeller efficiency, estimated at 5–7%, primarily due to the presence of recirculating flow and the resulting hydrodynamic losses. Numerical simulations indicated elevated flow velocity on the rear side of the impeller and within the orifices. Recirculation through these orifices ranged from 0.3 to 1.0 L/min per orifice, depending on rotational speed and differential pressure.

The total internal volume of the pump was 16 mL. Flow transitions remained smooth throughout the helical outlet region. Under ECMO operating conditions (pressure of 350 mmHg and flow rate of 5 L/min), peak tangential shear stress was 125 Pa, while average shear stress was approximately 40 Pa.

Prototype centrifugal pump

Based on preliminary computer simulations, a three-dimensional model of the centrifugal pump (CP) was developed, as shown in Fig. 3, a. Using this model, the prototype components were fabricated with a large-format medical 3D printer, the Formlabs 3BL (USA). The parts were produced via stereolithography (SLA), a laser-based 3D printing technology, using Gorky Liquid (Surgical) – a biocompatible, sterilizable surgical photopolymer – with a printing precision of 25 μm. The rotor features a working section mounted on a disk supported by a ball bearing, which also houses a magnet for the drive mechanism. The fully assembled prototype pump, prepared for bench testing, is depicted in Fig. 3, b.

The assembly includes a 4-pole magnet paired with a closure ring made from Steel 10, as well as a custom-fabricated support ball composed of durable aluminum oxide (Al_2O_3), also known as corundum or alundum. The CP housing features an outlet fitting with an internal diameter of 3/8 inch. The impeller is rotated externally via a magnetic coupling mechanism.

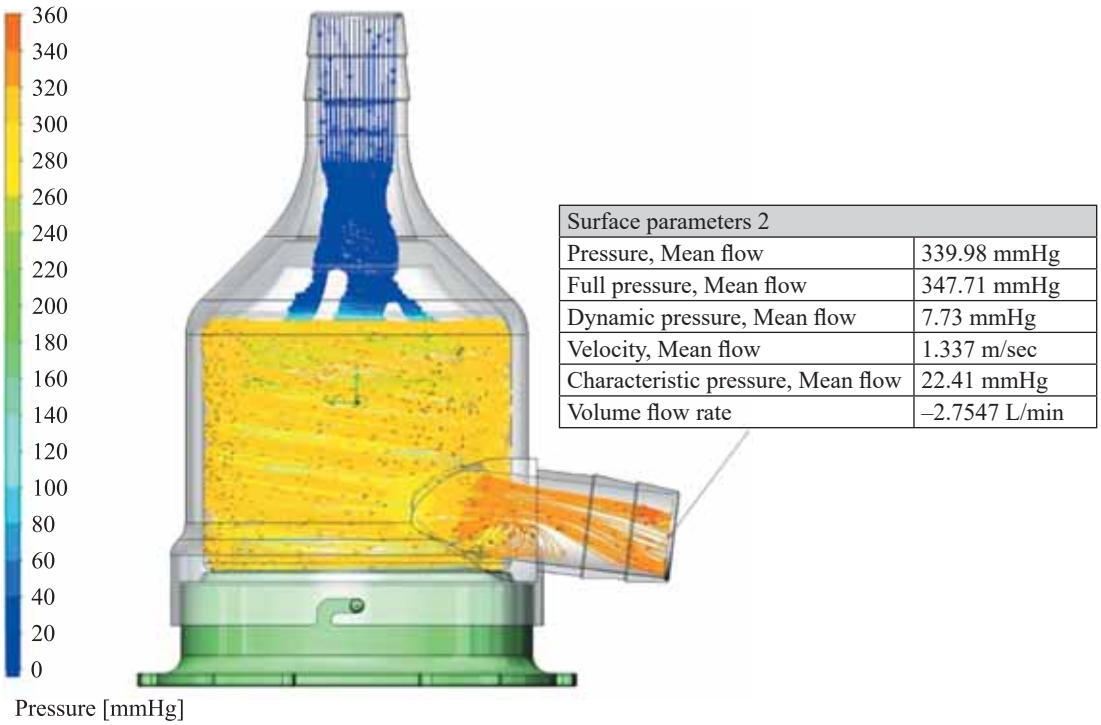

Surface parameters 2	
Pressure, Mean flow	339.98 mmHg
Full pressure, Mean flow	347.71 mmHg
Dynamic pressure, Mean flow	7.73 mmHg
Velocity, Mean flow	1.337 m/sec
Characteristic pressure, Mean flow	22.41 mmHg
Volume flow rate	–2.7547 L/min

Fig. 2. Particle trajectories at 7000 rpm impeller speed, 2.7 L/min flow and 340 mmHg pressure (ECMO mode)

Fig. 3. a, 3D model of the designed pump; b, model of the designed pump

Experimental study of HCC

The prototype testing was carried out in two sequential phases. The first phase involved validating the HCC derived from closed-loop computational simulations [8, 9]. Constant rotational speed studies were conducted within a circulatory test loop designed to emulate essential physiological elements such as vascular resistance, fluid inertia, and aortic compliance. The pump was driven using a Deltastream drive (Medos, Germany), as illustrated in Fig. 4. Distilled water served as the working fluid. Pump speeds ranging from 3000 to 7000 RPM were sufficient to achieve extracorporeal membrane oxygenation (ECMO) operating conditions. However, when the speed exceeded 8500 RPM, the impeller made

contact with the pump housing due to increased hydraulic lift forces.

In the second phase of testing, a hydrodynamic perfusion bench, described in detail in [10], was assembled. This bench replicates the configuration of an ECMO system and includes the pump, an oxygenator with an integrated heat exchanger, and an additional oxygenator. The latter is connected to a 5% CO_2 gas mixture and functions as a simulated "patient" (see Fig. 5).

For the pump efficiency study, anticoagulated donor blood diluted to a hematocrit of 25% was circulated through the system. This dilution was chosen to meet the minimum circuit volume requirement of approximately 700 mL.

Hemolysis parameters were assessed (N = 4) by calculating the normalized hemolysis index (NIH) using Formula, as described in [4].

Fig. 4. Evaluation of the HCC of the fabricated centrifugal pump head

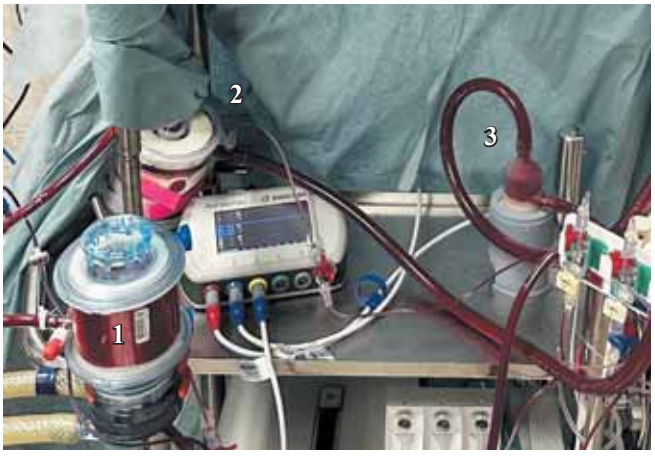

Fig. 5. Evaluation of oxygenating properties and hemolysis in ECMO mode (1, LivaNova oxygenator (INSPIRE, USA); 2, deoxygenator; 3, developed centrifugal pump)

$$\text{N.I.H. g / 100 l} = \Delta\text{freeHb} \times V \times \frac{100 - Ht}{100} \times \frac{100}{Q \times T},$$

where: Δfree Hb – increase in free plasma hemoglobin (g/L) during the sampling interval, V – circuit volume (L), Q – blood flow rate (L/min), Ht – hematocrit (%), T – pump operation time (min).

Throughout the experiment, the temperature of the circulating fluid was maintained at a constant 37.5 °C. The total duration of the tests was 6 hours. Upon completion of the experiments, the pumps were inspected for evidence of clot formation.

RESULTS

The HCC, presented in Fig. 6, demonstrates an agreement between the predicted and experimental results, with a deviation of 2.5 ± 0.5%.

The successful demonstration of the prototype centrifugal pump's operability and efficiency enabled progression to the second stage: a series of studies evaluating oxygenation performance and hemolysis under ECMO conditions. The pump effectively circulated blood through two oxygenators, achieving high levels of oxygen saturation.

The NIH of the pump was measured at 0.001 ± 0.001 g/100 L at the start of the experiment and 0.002 ± 0.001 g/100 L at the end – values that fall within acceptable limits for the given operating conditions. The blood hematocrit decreased from 25 ± 2% to 24 ± 2%, based on averaged data.

DISCUSSION

Calculations and experimental tests of the CP prototype showed a high correlation with the specified medical and technical requirements. Despite its small size, the pump delivers sufficient hydraulic power to achieve a pressure drop of 300–400 mmHg at a flow rate of 5–6 L/min.

The actual pressure drop deviated from theoretical predictions by no more than 3%. The HCC exhibited a banded structure, which is typical for CP performance profiles. In ECMO mode, the rotor operated at 6000–6500 rpm, which is much lower than the operational speed of the clinically used Deltastream pump (Medos, USA) [11].

The developed impeller design effectively minimized vortex formation and eliminated fluid stagnation zones. The calculated average tangential shear stress was approximately 40 Pa, remaining well below the erythrocyte damage threshold of 150 Pa [4]. Given the 500–600 RPM reduction in rotor speed compared to standard clinical devices, hemolysis levels observed in future experiments are expected to remain within acceptable limits.

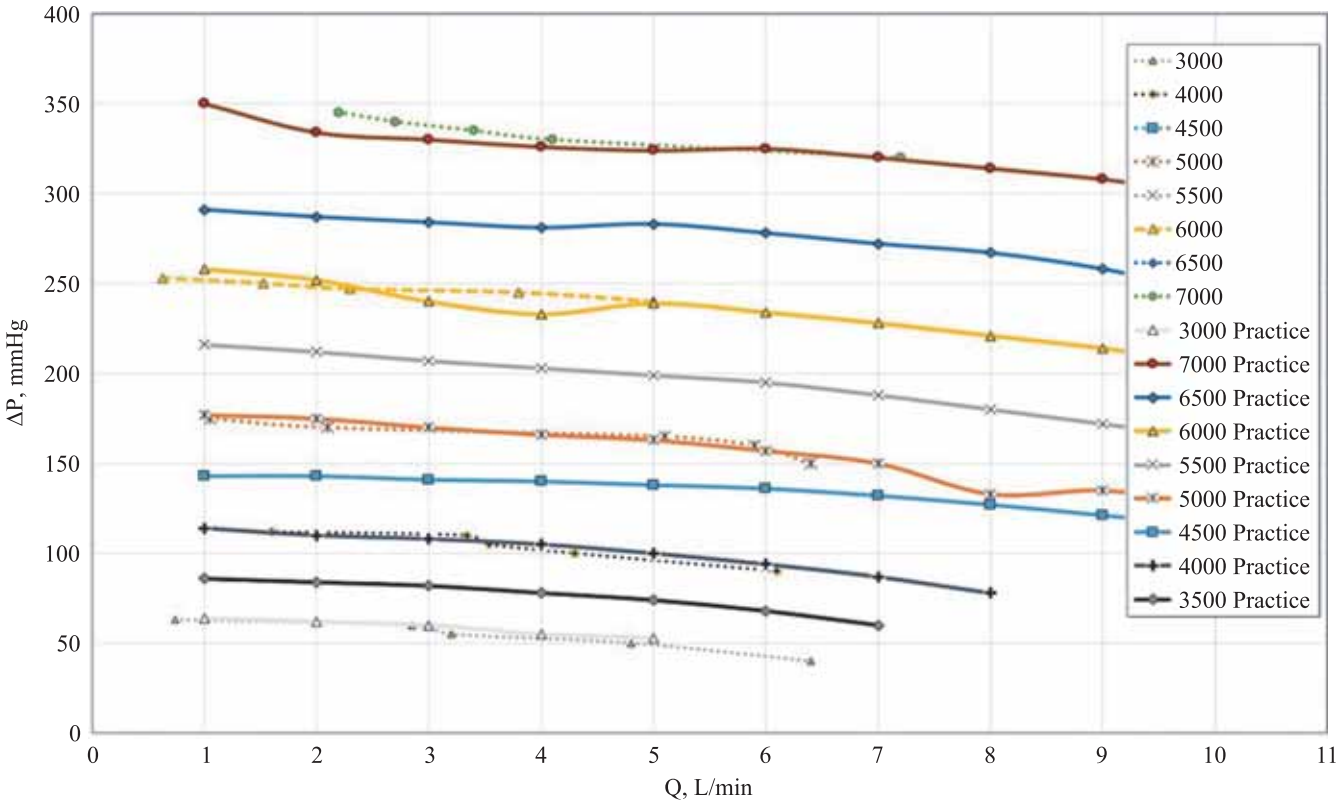

Fig. 6. Head-capacity curve of the pump. Dotted line indicates computer modeling, solid line shows bench test results

The use of straight vanes in the impeller design simplifies the manufacturing process of the pump. Evaluation of the proposed vane configuration showed an increase in head pressure while maintaining consistent fluid velocity throughout the flow path. The HCC of this model also indicates enhanced sensitivity to preload, which contributes to increased pulsatility – particularly beneficial in applications involving oxygenators and small-diameter cannulas.

The inclusion of additional ports proved to be an effective modification, facilitating improved pump flushing and enhancing non-thrombogenic properties without any significant compromise in hydraulic performance. A slight increase in impeller torque – up to 7% – was recorded, corresponding to a reduction in impeller efficiency by the same margin. This decrease is attributed to the presence of recirculation zones, which introduce hydrodynamic losses.

Numerical simulations confirmed elevated flow and velocity on the rear side of the impeller and within the added orifices, with secondary flow rates ranging from 0.3 to 1.0 L/min, depending on the head and flow rate.

In the final design, a closed impeller configuration was selected to minimize internal leakage flow while allowing for a larger operational clearance. During perfusion bench experiments, where the pump was integrated into a simulated ECMO circuit, the device showed good overall biocompatibility and low blood damage over a 6-hour test period (N = 4).

The maximum recorded value of NIH was 0.003 g/100 L, attributed primarily to limitations in the precision of the 3D printing process. No blood clots were observed during or after the experiments. The pump effectively overcame the combined resistance of two oxygenators, which totaled approximately 200 mmHg.

CONCLUSION

The presented results indicate that the developed centrifugal pump prototype exhibits strong potential for use in ECMO systems. Its hydraulic performance meets the requirements for conventional auxiliary circulatory support systems. Future work will focus on rotor optimization, comparative evaluation of alternative designs, development of a low-volume pump variant, and adaptation of the experimental models for production by casting.

The authors declare no conflict of interest.

REFERENCES

1. *Hill JD, O'Brien TG, Murray JJ, Dontigny L, Bramson ML, Osborn JJ, Gerbode F*. Prolonged extracorporeal oxygenation for acute post-traumatic respiratory failure (shock-lung syndrome). Use of the Bramston membrane lung. *N Engl J Med*. 1972; 286 (12): 629–634.
2. *Philipp A, Arlt M, Amann A, Lunz D, Müller T, Hilker M et al.* First experience with the ultra-compact mobile ex-

tracorporeal membrane oxygenationsystem Cardiohelp in interhospital transport. *Interact CardioVasc Thorac Surg*. 2011; 12 (6): 978–981.
3. *Dembinski R, Kopp R, Henzler D, Hochhausen N, Oslender N, Max M et al*. Extracorporeal Gas Exchange with the DeltaStream Rotary Blood Pump in Experimental Lung Injury. *Artif Organs*. 2003; 27 (6): 530–536.
4. *Thamsen B, Blümel B, Schaller J, Paschereit CO, Affeld K, Goubergrits L, Kertzscher U.* Numerical analysis of blood damage potential of the HeartMate II and HeartWare HVAD rotary blood pumps. *Artif Organs*. 2015; 39 (8): 651–659.
5. *Yu H, Janiga G, Thévenin D.* Computational fluid dynamics-based design optimization method for Archimedes screw blood pumps. *Artif Organs*. 2016; 4: 341–352.
6. *Nishida M, Yamane T, Tsukamoto Y, Ito K, Konishi T, Masuzawa T et al.* Shear evaluation by quantitative flow visualization near the casing surface of a centrifugal blood pump. *JSME Int J*. 2002; 45: 981–988.
7. *Kashiwa K, Nishimura T, Saito A, Kubo H, Fukaya A, Tamai H et al.* Left heart bypass support with the Rotaflow Centrifugal Pump® as a bridge to decision and recovery in an adult. *J Artif Organs*. 2012; 15 (2): 207–210.
8. *Kuleshov AP, Itkin GP*. Calculation of the main characteristics of a channel rotor when designing a centrifugal blood pump. *Biomedical Engineering*. 2019; 52: 311–315.
9. *Itkin GP, Bychnev AS, Kuleshov AP, Drobyshev AA.* Haemodynamic evaluation of the new pulsatile-flow generation method *in vitro*. *Int J Artif Organs*. 2020; 43 (3): 157–164.
10. *Rinaudo A, Pasta S*. Development of a self-pumping extracorporeal blood oxygenation device characterized by a rotating shaft withembedded fiber packages. *Int J Artif Organs*. 2020; 43 (6): 393–400.
11. *Gobel C, Arvand A, Eilers R, Marseille O, Bals C, Meyns B et al*. Development of the MEDOS/HIA DeltaStream Extracorporeal Rotary Blood Pump. *Artif Organs*. 2001; 25 (5): 358–365.

The article was submitted to the journal on 14.08.2024

DOI: 10.15825/1995-1191-2024-4-140-148

EFFECT OF PROLONGED CARDIAC GRAFT PRESERVATION ON ADHESION PROTEIN ACTIVATION AND SYNTHETIC ENDOTHELIAL FUNCTION

M.O. Zhulkov[1], N.A. Karmadonova[1], M.A. Surovtseva[1, 2], I.I. Kim[1, 2], O.V. Poveshchenko[1, 2], I.S. Zykov[1], A.R. Tarkova[1], D.A. Sirota[1, 3], A.V. Protopopov[1], A.G. Makaev[1], F.Yu. Kosimov[1], M.N. Murtazaliev[1], A.V. Guseva[1], K.A. Agaeva[1]

[1] Meshalkin National Medical Research Center, Novosibirsk, Russian Federation
[2] Research Institute of Clinical and Experimental Lymphology, Novosibirsk, Russian Federation
[3] Novosibirsk State Medical University, Novosibirsk, Russian Federation

Objective: to conduct a comparative study of the efficacy of Custodiol® cardioplegia (Custodiol HTK, Dr. Franz Köhler Chemie GmbH, Bensheim, Germany) and normothermic autoperfusion of heart graft as a part of an *ex vivo* cardiopulmonary complex (CPC). **Methods.** Landrace pigs weighing 50 ± 5 kg and aged 4–5 months (n = 10) were used as the model for a series of acute experiments. In the experimental group (n = 5), the CPC was conditioned by autoperfusion for 6 hours. In the control group, the heart's pumping function was restored after a 6-hour cold preservation with Custodiol®. The effectiveness of cardiac graft preservation methods was evaluated by measuring myocardial ischemic markers, endothelial synthetic function, and endothelial cell activation markers (E- and P-selectins, endothelial growth factor). **Results.** Following cardiac graft reperfusion, the control group exhibited a statistically significant increase in the concentration of myocardial ischemia markers; also, there was a significant decrease in the synthesis of endothelium-derived relaxing factor in the Custodiol® solution preservation group (378.5 [226.4; 539.7] *vs*. 542.1 [377.6; 853.2] μM/mL in the autoperfusion group, $p < 0.05$). The degree of coronary endothelial reperfusion injury/activation was several times higher in the control group than in the normothermic autoperfusion conditioning group. Moreover, cardiac output after a 6-hour graft conditioning was 0.63 [0.37; 0.80] and 0.37 [0.23; 0.37] L/min in the experimental and control groups, respectively ($p < 0.05$). **Conclusion.** Normothermic autoperfusion showed a significant advantage in preserving the morphofunctional status of the donor heart compared with cold preservation with Custodiol® during 6 hours of *ex vivo* graft conditioning.

Keywords: autoperfusion, heart preservation, normothermic perfusion, reperfusion injury, heart transplantation, cold preservation.

INTRODUCTION

Primary graft dysfunction is the leading cause of death and morbidity in cardiac transplant recipients [1]. Factors such as ischemia time, composition of the preservation solution, and preservation method may contribute to initial endothelial dysfunction and potentially influence long-term endothelial changes, including graft vasculopathy. This has led to an increasing use of myocardial and endothelial markers in both experimental and clinical studies to assess the quality of graft function preservation [2].

One of the inevitable events during the transplant reperfusion phase is the interaction between circulating neutrophils and the coronary endothelium. Endothelial injury represents the primary consequence of reperfusion, initiating a cascade that includes calcium overload in cardiomyocytes (the "calcium paradox"), tissue edema, and generation of reactive oxygen species by neutrophils. This damage begins within 2.5 to 5 minutes after the onset of reperfusion. It involves the initial slowing down or "rolling" of neutrophils along the endothelium, followed by firm adhesion and diapedesis of neutrophils into the myocardium. Once in the tissue, neutrophils interact with cardiomyocytes, leading to cellular necrosis [3].

Leukocyte adhesion to the vascular wall marks the early stage of both the immune and inflammatory responses to reperfusion. In post-ischemic myocardial tissue, neutrophil infiltration significantly impairs cardiac function [4]. Ischemia followed by reperfusion disrupts basal and agonist-stimulated nitric oxide (NO) synthesis [5], a factor known to modulate leukocyte adhesion to the endothelium. Reduced NO availability has been shown to increase leukocyte-endothelial interactions. The onset of reperfusion also triggers a sharp decline in endothelium-derived relaxing factor, alongside a spike in free radical production and P-selectin expression [3, 7].

Anti-adhesion therapy represents a promising new approach to mitigating ischemia-reperfusion injury (IRI).

Corresponding author: Alexander Makaev. Address: 15, Rechkunovskaya str., Novosibirsk, 630055, Russian Federation. Phone: (905) 198-33-31. E-mail: makaev_a@meshalkin.ru

One such strategy involves the use of monoclonal antibodies targeting specific adhesion molecules [8]. These adhesion-blocking antibodies help to reduce the extent of myocardial injury following reperfusion [9]. Although the therapeutic use of such anti-adhesion strategies shows potential for enhancing myocardial and coronary function recovery after cardiac surgery or transplantation, their use remains largely experimental at this stage.

Therefore, the continued investigation and clinical implementation of effective, cost-efficient methods for long-term conditioning of donor hearts is essential. Such advancements not only have the potential to expand the geographic scope of donor organ availability, thereby increasing transplant opportunities, but also to significantly improve long-term outcomes by reducing the incidence of graft vasculopathy.

MATERIALS AND METHODS

Landrace pigs (females), weighing 550 ± 5 kg and aged 4–5 months (n = 10), were used as the animal model for this series of experiments. Animal care, experimental procedures, monitoring, and euthanasia were conducted in accordance with the European Convention for the Protection of Vertebrate Animals Used for Experimental and Other Scientific Purposes (Strasbourg, March 18, 1986). The study was approved by the local bioethics committee (Protocol No. 2, dated September 1, 2022).

In the experimental group (n = 5), heart conditioning was performed using a 6-hour normothermic autoperfusion of the cardiopulmonary complex (CPC) *ex vivo*, followed by 1 hour of cold cardioplegia with Custodiol® HTK solution at 4 °C, and subsequent reperfusion via a circulatory assist device. The control group (n = 5) consisted of hearts preserved for 6 hours using standard cold cardioplegia with Custodiol® HTK solution, following conventional protocols (Fig. 1).

Preoperative preparation and anesthesia

On the day of the experiment, all animals were premedicated with Zoletil® 100, administered on an empty stomach. The dosage was individually adjusted based on the animal's weight and body size. Once anesthesia was induced, the surgical field and the neck area for vascular catheterization were prepared. The animal was then transferred to the operating table and positioned supine for tracheal intubation and placement of central arterial and venous catheters.

The procedures were performed under endotracheal anesthesia using sevoflurane and muscle relaxation with rocuronium bromide. Mechanical ventilation was delivered via a Fabius® Plus anesthesia-breathing workstation (Dräger, Germany) with inspiratory positive pressure of 20–30 cm H_2O, expiratory pressure of 5–8 cm H_2O, tidal volume of 8 ml/kg, and a respiratory rate of 12–14 breaths per minute.

Physiological parameters were continuously monitored using the IntelliVue MP70 patient monitor (Philips, Netherlands). During the procedure, we recorded invasive blood pressure within the heart chambers and major vessels, electrocardiographic data for arrhythmia detection, and core temperature of the organ complex.

Hematological parameters were assessed using an ABL 800 FLEX automatic blood analyzer (Radiometer, Denmark), in accordance with the manufacturer's instructions. Central hemodynamic monitoring was conducted via right heart catheterization using a Swan–Ganz catheter, complemented by a portable multifunctional ultrasound system (Philips CX50, Philips Ultrasound, USA) with ECG synchronization.

Coronary vascular resistance (CVR) was calculated using the following formula:

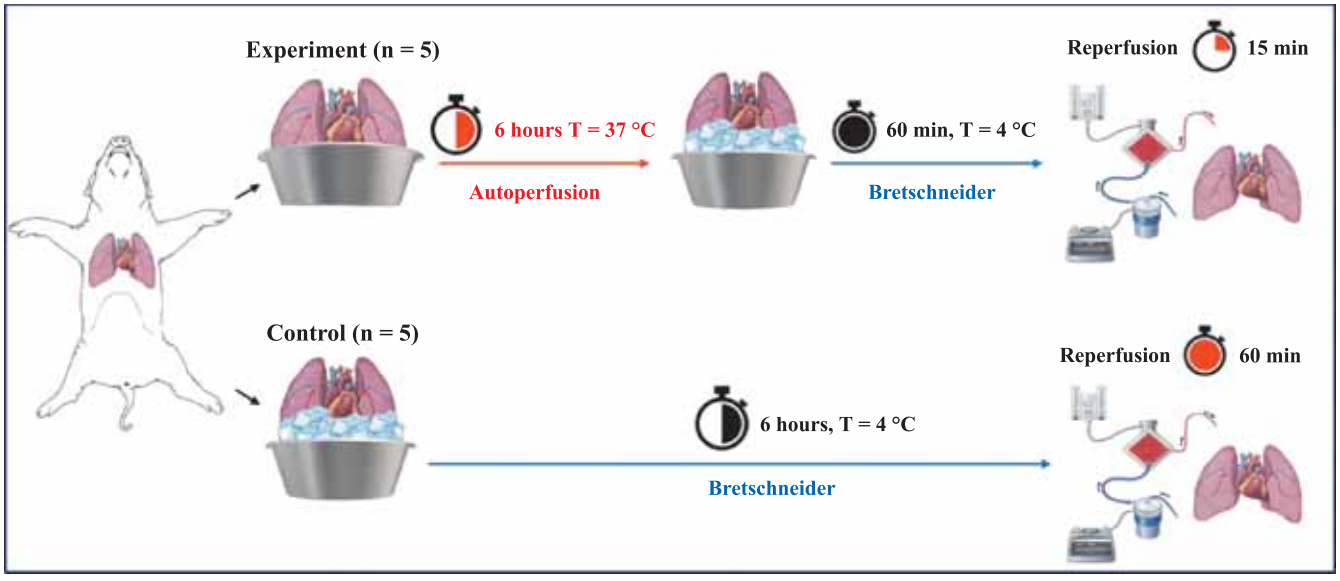

Fig. 1. Study design

$$CVR = \frac{mAP - mRAP}{CBF \times 100\ g},$$

where, mAP – mean aortic pressure, mRAP – mean right atrial pressure, and CBF – coronary blood flow.

Surgical technique for the experiment

A functional CPC was procured through midline sternotomy. Isolation of the CPC was started with removal of the pericardium and mobilization of the superior vena cava (SVC), then the brachiocephalic trunk (BCT), left subclavian artery (LSA), inferior vena cava (IVC) were isolated. The trachea was carefully separated from the esophagus using an electrocoagulator, achieving hemostasis. After heparin (3 mg/kg body weight) had been administered, the LSA was ligated as distally as possible, and an introducer was placed through the arterial stump to measure the aortic pressure and to guide diagnostic catheters. Then, the BCT was ligated and crossed, and an 18 Fr arterial cannula was inserted into the arterial stump and connected to the arterial reservoir. After clamping the descending thoracic aorta at the isthmus level, the arterial trunk was opened, and arterial blood was drawn into the reservoir. After blood level and arterial pressure were stabilized, 1–1.5 liters of Ringer's solution was injected into the femoral vein. After that, the vena cava was ligated and crossed, the trachea was crossed and reintubated with a cuffed tube. The functioning CPC was finally separated from the surrounding tissues, transferred to a container with warm saline (38 °C), the arterial trunk was clamped, and observation was continued for 6 hours (Fig. 2).

Throughout the autoperfusion period, a continuous infusion of 5% calcium chloride solution (3–5 mL/hour) and 10% glucose (5–10 mL/hour) was administered to maintain electrolyte and glucose levels within the physiological reference range. After 6 hours of normothermic autoperfusion of the CPC, cardioplegia was induced by injecting 2 liters of Custodiol® solution (Custodiol® HTK, Germany) into the aortic root. The CPC was subsequently stored in Custodiol® solution at 4 °C for 1 hour.

After cold storage, the heart was reperfused for 15–20 minutes using a cardiopulmonary bypass (CPB) machine primed with the animal's autologous blood. Electrical defibrillation was performed as needed. Once normothermia and spontaneous cardiac activity were restored, the CPC was filled with blood, isolated, and assessed via ultrasound imaging.

Tissue samples for histological examination were collected from the apex of the left ventricle and the middle lobes of the left and right lungs. Samples were fixed in 10% neutral buffered formalin, dehydrated through a graded series of ethanol solutions (increasing alcohol

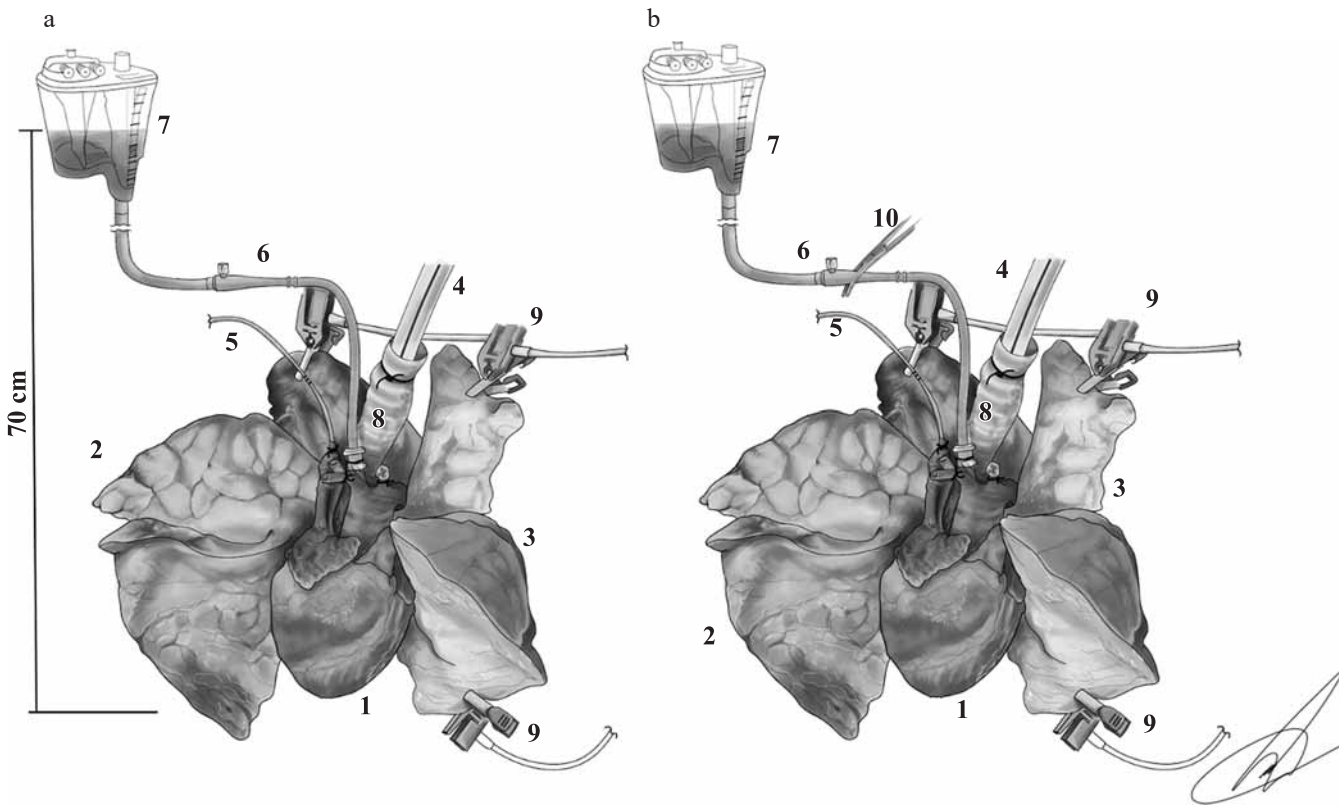

Fig. 2. Diagram of the isolated cardiopulmonary complex: a, stage of blood exfusion into the reservoir and preparation for transfer of the complex into a container; b, stage of final hemodynamic isolation of the cardiopulmonary complex; 1 – heart, 2 – right lung, 3 – left lung, 4 – intubation tube, 5 – Swan–Ganz catheter, 6 – arterial cannula, 7 – blood tank, 8 – trachea, 9 – electrocardiograph electrodes, 10 – clamp

by volume, ABV), and embedded in paraffin using a dispenser with integrated heating and cooling plates. Histological sections, 4–5 μm thick, were cut from paraffin blocks using a Microm HM 550 microtome (Thermo Scientific, Waltham, USA).

Prior to staining, the sections were deparaffinized in two changes of pure xylene for 10–15 minutes, then rehydrated through a graded series of ethanol (decreasing ABV, absolute to 70%) and finally rinsed in distilled water. Standard histological stains were applied, including hematoxylin and eosin, Van Gieson's stain with orcein for elastic fibers, and the periodic acid–Schiff (PAS) reaction.

Polarized light microscopy of the myocardium was performed using an Axio Scope.A1 microscope (Zeiss, Germany), equipped with an analyzer and polarizer, AxioCam HRm and HRc cameras (Zeiss, Germany), and ZEN Blue imaging software (Zeiss, Germany).

To prepare the extracts, left ventricular myocardial tissue was weighed, minced, and suspended in 1 mL of PBS, then stored at –70 °C. Samples were homogenized using a KZ-III-FP low-temperature tissue homogenizer (Servicebio Technology Co., Wuhan, China) at –40 °C with 3 mm ×2 and 4 mm ×1 steel balls, following the manufacturer's instructions. levels were centrifuged at 16,100×g for 5 minutes to remove tissue debris. Vascular endothelial growth factor (VEGF) and NO concentrations in tissue extracts were normalized to the total protein content of each sample. VEGF levels were quantified using a commercial ELISA kit (Vector-BEST, Novosibirsk, Russia), and NO levels were determined by measuring nitrite levels, a stable end product, using the Griess reagent (Sigma-Aldrich, Darmstadt, Germany), per the manufacturer's protocol. Briefly, 50 μL of tissue extract was mixed with 50 μL of Griess reagent in a 96-well plate, and absorbance was measured at 492 nm using a Stat FAX-2100 microplate reader (Awareness Technology Inc., USA). Nitrite levels were calculated from a standard calibration curve.

Serum troponin I was measured using a chemiluminescent immunoassay with ARCHITECT STAT Troponin-I reagents on the Architect i2000SR analyzer (Abbott, USA). To assess serum levels of troponin T, heart-type fatty acid-binding protein (H-FABP), E-selectin (SelE), and P-selectin (SelP), blood samples were centrifuged at 1,000×g for 20 minutes. Serum was aliquoted and stored at –80 °C until analysis. These biomarkers were quantified using sandwich ELISA kits (Cloud-Clone Corp., China) specific to swine antigens.

Statistical analysis was performed using Statistica 10.0 software (StatSoft Inc., USA). Descriptive statistics were applied to summarize the data. The significance of differences between groups was evaluated using the nonparametric Mann–Whitney U test for independent groups and the Wilcoxon signed-rank test for dependent groups. A p-value of less than 0.05 was considered statistically significant, in accordance with standard criteria for biomedical research.

RESULTS

In all experiments, graft reperfusion was performed using a CPB machine, maintaining consistent perfusion parameters (300–350 ml/min). However, by the 15th minute, a significant increase in aortic pressure and vascular resistance was observed in all hearts from the control group (Table 1).

At the same time, in all experiments within the control group, restoration of heart rhythm required multiple electrical defibrillation attempts (up to 10 discharges), followed by electrical cardiac stimulation. The reperfusion time required to wean the CPC from CPB, while maintaining an aortic root pressure of no less than 60 mmHg independently, was 87 [67; 102] minutes in the control group, compared to 19 [17.5; 22.5] minutes in the experimental group ($p < 0.05$).

The degree of ischemia and the effectiveness of the conditioning technique were assessed by measuring the levels of lactate, troponin I, troponin T, and H-FABP in

Table 1

Main hemodynamic parameters

Parameter \ Group	Control (n = 5)		Experimental (n = 5)		
	Before preservation	After reperfusion	T1	T6	After reperfusion
CO (L/min)	0.83 [0.74; 1.86]	0.37* [0.23; 0.37]	0.84 [0.78; 0.94]	0.57 [0.26; 0.88]	0.63# [0.37; 0.8]
HR (bpm)	96 [86; 105]	100 (ЭКС)	87 [78; 96]	98 [83; 116]	100 (ЭКС)
iABP (mmHg)	110 [75; 130]	162* [158; 210]	115 [65; 134]	112 [57; 128]	108 [84; 137]
CVR (mmHg·min/mL/100 g)	5.4 [4.2; 7.6]	13.9* [9.6; 15.8]	6.3 [5.3; 8.7]	7.1 [6.1; 10.3]	8.8# [5.3; 10.7]

Note. Data are presented as Me [Q1; Q3]. CO, cardiac output; HR, heart rate; iABP, invasive arterial blood pressure (aortic root); CVR, coronary vascular resistance; T1, 1st hour of autoperfusion; T6, 6th hour of autoperfusion; *, $p < 0.05$ compared with baseline (before preservation); #, $p < 0.05$ compared with control group after reperfusion.

Table 2

Myocardial ischemic markers

Indicator \ Group	Control (n = 5)		Experimental (n = 5)		
	Before preservation	After reperfusion	T1	T6	After reperfusion
Lactate (mmol/L)	3.3 [2.2; 4.5]	11.8* [10.1; 13.5]	5.8 [5.1; 6.7]	5.3 [4.7; 5.9]	7.1# [6.3; 8.4]
Troponin I (nmol/L)	175.84 [57.7; 309.9]	317,803.98* [44,509.9; 500,000.0]	144.8 [87.5; 187.7]	–	126,069*# [42,437.5; 141,583.1]
Troponin T (nmol/L)	0	988* [648; 1815.5]	0	442* [86.3; 881]	104.5*# [55.3; 344.3]
H-FABP (pg/mL)	0.2 [0.02; 1.1]	2.1* [0.1; 2.1]	0	0	0

Note. Data are presented as Me [Q1; Q3]; H-FABP, heart-type fatty acid-binding protein; T1, 1st hour of autoperfusion; T6, 6th hour of autoperfusion; *, $p < 0.05$ *vs.* baseline (before preservation); #, $p < 0.05$ *vs.* control group after reperfusion.

Table 3

Results of the study of myocardial extracts from the left ventricle of the heart

Indicator \ Group	Control (n = 5)		Experimental (n = 5)		
	Before preservation	After reperfusion	T1	Before preservation	After reperfusion
NO (μM/mL)	524.3 [335.1; 733.2]	378.5* [226.4; 539.7]	626.8 [566.5; 1288.5]	593.1 [442.8; 1003.8]	542.1# [377.6; 853.2]
VEGF (pg/mL)	701.8 [397.3; 1034.2]	978.1 [732.8; 1265.7]	742.3 [464.2; 1152.1]	789.3 [465.2; 1115.1]	777.8 [407.6; 1140.8]
SelE (ng/mL)	0.3 [0.05; 2.3]	4.4* [0.3; 8.1]	0	0.2 [0.1; 0.4]	0.2# [0.05; 0.2]
SelP (ng/mL)	1.8 [0.9; 2.6]	5.6* [2.8; 9.1]	1.3 [0.8; 1.8]	1.6 [1.1; 2.1]	2.4# [1.2; 3.2]

Note. Data are presented as Me [Q1; Q3]; NO, endothelium-derived relaxing factor; VEGF, vascular endothelial growth factor; SelE, selectin E; SelP, selectin P; T1, 1st hour of autoperfusion; T6, 6th hour of autoperfusion; *, $p < 0.05$ *vs.* baseline (before preservation); #, $p < 0.05$ *vs.* control group after reperfusion.

the blood flowing from the coronary sinus (Table 2). The control group showed statistically significant increases in lactate, troponin I, and troponin T levels following the reperfusion phase and restoration of cardiac function, compared to the autoperfusion group (Table 2).

The preservation of synthetic endothelial function was assessed by measuring the levels of endothelium-derived vasorelaxing factor (NO), endothelial growth factor (VEGF), and adhesion molecules E- and P-selectins (Table 3).

The study revealed that after 6 hours of preservation with Custodiol® solution, NO levels were significantly lower compared to the normothermic autoperfusion group (378.5 μM/mL *vs.* 542.1 μM/mL, respectively, $p < 0.05$). Additionally, the concentrations of adhesion molecules (E- and P-selectins) were significantly higher in the Custodiol® group compared to the autoperfusion group (4.4 ng/mL *vs.* 0.2 ng/mL for E-selectin and 5.6 ng/mL *vs.* 2.4 ng/mL for P-selectin, respectively, $p < 0.05$).

DISCUSSION

Myocardial reperfusion injury is primarily an iatrogenic phenomenon. A clear cause-and-effect relationship has been established between the degree of endothelial injury and post-ischemic contractile dysfunction in heart transplants [10]. Despite cold cardioplegia being the standard for donor organ preservation, graft function can deteriorate after four hours, particularly in organs from older donors [11]. This organ preservation method remains the leading risk factor for primary allograft dysfunction and mortality [12].

Despite the numerous benefits of *ex vivo* machine warm perfusion, this technology has not been widely adopted in most transplant centers over recent decades. The primary barrier is the high cost of such systems, which hinders their broader implementation in clinical practice [13]. However, evidence suggests that normothermic autoperfusion, as a method of prolonged *ex vivo* normothermic conditioning, is superior to static cold preservation [14]. Unlike machine perfusion techniques, autoperfusion of the donor heart provides optimal conditions for oxygen and energy substrate delivery to the graft, while preserving coronary blood flow's vasomotor autoregulation without subjecting the endothelial layer to excessive shear stress [15].

Recent studies have shown that reperfusion injury involves various components of the inflammatory response, with leukocyte-endothelial interactions playing a

central role [16]. The initial interaction between leukocytes and the endothelium triggers the subsequent pathophysiological stages of reperfusion injury – adhesion and migration of neutrophils across the endothelial barrier. Once in close proximity to cardiomyocytes, neutrophils release numerous cytotoxic factors that can lead to myocyte necrosis. The process of leukocyte adhesion to the endothelium begins with rolling along the endothelial surface, a process mediated by the release of adhesion molecules [17]. In the present study, it was demonstrated that 6-hour preservation of cardiac grafts with Custodiol® solution resulted in a significant increase in P-selectin levels compared to normothermic conditioning under autoperfusion conditions. The study of P-selectin is particularly significant because its expression is believed to play a critical role in leukocyte rolling and adhesion to the graft's endothelium [18].

Another reason for the interest in studying the expression of adhesion molecules and endothelial function is the high incidence of graft vasculopathy and the lack of effective treatment for this complication. Previous studies have shown that the intensity of arterial intimal thickening correlates with expression of P-selectin and vascular cell adhesion molecule-1 on endothelial cells in a rat model of chronic heart allograft rejection [19]. Administration of antibodies against P-selectin during reperfusion has been shown to reduce infarct size, decrease leukocyte adhesion to the coronary endothelium, and promote endothelial preservation [20]. Of particular interest are studies that have demonstrated P-selectin expression activation when isolated hearts were subjected to continuous perfusion with a blood-based perfusate [10].

These findings suggest that P-selectin release may not only indicate ischemia and reperfusion (where reperfusion acts as a rapid trigger for increased P-selectin expression) but could also be a general consequence of continuous perfusion through an extracorporeal circulation circuit. Interestingly, prior studies have shown that perfusion of rat hearts with crystalloid solution without an extracorporeal circulation circuit did not result in increased P-selectin levels [19]. In our study, we also observed increased P-selectin expression in the autoperfusion group after cardiac recovery using an extracorporeal circulation circuit. However, despite a twofold increase in P-selectin expression post-reperfusion compared to initial values, these changes were not statistically significant ($p > 0.05$). Similar results were observed for E-selectin expression, which was significantly increased in the control group, suggesting a higher degree of endothelial reperfusion injury in the control group compared to the autoperfusion group.

Another biomarker for myocardial ischemic injury is H-FABP, which plays a role in cellular fatty acid metabolism by reversibly binding and transporting long-chain polyunsaturated fatty acids from cell membranes to mitochondria. Plasma H-FABP levels begin to rise within 1 hour after myocardial ischemia, peak at 4–6 hours, and return to baseline within 24 hours [7]. In the present study, a statistically significant increase in H-FABP levels was observed in the control group compared to the autoperfusion group. There was no increase in H-FABP in the autoperfusion group, even after 6 hours of *ex vivo* cardiac conditioning, 60 minutes of cold ischemia, and reperfusion. This suggests the high efficiency of autoperfusion as a method for prolonged protection of the donor heart. Similar results were observed for lactate, troponin I, and troponin T levels in the blood flowing from the coronary sinus, highlighting the insufficient efficiency of Custodiol® solution for prolonged (6 hours) cardiac graft preservation. However, further research is needed to explore the predictive value of biomarkers of myocardial injury and endothelial dysfunction in determining the functional outcomes of transplantation.

CONCLUSION

Prolonged normothermic autoperfusion of a cardiac graft, compared to static cold preservation with Custodiol®, can better maintain the physiological conditions of the coronary endothelium and promote the synthesis of regulatory agents by endothelial cells. This, in turn, reduces the severity of IRI. The findings suggest that this method of long-term conditioning for cardiac transplants has significant potential in preventing vasculopathy.

This study was conducted as part of the project No. 23-25-10013, under Agreement No. 23-25-10013 dated April 20, 2023 with the Russian Science Foundation and Agreement No. p-52 dated April 03, 2023 with the Ministry of Science and Innovation Policy, Novosibirsk Oblast, Russian Federation.

The authors declare no conflict of interest.

REFERENCES

1. *Hosenpud JD, Bennett LE, Keck BM, Fiol B, Boucek MM, Novick RJ*. The Registry of the International Society for Heart and Lung Transplantation: sixteenth official report – 1999. *J Heart Lung Transplant*. 1999 Jul; 18 (7): 611–626.
2. *Stoica SC, Goddard M, Large SR*. The endothelium in clinical cardiac transplantation. *Ann Thorac Surg*. 2002 Mar; 73 (3): 1002–1008.
3. *Tsao PS, Aoki N, Lefer DJ, Johnson G 3rd, Lefer AM*. Time course of endothelial dysfunction and myocardial injury during myocardial ischemia and reperfusion in the cat. *Circulation*. 1990 Oct; 82 (4): 1402–1412.
4. *Kupatt C, Habazettl H, Zahler S, Weber C, Becker BF, Messmer K, Gerlach E*. ACE-inhibition prevents postischemic coronary leukocyte adhesion and leukocyte-dependent reperfusion injury. *Cardiovasc Res*. 1997 Dec; 36 (3): 386–395.
5. *Ma XL, Weyrich AS, Lefer DJ, Lefer AM.* Diminished basal nitric oxide release after myocardial ischemia and

reperfusion promotes neutrophil adherence to coronary endothelium. *Circ Res*. 1993 Feb; 72 (2): 403–412.
6. *Kubes P, Suzuki M, Granger DN*. Nitric oxide: an endogenous modulator of leukocyte adhesion. *Proc Natl Acad Sci USA*. 1991 Jun 1; 88 (11): 4651–4655.
7. *Patel KD, Zimmerman GA, Prescott SM, McEver RP, McIntyre TM.* Oxygen radicals induce human endothelial cells to express GMP-140 and bind neutrophils. *J Cell Biol*. 1991 Feb; 112 (4): 749–759.
8. *Boyle EM Jr, Pohlman TH, Cornejo CJ, Verrier ED.* Endothelial cell injury in cardiovascular surgery: ischemia-reperfusion. *Ann Thorac Surg*. 1996 Dec; 62 (6): 1868–1875.
9. *Forbess JM, Hiramatsu T, Nomura F, Miura T, Farrington GK, Sokolowski K et al.* Anti-CD11b monoclonal antibody improves myocardial function after six hours of hypothermic storage. *Ann Thorac Surg*. 1995 Nov; 60 (5): 1238–1244.
10. *Lefer AM, Tsao PS, Lefer DJ, Ma XL.* Role of endothelial dysfunction in the pathogenesis of reperfusion injury after myocardial ischemia. *FASEB J*. 1991 Apr; 5 (7): 2029–2034.
11. *Costanzo MR, Dipchand A, Starling R, Anderson A, Chan M, Desai S et al.* The International Society of Heart and Lung Transplantation Guidelines for the care of heart transplant recipients. *J Heart Lung Transplant*. 2010 Aug; 29 (8): 914–956.
12. *Banner NR, Thomas HL, Curnow E, Hussey JC, Rogers CA, Bonser RS et al.* The importance of cold and warm cardiac ischemia for survival after heart transplantation. *Transplantation*. 2008 Aug 27; 86 (4): 542–547.
13. *Pettit SJ, Petrie MC*. Transplantation of Hearts Donated After Circulatory-Determined Death. *Circ Heart Fail*. 2019 Apr; 12 (4): e005991.
14. *Tarkova AR, Zykov IS, Zhulkov MO, Protopopov AV, Smirnov YaM, Makaev AG et al.* Normothermic *ex vivo* heart and lung autoperfusion: assessment of functional status and metabolism. *Russian Journal of Transplantology and Artificial Organs.* 2023; 25 (4): 150–159.
15. *Zhulkov MO, Tarkova AR, Zykov IS, Makaev AG, Protopopov AV, Murtazaliyev MN et al.* Long-term normothermic autoperfusion of the cardiopulmonary complex *ex vivo* as a method of effective graft conditioning: an experimental study. *Circulatory pathology and cardiac surgery*. 2023; 27 (4): 33–42.
16. *Zhou M, Yu Y, Luo X, Wang J, Lan X, Liu P et al.* Myocardial Ischemia-Reperfusion Injury: Therapeutics from a Mitochondria-Centric Perspective. *Cardiology*. 2021; 146 (6): 781–792.
17. *Lasky LA*. Selectin-carbohydrate interactions and the initiation of the inflammatory response. *Annu Rev Biochem*. 1995; 64: 113–139.
18. Cell adhesion molecules: selectins and integrins – PubMed [Electronic resource]. URL: https://pubmed.ncbi.nlm.nih.gov/10647744/ (accessed: 18.01.2024).
19. *Koskinen PK, Lemström KB*. Adhesion molecule P-selectin and vascular cell adhesion molecule-1 in enhanced heart allograft arteriosclerosis in the rat. *Circulation*. 1997 Jan 7; 95 (1): 191–196.
20. *Weyrich AS, Ma XY, Lefer DJ, Albertine KH, Lefer AM. In vivo* neutralization of P-selectin protects feline heart and endothelium in myocardial ischemia and reperfusion injury. *J Clin Invest*. 1993 Jun; 91 (6): 2620–2629.

The article was submitted to the journal on 02.03.2024

DOI: 10.15825/1995-1191-2024-4-149-156

MODERN EXTRACORPOREAL CIRCULATORY SUPPORT SYSTEMS (CENTRIFUGAL PUMPS AND OXYGENATORS). LITERATURE REVIEW

O.Yu. Esipova[1], A.P. Kuleshov[1], V.K. Bogdanov[1], A.S. Esipov[2], N.V. Grudinin[1]

[1] Shumakov National Medical Research Center of Transplantology and Artificial Organs, Moscow, Russian Federation

[2] National Medical Research Center for High Medical Technologies, Krasnogorsk, Russian Federation

For more than 70 years, short-term mechanical circulatory support devices, as well as methods and skills for their implantation, have been continuously developed and improved. An in-depth study of each of the existing devices is important not only to optimize patient outcomes, but also to create a safer, more effective, smaller-sized new device. This review considers existing temporary circulatory support devices, as well as oxygenators, that supplement the system to protect lung function. Their main technical characteristics and the peculiarities of their application in clinical practice are given. Based on the literature review, we formulated the main directions of extracorporeal membrane oxygenation evolution in Russia.

Keywords: mechanical circulatory support, centrifugal pump, oxygenator, ECMO.

INTRODUCTION

Modern transplantology has greatly improved the treatment of critically ill patients by using innovative pharmacological therapies and advanced medical devices, allowing for organ support or replacement. Among these technologies, extracorporeal membrane oxygenation (ECMO) systems have emerged as a key intervention [1–3]. Currently, ECMO is a highly effective modality for managing acute cardiac and respiratory failure, serving both as a life-sustaining bridge to heart or lung transplantation.

Originally introduced as an experimental physiological technique, ECMO has evolved into a critical clinical tool. It plays a pivotal role in determining whether organ function can be restored or if definitive treatment through transplantation is necessary [4–10].

ECMO involves the cannulation of major blood vessels to connect the patient to an extracorporeal circuit, which includes essential components necessary for its function: cannulas, an oxygenator, and an extracorporeal pump. Oxygenators serve a dual role – oxygenating the blood and removing carbon dioxide [11–13]. Variations among oxygenators are primarily based on their structural design, priming volume, membrane gas exchange properties, and the pressure required to maintain a blood flow rate of 1–5 L/min to achieve adequate oxygenation. Extracorporeal pumps are responsible for generating the necessary pressure and flow within the circuit. In most modern ECMO systems, centrifugal pumps are employed due to their favorable performance characteristics [14, 15].

This review article highlights key advancements in the development and clinical application of the two primary components of an ECMO system: blood pumps and oxygenators.

EXTRACORPOREAL PUMPS FOR ECMO SYSTEM

Centrifugal pumps are a critical component of the extracorporeal circuit in ECMO systems. They are responsible for maintaining the patient's hemodynamic stability during a procedure by operating at predetermined parameters. These pumps can effectively compensate for circulatory insufficiency or partially substitute the heart's pumping function. They facilitate blood flow through the membrane oxygenator, enabling gas exchange by supplying oxygen and removing carbon dioxide, thus temporarily replacing pulmonary function.

Maquet Rotaflow (Maquet, Getinge Group, Germany)

The Maquet Rotaflow is a centrifugal pump (CP) specifically engineered to deliver continuous blood flow for the purpose of maintaining or replacing the pumping function of the heart (Fig. 1) [16–19]. In addition to

Fig. 1. Appearance of Maquet Rotaflow

Corresponding author: Olga Esipova. Address: 1, Shchukinskaya str., Moscow, 123182, Russian Federation. Phone: (925) 190-96-14. E-mail: olgadmitrieva2008@yandex.ru

the centrifugal pump, a continuous life support (PLT) system has been developed to provide both cardiac and respiratory support. The system is capable of generating blood flow rates ranging from 0.5 to 7 L/min. The PLT circuit is designed with a minimal number of primary components to reduce shear stress and turbulence.

The system features a 3 mm diameter, precision ball-bearing, low-friction aluminum oxide pump that drives a 4-blade impeller. The pump head is designed to utilize the potential of a radial magnetic drive. The system is automatic but can be manually started in the event of a failure.

The pump fill volume is 32 mL. The inlet and outlet cannulas are 3/8" in diameter; however, the system has been used in neonates and infants using special adapters to fit 1/4" size. The PLS kit includes a highly plasma-resistant polymethylpentene Quadrox iD oxygenator approved for continuous use for 14 days (shown in Fig. 2).

This system integrates an oxygenator and pump to deliver continuous extracorporeal circulatory support for up to 30 days. It features 3/8" inlet and outlet connectors and is capable of providing flow rates up to 7 L/min. These components are coated with biocompatible BIO-LINE or SOFTLINE materials (heparin-free) [20]. The oxygenator is designed with a distinctive membrane fiber arrangement that optimizes interaction with blood flow.

Fig. 2. Oxygenator Quadrox iD

Fig. 3. Extracorporeal head for the Medos Deltastream DP3 pump

Medos Deltastream DP3 Pump (XENIOS AG, Germany)

The Medos Deltastream DP3 is an ECMO pump approved for medium-term use of up to 14 days [21–24]. It is a diagonal flow pump that combines features of both centrifugal and axial pumps (Fig. 3). The DP3 is equipped with 3/8" and 1/4" inlet and outlet connectors, has a priming volume of 16 mL, and can generate flow rates of up to 8 L/min.

Flow rates vary by cannula size: up to 8 L/min with a 3/8" outlet and up to 2.4 L/min with a 1/4" outlet. The pump speed is adjustable between 100 and 10,000 rpm. A zero flow mode enables rapid shutdown by reducing the speed to prevent backflow. The system incorporates a ceramic bearing and magnetic clutch, and includes an optional pulsation mode adjustable between 40 and 90 wpm. The DP3 cannot be manually restarted; however, in the event of a failure, the portable console (weighing up to 10 pounds) is equipped with two 90-minute power batteries, ensuring temporary support during power or system failures. Additionally, the manufacturer offers a range of compatible adult and pediatric oxygenators.

CentriMag/PediVas (Abbott, USA)

The CentriMag and PediVAS are magnetically levitated centrifugal pumps designed to provide extracorporeal support for adult and pediatric patients, respectively [25–30]. The PediVAS system is suitable for use in both neonates and infants. It has a low priming volume of 14 mL, in contrast to the CentriMag's 31 mL (Fig. 4).

The inlet and outlet cannula diameters are 1/4" for the PediVAS and 3/8" for the CentriMag. Owing to differences in impeller design, the PediVAS can deliver flow rates of up to 1.7 L/min at 5500 rpm, while the CentriMag can reach up to 9.9 L/min at the same speed. This corresponds to a maximum working pressure of 540 mmHg for the PediVAS and 600 mmHg for the CentriMag.

Both devices are FDA-approved for up to 30 days of use for ECMO and ventricular assist applications. The PediVAS and CentriMag pump heads are compatible with the same console and system components (Fig. 5).

These CPs are magnetically levitated and operate without bearings, eliminating contact between the impeller and the housing. This design minimizes friction and heat generation, thereby reducing the risk of hemolysis and thrombosis. The motor is passively cooled through ambient-temperature convective airflow.

Medtronic Pumps (Medtronic Inc., USA)

Medtronic centrifugal pumps – specifically the Adult BPX-80 and Pediatric BP-50 – have been extensively used in open-heart surgery procedures [31–35]. These

Fig. 4. a, CentriMag centrifugal pump; b, PediVas centrifugal pump

Fig. 5. CentriMag drive system

pumps are available in two configurations: the BPX-80, with a priming volume of 80 mL for adult use, and the BP-50, with a 48 mL priming volume for pediatric patients. Both models feature a smooth vortex cone design (Fig. 6).

Both pumps are intended for short-term use. The BPX-80 features 3/8” inlet and outlet cannulae and can deliver flow rates of up to 8 L/min. The pediatric BP-50 pump provides flow rates of up to 1.5 L/min. These pumps are compatible with the Carmeda heparin-coated extracorporeal circuit (Carmeda AB, Sweden), which is designed to enhance biocompatibility.

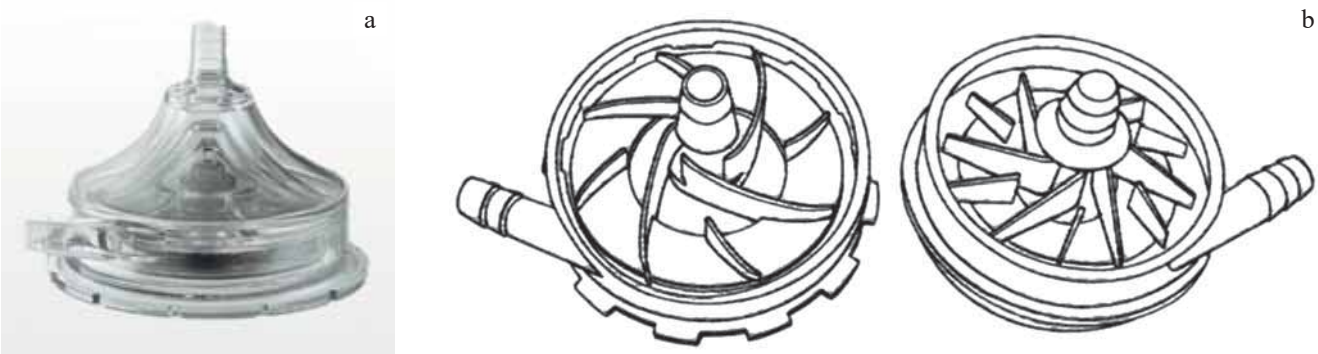

Fig. 6. a, BPX-80 centrifugal pump for adult patients; b, BP-50 centrifugal pump for pediatric patients

Fig. 7. a, Affinity centrifugal blood pump; b, Medtronic Bio-Console for pump control

The Affinity centrifugal blood pump (AP40), a second-generation model of the BPX-80, offers a reduced priming volume of 40 mL. It incorporates a smooth cone and low-profile fins optimized for minimizing hemolysis (Fig. 7, a). This pump is compatible with the Medtronic Bio-Console and includes a new remote actuator for impeller speed control (Fig. 7, b).

The Affinity centrifugal pump provides blood flow rates of up to 10 L/min at lower rotational speeds compared to earlier Medtronic models. Its design minimizes heat generation by reducing friction from moving components and ceramic spherical bearings. This pump

has shown low hemolysis, with less than 0.1 grams of hemoglobin released per 100 L of blood at a flow rate of 5 L/min [36].

Fig. 8. a, LivaNova Revolution centrifugal blood pump; b, Specialized pump control console

LivaNova Revolution (Sorin Group, UK)

The LivaNova Revolution is another centrifugal pump, featuring a priming volume of 57 mL and 3/8" inlet and outlet connectors (Fig. 8, a) [37]. It is operated via a specialized console and is fully integrated with the Sorin LivaNova control system (Fig. 8, b).

The open impeller design of the LivaNova Revolution pump facilitates easy priming and de-airing. Its housing features an injection-molded nylon magnet impregnated with ferromagnetic particles, enhancing the pump's durability. The LivaNova system can deliver flow rates of up to 8 L/min. The Revolution 5 centrifugal pump received FDA approval for use in ECMO systems for durations of up to 5 days.

Oxygenators for the ECMO system

A variety of oxygenators are currently available for both adult and pediatric ECMO systems. The key performance parameters of these devices have been analyzed and are summarized in Table 1 [38–44].

Table 1

Main technical specifications of oxygenators for an ECMO system

	Filling volume (mL)	Maximum blood flow rate (rpm)	Gas exchange surface area (m^2)	Heat exchange surface area (m^2)	Surface coating	Maximum usage time
Medos HILITE 800 (for pediatric patients)	55	0.8	0.32	0.074	Heparin coating	Long-term use
Medos HILITE 2400 (for adult patients)	95	2.4	0.65	0.16	Heparin coating	Long-term use
Medos HILITE 7000 (for adult patients)	275	7	1.9	0.45	Heparin coating	Long-term use
Getinge QUADROX iD (for adult patients)	250	7	1.8	–	Bioline coating	30 days
Getinge QUADROX iD (for pediatric patients)	81	2.8	0.8	0.15	Bioline coating	30 days
Eurosets ECMO (for adult patients)	225	7	1.81	0.08	Phosphorylcholine	14 days
Eurosets ECMO (for pediatric patients)	190	4	1.35	0.08	Phosphorylcholine	14 days
Paragon Pediatric (for pediatric patients)	175	4	1.23	0.2	Rheopak Albumin coating	15 days
Paragon Mini (for pediatric patients)	225	5	1.78	0.2	Rheopak Albumin coating	15 days
Paragon Midi (for adult patients)	250	7	1.95	0.4	Rheopak Albumin coating	15 days
Paragon Maxi (for adult patients)	290	9	2.44	0.4	Rheopak Albumin coating	15 days
LivaNova EOS (for adult patients)	150	5	12	0.14	Phosphorylcholine	5 days
LivaNova Lilliput II (for pediatric patients)	90	2.3	0.67	0.02	Phosphorylcholine	5 days
Novalung Minilung (for pediatric patients)	95	2.4	0.65	0.074	Heparin coating	29 days
Novalung iLA Membrane (for adult patients)	225	4.5	1.3	–	Heparin coating	29 days
Novalung XLung (for adult patients)	275	7	1.9	0.45	Heparin coating	29 days

Table 2

Summary data on extracorporeal pump application

	Advantages of extracorporeal pumps	Disadvantages of extracorporeal pumps
Maquet Rotaflow Pump	1. Minimal shear stress inside the pump cavities. 2. There is a switch to manual operation mode. 3. Continuous use for up to 14 days	High hemolysis rates
Medos Delta Stream DP3 Pump	1. Can create an optional pulsing operation mode from 40 to 90 beats/min. 2. Unique zero flow mode that prevents unwanted backflow. 3. A portable (~10 kg) console with two batteries for 90 minutes	No switch to manual operation
CentriMag Pump / PediVas Pump	Magnetic levitation that reduces the risk of hemolysis and thrombosis	No backup power supply
Medtronic BPX-80 / BP-50	1. There is a heparin-coated modification. 2. High preload sensitivity	High hemolysis rates. Short-term use
Medtronic Affinity	1. Low hemolysis rates. 2. High pump efficiency	Short-term use
Revolution LivaNova Pump	1. Low coefficient of friction due to unsealed bearings. 2. Easy filling and venting of pump cavities. 3. Nylon magnet impregnated with ferromagnetic particles, pressure-cast, with characteristics that, in combination with the impeller, increase the longevity of the pump	Only 2 channels for pressure measurement and two flow limits can be set. Short-term use

DISCUSSION

This review summarizes the key characteristics of pumps and oxygenators currently used in modern clinical ECMO practice. Based on the collected data, the main advantages and limitations of various extracorporeal pumps have been identified and are presented in Table 2.

In evaluating CPs for ECMO, considerations extend beyond the performance of oxygenators under varying flow and pressure conditions. Equally important are the pressure and flow requirements within the cannula connected to the patient. In many cases, particularly in patients with low body mass or small vessel diameter, smaller cannulas are required. For instance, at a flow rate of 5 L/min, a 5 mm diameter cannula can produce a pressure drop of up to 150 mmHg. This substantial resistance must be carefully factored into system design and patient management.

The growing number of ECMO procedures performed in intensive care and cardiac intensive care units over recent decades has demonstrated high survival rates among critically ill patients. Currently, the systems in use are predominantly imported, highlighting the need for the development of Russian-made CPs.

The development and implementation of domestically produced CPs is extremely important and essential. It would not only enhance the quality of medical care but also contribute to the creation of locally produced consumables required for clinical procedures.

At this stage, scientific data supporting the selection of specific pump models for further improvement are available. Advancing domestic CPs for clinical use will lay the foundation for the production of locally sourced consumables for ECMO procedures.

CONCLUSION

Based on the collected data, the use of magnetic levitation and centrifugal flow has proven to be both effective and safe for patient treatment. Reducing undesirable postoperative complications and promoting functional recovery are key clinical objectives in the application of ECMO systems in clinical practice.

In alignment with global standards for the development of such systems, medical and technical requirements have been formulated for the first Russian-made extracorporeal pump currently under development for ECMO circuits. Ongoing research will focus on three-dimensional mathematical modeling of the CP design, calculations for the key components, creation of prototypes, and testing them on hydrodynamic test benches to ensure compliance with specified medical and technical criteria.

The authors declare no conflict of interest.

REFERENCES

1. *Mugford M, Elbourne D, Field D*. Extracorporeal membrane oxygenation for severe respiratory failure in newborn infants. *Cochrane Database Syst Rev*. 2008; 3: CD001340.
2. *Sievert AN, Shackelford AG, McCall MM.* Trends and emerging technologies in extracorporeal life support: results of the 2006 ECLS survey. *J Extra Corpor Technol*. 2009; 41 (2): 73–78.
3. *Fleming GM, Gurney JG, Donohue JE, Remenapp RT, Annich GM.* Mechanical component failures in 28 171 neonatal and pediatric extracorporeal membrane oxygenation courses from 1987 to 2006. *Pediatr Crit Care Med*. 2009; 10 (4): 439–444.

4. *Gauthier SV, Poptsov VN, Spirina EA*. Extracorporeal membrane oxygenation in cardiac surgery and transplantology. M.: Triada, 2013; 272.
5. *Protti I, van Steenwijk MPJ, Meani P, Fresiello L, Meuwese CL, Donker DW*. Left Ventricular Unloading in Extracorporeal Membrane Oxygenation: A Clinical Perspective Derived from Basic Cardiovascular Physiology. *Curr Cardiol Rep*. 2024; 26 (7): 661–667.
6. *Turbendian HK, Gebhardt J, Scherkenbach P, Zawadzki MJ, Shillingford M*. A novel approach to delivery of extracorporeal support using a modified continuous flow ventricular assist device in a mid-volume congenital heart program. *Artif Organs*. 2021; 45 (1): 55–62.
7. *Abbasi A, Devers C, Sodha NR, Ventetuolo CE*. Extracorporeal Life Support in Adults with Acute Respiratory Failure: Current Evidence-Based Practices. *R I Med J*. 2019; 102 (10): 39–42.
8. *Madurka I, Bartók T, Kormosói-Tóth K, Schönauer N, Elek J, Bobek I*. Successful extracorporeal membrane oxygenation (ECMO) treatment in Legionella pneumonia. *Orv Hetil*. 2019; 160 (6): 235–240.
9. *Talor J, Yee S, Rider A, Kunselman AR, Guan Y, Undar A*. Comparison of perfusion quality in hollow-fiber membrane oxygenators for neonatal extracorporeal life support. *Artif Organs*. 2010; 34 (4): E110–E116.
10. *Vasavada R, Khan S, Qiu F, Kunselman A, Undar A*. Impact of oxygenator selection on hemodynamic energy indicators under pulsatile and nonpulsatile flow in a neonatal extracorporeal life support model. *Artif Organs*. 2011; 35 (6): E101–E107.
11. *Qiu F, Khan S, Talor J, Kunselman A, Undar A*. Evaluation of two pediatric polymethyl pentene membrane oxygenators with pulsatile and non-pulsatile perfusion. *Perfusion*. 2011; 26 (3): 229–237.
12. *Thiara AP, Hoel TN, Kristiansen F, Karlsen HM, Fiane AE, Svennevig JL*. Evaluation of oxygenators and centrifugal pumps for long-term pediatric extracorporeal membrane oxygenation. *Perfusion*. 2007; 22 (5): 323–326.
13. *Shen I, Levy FH, Vocelka CR, O'Rourke PP, Duncan BW, Thomas R, Verrier ED*. Effect of extracorporeal membrane oxygenation on left ventricular function of swine. *Ann Thorac Surg*. 2001; 71 (3): 862–867.
14. *Watterson PA, Woodard JC, Ramsden VS, Reizes JA*. VentrAssist hydrodynamically suspended, open, centrifugal blood pump. *Artif Organs*. 2000; 24 (6): 475–477.
15. *Lawson DS, Ing R, Cheifetz IM, Walczak R, Craig D, Schulman S et al.* Hemolytic characteristics of three commercially available centrifugal blood pumps. *Pediatr Crit Care Med*. 2005; 6 (5): 573–577.
16. *Han D, Leibowitz JL, Han L, Wang S, He G, Griffith BP, Wu ZJ.* Computational fluid dynamics analysis and experimental hemolytic performance of three clinical centrifugal blood pumps: Revolution, Rotaflow and CentriMag. *Med Nov Technol Devices*. 2022; 15: 100153.
17. *Horton S, Thuys C, Bennett M, Augustin S, Rosenberg M, Brizard C*. Experience with the Jostra Rotaflow and QuadroxD oxygenator for ECMO. *Perfusion*. 2004; 19 (1): 17–23.
18. *Ibrahim AE, Duncan BW, Blume ED, Jonas RA*. Long-term follow-up of pediatric cardiac patients requiring mechanical circulatory support. *Ann Thorac Surg*. 2000; 69 (1): 186–192.
19. *Wang S, Caneo LF, Jatene MB, Jatene FB, Cestari IA, Kunselman AR, Ündar A. In Vitro* Evaluation of Pediatric Hollow-Fiber Membrane Oxygenators on Hemodynamic Performance and Gaseous Microemboli Handling: An International Multicenter/Multidisciplinary Approach. *Artif Organs*. 2017; 41 (9): 865–874.
20. *Reser D, Seifert B, Klein M, Dreizler T, Hasenclever P, Falk V, Starck C.* Retrospective analysis of outcome data with regards to the use of Phisio®-, Bioline®- or Softline®-coated cardiopulmonary bypass circuits in cardiac surgery. *Perfusion*. 2012; 27 (6): 530–534.
21. *Lunz D, Philipp A, Judemann K, Amann M, Foltan M, Schmid C et al.* First experience with the deltastream(R) DP3 in venovenous extracorporeal membrane oxygenation and air-supported inter-hospital transport. *Interact Cardiovasc Thorac Surg*. 2013; 17 (5): 773–777.
22. *Heinsar S, Bartnikowski N, Hartel G, Farah SM, Seah EP, Wu E et al.* A comprehensive evaluation of hemodynamic energy production and circuit loss using four different ECMO arterial cannulae. *Artif Organs*. 2023; 47 (7): 1122–1132.
23. *Wang S, Force M, Moroi MK, Patel S, Kunselman AR, Ündar A*. Effects of Pulsatile Control Algorithms for Diagonal Pump on Hemodynamic Performance and Hemolysis. *Artif Organs*. 2019; 43 (1): 60–75.
24. *Okan Y, Sertac H, Erkut O, Taner K, Selen OI, Firat AH et al.* Initial Clinical Experiences With Novel Diagonal ECLS System in Pediatric Cardiac Patients. *Artif Organs*. 2017; 41 (8): 717–726.
25. *Borisenko O, Wylie G, Payne J, Bjessmo S, Smith J, Firmin R, Yonan N*. The cost impact of short-term ventricular assist devices and extracorporeal life support systems therapies on the National Health Service in the UK. *Interact Cardiovasc Thorac Surg*. 2014; 19 (1): 41–48.
26. *Dasse KA, Gellman B, Kameneva MV, Woolley JR, Johnson CA, Gempp T et al.* Assessment of hydraulic performance and biocompatibility of a MagLev centrifugal pump system designed for pediatric cardiac or cardiopulmonary support. *ASAIO J*. 2007; 53 (6): 771–777.
27. *Wang S, Sun W, Han D, Clark KP, Griffith BP, Wu ZJ. In vitro* study on device-induced damage to blood cellular components and degradation of von Willebrand factor in a CentriMag pump-assisted circulation. *Artif Organs*. 2024; 48 (9): 988–996.
28. *Jain M, Gadallah B, Das De S, Mehta V.* Implantation of short-term biventricular assist device (BiVAD) using the CentriMag™ system: the Manchester technique. *Indian J Thorac Cardiovasc Surg*. 2024; 40 (4): 521–525.
29. *Maul TM, Kocyildirim E, Marks JD, Bengston SG, Olia SE, Callahan PM et al.* Pre-clinical Implants of the Levitronix PediVAS® Pediatric Ventricular Assist Device – Strategy for Regulatory Approval. *Cardiovasc Eng Technol*. 2011; 2 (4): 263–275.
30. *Wang S, Rider AR, Kunselman AR, Richardson JS, Dasse KA, Undar A.* Effects of the pulsatile flow settings on

pulsatile waveforms and hemodynamic energy in a PediVAS centrifugal pump. *ASAIO J*. 2009; 55 (3): 271–276.
31. *Burda G, Trittenwein H, Carole H, Trittenwein G.* Testing of extracorporeal membrane oxygenation circuit related hemolysis using long-term stored packed red cells and fresh frozen plasma. *Artif Organs*. 2004; 28 (5): 496–499.
32. *Li P, Mei X, Ge W, Wu T, Zhong M, Huan N et al.* A comprehensive comparison of the *in vitro*. *Front Physiol*. 2023; 14: 1136545.
33. *Puentener P, Schuck M, Kolar JW.* The Influence of Impeller Geometries on Hemolysis in Bearingless Centrifugal Pumps. *IEEE Open J Eng Med Biol*. 2020; 1: 316–323.
34. *Fujiwara T, Nagaoka E, Watanabe T, Miyagi N, Kitao T, Sakota D et al.* New generation extracorporeal membrane oxygenation with MedTech Mag-Lev, a single-use, magnetically levitated, centrifugal blood pump: preclinical evaluation in calves. *Artif Organs*. 2013; 37 (5): 447–456.
35. *Hijikata W, Sobajima H, Shinshi T, Nagamine Y, Wada S, Takatani S, Shimokohbe A*. Disposable MagLev centrifugal blood pump utilizing a cone-shaped impeller. *Artif Organs*. 2010; 34 (8): 669–677.
36. Medtronic ECLS pumps [Internet]; http://www.medtronic.com/us-en/healthcare-professionals/therapies-procedures/cardiovascular/perfusion.html [updated 2024 August 15].
37. Revolution Livanova [Internet]; http://www.livanova.sorin.com/products/cardiac-surgery/perfusion/centrifugal-bloodpump/revolution [updated 2024 August 15].
38. *Glass K, Trivedi P, Wang S, Woitas K, Kunselman AR, Ündar A*. Building a Better Neonatal Extracorporeal Life Support Circuit: Comparison of Hemodynamic Performance and Gaseous Microemboli Handling in Different Pump and Oxygenator Technologies. *Artif Organs*. 2017; 41 (4): 392–400.
39. *Lemloh L, Bo B, Ploeger H, Dolscheid-Pommerich R, Mueller A, Kipfmueller F.* Hemolysis during Venovenous Extracorporeal Membrane Oxygenation in Neonates with Congenital Diaphragmatic Hernia: A Prospective Observational Study. *J Pediatr*. 2023; 263: 113713.
40. *Wang S, Moroi MK, Force M, Kunselman AR, Ündar A.* Impact of Heart Rate on Pulsatile Hemodynamic Performance in a Neonatal ECG-Synchronized ECLS System. *Artif Organs*. 2019; 43 (1): 81–89.
41. *Modi SP, D'Aloiso B, Palmer A, Smith S, Arlia P, Anselmi M et al.* Comparative analysis of oxygenator dysfunction in polymethylpentene oxygenators: A pilot study. *Perfusion*. 2024 Aug 1: 2676591241268402.
42. *Condello I, Lorusso R, Nasso G, Speziale G*. Long-term ECMO, efficiency and performance of EUROSETS adult A.L.ONE ECMO oxygenator. *J Cardiothorac Surg*. 2023; 18 (1): 95.
43. *Odish MF, Garimella PS, Crisostomo H, Yi C, Owens RL, Pollema T*. Using Cardiohelp, Quadrox, and Nautilus Extracorporeal Membrane Oxygenators as Vascular Access for Hemodialysis, Continuous Renal Replacement Therapy, and Plasmapheresis: A Brief Technical Report. *ASAIO J*. 2023; 69 (11): e455–e459.
44. *Fukuda M.* Evolutions of extracorporeal membrane oxygenator (ECMO): perspectives for advanced hollow fiber membrane. *J Artif Organs*. 2024; 27 (1): 1–6.
45. *Iwahashi H, Yuri K, Nosé Y.* Development of the oxygenator: past, present, and future. *J Artif Organs*. 2004; 7 (3): 111–120.

The article was submitted to the journal on 15.08.2024

DOI: 10.15825/1995-1191-2024-4-157-165

BIODEGRADABLE SILK-BASED PRODUCTS FOR REGENERATIVE MEDICINE

E.I. Podbolotova, O.I. Agapova

Shumakov National Medical Research Center of Transplantology and Artificial Organs, Moscow, Russian Federation

Silk is becoming one of the key materials in contemporary bioengineering and medicine due to its unique physicochemical and biological properties. This review article discusses the main components of silk, fibroin and sericin, their structure and functional characteristics, as well as their importance in the production of biocompatible and biodegradable materials. Modern methods of modifying silk to enhance its mechanical and biological properties are considered, including physical, chemical, and genetic manipulation. The use of silk in tissue engineering, development of medical implants, controlled drug delivery systems, and biosensors is given particular consideration. In conclusion, the prospects for further silk research targeted at creating innovative biomaterials for medical applications are discussed.

Keywords: silk, silk fibroin, tissue engineering, regenerative medicine.

Silk has captivated scientists and researchers for centuries due to its remarkable properties and wide range of applications. In the modern scientific landscape, interest in silk has grown substantially owing to its unique biological, chemical, and mechanical characteristics. Its exceptional biocompatibility, biodegradability, mechanical strength, and ability to be functionalized have positioned silk as a highly valuable material in the development of medical devices and bioengineered constructs.

COMPLEX CHARACTERISTICS

As a natural biopolymer, silk stands out for its superior physical and chemical properties, distinguishing it from other natural fibers. Its two primary components – fibroin and sericin – are integral to its structure and functionality. The chemical composition and interaction between these proteins play a key role in determining silk's properties and its wide-ranging applications.

Fibroin is the primary structural component of silk, responsible for its strength and elasticity [1]. Chemically, fibroin is a polypeptide composed of long chains of amino acids that form highly ordered structures known as β-sheets. These β-sheets are stabilized by strong hydrogen bonds between adjacent polypeptide chains, contributing to fibroin's distinctive mechanical properties [2]. In addition to these beta sheets, amorphous domains may also be present within the fibroin structure, providing enhanced flexibility to the material.

The structural integrity of fibroin is further reinforced by intermolecular hydrogen bonds that stabilize its three-dimensional structure and adds to its mechanical resilience.

Fibroin's amino acid composition is predominantly glycine (~50%), alanine (~30%), and serine (~10%) [3]. The high content of glycine and alanine is crucial to its structural properties. Glycine, with its minimal side chain (a single hydrogen atom), allows for tight packing of polypeptide chains, enabling the formation of compact and stable structures. Alanine, with a slightly larger methyl side chain, further stabilizes these structures, enhancing the overall strength of the material.

The high tensile strength of fibroin makes it an ideal material for creating sutures and biocompatible implants that must endure mechanical stress within the body [4]. Its notable elasticity enhances user comfort and enables implants and sutures to adapt to tissue movement and physiological changes [5].

The physicochemical properties of fibroin are critical to its broad range of biomedical applications. These properties include hydrophobicity, chemical resistance, and the capacity to be processed into diverse structural forms. Notably, fibroin exhibits low hygroscopicity [4], which contributes to its mechanical integrity and durability in moisture-rich environments – a characteristic particularly advantageous in reducing the risk of infection in medical settings.

Its chemical stability is another significant attribute; fibroin demonstrates resistance to a wide spectrum of chemical agents, including certain acids and alkalis. This resilience enhances its suitability for use in medical devices and materials that may encounter harsh chemical conditions. Furthermore, fibroin can be fabricated into a variety of formats – such as films, gels, and sutures – thereby extending its applications [6].

Corresponding author: Olga Agapova. Address: 5, Pehotnaya str., 123182, Moscow, Russian Federation.
Phone: (499) 190-66-19. E-mail: olya.agape@gmail.com

Sericin is the second major protein in silk and plays a critical role as a water-soluble binding agent that holds fibroin fibers together. Unlike the highly ordered structure of fibroin, sericin has an amorphous and less organized structure, rich in polar amino acids such as serine, tyrosine, and aspartic acid. These amino acids facilitate the formation of hydrogen bonds and strong interactions with water molecules, giving sericin its distinctive hydrophilic properties [7, 8].

Due to its high content of hydrophilic amino acids, sericin readily interacts with water, enabling it to retain moisture and form hydrogels. This property enhances its function as a natural adhesive, securing fibroin fibers and contributing to the overall integrity of silk.

The interaction between fibroin and sericin results in a cohesive and functionally efficient silk structure [9]. In natural silk cocoons, fibroin forms the structural core, while sericin coats and binds the fibers, adding strength, stability, and protection against environmental stressors.

The chemical composition of silk largely determines its suitability for various applications [10, 11]. Fibroin fibers, known for their high tensile strength and resistance to external stressors, are widely used in the production of wound dressings, medical implants, sutures, and other biomedical materials. Sericin's hydrophilic nature makes it ideal for cosmetic and medical products aimed at enhancing moisturization and adhesion.

One of silk's key advantages is its biocompatibility, a critical factor for materials used in medical and surgical procedures [5]. Silk fibroin (SF), in particular, integrates seamlessly into biological systems with minimal adverse reactions, largely due to its natural origin and favorable structural properties. As a natural protein, SF is readily recognized by the body, reducing the likelihood of inflammatory responses or immune rejection [12].

When in contact with living tissue, fibroin does not induce severe immune reactions such as inflammation or allergic responses. Its biocompatibility is further supported by its low toxicity and minimal mechanical irritation [13]. Moreover, SF actively supports tissue healing and regeneration. For example, fibroin-based films and scaffolds can function as temporary substrates that facilitate cell attachment, proliferation, and differentiation, thereby creating optimal conditions for tissue repair [14, 15].

BIODEGRADATION

Biodegradation is a crucial property of silk as it determines how silk behaves after implantation. Biodegradation refers to the process by which silk is naturally broken down and eliminated from the body through enzymatic and other biological mechanisms that degrade its polypeptide chains [16].

This property makes silk an ideal material for medical implants and other biodegradable biostructures, as it can be gradually absorbed and replaced by natural tissue. Consequently, this reduces the need for repeated surgical procedures and promotes faster patient recovery.

In addition, the biodegradation of silk products minimizes the risk of long-term inflammatory responses and other adverse effects. As a biodegradable material, silk is well-suited for creating temporary scaffolds that support tissue function until the body regenerates its lost tissue.

SF undergoes controlled biodegradation, allowing for precise regulation of the degradation timeline and rate [17]. Various processing techniques are employed to manipulate this process, including structural modifications and incorporation of specific additives [52, 53]. The biodegradation rate can also be influenced by environmental factors such as temperature, humidity, and enzymatic activity within body tissues.

It is also important to note that sericin, the second protein component of silk, is prone to biodegradation as well. Research has demonstrated that, unlike fibroin, which has a denser and more stable structure, sericin is water-soluble and, therefore, more readily biodegraded [54]. This property makes sericin particularly suitable for applications where a faster degradation rate is desired.

APPLICATION OF SILK FIBROIN IN TISSUE ENGINEERING AND REGENERATIVE MEDICINE

SF is widely used in tissue engineering, primarily to create biocompatible scaffolds that support tissue growth and regeneration [18]. Thanks to its structural strength and flexibility, SF-based matrices can be fabricated into various forms – films, scaffolds, and hydrogels – that closely mimic the natural extracellular matrix of tissues. These matrices facilitate cell adhesion, proliferation, and differentiation, making them effective in regenerating skin, bone, cartilage, and other tissues.

Research has shown that SF scaffolds promote the growth and migration of various cell types, including fibroblasts, osteoblasts, and chondrocytes, thereby aiding in the regeneration of damaged tissues [14, 15, 19]. Furthermore, SF can be modified with bioactive molecules, such as growth factors, to enhance its interaction with cells and further accelerate the regenerative process.

Examples of SF applications in tissue engineering include the creation of skin coatings for treating burns and wounds, as well as bone and cartilage substitutes [10, 14, 19]. Silk-based scaffolds and hydrogels can serve as temporary implants to support tissue regeneration following surgical procedures. In some cases, these materials are combined with other biomaterials, such as collagen or hyaluronic acid, to enhance both their mechanical strength and biological properties. Additionally, ongoing research focuses on creating three-dimensional printed structures made from silk proteins, which could be used for precise reconstruction of complex anatomical structures [20].

MEDICAL IMPLANTS

Silk is also widely employed in the production of medical implants [21]. A well-known example is surgical suture materials, which offer high tensile strength and minimal immune response [22]. Beyond sutures, silk proteins are used in developing a range of implants, including skeletal fixators, vascular prostheses, and devices for nerve tissue repair. The biocompatibility and mechanical strength of these silk-based implants ensure their stable integration with biological tissues and reliable long-term function.

For instance, SF-based skeletal fixators are used to stabilize and support bone structures in the treatment of fractures and other bone injuries [23, 24]. Unlike traditional metal fixators, silk-based structures are immune to corrosion and can be fully bioresorbable once the healing process is complete. This property reduces the risk of long-term complications and eliminates the need for additional surgeries to remove the fixators.

Silk vascular prostheses are being developed as replacements for damaged or blocked blood vessels [25–27]. Due to its excellent mechanical properties, silk can be processed to replicate the elasticity and strength of natural blood vessels. Furthermore, these silk prostheses can be modified to enhance anticoagulant properties, which helps reduce the risk of thrombosis.

In nerve tissue repair, silk scaffolds are being developed to support the growth and directed repair of nerve fibers [28]. Silk can be used to create microtubules and other structures that guide axon growth, promoting functional recovery from peripheral nervous system injuries. Experimental studies have shown that silk-based implants can significantly enhance nerve fiber regeneration, restoring both sensory and motor functions in animal models [29–32].

CONTROLLED DRUG DELIVERY

Controlled drug delivery is another significant application of silk proteins in medicine. SF microspheres and nanoparticles can be used to encapsulate and deliver a range of drugs, including antibacterial agents, anticancer drugs, and proteins. The unique properties of fibroin allow for the regulation of drug release rates, enabling sustained and controlled therapy [33, 34].

For example, fibroin nanoparticles can be used to deliver anticancer drugs directly to tumor cells, minimizing damage to healthy tissues and reducing side effects [35]. Additionally, fibroin microspheres are ideal for vaccine delivery, providing a gradual release of antigens and stimulating a sustained immune response [36, 37]. This approach is particularly valuable for the development of vaccines targeting chronic infections and cancers, where long-term and stable immune system activation is essential.

BIOSENSORS AND DIAGNOSTIC DEVICES

Recently, researchers have been exploring the use of silk in the development of biosensors and diagnostic devices. Thanks to its biocompatibility and functionalizability, silk provides an ideal foundation for sensors that can detect biomolecules, pathogens, and other critical analytical targets [38]. These sensors have potential applications in disease diagnosis, treatment monitoring, and the development of personalized medical strategies.

Examples of silk-based biosensors include devices designed to monitor glucose levels in diabetic patients, detect specific biomarkers for early cancer diagnosis, and track the condition of wound surfaces to prevent infections [39, 40]. These sensors are not only useful in medical settings but can also be employed in home care, making diagnostics more accessible and convenient for patients. Furthermore, they can be integrated into wearable medical devices, enabling continuous monitoring of a patient's condition and facilitating early detection of any changes [55].

MODIFIED SILK

Genetically modified silkworms can produce silk enriched with functional peptides and proteins, such as antibacterial agents or growth factors [41]. These genetically modified silks may exhibit enhanced mechanical and biological properties compared to natural silk. For instance, the incorporation of genes encoding elastin-like peptides can improve the elasticity and strength of silk fibers [56]. Additionally, the addition of antimicrobial peptides can make silk more resistant to bacterial infections [57].

Silk proteins are also used in the fabrication of composite materials with enhanced properties. By combining SF with other biomaterials, such as collagen, chitosan, or carbon nanotubes, it is possible to create materials with unique mechanical and biological characteristics [42–44]. These composites have applications in medical implants, tissue engineering, and biosensors. For example, composites made from SF and carbon nanotubes show potential in cardiac tissue engineering for heart repair [45].

Chemical modification of fibroin involves adding various functional groups and molecules to its surface [46]. For instance, incorporating antibacterial agents can make fibroin resistant to bacterial infections [47]. Additionally, modification with growth factors and other bioactive molecules enhances the interaction of silk fibroin (SF) with cells, promoting regenerative processes. Chemically modified fibroin has been shown to significantly improve tissue engraftment and regeneration [48].

Physical modification of silk focuses on altering its structure and morphology to enhance its mechanical and biological properties. For example, creating porous structures can improve permeability and biocompatibi-

lity, which is crucial for tissue engineering applications [49, 50]. Nanotechnology enables the fabrication of silk nanostructures with unique properties, such as increased strength and elasticity. Furthermore, physically modified SF has been shown to improve cell adhesion and proliferation, which aids in tissue regeneration and wound healing.

COMPARATIVE CHARACTERISTICS OF SILK-BASED MATERIALS AND THEIR APPLICATIONS

To clearly compare the characteristics of silk-based materials in various fields of application, Table provides an overview of key properties and benefits. It summarizes the use of fibroin and other silk components in tissue engineering, medical implants, biosensors, and drug delivery systems.

Table

Silk application in medicine and biotechnology

Area of application	Material	Product	Result	Manufacturing method	Article
Tissue engineering	Fibroin	Corneal regeneration membranes	Stimulates cell growth, supports cell functional activity	Irrigation method	[14, 15]
Tissue engineering	Natural silk fabrics	Tissue regeneration scaffolds	Supports tissue regeneration	Chemical treatment of silk fabrics	[18]
Tissue engineering	Fibroin	Bone regeneration scaffold	Supports cell growth and regeneration	Irrigation method, freeze-thaw	[19]
Medical implants	Silk threads	Surgical threads	Minimal body reaction	Antibacterial treatment, thread tube weaving	[22]
Medical implants	Silk threads	Vascular prostheses	Enhanced tissue integration, excellent biocompatibility	Electrospinning	[25]
Medical implants	Silk threads	Endovascular prostheses	Reliability and long-term stability	Thread tube weaving, chemical treatment	[26]
Medical implants	Silk threads	Elastic vascular prostheses	Reduced risk of thrombosis	Thread tube weaving, chemical treatment	[27]
Neuroregeneration	Fibroin	Nerve regeneration hydrogels	Enhanced regeneration	Chemical modification	[29]
Neuroregeneration	Fibroin	Regeneration nanofiber tubes	Directed growth support	Electrospinning	[30]
Neuroregeneration	Fibroin	Nerve scaffolds	Accelerated regeneration	3D printing	[31]
Neuroregeneration	Fibroin	Hydrogels loaded with stem cells for brain regeneration	Function restoration after stroke	Cell integration into hydrogels	[32]
Drug delivery	Fibroin nanoparticles	Encapsulation of anticancer drugs	Precise delivery, minimization of side effects	Encapsulation	[35]
Drug delivery	Fibroin	Microspheres for DNA vaccine delivery	Improved immunogenicity	Encapsulation	[36]
Drug delivery	Fibroin	Microneedles for transdermal vaccine delivery	Efficient and painless delivery	Chemical treatment, casting of needle molds	[37]
Biosensors	Fibroin	Electrochemical glucose biosensors	Continuous glucose monitoring	Chemical treatment, casting of needle molds	[39]
Biosensors	Fibroin	Colorimetric biosensors on stable platforms	Accurate diagnosis, reuse	Chemical modification	[40]
Genetically modified silkworm	Fibroin	Components for enhancing mechanical properties	Enhanced mechanical properties	Use of transgenic silkworms	[41]
Tissue engineering	Fibroin	Composite matrices for bone regeneration	Enhanced cell adhesion and proliferation	Modification with nano-hydroxyapatite and gelatin	[42]

End of table

Area of application	Material	Product	Result	Manufacturing method	Article
Tissue engineering	Fibroin	Cardiomyocyte matrices	Enhanced cardiomyocyte function	Electrospinning	[45]
Chemical modification	Fibroin	Modified fibroin	Enhanced properties	Serine-based chemical modification	[46]
Tissue engineering	Fibroin	Hydrogels for growth factor delivery	Growth factor delivery	Chemical treatment, UV irradiation	[48]
Tissue engineering	Fibroin	Hydrogels for bone tissue engineering	Enhanced properties	Sequential addition and porogen leaching	[50]
Medical implants	Fibroin Antheraea pernyi	Modified implants	Increased resistance to degradation	Acylation by succinyl anhydride	[52]
Pharmacology	Fibroin-based nanoparticles	Nanocapsules for drug delivery	Controlled drug release	Self-organization of fibroin into nanostructures	[53]
Biosensors	Fibroin	Biosensors and wearable devices	Continuous health monitoring	Formation of flexible fibroin films	[55]
Genetically modified silkworm	Transgenic silk with antibacterial peptides	Antibacterial sutures	Resistance to bacterial infections	Genetic modification of silkworms	[57]

CONCLUSION

Silk and fibroin continue to be among the most promising materials for research and development across a range of scientific disciplines. The growing scientific interest in silk is driven by its unique properties and broad potential for application in various fields.

A primary area of focus is the development of innovative biomedical materials. For example, biodegradable silk- and fibroin-based implants are being investigated for their potential to repair damaged tissues and organs [51]. Ongoing research aims to create advanced dressings and suture materials that offer enhanced mechanical properties and promote tissue regeneration [18].

The authors declare no conflict of interest.

REFERENCES

1. *Amirova TS, Ibragimov AA, Nazarov OM, Saminov KhN.* Analysis of the structure of silk sericin and fibroin. *Universum: Chemistry and Biology*. 2024; 1 (6): 28–31. [In Russ, English abstract]. doi: 10.32743/UniChem.2024.120.6.17463.
2. *Cheng Y, Koh LD, Li D, Ji B, Han MY, Zhang YW.* On the strength of β-sheet crystallites of Bombyx mori silk fibroin. *J R Soc Interface*. 2014 Apr 30; 11 (96): 20140305. doi: 10.1098/rsif.2014.0305.
3. *Zhou CZ, Confalonieri F, Jacquet M, Perasso R, Li ZG, Janin J.* Silk fibroin: structural implications of a remarkable amino acid sequence. *Proteins*. 2001 Aug 1; 44 (2): 119–122. doi: 10.1002/prot.1078. PMID: 11391774.
4. *Altman GH, Diaz F, Jakuba C, Calabro T, Horan RL, Chen J et al.* Silk-based biomaterials. *Biomaterials*. 2003 Feb; 24 (3): 401–416. doi: 10.1016/s0142-9612(02)00353-8. PMID: 12423595.
5. *Vepari C, Kaplan DL.* Silk as a biomaterial. *Prog Polym Sci*. 2007; 32 (8–9): 991–1007. doi: 10.1016/j.progpolymsci.2007.05.013. PMID: 19543442.
6. *Rockwood DN, Preda RC, Yücel T, Wang X, Lovett ML, Kaplan DL.* Materials fabrication from Bombyx mori silk fibroin. *Nat Protoc*. 2011 Sep 22; 6 (10): 1612–1631. doi: 10.1038/nprot.2011.379. PMID: 21959241.
7. *Lee HG, Jang MJ, Park BD, Um IC.* Structural characteristics and properties of redissolved silk sericin. *Polymers (Basel)*. 2023 Aug 14; 15 (16): 3405. doi: 10.3390/polym15163405. PMID: 37631462.
8. *Kunz RI, Brancalhão RM, Ribeiro LF, Natali MR.* Silkworm sericin: properties and biomedical applications. *Biomed Res Int*. 2016; 2016: 8175701. doi: 10.1155/2016/8175701.
9. *Du S, Zhang J, Zhou WT, Li QX, Greene GW, Zhu HJ et al.* Interactions between fibroin and sericin proteins from Antheraea pernyi and Bombyx mori silk fibers. *J Colloid Interface Sci*. 2016 Sep 15; 478: 316–323. doi: 10.1016/j.jcis.2016.06.030. Epub 2016 Jun 10. PMID: 27314644.
10. *Nguyen TP, Nguyen QV, Nguyen VH, Le TH, Huynh VQN, Vo DN et al.* Silk fibroin-based biomaterials for biomedical applications: a review. *Polymers (Basel)*. 2019 Nov 24; 11 (12): 1933. doi: 10.3390/polym11121933. PMID: 31771251.
11. *Liu J, Shi L, Deng Y, Zou M, Cai B, Song Y et al.* Silk sericin-based materials for biomedical applications.

Biomaterials. 2022 Aug; 287: 121638. doi: 10.1016/j.biomaterials.2022.121638. Epub 2022 Jun 17. PMID: 35921729.

12. *Luangbudnark W, Viyoch J, Laupattarakasem W, Surakunprapha P, Laupattarakasem P.* Properties and biocompatibility of chitosan and silk fibroin blend films for application in skin tissue engineering. *ScientificWorldJournal*. 2012; 2012: 697201. doi: 10.1100/2012/697201. Epub 2012 May 22. PMID: 22701367.
13. *Ode Boni BO, Bakadia BM, Osi AR, Shi Z, Chen H, Gauthier M et al.* Immune Response to Silk Sericin-Fibroin Composites: Potential immunogenic elements and alternatives for immunomodulation. *Macromol Biosci*. 2022 Jan; 22 (1): e2100292. doi: 10.1002/mabi.202100292. Epub 2021 Nov 10. PMID: 34669251.
14. *Madden PW, Lai JN, George KA, Giovenco T, Harkin DG, Chirila TV.* Human corneal endothelial cell growth on a silk fibroin membrane. *Biomaterials*. 2011 Jun; 32 (17): 4076–4084. doi: 10.1016/j.biomaterials.2010.12.034. Epub 2011 Mar 21. PMID: 21427010.
15. *Liu J, Lawrence B, Liu A, Schwab I, Oliveira L, Rosenblatt M.* Silk fibroin as a biomaterial substrate for corneal epithelial cell sheet generation. *Invest Ophthalmol Vis Sci*. 2012; 53 (7): 4130–4138. doi: 10.1167/iovs.12-9876.
16. *Li G, Sun S.* Silk fibroin-based biomaterials for tissue engineering applications. *Molecules*. 2022 Apr 25; 27 (9): 2757. doi: 10.3390/molecules27092757. PMID: 35566110.
17. *Lu Q, Zhang B, Li M, Zuo B, Kaplan DL, Huang Y et al.* Degradation mechanism and control of silk fibroin. *Biomacromolecules*. 2011 Apr 11; 12 (4): 1080–1086. doi: 10.1021/bm101422j. Epub 2011 Feb 25. PMID: 21361368.
18. *Safonova LA, Bobrova MM, Efimov AE, Agapova OI, Agapov II.* Biodegradable materials based on natural silk fabric as promising scaffolds for tissue engineering and regenerative medicine. *Russian Journal of Transplantology and Artificial Organs*. 2020; 22 (4): 105–114. [In Russ, English abstract].
19. *Kotliarova MS, Arkhipova AYu, Moysenovich AM, Kulikov DA, Kulikov AV, Kon'kov AS et al.* Biodegradable scaffolds based on fibroin for bone tissue regeneration. *Vestnik Moskovskogo universiteta*. Series 16. Biology. 2017; 4: 222–228. [In Russ, English abstract].
20. *Midha S, Ghosh S.* Silk-based bioinks for 3D bioprinting. *Regenerative Medicine: Laboratory to Clinic*. 2017: 259–276. doi: 10.1007/978-981-10-3701-6_15.
21. *Shabbirahmed AM, Sekar R, Gomez LA, Sekhar MR, Hiruthyaswamy SP, Basavegowda N, Somu P.* Recent developments of silk-based scaffolds for tissue engineering and regenerative medicine applications: A special focus on the advancement of 3D printing. Biomimetics. 2023 Jan 16; 8 (1): 16. doi: 10.3390/biomimetics8010016.
22. *Chen X, Hou D, Wang L, Zhang Q, Zou J, Sun G.* Antibacterial Surgical Silk Sutures Using a high-performance slow-release carrier coating system. *ACS Appl Mater Interfaces*. 2015 Oct 14; 7 (40): 22394–22403. doi: 10.1021/acsami.5b06239. Epub 2015 Sep 29. PMID: 26378964.
23. *Foppiani JA, Taritsa IC, Foster L, Patel A, Hernandez Alvarez A, Lee D et al.* Redefining surgical materials: applications of silk fibroin in osteofixation and fracture repair. *Biomimetics (Basel)*. 2024 May 11; 9 (5): 286. doi: 10.3390/biomimetics9050286. PMID: 38786496.
24. *Ding Z, Cheng W, Mia MS, Lu Q.* Silk biomaterials for bone tissue engineering. *Macromol Biosci*. 2021 Aug; 21 (8): e2100153. doi: 10.1002/mabi.202.
25. *Settembrini A, Buongiovanni G, Settembrini P, Alessandrino A, Freddi G, Vettor G, Martelli E. In vivo* evaluation of silk fibroin small-diameter vascular grafts: state of art of preclinical studies and animal models. *Front Surg*. 2023 May 26; 10: 1090565. doi: 10.3389/fsurg.2023.1090565.
26. *Liu Z, Li G, Zheng Z, Li Y, Han Y, Kaplan DL et al.* Silk fibroin-based woven endovascular prosthesis with heparin surface modification. *J Mater Sci Mater Med*. 2018 Apr 12; 29 (4): 46. doi: 10.1007/s10856-018-6055-3. PMID: 29651619.
27. *Tanaka T, Abe Y, Cheng CJ, Tanaka R, Naito A, Asakura T.* Development of small-diameter elastin-silk fibroin vascular grafts. *Front Bioeng Biotechnol*. 2021 Jan 14; 8: 622220. doi: 10.3389/fbioe.2020.622220. PMID: 33585421.
28. *Millesi F, Weiss T, Radtke C.* Silk biomaterials in peripheral nerve tissue engineering. *Advances in Silk Biomaterials*. 2020: 107–128. doi: 10.1007/978-3-030-06217-0_5-1.
29. *Gu X, Chen X, Tang X, Zhou Z, Huang T, Yang Y et al.* Pure-silk fibroin hydrogel with stable aligned micropattern toward peripheral nerve regeneration. *Nanotechnology Reviews*. 2021; 10: 10–19. doi: 10.1515/ntrev-2021-0002.
30. *Zhang F, Liu R, Zuo B, Qin J.* Electrospun silk fibroin nanofiber tubes for peripheral nerve regeneration. *4th International Conference on Bioinformatics and Biomedical Engineering (iCBBE)*. 2010: 1–4. doi: 10.1109/ICBBE.2010.5514821.
31. *Jiang JP, Liu XY, Zhao F, Zhu X, Li XY, Niu XG et al.* Three-dimensional bioprinting collagen/silk fibroin scaffold combined with neural stem cells promotes nerve regeneration after spinal cord injury. *Neural Regen Res*. 2020 May; 15 (5): 959–968. doi: 10.4103/1673-5374.268974. Erratum in: *Neural Regen Res*. 2020 Oct; 15 (10): 1961. doi: 10.4103/1673-5374.280332. PMID: 31719263.
32. *Fernández-García L, Pérez-Rigueiro J, Martinez-Murillo R, Panetsos F, Ramos M, Guinea GV et al.* Cortical reshaping and functional recovery induced by silk fibroin hydrogels-encapsulated stem cells implanted in stroke animals. *Front Cell Neurosci*. 2018 Sep 6; 12: 296. doi: 10.3389/fncel.2018.00296. PMID: 30237762.
33. *Pritchard EM, Kaplan DL.* Silk fibroin biomaterials for controlled release drug delivery. *Expert Opin Drug Deliv*. 2011 Jun; 8 (6): 797–811. doi: 10.1517/17425247.2011.568936. Epub 2011 Apr 1. PMID: 21453189.
34. *Rajendra P, Nidamanuri B, Balan A, Venkatachalam S, Jawahar N.* A review on structure, preparation and applications of silk fibroin-based nano-drug delivery systems.

J Nanoparticle Res. 2022; 24: 55. doi: 10.1007/s11051-022-05526-z.

35. *Kucharczyk K, Florczak A, Deptuch T, Penderecka K, Jastrzebska K, Mackiewicz A et al.* Drug affinity and targeted delivery: double functionalization of silk spheres for controlled doxorubicin delivery into Her2-positive cancer cells. *J Nanobiotechnology*. 2020 Mar 30; 18 (1): 56. doi: 10.1186/s12951-020-00609-2. PMID: 32228620.
36. *Liu Y, Lv Z, Zhang C, Zhu X, Shi T, Zhong S et al.* Preparation and immunogenicity of silk fibroin/chitosan microspheres for DNA vaccine delivery against infectious bursal disease virus. *Shengwu Gongcheng Xuebao / Chinese Journal of Biotechnology*. 2014; 30 (3): 393–403. doi: 10.13345/j.cjb.130344.
37. *Stinson JA, Raja WK, Lee S, Kim HB, Diwan I, Tutunjian S et al.* Silk fibroin microneedles for transdermal vaccine delivery. *ACS Biomater Sci Eng*. 2017 Mar 13; 3 (3): 360–369. doi: 10.1021/acsbiomaterials.6b00515. Epub 2017 Jan 17. PMID: 33465933.
38. *Ru M, Hai AM, Wang L, Yan S, Zhang Q.* Recent progress in silk-based biosensors. *Int J Biol Macromol*. 2023 Jan 1; 224: 422–436. doi: 10.1016/j.ijbiomac.2022.10.134. Epub 2022 Oct 18. PMID: 36270404.
39. *Zhao L, Wen Z, Jiang F, Zheng Z, Lu S.* Silk/polyols/GOD microneedle based electrochemical biosensor for continuous glucose monitoring. *RSC Adv*. 2020 Feb 10; 10 (11): 6163–6171. doi: 10.1039/c9ra10374k. PMID: 35496012.
40. *Márquez A, Santiago S, Dos Santos MV, Aznar-Cervantes SD, Domínguez C, Omenetto FG et al.* Reusable colorimetric biosensors on sustainable silk-based platforms. *ACS Appl Bio Mater*. 2024 Feb 19; 7 (2): 853–862. doi: 10.1021/acsabm.3c00872. Epub 2024 Jan 25. PMID: 38270977.
41. *Dai X, Ye X, Shi L, Yu S, Wang X, Zhong B.* High mechanical property silk produced by transgenic silkworms expressing the Drosophila Dumpy. *Front Bioeng Biotechnol*. 2024 Feb 12; 12: 1359587. doi: 10.3389/fbioe.2024.1359587. PMID: 38410165.
42. *Moisenovich MM, Arkhipova AYu, Orlova AA, Drutskaya MS, Volkova SV, Zacharov SE et al.* Composite scaffolds containig silk fibroin, gelatin, and hydroxyapatite for bone tissue regeneration and 3D cell culturing. *Acta Naturae*. 2014; 6 (1): 103–109. [In Russ, English abstract].
43. *Li F, Zheng Z, Luo T, Liu J, Wu J, Wang X et al.* Silk microfiber-reinforced silk composite scaffolds: fabrication, mechanical properties, and cytocompatibility. *J Mater Sci*. 2016; 51: 7121–7131. doi: 10.1007/s10853-015-9613-9.
44. *Li ZH, Ji S, Wang YZ, Shen XC, Liang H.* Silk fibroin-based scaffolds for tissue engineering. *Front Mater Sci*. 2013; 7: 217–234. doi: 10.1007/s11706-013-0214-8.
45. *Zhao G, Zhang X, Li B, Huang G, Xu F, Zhang X.* Solvent-free fabrication of carbon nanotube/silk fibroin electrospun matrices for enhancing cardiomyocyte functionalities. *ACS Biomater Sci Eng*. 2020 Mar 9; 6 (3): 1630–1640. doi: 10.1021/acsbiomaterials.9b01682. Epub 2020 Feb 3. PMID: 33455382.
46. *Liu X, Xia Q, Zhou J, Zhang Y, Ju H, Deng Z.* Chemical modification of silk fibroin through serine amino acid residues. *Materials (Basel)*. 2022 Jun 22; 15 (13): 4399. doi: 10.3390/ma15134399. PMID: 35806524.
47. *Ghalei S, Handa H.* A review on antibacterial silk fibroin-based biomaterials: current state and prospects. *Mater Today Chem*. 2022 Mar; 23: 100673. doi: 10.1016/j.mtchem.2021.100673. Epub 2021 Dec 9. PMID: 34901586.
48. *Fathi-Achachelouei M, Keskin D, Bat E, Vrana NE, Tezcaner A.* Dual growth factor delivery using PLGA nanoparticles in silk fibroin/PEGDMA hydrogels for articular cartilage tissue engineering. *J Biomed Mater Res B Appl Biomater*. 2020 Jul; 108 (5): 2041–2062. doi: 10.1002/jbm.b.34544. Epub 2019 Dec 24. PMID: 31872975.
49. *Xiao M, Yao J, Shao Z, Chen X.* Silk-based 3D porous scaffolds for tissue engineering. *ACS Biomater Sci Eng*. 2024 May 13; 10 (5): 2827–2840. doi: 10.1021/acsbiomaterials.4c00373. Epub 2024 May 1. PMID: 38690985.
50. *Burger D, Beaumont M, Rosenau T, Tamada Y.* Porous silk fibroin/cellulose hydrogels for bone tissue engineering via a novel combined process based on sequential regeneration and porogen leaching. *Molecules*. 2020 Nov 3; 25 (21): 5097. doi: 10.3390/molecules25215097. PMID: 33153040.
51. *Ma L, Dong W, Lai E, Wang J.* Silk fibroin-based scaffolds for tissue engineering. *Front Bioeng Biotechnol*. 2024 Apr 25; 12: 1381838. doi: 10.3389/fbioe.2024.1381838.
52. *Dai X, Li X, Zhang C, Wang L, Ma C, Yang W, Li M.* Acylation modification of Antheraea pernyi silk fibroin using succinic anhydride and its effects on enzymatic degradation behavior. *J Chem*. 2013. doi: 10.1155/2013/640913.
53. *Lu Q, Zhu HS, Zhang CC, Zhang F, Zhang B, Kaplan DL*. Silk self-assembly mechanisms and control from thermodynamics to kinetics. *Biomacromolecules*. 2012; 13: 826–832.
54. *Baltayeva MM, Babadjanova DD, Eshchanov KO.* Sericin and its meaning. *Universum: tekhnicheskie nauki*. 2022; 1 (94): 89–92. [In Russ, English abstract].
55. *Song Y, Hu C, Wang Z, Wang L.* Silk-based wearable devices for health monitoring and medical treatment. *iScience*. 2024 Mar 27; 27 (5): 109604. doi: 10.1016/j.isci.2024.109604.
56. *Shen X, Shi H, Wei H, Wu B, Xia Q, Yeo J, Huang W.* Engineering natural and recombinant silks for sustainable biodevices. *Front Chem*. 2022; 10: 881028. doi: 10.3389/fchem.2022.881028.
57. *Li Z, Jiang Y, Cao G, Li J, Xue R, Gong C.* Construction of transgenic silkworm spinning antibacterial silk with fluorescence. *Mol Biol Rep*. 2015; 42 (1): 19–25. doi: 10.1007/s11033-014-3735.

The article was submitted to the journal on 13.08.2024

DOI: 10.15825/1995-1191-2024-4-166-170

NATIVE LIVER FIBROSIS IN PEDIATRIC LIVER RECIPIENTS: ASSOCIATION WITH GENETIC POLYMORPHISM IN THE *TGFB1* GENE

O.M. Tsirulnikova[1, 2], O.E. Gichkun[1, 2], R.M. Kurabekova[1], E.A. Stakhanova[1], I.E. Pashkova[1], E.A. Vakurova[2], O.P. Shevchenko[1, 2]

[1] Shumakov National Medical Research Center of Transplantology and Artificial Organs, Moscow, Russian Federation

[2] Sechenov University, Moscow, Russian Federation

Objective: to examine the relationship between native liver fibrosis and *TGFB1* gene polymorphism in pediatric liver recipients. **Materials and methods.** Fibrosis of varying severity was diagnosed (METAVIR scale) based on histological analysis of the native liver of children (45 boys and 62 girls aged 3 to 73 months). Genomic DNA was genotyped by real-time polymerase chain reaction using TaqMan probes. **Results.** The prevalence of the *TGFB1* single nucleotide polymorphisms (SNPs) rs1800469, rs1800470, and rs1800471 was examined in both children with liver fibrosis of varying severity and in healthy individuals. The distribution of rs1800470 in children with fibrosis was 50% homozygotes of major allele, 29% heterozygotes and 21% homozygotes of minor allele. This distribution was not consistent with the Hardy–Weinberg principle ($p = 0.00026$). Conclusion. Liver fibrosis in pediatric liver recipients is linked to the rs1800470 polymorphism of the *TGFB1* gene. Carriage of the heterozygous rs1800470 genotype may be a protective factor against liver fibrosis in children with liver failure.

Keywords: liver fibrosis, biliary atresia and hypoplasia, pediatric liver recipients, rs1800469, rs1800470, rs1800471.

INTRODUCTION

In recent years, substantial progress has been achieved in developing a highly effective treatment system for children with congenital hepatobiliary disorders. Advanced surgical techniques for LT have been introduced, many of which are recognized as globally pioneering – including procedures involving ABO-incompatible donors. The number of LTs has notably increased, even among very young pediatric patients. Arguably, the most remarkable accomplishment in this field has been the complete fulfillment of the national demand for pediatric LT, offering a full recovery to patients who were once considered untreatable [1, 2].

Key areas of current research include identifying genetic predisposition patterns, improving methods for predicting disease progression, and developing strategies to prevent post-LT complications. One promising direction for integration into clinical pediatric practice is the investigation of gene polymorphisms that influence the expression of key factors regulating the formation, development, and function of the hepatobiliary system in children before and after birth.

Previous studies have demonstrated that children with liver failure of various etiologies exhibit a distinct distribution of rare haplotypes of the *TGF-β1* (transforming growth factor beta 1) gene, which regulates the expression of the key profibrogenic cytokine *TGF-β1*, compared to healthy individuals. The clinical relevance of three single nucleotide polymorphisms (SNPs) in the TGFB1 gene – rs1800469, rs1800470, and rs1800471 – has been established, particularly in relation to post-transplant complications such as graft rejection and infections [3, 4].

However, the broad spectrum of liver diseases among the studied patients – including congenital cholestatic and metabolic disorders, as well as acquired cirrhosis and hepatitis – limits the ability to isolate the role of TGFB1 gene polymorphisms. This necessitates further investigation in more homogeneous patient groups. Cirrhosis, a terminal stage of liver fibrosis, is characterized by excessive production and accumulation of extracellular matrix, leading to partial or complete impairment of hepatic function. The fibrotic process involves hepatocytes, lymphocytes, and a cascade of proinflammatory and profibrogenic cytokines [5, 6].

The aim of the present study was to analyze the association between native liver fibrosis and SNPs in the *TGF-β1* gene – rs1800469, rs1800470, and rs1800471 – in pediatric LT recipients during the early post-transplant period. The findings of this research are expected to clarify the role of *TGF-β1* gene polymorphisms in the pathogenesis of liver fibrosis and to evaluate their potential

Corresponding author: Rivada Kurabekova. Address: 1, Shchukinskaya str., Moscow, 123182, Russian Federation. Phone: (499) 190-53-41. E-mail: kourabr@yandex.ru

clinical value in predicting fibrosis risk in pediatric liver recipients.

MATERIALS AND METHODS

The study included 107 pediatric LT recipients (45 boys and 62 girls) aged 3 to 73 months (median age: 8 months), and a control group of 199 healthy individuals (79 males and 120 females) with a mean age of 32.7 ± 9.6 years.

Indications for LT in the pediatric cohort were end-stage liver disease resulting from the following conditions: biliary atresia (n = 61), biliary tract hypoplasia (n = 8), Alagille syndrome (n = 8), Caroli's disease (n = 8), Byler's disease (n = 6), and other rare hepatic disorders (n = 16), including Crigler–Najjar syndrome, glycogen storage disease type I (Von Gierke disease), alpha-1 antitrypsin deficiency, tyrosinemia, fulminant hepatitis, autoimmune hepatitis, and cryptogenic cirrhosis.

Liver fibrosis of varying severity was diagnosed in the recipients based on macroscopic and histologic examination of the native liver explants obtained during transplantation, evaluated according to the METAVIR scoring system: F1 (stellate enlargement of portal tracts without septa) in 5 cases, F2 (portal expansion with isolated porto-portal septa) in 9 cases, F3 (numerous septa without cirrhosis) in 14 cases, and F4 (cirrhosis) in 79 cases.

All patients received treatment and underwent comprehensive clinical, laboratory, and instrumental evaluation in accordance with the protocols at Shumakov National Medical Research Center of Transplantology and Artificial Organs. LT was performed using grafts from living-related donors. Post-transplant, recipients were maintained on double- or triple-drug immunosuppressive therapy regimens.

The detailed methodology and statistical analysis employed in this study have been previously described in our publication, "Association between the Tgfb1 Gene Haplotype and Liver Diseases in Children" [7].

RESULTS AND DISCUSSION

Fig. 1 illustrates the distribution frequencies of three polymorphic variants of the *TGF-β1* gene – rs1800469, rs1800470, and rs1800471 – among pediatric liver recipients with fibrosis.

Comparative analysis of genotype frequencies of the studied SNPs between children with liver fibrosis and healthy controls revealed no statistically significant differences for rs1800469 and rs1800471. However, a significant difference was observed in the distribution of rs1800470 genotypes between the two groups (Fig. 2).

As shown in Fig. 2, a statistically significant difference was observed in the distribution of the heterozygous genotype of rs1800470. In children with liver fibrosis, the AG genotype was 1.6 times less frequent than in healthy individuals ($\chi^2 = 9.4778$, $p = 0.0236$).

In healthy individuals, all three SNPs conformed to Hardy–Weinberg equilibrium. Among children with liver fibrosis, rs1800469 and rs1800471 also demonstrated equilibrium ($\chi^2 = 1.7648$, $p = 0.23$; $\chi^2 = 0.1236$, $p = 0.99$, respectively). However, the distribution of rs1800470 significantly deviated from Hardy–Weinberg expectations ($\chi^2 = 13.7673$, $p = 0.00026$).

These findings suggest that among the three studied SNPs in the TGF-β1 gene, rs1800470 displays a notable deviation from Hardy–Weinberg equilibrium in the group of children with liver fibrosis. This deviation may reflect a potential medical significance of this locus under study.

A comparative analysis of genotype frequencies in children with liver fibrosis and healthy individuals was conducted using different allelic interaction models, including codominant, dominant, recessive, and over dominant (Table).

Table shows significant differences in the distribution of rs1800470 SNP genotypes in codominant (OR = 0.49, CI 0.29–0.84, p = 0.0088) and over dominant (OR = 0.47, CI 0.28–0.77, p = 0.0024) models. The findings suggest that, in both models, the heterozygous AG genotype is significantly less frequent in children with liver fibrosis, potentially serving as a protective factor against

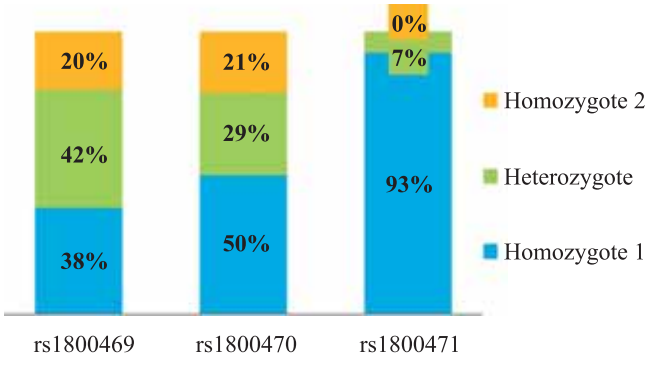

Fig. 1. Distribution of genotypes rs1800469, rs1800470 and rs1800471 of the TGFB1 gene in pediatric liver recipients with liver fibrosis

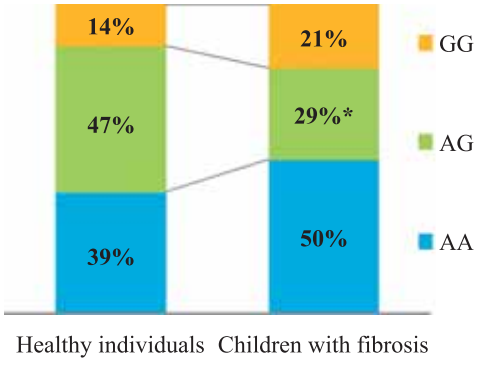

Fig. 2. Distribution of rs1800470 genotypes of the TGFB1 gene in healthy individuals and in pediatric liver recipients with liver fibrosis. * $p < 0.05$ *vs.* healthy individuals

Table

Distribution of the TGFB1 polymorphism rs1800470 in children with liver fibrosis and in healthy individuals in different m odels

SNPs/Model	Genotype	Frequency, % children with fibrosis	Frequency, % healthy individuals	OR (95% CI)	P value
Codominant	AA	50.0	39.4	1.00	0.0088*
	AG	29.2	47.0	0.49 (0.29–0.84)	
	GG	20.8	13.6	1.20 (0.62–2.33)	
Dominant	AA	50.0	39.4	1.00	0.076
	AG-GG	50.0	60.6	0.65 (0.40–1.05)	
Recessive	AA-AG	79.2	86.4	1.00	0.11
	GG	20.8	13.6	1.66 (0.89–3.09)	
Over dominant	AA-GG	70.8	53.0	1.00	0.0024*
	AG	29.2	47.0	0.47 (0.28–0.77)	

* – $p < 0.05$.

its development. No significant differences in genotype distribution were observed in the other models. It is important to note that in our previous study, the distribution of the rs1800470 polymorphism in 225 children with end-stage liver failure did not show significant differences compared to healthy individuals. This discrepancy can likely be attributed to the absence of liver fibrosis in some recipients, where the indication for transplantation was based on conditions such as hepatitis and metabolic liver diseases, rather than liver fibrosis [7].

Our data show significant differences in the frequency of *TGF-β1* gene polymorphisms between children with liver fibrosis and healthy individuals, suggesting a potential association between these genetic variants and susceptibility to liver fibrosis.

Several studies have investigated the role of *TGF-β1* gene polymorphisms in liver fibrosis in adult patients, but their results have been inconsistent. The authors suggest that these discrepancies may be attributed to the ethnic origin of the populations studied [8–10]. While some studies in European populations show a link between liver fibrosis and *TGF-β1* gene polymorphisms, this association has not been consistently observed in some Asian populations. Furthermore, research has indicated that *TGF-β1* gene polymorphisms could also play a role in the development of myocardial fibrosis and myocardial infarction [11–13].

The findings of our study may hold both scientific and practical significance. They contribute to a deeper understanding of the role of *TGF-β1* gene polymorphisms in the development of tissue fibrosis and may be useful in assessing individual risk for fibrosis or identifying new therapeutic targets. Moreover, the presence of genotypes associated with an increased risk of fibrosis could be valuable in predicting post-transplant complications or individual responses to immunosuppressive therapy – areas that warrant further investigation.

CONCLUSION

Liver fibrosis remains a significant clinical issue, with its causes and underlying mechanisms still under active investigation. In the present study, liver fibrosis was linked to TGF-β1 gene polymorphisms. Specifically, among pediatric liver recipients with verified native liver fibrosis, the heterozygous genotype at the rs1800470 locus of the TGF-β1 gene was found to be 1.6 times less frequent compared to healthy individuals. This finding suggests a potential protective role of the heterozygous rs1800470 variant against the development of liver fibrosis. Continued investigation into the TGF-β1 gene polymorphisms may enable personalized prediction of post-transplant complications.

The authors declare no conflict of interest.

REFERENCES

1. *Gautier SV, Khomyakov SM*. Organ donation and transplantation in the Russian Federation in 2023. 16th Report from the Registry of the Russian Transplant Society. *Russian Journal of Transplantology and Artificial Organs*. 2024; 26 (3): 8–31. (In Russ.). https://doi.org/10.15825/1995-1191-2024-3-8-31.
2. *Kurabekova RM, Gichkun OE, Tsirulnikova OM, Pashkova IE, Vakurova EA, Shevchenko OP, Gautier SV*. High incidence of rare TGFB1 haplotypes in children with biliary atresia. *Russian Journal of Transplantology and Artificial Organs*. 2024; 26 (3): 168–175. (In Russ.). https://doi.org/10.15825/1995-1191-2024-3-168-175.
3. *Ge YZ, Wu R, Lu TZ, Jia RP, Li MH, Gao XF et al.* Combined effects of TGFB1 +869 T/C and +915 G/C polymorphisms on acute rejection risk in solid organ transplant recipients: A systematic review and meta-analysis. *PLoS One.* 2014; 9 (4): e93938. doi: 10.1371/journal.pone.0093938.
4. *Liu K, Liu X, Gu S, Sun Q, Wang Y, Meng J, Xu Z.* Association between TGFB1 genetic polymorphisms and chronic allograft dysfunction: a systematic review and meta-analysis. *Oncotarget.* 2017; 8 (37): 62463–62469.

5. *Leask A, Abraham DJ.* TGF-beta signaling and the fibrotic response. *FASEB J.* 2004; 18 (7): 816–827.
6. *de Brito WB, Queiroz MAF, da Silva Graça Amoras E, Lima SS, da Silva Conde SRS, Dos Santos EJM et al.* The TGFB1 -509C/T polymorphism and elevated TGF-β1 levels are associated with chronic hepatitis C and cirrhosis. *Immunobiology.* 2020; 225 (5): 152002. doi: 10.1016/j.imbio.2020.152002.
7. *Kurabekova RM, Gichkun OE, Tsirulnikova OM, Pashkova IE, Fomina VA, Shevchenko OP, Gautier SV.* Analysis of the Association between the Tgfb1 Gene Haplotype and Liver Diseases in Children. *Acta Naturae.* 2023; 15 (3): 75–81. doi: 10.32607/actanaturae.19425.
8. *Iriyoda TMV, Flauzino T, Costa NT, Lozovoy MAB, Reiche EMV, Simão ANC.* TGFB1 (rs1800470 and rs1800469) variants are independently associated with disease activity and autoantibodies in rheumatoid arthritis patients. *Clin Exp Med.* 2022; 22 (1): 37–45. doi: 10.1007/s10238-021-00725-9.
9. *Zhang XX, Bian RJ, Wang J, Zhang QY.* Relationship between cytokine gene polymorphisms and acute rejection following liver transplantation. *Genet Mol Res.* 2016; 15 (2): 15027599.
10. *Guo P, Sun X, Feng X, Zhang C.* Transforming growth factor-β1 gene polymorphisms with liver cirrhosis risk: A meta-analysis. *Infect Genet Evol.* 2018; 58: 164–170. doi: 10.1016/j.meegid.2017.12.019.
11. *Sudomoina MA, Sukhinina TS, Barsova RM, Favorov AV, Sakhnovich RM, Titov BV et al.* Comprehensive analysis of the association of inflammatory gene polymorphisms with myocardial infarction. *Molecular biology.* 2010; 44 (3): 463–471.
12. *Barsova RM, Titov BV, Matveeva NA, Favorov AV, Rybalkin IN, Vlasik TN et al.* Contribution of the TGFB1 Gene to Myocardial Infarction Susceptibility. *Acta Naturae.* 2012; 4 (2): 74–79.
13. *Gichkun OE, Shevchenko OP, Kurabekova RM, Mozheiko NP, Shevchenko AO.* The rs1800470 Polymorphism of the TGFB1 Gene Is Associated with Myocardial Fibrosis in Heart Transplant Recipients. *Acta Naturae.* 2021; 13 (4): 42–46. doi: 10.32607/actanaturae.11469.

The article was submitted to the journal on 22.10.2024

DOI: 10.15825/1995-1191-2024-4-171-177

THE FIRST EXPERIENCE IN NORMOTHERMIC *EX VIVO* KIDNEY PERFUSION (CASE REPORT)

A.V. Shabunin[1, 2], M.G. Minina[1, 3], P.A. Drozdov[1, 2], V.M. Sevostyanov[1], N.V. Grudinin[1, 3], V.K. Bogdanov[1, 3], D.A. Bankeev[1, 3], E.A. Tenchurina[1]

[1] Botkin Hospital, Moscow, Russian Federation
[2] Russian Medical Academy of Continuous Professional Education, Moscow, Russian Federation
[3] Shumakov National Medical Research Center of Transplantology and Artificial Organs, Moscow, Russian Federation

Objective: to assess if normothermic *ex vivo* machine perfusion (NMP) of a kidney from an expanded criteria donor (ECD) is feasible and safe. **Materials and methods.** NMP of the right kidney from an ECD was performed on a device developed at Botkin Hospital. A solution based on donor's blood with the addition of Ringer's lactate solution and human albumin was used for perfusion. The temperature in the circuit was maintained at 37 °C. Perfusion lasted for 203 minutes, after which the renal resistive index was almost halved from 0.33 to 0.16. 120 ml of urine was obtained. Results. The right kidney was successfully transplanted after perfusion. There was immediate function of the right renal graft in the postoperative period. The recipient's serum creatinine level was 530 μmol/L on day 1 following transplantation and 170 μmol/L on day 14 of discharge. The left kidney was preserved by static cold storage and further transplanted to the recipient. **Conclusion.** The use of NMP to preserve grafts obtained from ECDs is safe and feasible in clinical practice. Further studies are required to determine the clear indications for its use and to formulate an optimal procedure for its implementation.

Keywords: expanded criteria donor, kidney transplantation, perfusion devices.

INTRODUCTION

Organ transplantation is a remarkable achievement of the 20th century that has prolonged the lives of many thousands of patients. However, a major challenge in this field remains the persistent imbalance between the demand for donor organs and their limited availability [1]. One potential strategy to address this shortage is the use of expanded criteria donors (ECDs) [2]. In the context of kidney transplantation, ECDs are typically defined as donors aged 60 years and above, or those aged 50–59 years who present with at least two of the following comorbidities: cerebrovascular cause of death, a history of hypertension, or a serum creatinine level exceeding 132 μmol/L [3]. Despite this approach, organs from ECDs are often considered suboptimal due to concerns over their pathological condition and uncertainties regarding their functional adequacy post-transplant.

Traditional kidney preservation techniques rely primarily on hypothermia. By lowering tissue temperature, enzymatic activity is significantly slowed, with metabolic rates decreasing by approximately two- to threefold for every 10 °C decrease in temperature [4]. Hypothermia slows down adenosine triphosphate (ATP) depletion in the cell, preventing the breakdown of cellular structures. However, as the duration of cold preservation increases, ATP levels continue to decline, eventually leading to cellular necrosis [4, 5].

Cold ischemia time (CIT) is a well-established independent risk factor for post-transplant organ dysfunction and is closely associated with delayed graft function [6]. This is particularly relevant for organs retrieved from ECDs, which are inherently more susceptible to ischemic damage due to pre-existing risk factors that contribute to graft vulnerability [7–9]. While organ donation programs implement various strategies to minimize CIT – especially for ECD organs – logistical constraints often limit the effectiveness of these efforts. As a result, there is a growing interest in modifying mechanical preservation methods, such as dynamic perfusion, to reduce static cold storage duration and improve graft outcomes.

In the past decade, organ perfusion at subnormothermic and normothermic temperatures has garnered significant research interest. Unlike traditional approaches that suppress cellular activity, normothermic conditions aim to preserve aerobic metabolism and promote the restoration of cellular function. This strategy offers several potential advantages over static cold storage (SCS) and hypothermic machine perfusion, including minimizing or avoiding cold ischemia-induced injury. By maintaining physiologic conditions, normothermic machine perfusi-

Corresponding author: Elmira Tenchurina. Address: 5, Vtoroy Botkinskiy proezd, Moscow, 125284, Russian Federation. Phone: (967) 113-87-64. E-mail: arimle@inbox.ru

on (NMP) can activate cellular recovery mechanisms and enable functional assessment of donor kidneys.

To explore the clinical applicability of NMP within our hospital setting, we developed a preliminary perfusion protocol. Using this approach, we perfused one kidney from a donor older than 60 years prior to transplantation. Both kidneys were subsequently transplanted into recipients at Botkin Hospital. The clinical details and outcomes of this case are presented below.

CLINICAL CASE

Donor characteristics

The donor was a 65-year-old male who succumbed to a traumatic brain injury. He remained in the intensive care unit for 55 hours prior to organ procurement. During this period, there were no episodes of circulatory arrest or hypotension. Peak vasopressor support did not exceed 350 ng/kg/min. Initial laboratory values showed a urea level of 4.3 mmol/L and a serum creatinine level of 92.0 μmol/L.

Following the declaration of brain death, the heart, liver, and both kidneys were retrieved. Examination of the right and left kidneys revealed medium-sized organs with a homogeneous color and no tumor-like formations. Each kidney had a single renal artery originating from the aorta, which exhibited atherosclerotic changes, and a single renal vein. Both kidneys were deemed suitable for transplantation and were subsequently transported to Botkin Hospital.

Kidney preservation under normothermic machine perfusion

The NMP circuit was developed at Botkin Hospital and is based on a Maquet heart-lung machine equipped with a roller pump and a Skipper AF Plus oxygenator (Eurosets). A custom-designed perfusion container, created using 3D modeling, was used to accommodate the kidney during NMP. A view of the right kidney within this container during perfusion is shown in Fig. 1.

The perfusion circuit was primed with 1200 ml of perfusate composed of donor blood collected prior to in situ cold perfusion (800 ml), Ringer's lactate solution, and human albumin, adjusted to achieve a target hematocrit of 15–25%. The right kidney graft was positioned in the perfusion container and connected to both arterial and venous circuits. A thin venous catheter was inserted into the ureter to facilitate urine drainage. Synthetic glucocorticoids, heparin, glucose, insulin, prostaglandin E1, amino acid solution, antibiotics, and sodium bicarbonate were injected into the circuit during perfusion. The perfusion temperature was maintained at 37 °C using a stationary Maquet temperature control device.

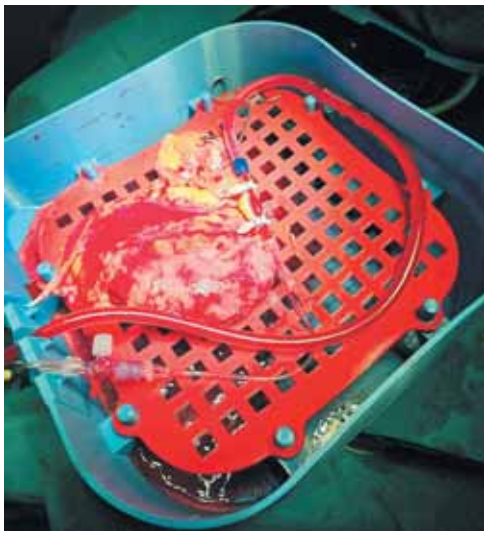

Fig. 1. View of a donor kidney in a normothermic perfusion container

Arterial blood samples were taken periodically to monitor acid–base balance, electrolyte levels, and other biochemical parameters. Renal artery pressure was continuously measured and displayed on a separate monitor. Perfusion pressure increased from 90 mmHg at the start to 130 mmHg by the end of the procedure. Urine output was quantitatively measured throughout the perfusion.

The interval between initiation of in situ cold perfusion during organ retrieval and commencement of ex vivo NMP was 300 minutes (5 hours). NMP lasted for 203 minutes. Details are presented in Table 1.

At 15 minutes after initiation of perfusion, urine output was 10 ml. Over the full duration of perfusion, a total of 120.0 ml of urine was produced. Clinical and biochemical analysis of the urine was performed, as detailed in Table 2.

Upon completion of NMP, the right kidney was deemed suitable for transplantation and was successfully transplanted into the recipient. The left kidney was transplanted without undergoing additional perfusion.

Result of zero-time kidney biopsies

The right kidney biopsy revealed 15 glomeruli, which appeared anemic and ischemic. Tubular structures demonstrated granular protein dystrophy and epithelial cell necrosis. Arterioles and interstitium showed no pathological features. The left kidney biopsy contained 7 glomeruli, one of which was globally sclerotic. Several glomeruli showed signs of anemia and ischemia. Tubules exhibited granular protein dystrophy and epithelial cell necrosis. Two muscular arteries and the arterioles were without pathological findings. Microfocal interstitial sclerosis was observed.

Conclusion: Findings are consistent with mild to moderate acute tubular necrosis in both kidneys.

Right kidney transplant recipient: *The recipient was a 52-year-old woman with end-stage CKD secondary to polycystic kidney disease. She had been undergoing renal replacement therapy (RRT) via hemodialysis since 2019 and was placed on the transplant waiting list on January 9, 2020. Kidney transplantation was performed on October 10, 2023.*

Cold kidney storage lasted 300 minutes prior to NMP and 132 minutes following NMP. Upon restoration of blood flow, there were no visible signs of reperfusion syndrome, and urine outflow via the ureter was observed.

A Doppler ultrasound scan performed immediately post-transplantation revealed a resistive index (RI) of 0.75 (see Fig. 2).

Table 1

Parameters of normothermic *ex vivo* kidney perfusion

Measurement time points / Perfusion parameters	Donor blood from the bag (before perfusion)	0 min, start of perfusion	15 min	45 min	90 min	180 min
Renal artery pressure, mmHg		60	90	96	134	130
Perfusion rate, mL/min		180	400.0	430.0	800.0	800.0
Perfusion pressure/rate ratio, resistive index		0.33	0.22	0.22	0.16	0.16
Perfusion temperature, °C		–	37.0	37.1	37.1	37.0
Diuresis, mL		–	10.0	–	30.0	80.0
pH	6.83	6.72	7.22	7.48	7.56	7.99
pO_2, mmHg	153.0	190.0	180.0	197.0	278.0	293.0
pCO_2, mmHg	120.8	34.4	16.8	9.3	9.4	7.0
K^+, mmol/L	2.6	3.0	2.9	2.8	3.0	3.3
Na, mmol/L	153.0	152.0	149.0	151.0	154.0	162.0
BE, mmol/L	–13.0	–30.0	–21.0	–17.0	–14.0	2.0
Hct, %	<15.0	<15.0	<15.0	<15.0	<15.0	<15.0
Glucose, mmol/L	35.2	10.7	8.3	8.3	9.4	15.0
Urea, mmol/L			2.0			1.7
Creatinine, μmol/L			44.0			44.0

Note: pO_2, partial pressure of oxygen; pCO_2, partial pressure of carbon dioxide; K^+, potassium; Na, sodium; BE, base excess; Hct, hematocrit.

Table 2

Analysis of a urine sample produced by kidney during *ex-vivo* normothermic perfusion

Parameters	120th minute of perfusion
Urinalysis	
Color	Light yellow
Transparency	Full
Specific weight	1.018
pH	5.5
Glucose, mmol/L	not detected
Protein, g/L	0.1
Ketone bodies, mmol/L	not detected
Urobilinogen, mmol/L	3.4
Leukocytes, count/μL	15.0
Epithelium, per field of view	0–5
Erythrocytes, per field of view	40.0
Cylinders, per field of view	0
Urine chemistry	
K^+, mmol/L	49.0
Na^+, mmol/L	62.0
Albumin, mg/L	573.72
Creatinine, μmol/L	181.0

Note: K^+, potassium; Na, sodium.

Urine output on postoperative day 1 was 600 mL. Postoperative hemodialysis was not required. By the time of discharge on postoperative day 14, daily urine output had increased to 1900 mL. Laboratory values at discharge showed a blood urea level of 25.1 mmol/L and a serum creatinine level of 170 μmol/L (see Table 3).

Left kidney transplant recipient (non-perfused): *A 54-year-old woman with end-stage CKD secondary to chronic glomerulonephritis and nephrosclerosis. She had been receiving RRT via hemodialysis since September 2021 and was placed on the transplant waiting list on May 13, 2022. Her first kidney transplantation was performed on November 18, 2022; however, the graft was removed on postoperative day 7. A kidney re-transplantation was successfully performed on October 10, 2023, with evidence of primary graft function. On postoperative day 1, serum creatinine was 752 μmol/L and blood urea was 20.6 mmol/L. Urine output reached 600 mL within the first 24 hours. No postoperative hemodialysis was required. At the time of discharge on day 14, the patient had a daily urine output of 1900 mL, a blood urea level of 25.1 mmol/L, and a serum creatinine level of 170 μmol/L (see Table 3).*

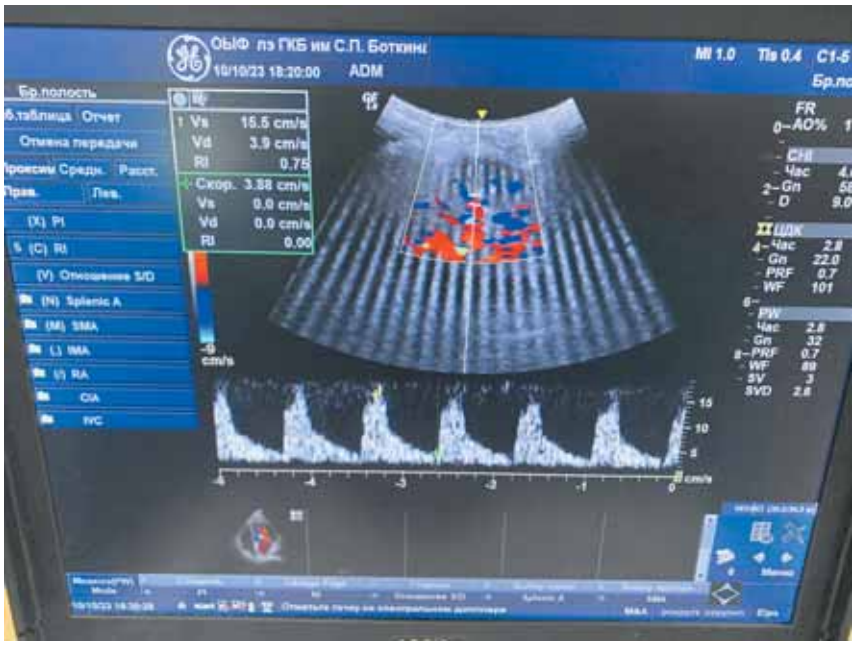

Fig. 2. Doppler ultrasound of the right kidney graft upon completion of transplantation to the recipient

Table 3

Characteristics of right kidney recipient

Characteristics	Right kidney recipient
Gender, male/female	Female
Age, years	52
Diagnosis	Stage 5 CKD, Polycystic kidney disease
Start of hemodialysis	2019
Number of HLA-A, B, Dr mismatches	4
Total cold ischemia time, min	432.0
Resistive index RI, at the end of surgery	0.75
RI, day 1	0.8
RI, day 7	0.76
RI , at discharge	0.67
Graft function	Primary
Number of hemodialysis sessions after transplantation	0
Urea/creatinine, day 1, mmol/L, μmol/L	14.1/530
Urea/creatinine, day 6, mmol/L, μmol/L	26.7/300
Urea/creatinine at discharge, mmol/L, μmol/L	25.1/170
Diuresis, day 1, mL	600
Diuresis at discharge, mL	1900
Inpatient stay, bed days	14

Note: RI, resistive index.

DISCUSSION

NMP represents a paradigm shift in donor organ preservation, offering the dual advantage of organ recovery and real-time functional assessment prior to transplantation. This report presents the first documented case of normothermic kidney perfusion (NKP) in clinical practice in Russia. The choice of a donor aligns with the current international strategy of using NMP for ECDs and donors after circulatory death. In this case, the donor was a 65-year-old individual who died from traumatic brain injury, with biochemical markers of renal function within normal reference ranges.

The perfusion circuit, composition of the perfusate, and perfusion protocol are similar to those described by Nicholson and Hosgood [10], leading experts from the United Kingdom with extensive experience in NKP. In 2013, Nicholson and Hosgood [10] published the results of the first clinical application of NMP. Between December 2010 and August 2012, they subjected 18 kidneys

from ECDs to NMP. The transplant outcomes were compared with a control group of 47 recipients who received kidneys from ECDs preserved using static cold storage between March 2008 and August 2012 at the same transplant center. Both groups were comparable in terms of donor and recipient age, cold ischemia time, and were limited to first-time kidney transplant recipients.

During perfusion, renal blood flow was continuously monitored. The intrarenal resistive index (RI) was calculated as the ratio of mean arterial pressure to perfusion rate, measured every 5 minutes during the first 15 minutes and then every 15 minutes until the end of perfusion. Total urine output was recorded, and blood gas analysis was performed before and after perfusion to assess acid-base balance [10].

In our case, kidney perfusion was initiated at an arterial pressure of 60 mmHg, which gradually increased throughout the procedure, reaching 130 mmHg by the 180th minute. The perfusion rate also rose progressively, from 180.0 ml/min to 800.0 ml/min. RI decreased almost twofold during the perfusion, from 0.33 to 0.16. The temperature within the perfusion circuit was consistently maintained at 37 °C.

Nicholson et al. [10] reported more moderate perfusion parameters, maintaining mean arterial pressures between 52 and 70 mmHg during NMP. While all kidneys in their study demonstrated some fluctuations in RI during the initial 15 minutes of perfusion, a general downward trend in RI was observed. The authors found a statistically significant correlation between RI and donor age ($p = 0.027$), as well as between RI and reduced urine output during perfusion ($p = 0.035$).

Similar perfusion characteristics were reported by Canadian authors in their publication detailing the first clinical experience with normothermic perfusion in North America [11]. In their protocol, arterial pressure was initially set at 75 mmHg and maintained at 65 mmHg by adjusting the centrifugal pump speed. At the start of perfusion (0 hour), median renal artery blood flow was 279 mL/min (range: 60–547 mL/min), which increased over time. After one hour of perfusion, median flow had risen to 346 mL/min (range: 206–680 mL/min).

In our case, the partial pressure of oxygen (pO_2) at the beginning of NMP was below 200.0 mmHg (measured at 190.0 mmHg) and progressively increased throughout the procedure, reaching 293.0 mmHg by the end. The perfusate was prepared using the donor's blood, which was transported in a blood collection bag. Initial analysis of the acid-base status of the perfusate revealed severe acidosis, with a pH of 6.83, markedly elevated pCO_2 (120.8 mmHg), significant base deficit, and extremely high glucose levels. These findings are consistent with anaerobic conditions during donor blood preservation.

Most of these abnormalities were rapidly corrected following the initiation of perfusion, owing to the combined effects of the roller pump and oxygenator, as well as the introduction of sodium bicarbonate solution, potassium chloride to correct hypokalemia, and short-acting insulin to manage hyperglycemia. However, a persistent base (alkali) deficit was observed throughout most of the perfusion, despite repeated sodium bicarbonate administration. We hypothesize this may be due to impaired hydrogen ion excretion and bicarbonate reabsorption, indirectly indicating suboptimal renal function during perfusion – though this hypothesis requires further investigation.

Urine output was first noted at the 15th minute of perfusion. Due to the absence of further active diuresis, furosemide was introduced into the circuit, resulting in a positive diuretic response.

Overall, analysis of both hemodynamic and metabolic parameters during perfusion underscores the importance of strict adherence to protocol. Introduction of drugs into the circuit should be performed through the designated perfuser to prevent abrupt fluctuations in perfusate composition, especially during extended perfusion sessions. In this case, NMP lasted for 203 minutes.

In the study by Mazilescu et al. [11], 13 human kidney grafts were perfused for a median duration of 171 minutes (range: 44–275 minutes). One of the notable findings was the consistently high oxygen level in the perfusate, with a reported median pO_2 of 562 mmHg. A single dose of bicarbonate solution was administered, following which the pH remained stable throughout the perfusion period. Urine output was not observed in 2 of the 13 cases. The authors highlighted a high degree of variability in urine production across the cohort, with a median of 16 mL and a range of 1–104.5 mL during perfusion.

In our study, lactate levels in the perfusate were not measured. However, Mazilescu et al. [11] reported that lactate concentrations remained relatively stable during perfusion, with a median value of 11.6 mmol/L at baseline (range: 7.9–15.25 mmol/L) and 10.13 mmol/L at the end of perfusion (range: 3.06–15.6 mmol/L). These findings suggest that stable lactate levels, despite being relatively high, may be indicative of satisfactory renal perfusion. The authors found no significant differences in perfusion characteristics between grafts that developed delayed graft function and those with immediate (primary) function. Specifically, renal blood flow and intrarenal RI at baseline (313 *vs.* 260 mL/min, $P = 0.23$; RI 0.25 *vs.* 0.31, $P = 0.41$) and at the end of perfusion (550 *vs.* 372 mL/min, $P = 0.12$; RI 0.14 *vs.* 0.19, $P = 0.12$) were comparable between the two groups. Similarly, perfusate parameters, including pH, lactate, pO_2, pCO_2, and urine production during perfusion did not differ significantly

and showed no correlation with post-transplant graft function or urine output.

It is also worth noting that Mazilescu et al. used a perfusate based on dextran/albumin (Steen solution) supplemented with red blood cells – a composition commonly used in *ex vivo* lung and liver perfusion studies [12, 13]. This solution provides high oncotic pressure, which may account for the generally low urine output observed during perfusion. The authors highlight that future research should shift focus toward analyzing the composition of urine produced during perfusion, rather than volume alone, as a more meaningful indicator of post-transplant kidney function.

CONCLUSION

Our initial experience with normothermic perfusion of a donor kidney demonstrated the safety and technical feasibility of this technique in clinical practice. Moving forward, there is a need to develop a structured study protocol to assess the applicability and effectiveness of NMP in kidneys retrieved from donors following an out-of-hospital cardiac arrest.

The authors declare no conflict of interest.

REFERENCES

1. *Lewis A, Koukoura A, Tsianos GI, Gargavanis AA, Nielsen AA, Vassiliadis E.* Organ donation in the US and Europe: the supply *vs.* demand imbalance. *Transplant Rev (Orlando)*. 2021 Apr; 35 (2): 100585.
2. *Summers DM, Watson CJ, Pettigrew GJ, Johnson RJ, Collett D, Neuberger JM, Bradley JA.* Kidney donation after circulatory death (DCD): state of the art. *Kidney Int.* 2015 Aug; 88 (2): 241–249.
3. *Port FK, Bragg-Gresham JL, Metzger RA, Dykstra DM, Gillespie BW, Young EW et al.* Donor characteristics associated with reduced graft survival: an approach to expanding the pool of kidney donors. *Transplantation.* 2002 Nov 15; 74 (9): 1281–1286.
4. *Van't Hoff MJH*. Etudes de dynamique chimique. *Recueil des Travaux Chimiques des Pays-Bas.* 2010; 3 (10): 333–336.
5. *Kalogeris T, Baines CP, Krenz M, Korthuis RJ.* Ischemia/reperfusion. *Compr Physiol*. 2016 Dec 6; 7 (1): 113–170.
6. *Summers DM, Johnson RJ, Hudson A, Collett D, Watson CJ, Bradley JA.* Effect of donor age and cold storage time on outcome in recipients of kidneys donated after circulatory death in the UK: a cohort study. *Lancet.* 2013 Mar 2; 381 (9868): 727–734.
7. *Collins MG, Chang SH, Russ GR, McDonald SP.* Outcomes of transplantation using kidneys from donors meeting expanded criteria in Australia and New Zealand, 1991 to 2005. *Transplantation.* 2009 Apr 27; 87 (8): 1201–1209.
8. *Fraser SM, Rajasundaram R, Aldouri A, Farid S, Morris-Stiff G, Baker R et al.* Acceptable outcome after kidney transplantation using "expanded criteria donor" grafts. *Transplantation.* 2010 Jan 15; 89 (1): 88–96.
9. *Metzger RA, Delmonico FL, Feng S, Port FK, Wynn JJ, Merion RM.* Expanded criteria donors for kidney transplantation. *Am J Transplant*. 2003; 3 (4): 114–125.
10. *Nicholson ML, Hosgood SA.* Renal transplantation after *ex vivo* normothermic perfusion: the first clinical study. *Am J Transplant*. 2013 May; 13 (5): 1246–1252.
11. *Mazilescu LI, Urbanellis P, Kim SJ, Goto T, Noguchi Y, Konvalinka A et al.* Normothermic *Ex Vivo* Kidney Perfusion for Human Kidney Transplantation: First North American Results. *Transplantation.* 2022 Sep 1; 106 (9): 1852–1859.
12. *Cypel M, Yeung JC, Liu M, Anraku M, Chen F, Karolak W et al.* Normothermic *ex vivo* lung perfusion in clinical lung transplantation. *N Engl J Med*. 2011 Apr 14; 364 (15): 1431–1440.
13. *Selzner M, Goldaracena N, Echeverri J, Kaths JM, Linares I, Selzner N et al.* Normothermic *ex vivo* liver perfusion using steen solution as perfusate for human liver transplantation: first North American results. *Liver Transpl*. 2016 Nov; 22 (11): 1501–1508.

The article was submitted to the journal on 28.05.2024

DOI: 10.15825/1995-1191-2024-4-178-183

BACTERIAL TRANSLOCATION IN DECEASED ORGAN DONORS

O.V. Petkevich[1], V.M. Mitsura[1, 2], V.N. Martinkov[1], D.L. Dugin[1], Z.A. Dundarov[2]

[1] Republican Research Center for Radiation Medicine and Human Ecology, Gomel, Republic of Belarus
[2] Gomel State Medical University, Gomel, Republic of Belarus

Objective: to ascertain the prevalence and risk factors for bacterial translocation (BT) in brain-dead donors (BDDs) during organ and tissue retrieval in health care facilities. **Materials and methods**. The study included 62 BDDs, featuring 44 males (71%) and 18 females (29%), aged 17 to 64 years. Organ was retrieved in health-care institutions located in Gomel Oblast in 2019–2022. Bacteriological examination of biopsy material taken from different parts of the intestine, mesenteric lymph nodes (MLNs) and spleen was carried out. The presence of BT was validated when bacterial growth was obtained from homogenized MLNs and(or) spleen by isolating an identical strain from the intestinal lumen. The anthropometric characteristics of BDDs, hematologic, biochemical parameters, and the length of stay in the intensive care unit (ICU) were assessed. **Results.** Evidence of bacterial translocation was detected in 22 BDDs (35.5%, 95% CI 24.7–48.0). Growth in MLNs and in spleen biopsies was noted in 21 (95.5%) and 7 (31.8%) patients, respectively. The BDDs were categorized into two groups depending on the presence of BT, and the main characteristics were compared. ROC analysis was used to determine the prognostic significance of the main parameters. Risk factors for BT were serum sodium level >144 mmol/L (AUC = 0.759) at the time of retrieval, weight >89 kg (AUC = 0.756), BMI >27.5 (AUC = 0.709), decreased hemoglobin <126 g/L (AUC = 0.665), and ICU stay >2 days (AUC = 0.656). **Conclusion.** Bacterial translocation is found in 35.5% of BDD cases, and it is accompanied by penetration of bacteria and yeast-like fungi into the MLNs and spleen. Bacterial translocation is linked to excess body weight, hypernatremia, prolonged ICU stay, and decreased hemoglobin levels at the time of retrieval. These factors should be taken into account in the medical management of brain-dead donors (organ donor conditioning).

Keywords: deceased organ donor, bacterial translocation, organ transplantation, transplantation coordination.

INTRODUCTION

Despite significant advances in therapeutic techniques, organ transplantation remains the only definitive treatment for end-stage organ diseases and is often the sole option when all other conservative treatments have failed [1–3]. With the continuous increase in the number of patients on the transplant waiting list and a decrease in the number of suitable donors, there is a growing organ shortage. This has led to the necessity of expanding the criteria for selecting viable donors. As a result, there is a trend towards accepting older organ donors (brain-dead donors, BDDs), extending the duration of the donor's stay in the intensive care unit (ICU), and adopting more flexible criteria for various homeostatic parameters, such as serum sodium levels, hyperglycemia, and acid-base balance shifts. In addition, there is consideration for donors with sanitized infectious foci [4–6].

Brain death triggers numerous pathological processes that directly impact both the quantity and quality of organs available for transplantation. With the expansion of eligibility criteria for organ donors and prolonged stays in the ICU with highly invasive medical support, a deeper understanding of the underlying pathophysiology of transplant-related organ dysfunction is essential to fully optimize the donor pool [5]. In kidney and liver transplantation, recipients of allografts harvested from deceased donors with a beating heart experience a significantly higher rate of post-transplant complications, such as acute rejection or chronic graft dysfunction, compared to those receiving organs from living donors, leading to worse overall transplant outcomes [6]. The decline in transplant effectiveness cannot be solely attributed to differences in the antigenic composition of donor-recipient pairs. Some studies suggest that the strength of immune response is more closely related to the extent of injury to the donor organ than to the degree of mismatches in donor and recipient human leukocyte antigens (HLA) [7].

Bacterial endotoxemia is a cytotoxic factor that causes injury to potential donor organs, primarily due to increased intestinal permeability. Bacterial translocation (BT) can occur in up to 30–40% of critically ill patients, according to various sources, and is directly associated with elevated inflammatory markers and reduced activity of blood coagulation factors. In response to these inflammatory markers, antigen-presenting T cells trigger cytotoxic reactions, leading to organ damage and dysfunction [8–11].

Corresponding author: Oleg Petkevich. Address: 290, Ilyicha str., Gomel, 246040, Republic of Belarus.
Phone: +375 232 530830 (fax); +375296587154 (mob.). E-mail: tcgomel@gmail.com

Given this, it can be concluded that BT is a common condition in potential organ donors. However, the precise mechanisms and factors that correlate with the risk of BT development in effective organ donors are still not fully understood. Identifying these factors and implementing measures to mitigate them could reduce the incidence of organ donor injury and ultimately improve transplant outcomes [6–8].

Objective: to determine the prevalence and risk factors for BT in brain-dead donors (BDDs) during organ and tissue procurement in healthcare facilities.

MATERIALS AND METHODS

This observational cohort study included BDDs from whom solid organs were procured, following the legal methodology established for organ donation. Organ procurement was carried out at healthcare facilities in Gomel Oblast (Belarus) from 2019 to 2022. The exclusion criterion was the inability to obtain biopsy material due to a lack of access to the abdominal cavity during procurement (e.g., mono-heart procurement without laparotomy, lung procurement, or heart-lung procurement without laparotomy, vascular allograft procurement). The study received approval from the Ethics Committee of Gomel State Medical University.

The study included 62 BDDs, comprising 44 males (71%) and 18 females (29%), aged between 17 and 64 years. Brain death resulted from traumatic brain injury in 19 cases (30.6%) and non-traumatic brain injury in 43 cases (69.4%). Among the non-traumatic cases, 36 (58.1%) were due to intracranial hemorrhage and 7 (11.3%) to atherothrombotic cerebral circulatory disorders.

All BDDs were managed in the ICU and received enteral nutrition as follows:

– 16 donors (25.8%) received enteral nutrition based on the clinical protocol of the Ministry of Health of the Republic of Belarus;
– 19 donors (30.6%) received standardized enteral nutrition ("Enterolin," 1 kcal/mL) at a dosage of 20 mL/kg/day, in accordance with national clinical guidelines for intensive care in cerebrovascular insufficiency;
– 27 donors (43.6%) received standardized "Enterolin" enteral nutrition with continuous administration via enteral pumps, accompanied by pharmacological support (prokinetics, eubiotics, and antacids) at therapeutic dosages.

The anthropometric parameters, key hematological and biochemical indicators, as well as ICU length of stay, were assessed for all BDDs. The characteristics of BDDs at the time of organ retrieval are presented in Table 1.

Table 1

Characteristics of BDDs at the time of retrieval

Indicator	M ± SD
Age (years)	46.8 ± 10.7
Height (cm)	174.4 ± 6.7
Weight (kg)	80.9 ± 10.9
Body mass index (kg/m^2)	26.6 ± 3.5
ICU stay (days)	3.7 ± 2.3
Hemoglobin (g/L)	139.7 ± 16.1
Red blood cells (×10^{12}/L)	4.19 ± 0.79
Hematocrit (L/L)	0.42 ± 0.04
Platelets (×10^9/L)	274.0 ± 72.5
Leukocytes (×10^9/L)	11.4 ± 3.5
Urea (mmol/L)	5.9 ± 1.3
Creatinine (μmol/L)	76.7 ± 21.0
pH	7.39 ± 0.03
Lactate (mmol/L)	1.28 ± 0.51
Na (mmol/L)	146.0 ± 8.6
K (mmol/L)	4.23 ± 0.44

Bacteriological analysis was performed on biopsy samples taken from various sections of the intestine, mesenteric lymph nodes (MLNs), and spleen. BT was confirmed when bacterial growth was detected in homogenates of the MLNs and/or spleen, with identification of a strain identical to that isolated from the intestinal lumen.

Statistical processing and data analysis were conducted using SPSS Statistics for Windows, version 26 (IBM Corp., USA). Quantitative variables are presented as mean ± standard deviation (M ± SD). The Mann–Whitney U test was applied to compare quantitative variables between two independent groups. The predictive value of various parameters was evaluated using receiver operating characteristic (ROC) curve analysis in MedCalc version 19.4.1. The area under the curve (AUC), along with the corresponding 95% confidence interval (CI), sensitivity (Se), and specificity (Sp) at the determined cut-off points, were calculated. A p-value of less than 0.05 was considered statistically significant.

RESULTS

BT signs were detected in 22 BDDs (35.5%; 95% CI: 24.7–48.0). In most cases, microorganisms characteristic of the intestinal microflora were detected in MLNs (21 patients, 95.5%), and in a smaller proportion of cases, in the spleen biopsy samples (7 patients, 31.8%). The detected microorganisms included *Enterococcus faecium*, *Escherichia coli*, *Klebsiella pneumoniae*, *clostridia*, *Staphylococcus haemolyticus*, and yeast fungi such as *Candida albicans* and *Saccharomyces cerevisiae* found in various combinations.

Based on the presence or absence of BT, the BDDs were divided into two groups, and their main clinical and laboratory characteristics were compared (Table 2).

ROC analysis was performed to evaluate the predictive value of parameters that demonstrated statistical

significance at $p < 0.1$ between groups, and to determine their boundary values. The results are presented in descending order of AUC in Table 3 and illustrated in Figs. 1 and 2.

Table 2

Comparison of the characteristics of BDDs by the presence of bacterial translocation

Indicator	Group 1 (BT), n = 22	Group 2 (no BT), n = 40	P
Age (years)	48.0 ± 10.1	46.4 ± 11.2	0.802
Height (cm)	175.0 ± 6.4	173.7 ± 6.9	0.338
Weight (kg)	87.5 ± 10.8	77.0 ± 6.9	**0.0007**
Body mass index (kg/m^2)	27.8 ± 3.6	26.1 ± 3.2	**0.071**
Stay in ICU (days)	4.0 ± 2.7	2.5 ± 1.9	**0.044**
Hemoglobin (g/L)	130.5 ± 16.4	142.0 ± 15.3	**0.033**
Erythrocytes (×10^{12}/L)	4.51 ± 0.80	4.05 ± 0.78	0.216
Hematocrit (l/L)	0.41 ± 0.04	0.42 ± 0.05	0.844
Platelets (×10^9/L)	250.0 ± 74.9	278.5 ± 71.2	0.353
Leukocytes (×10^9/L)	12.0 ± 3.5	11.0 ± 3.5	0.269
Urea (mmol/L)	5.8 ± 4.3	5.7 ± 1.3	0.901
Creatinine (μmol/L)	82.5 ± 21.8	72.0 ± 20.8	0.594
pH	7.38 ± 0.03	7.39 ± 0.03	0.901
Lactate (mmol/L)	1.25 ± 0.54	1.15 ± 0.48	0.765
Na (mmol/L)	152.5 ± 7.4	143.0 ± 8.1	**0.0006**
K (mmol/L)	4.20 ± 0.46	4.20 ± 0.42	0.594

Table 3

Prognostic significance of laboratory and clinical parameters (in descending order of AUC)

Indicator	AUC; 95% CI	Cut-off	Se, %	Sp, %
Na (mmol/L)	0.759; 0.633–0.858	>148	81.8	75.0
Weight (kg)	0.756; 0.631–0.856	>89	50.0	87.5
Body mass index (kg/m^2)	0.709; 0.579–0.817	>27.5	68.2	72.5
Hb (g/L)	0.665; 0.534–0.780	≤126	45.5	87.5
ICU stay (days)	0.656; 0.524–0.772	>2	72.7	50.0

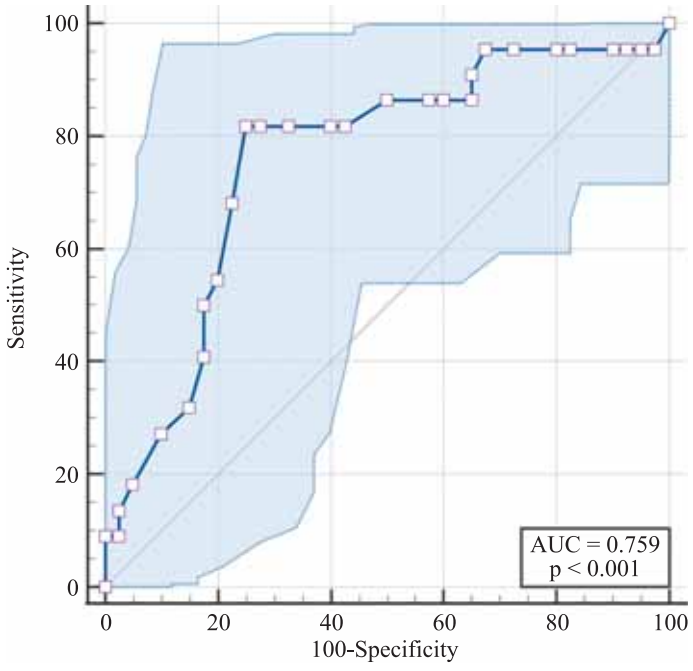

Fig. 1. Prognostic significance of serum sodium levels at the time of retrieval for the presence of BT in BDDs

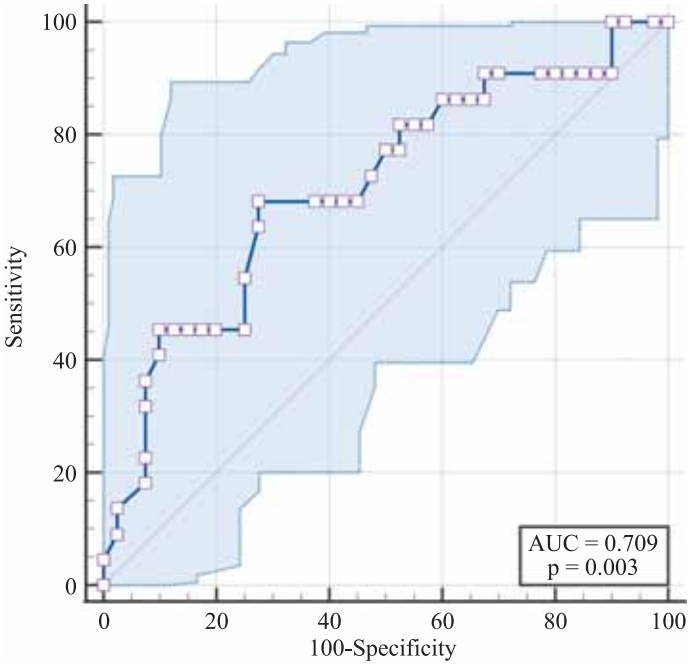

Fig. 2. Prognostic significance of serum sodium levels at the time of organ retrieval for the presence of BT in BDDs

DISCUSSION

The analysis identified the most significant predictor of BT in BDDs as a serum sodium level exceeding 148 mmol/L at the time of organ procurement, followed by a body weight over 89 kg (BMI >27.5). Additionally, a hemoglobin level ≤126 g/L and an ICU stay longer than two days were also associated with an increased risk of BT. Given the comparable predictive value of body weight and BMI, we recommend prioritizing BMI as a more objective and standardized metric, as it accounts for the donor's height.

Our findings align with previous reports indicating that hypernatremia and excessive body weight in BDDs are significant factors contributing to increased intestinal permeability [8, 9]. These observations underscore the importance of careful medical monitoring of potential organ donors prior to organ retrieval. The presence of BT may be associated with endotoxinemia, which can result in donor allograft injury and negatively affect post-transplant graft function [12].

CONCLUSION

The incidence of BT among effective organ donors was found to be 35.5%, characterized by the penetration of bacteria and yeast-like fungi into the MLNs and spleen. BT was significantly associated with excess body weight, hypernatremia, prolonged ICU stay, and reduced hemoglobin levels at the time of organ procurement. These findings highlight the importance of considering these risk factors during medical management of potential organ donors, as BT may contribute to allograft dysfunction and adversely impact transplant outcomes.

The authors declare no conflict of interest.

REFERENCES

1. *Reznik ON, Reznik AO*. Social bases for the dialogue on deceased organ donation. *Russian Journal of Transplantology and Artificial Organs*. 2023; 25 (4): 174–180. (In Russ.). https://doi.org/10.15825/1995-1191-2023-4-174-180.
2. *Salimov UR, Shcherba AE, Rummo OO*. Bacterial complications after liver transplantation. Promising directions for further research. *Transplantologiya. The Russian Journal of Transplantation*. 2023; 15 (2): 238–250. (In Russ.). https://doi.org/10.23873/2074-0506-2023-15-2-238-250.
3. *Shabunin AV, Loran OB, Pushkar DYu, Veliev EI, Minina MG, Drozdov PA et al*. Integrated strategy for preventing delayed renal graft function. *Russian Journal of Transplantology and Artificial Organs*. 2023; 25 (2): 8–14. (In Russ.). https://doi.org/10.15825/1995-1191-2023-2-8-14.
4. *Kuzmin DO, Manukovsky VA, Bagnenko SF, Reznik ON, Ananiev AN, Vorobyeva OA et al*. Use of polyclonal antibodies in brain-dead donors in kidney transplantation. *Russian Journal of Transplantology and Artificial Organs*. 2022; 24 (4): 124–134. (In Russ.). https://doi.org/10.15825/1995-1191-2022-4-124-134.
5. *Bera KD, Shah A, English MR, Harvey D, Ploeg RJ*. Optimisation of the organ donor and effects on transplanted organs: a narrative review on current practice and future directions. *Anaesthesia*. 2020 Sep; 75 (9): 1191–1204. https://doi.org/10.1111/anae.15037.
6. *Tsiuryn YO, Yakubtsevich RE*. Modern view on the donor management of brain-dead donors. *Journal of the Grod-*

no State Medical University. 2022; 20 (5): 485–493. (In Russ.). https://doi.org/10.25298/2221-8785-2022-20-5-485-493.

7. *Zirpe K, Gurav S*. Brain Death and Management of Potential Organ Donor: An Indian Perspective. *Indian J Crit Care Med*. 2019 Jun; 23 (Suppl 2): S151–S156. doi: 10.5005/jp-journals-10071-23194. PMID: 31485125; PMCID: PMC6707496.
8. *Kane TD, Johnson SR, Alexander JW, Craycraft TK*. Bacterial translocation in organ donors: clinical observations and potential risk factors. *Clin Transplant*. 1997; 11 (4): 271–274.
9. *Uçar Bİ, Uçar GI.* Intestinal Barrier Dysfunction, Bacterial Translocation and Inflammation: Deathly Triad in Sepsis. *Infections and Sepsis Development*. *IntechOpen*. 2021 Oct 27: 303–328. doi: 10.5772/intechopen.99554.
10. *Moharem HA, Fetouh FA, Darwish HM, Ghaith D, Elayashy M, Hussein A et al.* Effects of bacterial translocation on hemodynamic and coagulation parameters during living-donor liver transplant. *BMC Anesthesiol*. 2018 Apr 25; 18 (1): 46. doi: 10.1186/s12871-018-0507-7. PMID: 29699477; PMCID: PMC5921288.
11. *Rodríguez-Laiz GP, Zapater P, Melgar P, Alcázar C, Franco M, Giménez P et al.* Liver Transplantation Group. Bacterial DNA translocation contributes to systemic inflammation and to minor changes in the clinical outcome of liver transplantation. *Sci Rep*. 2019 Jan 29; 9 (1): 835. doi: 10.1038/s41598-018-36904-0. PMID: 30696924; PMCID: PMC6351615.
12. *Carron C, Pais de Barros JP, Gaiffe E, Deckert V, Adda-Rezig H, Roubiou C et al.* End-Stage Renal Disease-Associated Gut Bacterial Translocation: Evolution and Impact on Chronic Inflammation and Acute Rejection After Renal Transplantation. *Front Immunol*. 2019 Aug 16; 10: 1630. doi: 10.3389/fimmu.2019.01630.

The article was submitted to the journal on 04.04.2024

DOI: 10.15825/1995-1191-2024-4-184-188

PROMOTING ORGAN DONATION IN RUSSIA: PROBLEMS AND PROSPECTS

G.N. Komkova[1], E.N. Toguzaeva[1], A.V. Basova[1, 2], M.S. Karamysheva[1]

[1] Saratov State University, Saratov, Russian Federation
[2] Saratov State Medical University, Saratov, Russian Federation

Transplantation helps to save the lives of patients with end-stage diseases of the liver, heart, lungs, and kidney. **Objective:** to study the strategies for advancing the idea of organ donation in the Russian Federation. **Materials and methods.** Scholarly publications by Russian researchers on the issue at hand. The study's methodology was based on application of general and specific scientific methods of theoretical analysis. **Results.** An assessment of how opportunities were used to legitimately promote the idea of donation was conducted. **Conclusion.** Modern ways and methods of promoting the idea of organ donation will help to introduce into public attention the importance of organ donation for transplantation.

Keywords: organ transplantation, deceased donation, donor.

INTRODUCTION

Promotion of the idea of organ donation has become a cornerstone in the advancement of solid organ transplantation programs in Russia [1]. There has been a consistent year-on-year increase in the number of transplant procedures, with 3,057 organ transplants performed in 2023 alone [2]. The establishment of new transplant centers and programs across the Russian Federation has further enhanced transplant activity, expanded waiting lists, and improved access to high-tech medical care for the population [2].

The growth in the number of transplant centers, professional training of physicians across various specialties, and active educational initiatives in the field of organ transplantation and donation have all contributed to shaping a positive public perception of this type of medical care. These efforts support the internal acceptance of transplantation, foster an understanding of its social significance, and underscore its vital role in modern healthcare systems [1].

Objective: to examine current approaches to promoting the idea of organ donation in the Russian Federation.

MATERIALS AND METHODS

Analysis of Russian scholarly publications on the promotion of the idea of organ donation. Using general theoretical methods (analysis, synthesis, comparison, generalization), general scientific approaches (comparative legal analysis), and specific scientific methods (concretization, comparative jurisprudence), an analysis of Russian scholarly publications on the promotion of the idea of organ donation in Russia and abroad was conducted. This analysis considered the current legal frameworks and prevailing social realities.

RESULTS AND DISCUSSION

Both the state and society are faced with a critical challenge: instilling in the public consciousness the importance, humanitarian nature, and significance of organ donation. In this context, the idea of addressing the problem of organ shortage through advancement and popularization of living donation warrants broader public and academic discourse.

As Rustamov and Turaeva emphasized, the primary objective of any form of propaganda is to shape public opinion and establish a life position that aligns with the interests of a particular subject [3]. Based on its intended impact, propaganda can be classified into two categories: constructive, which unites citizens around universally recognized values, and destructive, which fosters anti-humanist beliefs [3].

Based on the ways of disseminating knowledge and forming beliefs, the promotion of organ donation can be categorized into three main forms: oral (live communication, radio, television), print (publications in mass media), and virtual (Internet portals, websites, social networks).

The oral form – such as lectures, discussions, or meetings with healthcare professionals – involves direct, personal communication. This format allows for a more flexible and adaptive engagement with the audience, depending on their mood, level of awareness, and openness to the subject.

Dissemination of information through print media can reach a wide audience, although it primarily influences

Corresponding author: Alla Basova. Address: 112, Bolshaya Kazachya str., Saratov, 410012, Russian Federation. Phone: (8452) 67-76-20. E-mail: allsar@rambler.ru

the older and middle-aged population. Oral communication offers opportunities like thematic TV and radio programs featuring public figures, celebrities, and athletes, that would promote the idea of organ donation. The creation of documentary and feature films addressing this topic also holds strong potential for impact.

In the digital sphere, social networks offer a particularly powerful tool for reaching younger and middle-aged audiences. Bloggers, especially those covering topics related to health and lifestyle, act as opinion leaders with vast subscriber bases often numbering in the hundreds of thousands or even millions.

Each mode of communication serves a specific purpose. Oral communication fosters personal engagement and helps dismantle psychological barriers, such as fear or cultural taboos surrounding organ donation. Traditional media, particularly print and broadcast, aims to convey the broader social and ethical importance of organ donation to a large audience. Digital media and social networks help normalize and popularize the topic.

In summary, oral communication makes the topic discussable, traditional media makes it socially relevant and supported, while social media makes it culturally appealing.

In addition, the role of the media in promoting organ donation cannot be underestimated. Well-executed information campaigns that feature compelling, real-life stories of transplant recipients, people of various ages who have received a second chance at life, have the potential to significantly shift public attitudes toward transplantation, presenting it as an essential and life-affirming aspect of modern medicine. Social networks serve as a powerful platform in this regard, enabling broad outreach and formation of active, engaged communities that support the idea of donation.

In accordance with article 8 of the Law of the Russian Federation dated December 22, 1992 No. 4180-I "On the Transplantation of Human Organs and (or) Tissues", there is a legal presumption of consent for deceased organ donation in Russia [4]. However, in practice, relatives of the deceased often object to autopsy and organ retrieval based on personal convictions or religious beliefs.

For example, according to a study by Reshetnikov conducted at the Volga Region Organ and Tissue Donation Coordination Center, relatives of potential donors were asked for consent to retrieve organs for transplantation. These conversations were conducted with the aim of preventing potential conflicts. Out of 124 individuals approached, only 79 (63.7%) gave their consent, while 45 (36.3%) refused [5]. Given that a single organ donor can potentially save up to seven lives, the refusal to retrieve organs from 45 individuals could mean that as many as 315 critically ill patients were deprived of life-saving transplantation.

In his conclusions, Reshetnikov emphasized that the most important factor influencing public attitudes toward organ donation is the level of awareness about the humanity of transplantology and the vital role this medical field plays in saving lives [5].

In his paper, Reznik outlined the key stages in advancing what he termed the "concept of the sociology of posthumous donation". These include: (1) conducting sociological research involving focus groups, such as medical students, physicians from various fields, and professionals engaged in donor programs; (2) developing standardized informational and educational materials; and (3) disseminating knowledge about postmortem organ donation as a form of social interaction [6].

The study of spiritual, moral, and traditional religious views among the Russian population reveals several factors that hinder citizens' willingness to participate in organ donation. One of the identified issues is the fragmented legal regulation surrounding the promotion of organ donation through social advertising.

Given that Orthodox Christianity and Islam are the most commonly practiced religions in Russia, understanding the perspectives of these faith traditions on organ donation is of particular importance for the effective promotion of donation initiatives.

Some studies have explored the influence of religious beliefs and social attitudes on organ donation in Russia. For instance, Kochetkov and Zudin conducted a questionnaire-based survey at a city hospital in Nizhny Novgorod Oblast to assess attitudes toward deceased organ donation programs. Among the 130 patients surveyed, 75.4% identified as religious. Notably, within this group, the willingness to sign consent for deceased organ donation was significantly lower compared to non-religious respondents [8].

A more recent study titled "Readiness and Attitude to Types of Donation Among youth" (a mass survey in Kazan, 2023) found that while 70% of young respondents expressed a generally positive attitude toward donation, only 53% confirmed their personal readiness to become a donor [9].

It is important to note that these religions exert considerable influence not only on believers but also on societal values as a whole. As such, the inclusion of religious leaders in public education campaigns about the significance and humanitarian value of organ donation can be a vital component in overcoming resistance and increasing public support [7].

It is evident that raising public awareness about organ donation requires a comprehensive and multifaceted approach. A key component is the implementation of educational campaigns within academic institutions, where students can acquire fundamental knowledge about organ transplantation and understand the societal importance of donation. Integration of specialized courses and interactive activities into the educational curriculum can foster a positive attitude toward organ donation among young people, promoting it as an individually responsible and

socially supported practice aimed at preserving health, extending active life, and reinforcing human solidarity.

Finally, it is necessary to develop specialized institutions and support programs that would provide guidance and counseling to both potential donors and their families. Ensuring transparency in the donation process, upholding legal safeguards, and embracing innovative technologies in the field of individual donation can significantly enhance public trust, ultimately saving more lives.

The analysis of scientific literature has identified a promising avenue for enhancing public awareness of the importance and necessity of organ donation: the organization and implementation of educational and informational activities aimed at shaping the public's understanding of organ donation.

In this context, it is crucial to single out the implementation of specialized programs. These programs consist of a series of initiatives designed to provide as many people as possible with accurate and reliable information about organ donation and transplantation.

Educational projects should become a central component of efforts to develop transplant programs. Their goal is to disseminate accurate knowledge about organ transplantation, the patients who rely on it, and the diseases for which organ transplants offer the only hope of survival. These projects should also work to dispel myths surrounding donation and promote the importance of postmortem donation [1].

In many countries around the world, including Brazil, Italy, Spain, Japan, Singapore, Germany, and France, social advertising promoting organ donation is an ongoing effort, particularly targeting young people. Printed visual materials are produced and displayed in public spaces and educational institutions. Examples of such campaigns include posters with messages like "Give Life", "Save Seven Lives", and "Become a Hero. Be an Organ Donor" [10].

In Kazan, in 2024, the All-Russian Exhibition of Social Advertising on Organ Donation, titled "The Real Power is Inside You", was held to raise public awareness about patients waiting for organ transplants [11].

The official portal of the Russian Ministry of Health has a dedicated section on bone marrow and organ donation for transplantation in the section "Organ donation for transplantation", where people can ask questions, read the latest news, and learn about patient stories [1].

The information resource "National Association in the Field of Donation and Transplantology" (https://nadit.ru/) features social advertising in the form of animated mini-movies highlighting the importance of organ donation, such as "Life is the Best Gift", "Thank You, Donor!", "Leaving, I Give You Life", and "Transplantation? I Am for It!" These videos, along with real stories of individuals who became organ donors after sudden death, emphasize how they saved lives [12].

Additionally, the activities of various non-profit organizations deserve recognition. For instance, the charity foundation "Life as a Miracle" supports children waiting for or undergoing liver transplants, while the charity organization "Own Atmosphere" aids individuals in need of lung transplants. The public organization "NEFRO-LIGA" brings together patients with kidney diseases, those undergoing dialysis, and individuals in recovery after kidney transplants, along with their families. The association "RusTransplant" offers vital information for patients, and NEFRO-LIGA continues its support for kidney disease patients and their families.

Shumakov National Medical Research Center of Transplantology and Artificial Organs is a flagship in the field of transplantology in Russia. The Center's management and staff actively promote public awareness by organizing press conferences, educational lectures, and public events dedicated to transplantation and organ donation. It plays a key role in initiatives such as the nationwide "Donor Day" campaign across various regions of the Russian Federation and the All-Russian Transplant Games for individuals living with transplanted organs. In collaboration with the Life as a Miracle Foundation, the Center has also launched online platforms like "Пропечень.рф" and "100 Questions to a Transplantologist", with project answers broadcast in the Moscow subway [1].

Demonstrating medical achievements not only confirms that organ donation saves lives and restores health – enabling recipients to live fully, work, raise families, and enjoy life – but also helps ordinary citizens understand the profound social challenges faced by people with end-stage organ failure, when the only chance for survival is transplantation. Initiatives such as the publication of patient stories in the media, as well as themed photo exhibitions in Moscow parks and on the grounds of the Shumakov Center, allow the public to witness the transformative power of modern transplantation and appreciate the societal value of organ donation.

CONCLUSION

Promoting the idea of organ donation is a complex yet vitally important educational endeavor. It involves targeted and systematic efforts by public organizations to disseminate scientific knowledge and shape spiritual and moral values rooted in the recognition of the life-saving importance of organ donation. Despite the sensitivity of the topic, its deeply humane goals underscore the necessity of open and thoughtful public dialogue.

The creation of well-crafted social advertising on organ donation has proven to be an effective tool for strengthening positive public opinion on this issue in the Russian Federation [10]. The analysis conducted supports the conclusion that it is both timely and advisable to enhance existing educational and informational efforts. Moreover, the development of new platforms

and projects that consistently highlight the value and necessity of donation will help foster a more informed and supportive public attitude, ultimately increasing the willingness of the Russian population to embrace the idea of organ donation.

This research was supported by the Russian Science Foundation, Grant No. 24-28-00386, "Propaganda in Russian Law: Transformational and Institutional Changes". More information is available at: https://rscf.ru/project/24-28-00386/.

The authors declare no conflict of interest.

REFERENCES

1. Resurs podderzhki: kak informirovanie obshchestva o donorstve organov spasaet zhizni [Internet]. https://donorstvo.org/articles/133.
2. *Gautier SV, Khomyakov SM.* Organ donation and transplantation in the Russian Federation in 2023. 16th Report from the Registry of the Russian Transplant Society. *Russian Journal of Transplantology and Artificial Organs*. 2024; 26 (3): 8–31. https://doi.org/10.15825/1995-1191-2024-3-8-31.
3. *Rustamov RR, Turaeva SH.* Types of propaganda, its goals and objectives. *Bulletin of Science*. 2020; 5 (11): 58–62.
4. Konsul'tantPljus [Internet]. Zakon Rossiyskoy Federatsii ot 22.12.1992 № 4180-1 "O transplantatsii organov i(ili) tkaney cheloveka" (red. ot 1.05.2022). [cited 2024 March 14]. Available from: https://www.consultant.ru/document/cons_doc_LAW_4692/.
5. *Reshetnikov AV, Romanov SV, Abaeva OP, Smirnova GYu.* The attitude of Russians to posthumous donation (on the example of the region). *Sociological research*. 2019; 4: 70–76. doi 10.31857/S013216250004587-8.
6. *Reznik ON, Reznik OA.* The social foundations of the dialogue on posthumous organ donation. *Russian Journal of Transplantology and Artificial Organs.* 2023; 25 (4): 174–180. doi: 10.15825/1995-1191-2023-4-174-180.
7. *Andrianov AV.* Legislation and religions of the Russian Federation (Russian Orthodox Church, Judaism, Islam and Buddhism) on ethical issues of transplantation. *Ipatievsky Bulletin*. 2015; 3 (3): 175–209.
8. *Kochetkova AV, Zudin SD.* On the importance of the religious factor for posthumous organ donation. *Ilyinsky readings 2022. Collection of materials of the school-conference of young scientists and specialists.* M., 2022: 193–194.
9. *Savelieva ZhV, Fayzullina LR*. Readiness and attitude to types of donation among youth (according to mass survey in Kazan). *The Kazan socially-humanitarian bulletin*. 2023; 2 (59): 43–47. doi: 10.26907/2079-5912.2023.2.43-47.
10. *Anisimov AA, Abdullina AR, Raimova AT, Anisimov UA.* Social advertising as a tool for building trust in organ donation. *Transplantation.* 2023; 15 (2): 226–237. doi: 10.23873/2074-0506-2023-15-2-226-237.
11. Vystavka social'noj reklamy donorstva organov otkrylas' v Kazani [Internet]. https://www.tatar-inform.ru/news/vystavka-socialnoi-reklamy-donorstva-organov-otkrylas-v-kazani-5951429.
12. The page of the information resource "National Association in the field of donation and transplantation" [Internet]. [cited 2024 February 16]. Available from: https://nadit.ru/.

The article was submitted to the journal on 14.10.2024

DOI: 10.15825/1995-1191-2024-4-189-200

EXPERIMENTAL STUDY OF A NEW DEXTRAN-40-BASED COMBINED SOLUTION ON A SMALL LABORATORY ANIMAL MODEL

N.V. Grudinin[1], V.K. Bogdanov[1], I.V. Pashkov[1], O.Yu. Esipova[1], A.P. Kuleshov[1], N.P. Mozheiko[1], E.A. Volkova[1], S.V. Gautier[1, 2]

[1] Shumakov National Medical Research Center of Transplantology and Artificial Organs, Moscow, Russian Federation

[2] Sechenov University, Moscow, Russian Federation

Background. Organ shortage remains an unsolved issue in the field of transplantology. It is particularly severe in such a progressive area as lung transplantation. The creation of extracorporeal systems for rehabilitation of donor organs has been made possible by perfusion techniques; however, the search for the best perfusion and preservation solutions remains important. **Objective:** to evaluate the efficacy of the developed solution for preservation and normothermic *ex vivo* lung perfusion (EVLP), as well as to conduct a comparative analysis with the standard perfusion solution for EVLP. **Materials and methods.** Experimental studies on small animal models were conducted. All animals were divided into 2 groups – control and experimental. The study stages consisted of: procurement of donor lungs, static cold storage, EVLP and orthotopic left lung transplantation. In the experimental group, the lungs were preserved using an experimental solution, while in the control group, they were preserved in PERFADEX® Plus (XVIVO, Sweden). Static cold storage lasted for 10 hours. Orthotopic left lung transplantation was performed after EVLP. The follow-up period was 2 hours, after which blood samples and sections of the transplanted lung were taken for morphological examination. Upon completion of the experiment, the animal was removed from the experiment by exsanguination. **Results.** Respiratory index at the end of perfusion was statistically significantly higher in the experimental group (434 mmHg) than that of the control group (394 mmHg). Pulmonary vascular resistance (PVR) in both groups had a downward trend, which is a good prognostic sign of the efficacy of perfusion agents. PVR was lower in the experimental group compared to the control group – 36 versus 89 dynes/sec/cm^{-5}. **Conclusion.** The developed combined dextran-40-based solution showed its effectiveness as a preservation agent for static cold storage and as a perfusion solution for EVLP.

Keywords: lung transplantation, ex vivo lung perfusion, preservative solutions, perfusion solution.

INTRODUCTION

Lung transplantation (LT) has become a highly effective therapeutic option for end-stage lung disease, but access is limited by the insufficient number of donor organs available [1, 2]. Expanding donor selection criteria allows for more organs to be transplanted, but this also increases the risk of primary graft dysfunction with the use of "marginal" or compromised organs [3, 4].

Normothermic *ex vivo* lung perfusion (EVLP) allows for objective assessment of compromised lungs that were previously deemed unsuitable for transplantation. EVLP not only enables evaluation of the organ but also extends preservation times, offering logistical advantages. Moreover, recent developments have highlighted the potential of EVLP as a therapeutic platform for reconditioning donor lungs. Clinical trials have demonstrated the safety and feasibility of transplanting organs assessed through EVLP, with survival rates comparable to those of organs preserved using traditional cold static storage methods [5–7].

The success of EVLP is largely attributed to the pioneering work of Professor Stig Steen, who performed the first human LT following *ex vivo* assessment [8]. A key factor in the success of this perfusion technique was Steen's human albumin-based perfusion solution, known as the Steen Solution™. Human serum albumin, a primary component of the solution, maintains physiologically relevant colloid osmotic pressure, minimizing lung damage [9]. Additionally, the presence of dextran 40 in the solution helps reduce the negative impact of leukocytes on the vascular endothelium [10].

Despite the positive properties of the solution, lungs are still susceptible to ischemia-reperfusion injury (IRI) during EVLP. IRI is characterized by an acute inflammatory response and increased oxidative stress, both of which contribute to primary graft dysfunction in the early

Corresponding author: Nikita Grudinin. Address: 1, Shchukinskaya str., Moscow, 123182, Russian Federation. Phone: (903) 805-63-58. E-mail: Zbignev.religa@mail.ru

postoperative period [11–13]. It is well established that proinflammatory cytokines in the perfusate and tissue increase significantly over time, even during successful perfusions [14, 15]. The duration of perfusion directly correlates with the degree and severity of LT injury [16, 17].

There is still incomplete understanding of the pathophysiological events occurring during EVLP, and as a result, existing perfusion solutions continue to evolve in terms of composition and addition of new adjuvants. In this context, a combined solution for both preservation and normothermic EVLP has been developed. Unlike the original Steen Solution™, this new solution features dextran 40 and a modified electrolyte composition as its base.

This study aimed to evaluate the efficacy of this experimental solution in comparison to the original Steen Solution™, which is widely regarded as the gold standard for EVLP in clinical practice worldwide.

MATERIALS AND METHODS

Experiments were conducted using small animal models, specifically male Wistar rats weighing 250–300 g. The following stages were carried out in the series of experiments:

– Lung procurement;
– Static hypothermic storage;
– *Ex vivo* lung perfusion;
– Orthotopic left lung transplantation.

In the experimental group, donor lungs were preserved using the experimental solution, while in the control group, Perfadex Plus was used as the preserving agent. In all cases, static hypothermic storage was maintained for 10 hours.

The animals were divided into two equal groups: donors (n = 30) and recipients (n = 30). The donor group was further divided into two subgroups:

Group 1 – EVLP using the experimental solution (n = 15);

Group 2 – EVLP with Steen Solution™ solution (n = 15).

After *ex vivo* perfusion, orthotopic left lung transplantation (OLLT) was performed. A follow-up period of two hours was observed, after which blood samples and tissue sections of the transplanted lung were collected for morphological analysis.

Donor lung procurement procedure

The donor animal was placed in a specialized anesthesia induction chamber, where sedation was induced using an isoflurane vaporizer (RWD R5835, China) at a flow rate of 1 L/min and a concentration of 5 vol/%. The depth of anesthesia was monitored by assessing the animal's response to pain stimuli and respiratory rate. Tracheal intubation was performed using a 14 G IV catheter, and the intubation tube was connected to the SAR-830/AP Ventilator (CWE, USA) circuit. Mechanical ventilation (MV) was initiated with 100% oxygen and the following parameters: respiratory rate (RR) 85/min, respiratory volume (V_{RV}) 1.2 mL, flow volume (V_{FV}) 700 mL/min, peak pressure (P_{peak}) 8 cmH_2O, positive end-expiratory pressure (PEEP) 3 cmH_2O, and isoflurane flow at 3.5 vol/%. A median sternotomy was performed, and after dissection of lung tissues and hilar structures, 500 units of heparin were injected through a puncture of the right ventricular apex. After a 3-minute exposure, 12 mL of whole donor blood was drawn into a heparinized syringe. A 2.0/2.5 mm cannula was then inserted into the right ventricle and advanced into the pulmonary artery, while a 2 mm diameter metal angular cannula was placed into the left ventricle for adequate perfusate drainage.

The donor lungs were preserved by antegrade perfusion with Perfadex Plus solution at 4 °C, using a syringe pipette to deliver 20 mL of solution at a rate of 200 mL/h (3.3 mL/min) for an exposure time of 6 minutes [18].

During preservation, the MV parameters were adjusted with atmospheric air as follows: respiratory rate (RR) 40/min, V_{RV} 1.5 mL, V_{FV} 300 mL/min, P_{peak} 6 cmH_2O, and PEEP 3 cmH_2O. After graft preservation, the diaphragm, superior vena cava, pulmonary ligaments, and pleura were dissected. The trachea was separated from the esophagus. Once the lungs were fully mobilized, a 14 G plastic cannula was inserted into the tracheal lumen for subsequent ventilation under *ex vivo* lung perfusion (EVLP) conditions. Following the procurement process, the lung graft was placed in a sterile container filled with 30 mL of Perfadex Plus solution for static hypothermic storage, where it was preserved for 10 hours.

Normothermic *ex vivo* lung perfusion procedure

In the experimental group, the perfusion circuit was filled with 10 mL of the dextran 40-based experimental solution and 12 mL of whole donor blood. In the control group, the extracorporeal circuit was filled with 20 mL of Steen Solution. The following adjuvants were added to the solution in all groups: Glucose 40% (4 U), $NaHCO_3$ 4.8% (2 U), Vasaprostane (10 μg), Insulin P (3 U), Methylprednisolone (20 mg), Cefazolin (0.5 mg/mL), and Heparin (300 U).

Once the solution temperature reached 25 °C during continuous recirculation, the perfusate was analyzed for acid-base and electrolyte parameters, as well as glucose concentration.

For deaeration, the graft was retrogradely filled at a rate of 1 mL/min through the left atrium cannula, passi-

vely with a water column, until the solution appeared in the pulmonary artery cannula. After this, the pump was stopped, and the perfusion line was connected to the pulmonary artery cannula. Initial volumetric perfusion rate was set at 1.2 mL/min, which represents 15% of the target perfusion rate. The required 100% perfusion rate was calculated based on the estimated mass of the lung graft, as determined by the following formula (1):

$$V = 0.0053 \times m - 0.48, \quad (1)$$

where m is animal weight in grams.

The estimated lung graft mass was calculated based on a perfusion rate of 6 mL/min/gram [18, 19]. MV of the lung graft was initiated 15 minutes after the onset of normothermic machine perfusion, upon reaching a temperature of 33 °C. During this period, perfusion parameters were recorded, and pulmonary vascular resistance was calculated.

Gas and electrolyte composition of the perfusate was analyzed before the start of graft perfusion and then at 15-minute intervals. Samples were taken simultaneously from two points in the perfusion circuit: the outflow perfusate from the left atrium and the circulating perfusate sampled after the oxygenator. Comparing oxygen and carbon dioxide levels from these two sampling points enabled evaluation of perfusion efficiency and assessment of the graft's functional status.

At 120 minutes, a final analysis of gas and electrolyte composition was performed. Machine perfusion was then discontinued, and MV was continued. For further preservation, 20 mL of the dextran 40-based experimental solution cooled to 4 °C was infused into the pulmonary artery via the perfusion system at a rate of 200 mL/hour.

Orthotopic left lung transplantation

Lung implantation was performed using the cuff technique to minimize warm ischemia time and reduce variability due to surgical technique [20]. The principle of this method involves using intravenous catheter segments as cuffs to secure the graft vessels and facilitate implantation into the recipient's corresponding vessels. Specifically, 14 G catheters were used for bronchial implantation, 16 G for the pulmonary artery, and 14–16 G for the pulmonary vein depending on vessel diameter [21, 22].

To minimize warm ischemia and provide local cooling during cuff placement, the graft was irrigated with dextran 40-based preservation solution at 4 °C. The graft was suspended by the lung root and stabilized using a flexible holder. Donor lung vessels were passed through their respective cuffs, with the vascular edges folded over the cuff body and secured using a 7/0 Prolene ligature. The bronchial cuff was prepared and implanted in a similar fashion. This procedure took an average of 30 minutes.

Following anesthesia induction and initiation of MV, the recipient animal was positioned in right lateral decubitus on the operating table. A thoracotomy was performed through the 5th intercostal space, with resection of the 4th rib [23, 24]. The native lung's vascular structures were mobilized, and a vascular clamp was applied to the lung root before removal of the left lung. To prevent twisting of vascular anastomoses, the left main bronchus was implanted first. For ease of cuff placement, the pulmonary artery and veins were incised transversely, and the corresponding cuffs were inserted and secured with ligatures. Upon completion of all anastomoses, the vascular clamp was released to initiate graft reperfusion.

The follow-up period was 2 hours, after which blood was selectively collected from the pulmonary artery and pulmonary veins for gas analysis.

Morphological study

Following perfusion, samples of the right lung parenchyma were fixed in 10% neutral buffered formaldehyde (pH 7.4) for 24 hours. Similarly, 2 hours after transplantation, samples of the left lung parenchyma were collected and fixed in 10% formaldehyde under identical conditions. For paraffin embedding, the tissue specimens were dehydrated using isopropyl alcohol and cleared with petroleum ether. The samples were then embedded in paraffin blocks and sectioned at a thickness of 5 μm.

Histological sections were stained with hematoxylin and eosin (H&E) for microscopic examination. Microscopic analysis was conducted using a Leica DM 750 light microscope (Leica, Germany), equipped with a 10× eyepiece and objective lenses of 4×, 10×, 40×, and 100× magnification. Digital images of the histological sections were captured using an ICC50 camera (Leica, Germany).

Samples were assessed for vascular thrombosis, hemorrhage, interstitial and alveolar edema, and cellular infiltration.

Statistical data processing methods

Statistical analysis was conducted using the licensed SAS Enterprise Guide 9.4 software. All variables were tested for normality using the Kolmogorov–Smirnov and Shapiro–Wilk tests. For normally distributed data, parametric statistical methods were applied; in the case of non-normally distributed data, non-parametric methods were used. Group comparisons for variables such as oxygenation index, pulmonary vascular resistance, pulmonary arterial pressure, lactate, glucose, buffer bases, and peak inspiratory pressure were performed using the Kruskal–Wallis test. A p-value <0.05 was considered statistically significant. Box-and-whisker plots were generated using SAS Enterprise Guide 9.4.

RESULTS

The experimental study comprised two main phases: EVLP and OLLT in recipient animals. During the EVLP procedure, key indicators reflecting the functional status of the donor lungs were continuously monitored and recorded in both groups. These indicators included oxygenation index (OI) (Fig. 1), pulmonary artery pressure (PAP), and pulmonary vascular resistance (PVR). Comparative analysis of these parameters between the groups was performed using the Kruskal–Wallis test, with p-values <0.05 considered statistically significant.

OI is a key measure of gas transport during lung perfusion, with a lower acceptable value typically considered at 350. The study observed high OI values in both groups. At the beginning of the procedure, median OI in the control group (Steen Solution) was 498.5 [460; 537], and in the experimental group, it was 518 [483; 553]. Statistical analysis revealed no significant differences between the groups ($p > 0.05$). Throughout the *ex vivo* procedure, the PaO_2/FiO_2 ratio remained comparable between the two groups; however, a significant increase in OI was noted in the experimental group in the final analysis. Specifically, median OI in the Steen Solution group was 394.4 [373; 416], while in the experimental group, it increased to 434.7 [422; 447], with the difference reaching statistical significance ($p < 0.0001$).

While the volumetric perfusion rates were identical in both groups during EVLP, differences in PAP were observed (Fig. 2).

In the control group, initial PAP values were within the acceptable threshold of 15 mmHg, with a median of 9.07 [7.7; 10.4] mmHg. Throughout the EVLP procedure, PAP fluctuations in this group were minimal, with a final median value of 8.47 [7.2; 9.8] mmHg. In contrast, the experimental group demonstrated a consistently lower PAP, showing a downward trend from an initial median of 4.45 [3.3; 5.6] mmHg to 3.4 [2.9; 3.9] mmHg by the end of perfusion. This notable difference in PAP dynamics played a crucial role in calculating PVR values, which served as an objective indicator of vascular compliance in donor lungs during EVLP (Fig. 3).

Median PVR in the control group was 604.3 [515; 693] Dynes/sec/cm^{-5}, whereas in the experimental group, it did not exceed 297.8 [223; 373] Dynes/sec/cm^{-5}. These differences were statistically significant. Although both groups exhibited a marked downward trend in PVR during the EVLP procedure, by the end, the group using the experimental dextran 40-based solution demonstrated significantly lower vascular resistance compared to the Steen Solution™ group, with median values of 35.8 [31; 41] *vs.* 89.1 [75; 103] Dynes/sec/cm^{-5}, respectively ($p < 0.0001$).

Lactate level dynamics were monitored throughout the perfusion period (Fig. 4).

Lactate dynamics had a general upward trend throughout the EVLP procedure, as expected due to the absence of metabolic pathways for lactate clearance in the *ex vivo* setting. While no statistically significant differences were noted between the groups at the 60- and 90-minute

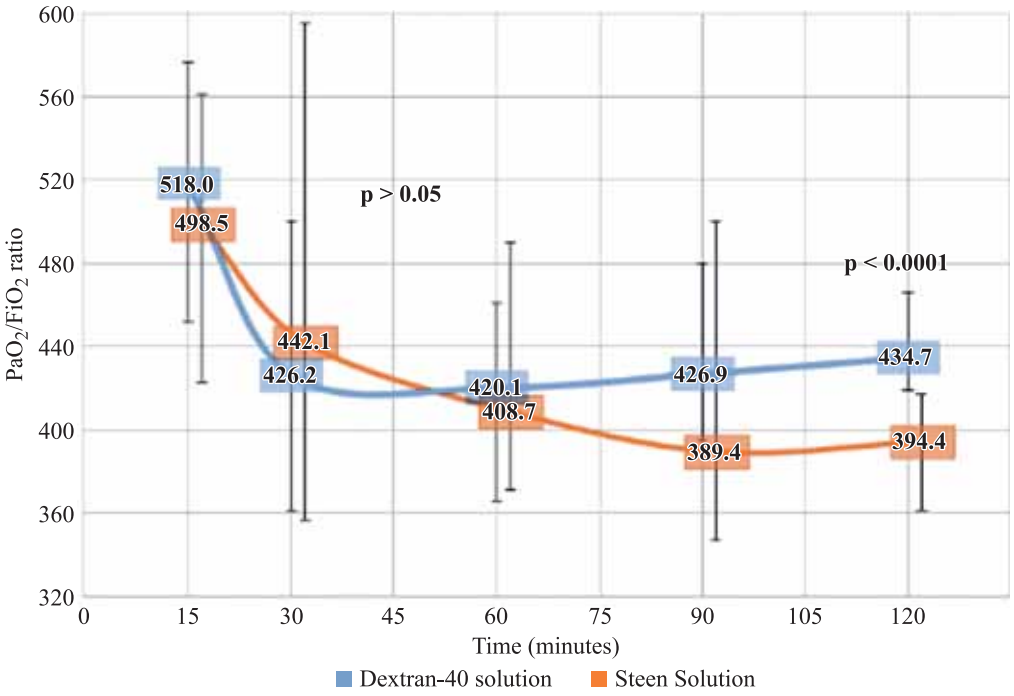

Fig. 1. Dynamics of oxygenation index during EVLP. The indices are presented as median, vertical lines indicate interquartile range, p is statistical significance

marks, the experimental solution group demonstrated narrower fluctuation ranges in median lactate levels. Importantly, at the final measurement point, the maximum lactate values were significantly lower in the experimental group – 7.5 [7.2; 7.6] mmol/L compared to 7.87 [7.8; 8.5] mmol/L in the Steen Solution™ group.

After EVLP, OLLT was performed. To assess the functional integrity of the graft post-transplant, OI (Fig. 5) and lactate levels (Fig. 6) were measured twice during the 120-minute post-transplant follow-up period.

After implantation of donor lung, OI values in the group perfused with the experimental dextran 40-based

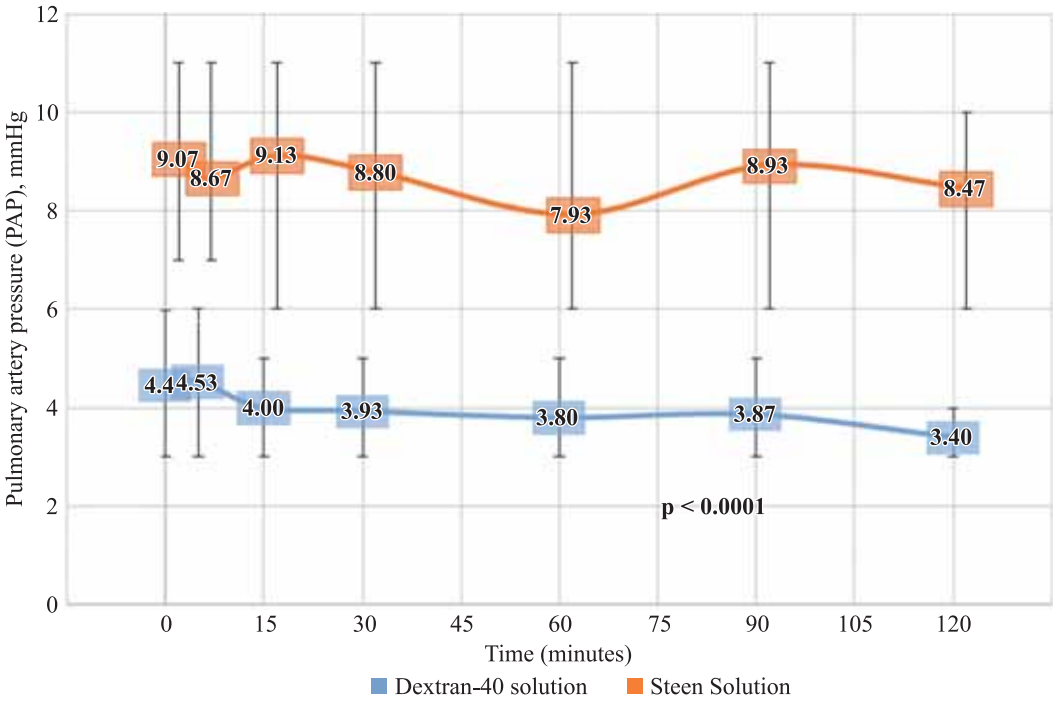

Fig. 2. Dynamics of pulmonary artery pressure during EVLP. The indices are presented as median, vertical lines indicate interquartile range, p is statistical significance

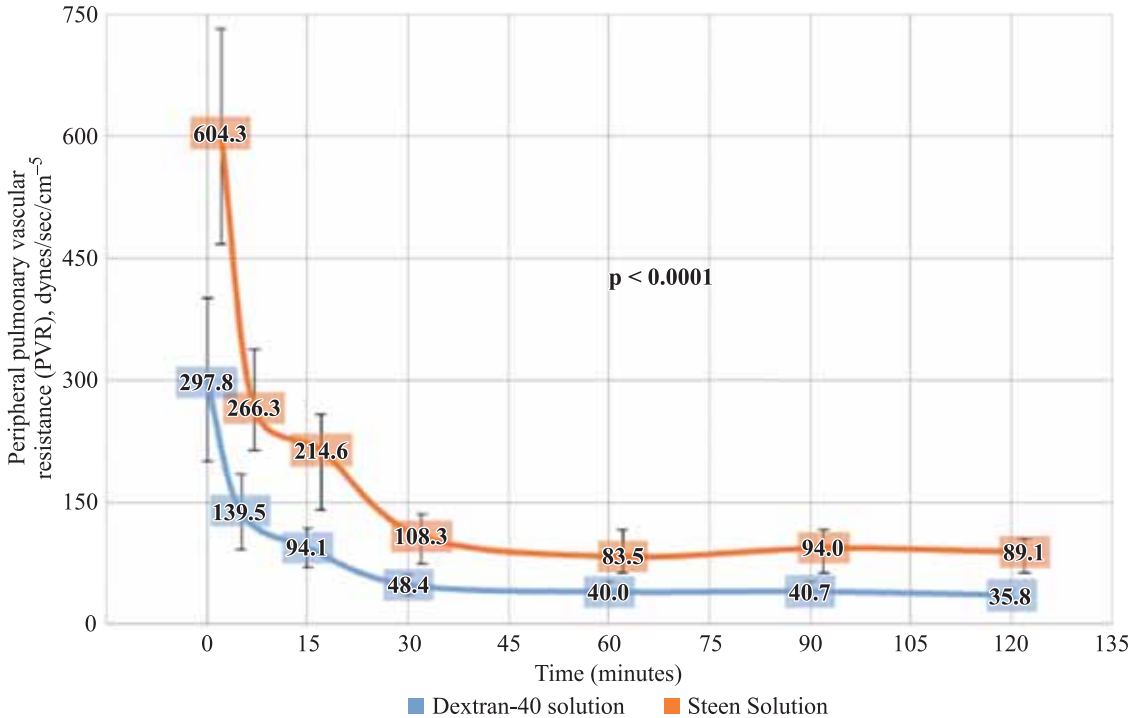

Fig. 3. Dynamics of peripheral vascular resistance during EVLP. The indices are presented as median, vertical lines indicate interquartile range, p is statistical significance

solution remained significantly elevated, consistently exceeding the critical threshold of 350. The Steen Solution™ group exhibited borderline OI values during EVLP, and after two hours of post-transplant monitoring, median OI had declined to 122 [113; 131]. Meanwhile, in the experimental group, median OI remained at 364 [353; 375] (p = 0.000).

Lactate levels, serving as an indirect marker of IRI, remained within the permissible range (below 10 mmol/L) in both groups. However, they were significantly elevated in the group where EVLP was performed using Steen Solution™. After 120 minutes of follow-up, the median lactate level in the control group was 8 [7; 9] mmol/L, compared to 6 [5; 6] mmol/L in the experimental group. This, alongside the OI, indicates a reduced functional

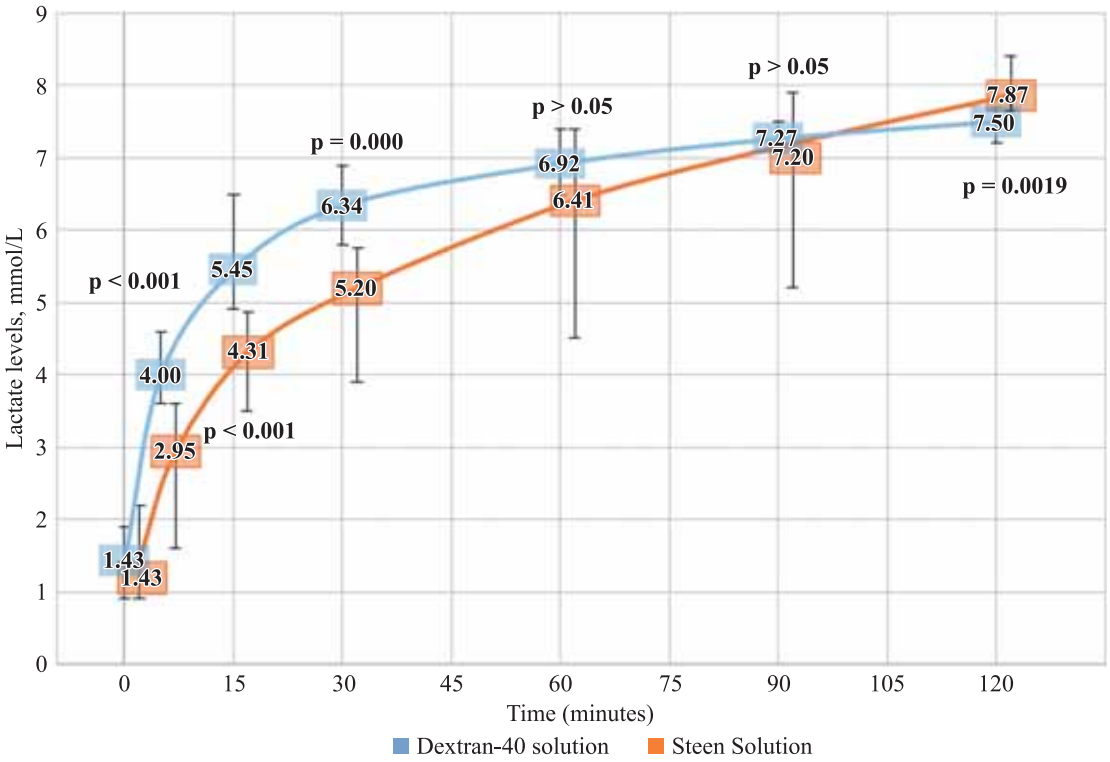

Fig. 4. Dynamics of changes in lactate levels during EVLP. The indices are presented as median, vertical lines indicate interquartile range, p is statistical significance

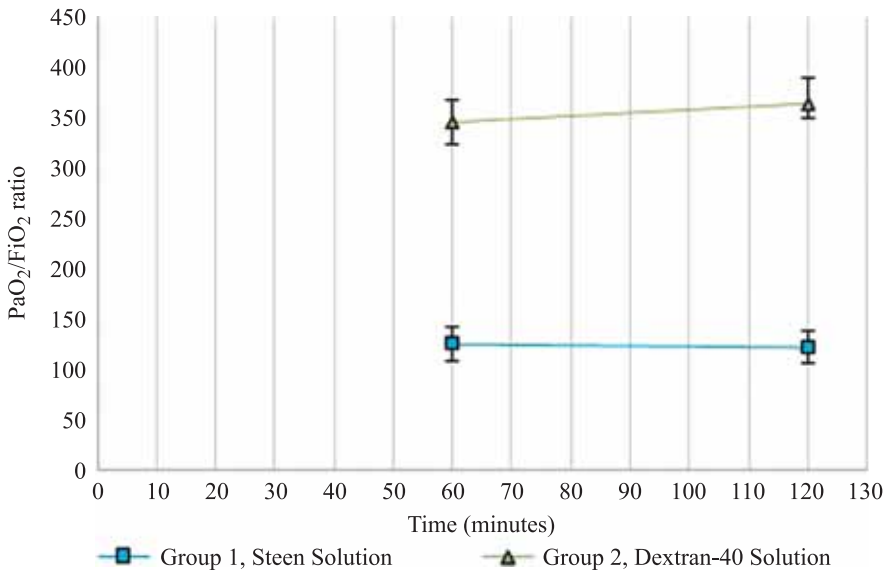

Fig. 5. Dynamics of oxygenation index after transplantation. The indices are presented as median, vertical lines indicate interquartile range, p is statistical significance

status of the donor lung. The differences were statistically significant (p = 0.043).

Histopathological evaluation post-EVLP

Microscopic examination of lung specimens was done at 100× magnification (Fig. 7, a) and 200× magnification (Fig. 7, b). Each sample was assessed across the entire tissue section.

Upon completion of the 120-minute perfusion procedure, lung tissue samples were collected for histological analysis. Microscopic examination revealed occasional focal disruptions of the alveolar-capillary membrane, although the overall integrity of the lung parenchyma was preserved. The alveolar spaces appeared distended, but no signs of edema were observed. Mild thickening was noted in the alveolar septa and peribronchovascular regions.

Histopathological evaluation post-transplant

Histological evaluation of the transplanted lung specimens was performed at 100× magnification (Fig. 8, a) and 200× magnification (Fig. 8, b), across the entire tissue section in each case.

After OLLT, histological examination of the lung tissue was conducted. Most sections demonstrated preserved architecture of the lung parenchyma with well-expanded alveoli and no evident structural defects. Occasional microatelectasis was observed in isolated lung

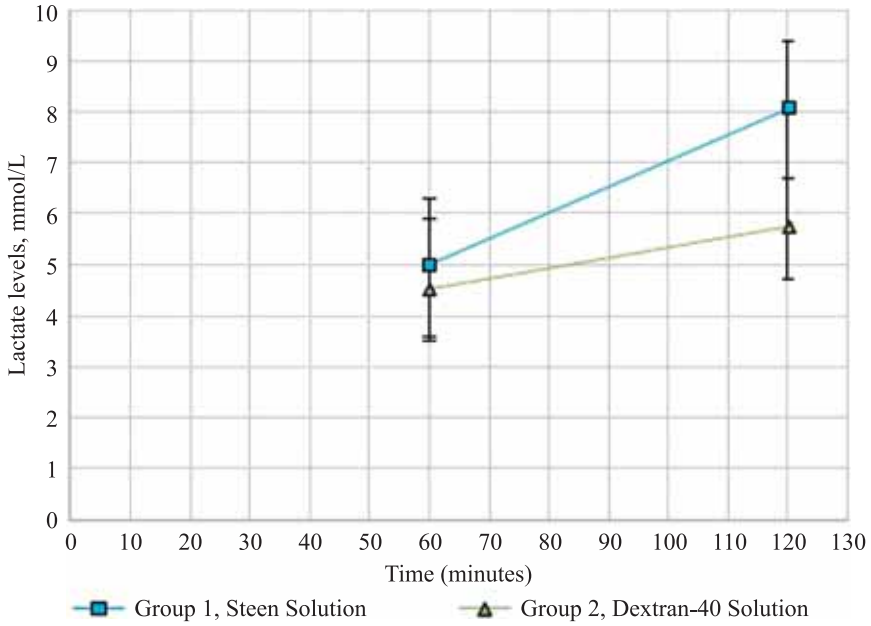

Fig. 6. Dynamics of changes in lactate levels after transplantation. The indices are presented as median, vertical lines indicate interquartile range, p is statistical significance

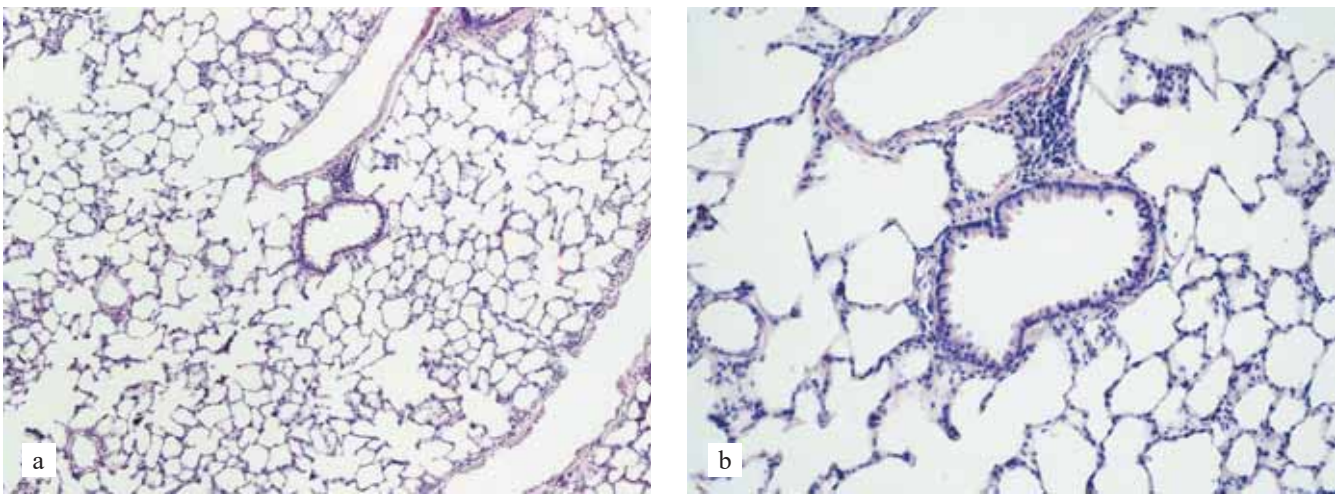

Fig. 7. Results of morphologic studies: a, histologic picture of donor right lung parenchyma after 120 minutes of EVLP, 100× magnification; b, histologic picture of donor right lung parenchyma after 120 minutes of EVLP, 200× magnification

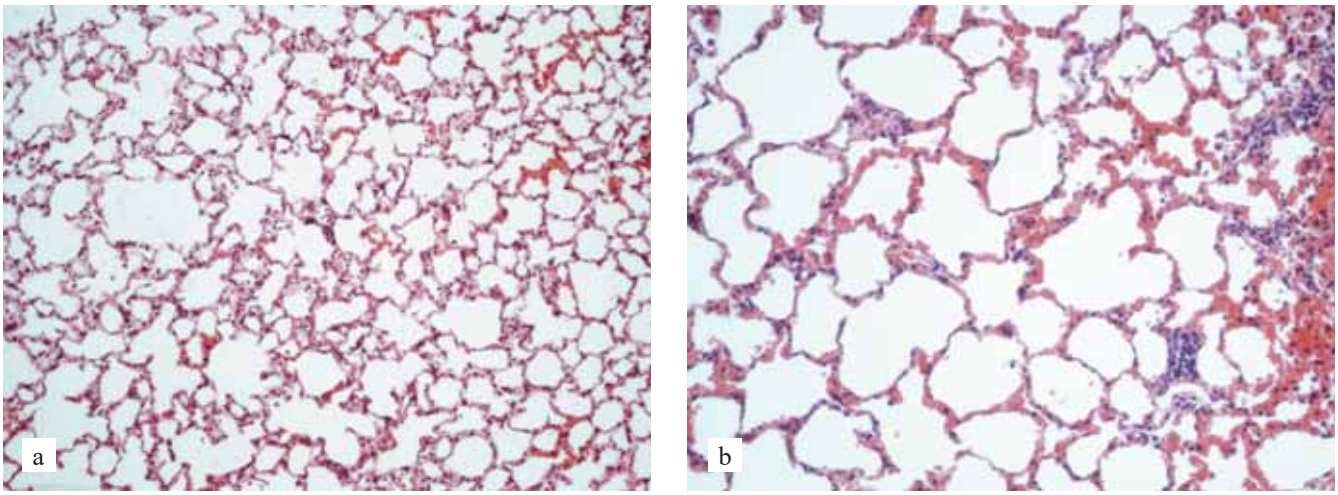

Fig. 8. Results of morphologic studies: a, histologic picture of donor left lung parenchyma 24 hours after transplantation, 100× magnification; b, histologic picture of donor left lung parenchyma 24 hours after transplantation, 200× magnification

segments. Mild thickening was noted in the alveolar spaces and peribronchovascular regions. Vascular congestion within the microcirculatory bed was present, along with sporadic foci of minor intraalveolar hemorrhage. Slight interalveolar septal edema was identified. The observed morphological picture in both groups is consistent with physiological changes following EVLP and subsequent transplantation and are not indicative of pathological alterations.

DISCUSSION

EVLP has become a crucial component of LT programs globally. While it has primarily been used for quality assessment of suboptimal donor lungs, its potential for active treatment and functional restoration of donor organs is even greater. One key element of the EVLP procedure is the perfusion solution, which enables the perfusion of isolated lungs without causing edema. Currently, the human albumin-based buffer solution known as Steen Solution™ is commercially available. Clinical studies have demonstrated its high efficacy in EVLP, employing various protocols and perfusion durations. Notably, Steen Solution can be used with or without the addition of donor blood. However, several studies have raised both positive and negative aspects regarding the addition of erythrocyte mass [25]. Despite the widespread clinical use of Steen Solution™, many research teams are developing alternative perfusion solutions.

The development of new solutions is driven by the need to identify the most optimal formulation for lung perfusion. A key factor in this search is the high cost of Steen Solution™ and, consequently, the financial limitations it imposes on the EVLP procedure. The high cost has significantly hindered the broader use of EVLP for both evaluation and rehabilitation of donor lungs. This study demonstrated the efficacy of a novel dextran 40-based combination solution. One of the main advantages of this experimental solution is its versatility, as it can be used both as a preservation agent for static hypothermic storage and as a perfusion solution during EVLP.

The study evaluated the efficacy of this experimental solution in a rat EVLP model, followed by single-lung transplantation. A static hypothermic storage period of 12 hours was chosen, as it is considered appropriate for clinical practice and models expanded criteria donation. In most translational *ex vivo* perfusion studies, the perfusion is typically carried out in pig models [26].

Experimental models using large animals are often associated with high maintenance costs and complex logistics. One potential solution to this issue is the use of small laboratory animals as experimental models. While such studies are economically advantageous, they present technical challenges in perfusion. To date, only one EVLP system designed specifically for rats, developed by Harvard Apparatus, is commercially available. Many research teams, however, have opted to design their own benches tailored to specific lung perfusion research needs, aiming to reduce the cost of consumables [27]. In our study, we used a custom-designed low-volume bench with a filling volume of just 25 mL, compared to foreign systems where the primary filling volume typically ranges from 150 mL [28–31]. This compact bench setup enabled a thorough analysis of the properties of the experimental solution, especially as the addition of donor blood was essential as the primary adjuvant. In contrast, experimental platforms with circuit filling volumes over 50 mL complicate the use of donor blood, significantly limiting their utility.

As a result of the study, the respiratory index (RI) at the end of perfusion was statistically significantly higher in the experimental group compared to the control group – 434 mmHg versus 394 mmHg, respectively. Des-

pite the higher RI in the experimental group, both groups surpassed the minimum threshold value of 350 mmHg, indicating that the perfusion was effective. PVR decreased in both groups, which is a positive prognostic indicator of perfusion efficacy. However, PVR in the experimental group was significantly lower than in the control group – 36 *vs.* 89 Dynes/sec/cm^{-5}, respectively. Morphological analysis showed that lung parenchyma architecture was preserved, with isolated areas of neutrophilic infiltration observed. Some sections displayed areas of alveolar-capillary membrane rupture. Slight thickening of alveolar air spaces and peribronchovascular connective tissue was noted in both groups. These findings highlight the positive attributes of the developed solution compared to the original Steen Solution™. The possibility of using the experimental solution for both preservation and EVLP provides clear advantages over the foreign counterpart. The study demonstrates the recovery of lung function after prolonged hypothermic storage, as evidenced by the increase in RI and decrease in PVR during perfusion.

CONCLUSION

The dextran 40-based combined solution showed its effectiveness both as a preservative agent for static hypothermic storage and as a perfusion solution for EVLP. The use of a low-volume bench for experimental studies in a rat model enhanced the efficiency of lung graft function analysis while reducing consumable costs. Donor lungs preserved and perfused with the experimental solution exhibited better RI and lower PVR compared to the original Steen Solution™, highlighting its efficacy. Recovery of lung function after prolonged hypothermic storage was confirmed by an increase in RI and a decrease in PVR during perfusion, indicating safe and adequate preservation of the graft. Therefore, the developed dextran 40-based solution presents a promising and effective alternative for preservation and *ex vivo* perfusion of donor lungs when compared to existing foreign solutions.

The authors declare no conflict of interest.

REFERENCES

1. NHS Blood and Transplant: annual activity report; 2022. Available at: https://www.odt.nhs.uk/statistics-and-reports/organ-specific-reports/.
2. *Ojo AO, Heinrichs D, Emond JC, McGowan JJ, Guidinger MK, Delmonico FL, Metzger RA*. Organ donation and utilization in the USA. *Am J Transplant*. 2004; 4 (9): 27–37. doi: 10.1111/j.1600-6135.2004.00396.x.
3. *Mulligan MJ, Sanchez PG, Evans CF, Wang Y, Kon ZN, Rajagopal K et al.* The use of extended criteria donors decreases one-year survival in high-risk lung recipients: a review of the United Network of Organ Sharing Database. *J Thorac Cardiovasc Surg*. 2016; 152 (3): 891–898.e2. doi: 10.1016/j.jtcvs.2016.03.096.
4. *Botha P, Trivedi D, Weir CJ, Searl CP, Corris PA, Dark JH, Schueler SV.* Extended donor criteria in lung transplantation: impact on organ allocation. *J Thorac Cardiovasc Surg*. 2006; 131 (5): 1154–1160. doi: 10.1016/j.jtcvs.2005.12.037.
5. *Valenza F, Rosso L, Coppola S, Froio S, Palleschi A, Tosi D et al. Ex vivo* lung perfusion to improve donor lung function and increase the number of organs available for transplantation. *Transpl Int*. 2014; 27 (6): 553–561. doi: 10.1111/tri.12295.
6. *Cypel M, Yeung JC, Liu M, Anraku M, Chen F, Karolak W et al.* Normothermic *ex vivo* lung perfusion in clinical lung transplantation. *N Engl J Med*. 2011; 364 (15): 1431–1440. doi: 10.1056/NEJMoa1014597.
7. *Sanchez PG, Chan EG, Davis RD, Hartwig M, Machuca T, Whitson B et al.* Normothermic *ex vivo* lung perfusion (novel) as an assessment of extended criteria donor lungs: a prospective multi-center clinical trial. *J Heart Lung Transplant*. 2022; 41 (4): S40–S41. doi: 10.1016/j.healun.2022.01.092.
8. *Steen S, Sjöberg T, Pierre L, Liao Q, Eriksson L, Algotsson L*. Transplantation of lungs from a non-heart-beating donor. *Lancet*. 2001; 357 (9259): 825–829. doi: 10.1016/s0140-6736(00)04195-7.
9. *Levitt DG, Levitt MD.* Human serum albumin homeostasis: a new look at the roles of synthesis, catabolism, renal and gastrointestinal excretion, and the clinical value of serum albumin measurements. *Int J Gen Med*. 2016; 9: 229–255. doi: 10.2147/ijgm.S102819.
10. *Termeer CC, Weiss JM, Schöpf E, Vanscheidt W, Simon JC*. The low molecular weight Dextran 40 inhibits the adhesion of T lymphocytes to endothelial cells. *Clin Exp Immunol*. 1998; 114 (3): 422–426. doi: 10.1046/j.1365-2249.1998.00729.x.
11. *Laubach VE, Sharma AK*. Mechanisms of lung ischemia-reperfusion injury. *Curr Opin Organ Transplant*. 2016; 21 (3): 246–252. doi: 10.1097/mot.0000000000000304.
12. *Cypel M, Yeung JC, Hirayama S, Rubacha M, Fischer S, Anraku M et al.* Technique for prolonged normothermic *ex vivo* lung perfusion. *J Heart Lung Transplant*. 2008; 27 (12): 1319–1325. doi: 10.1016/j.healun.2008.09.003.
13. *Cypel M, Rubacha M, Yeung J, Hirayama S, Torbicki K, Madonik M et al.* Normothermic *ex vivo* perfusion prevents lung injury compared to extended cold preservation for transplantation. *Am J Transplant*. 2009; 9 (10): 2262–2269. doi: 10.1111/j.1600-6143.2009.02775.x.
14. *Andreasson ASI, Borthwick LA, Gillespie C, Jiwa K, Scott J, Henderson P et al*. The role of interleukin-1β as a predictive biomarker and potential therapeutic target during clinical *ex vivo* lung perfusion. *J Heart Lung Transplant*. 2017; 36 (9): 985–995. doi: 10.1016/j.healun.2017.05.012.
15. *Kakishita T, Oto T, Hori S, Miyoshi K, Otani S, Yamamoto S et al.* Suppression of inflammatory cytokines during

ex vivo lung perfusion with an adsorbent membrane. *Ann Thorac Surg*. 2010; 89 (6): 1773–1779. doi: 10.1016/j.athoracsur.2010.02.077.

16. *Erasmus ME, Fernhout MH, Elstrodt JM, Rakhorst G.* Normothermic *ex vivo* lung perfusion of non-heart-beating donor lungs in pigs: from pretransplant function analysis towards a 6-h machine preservation. *Transpl Int*. 2006; 19 (7): 589–593. doi: 10.1111/j.1432-2277.2006.00318.x.
17. *Brandes H, Albes JM, Conzelmann A, Wehrmann M, Ziemer G.* Comparison of pulsatile and nonpulsatile perfusion of the lung in an extracorporeal large animal model. *Eur Surg Res*. 2002; 34 (4): 321–329. doi: 10.1159/000063067.
18. *Van Zanden JE, Leuvenink HGD, Verschuuren EAM, Erasmus ME, Hottenrott MC.* A translational rat model for *ex vivo* lung perfusion of pre-injured lungs after brain death. *PLoS One*. 2021; 16 (12): e0260705. doi: 10.1371/journal.pone.0260705.
19. *Noda K, Shigemura N, Tanaka Y, Bhama JK, D'Cunha J, Luketich JD, Bermudez CA.* Successful prolonged *ex vivo* lung perfusion for graft preservation in rats. *Eur J Cardiothorac Surg*. 2014; 45 (3): e54–e60. doi: 10.1093/ejcts/ezt598.
20. *Wang W, Qian J, Zhu M, Wang Y, Pan Y.* Normothermic *ex vivo* lung perfusion outperforms conventional cold preservation in a deceased rat lung. *Ann Transl Med*. 2022; 10 (2): 99. doi: 10.21037/atm-22-42.
21. *Ohsumi A, Kanou T, Ali A, Guan Z, Hwang DM, Waddell TK et al.* A Method for Translational Rat *Ex vivo* Lung Perfusion Experimentation. *Am J Physiol Lung Cell Mol Physiol*. 2020; 319 (1): L61–L70. doi: 10.1152/ajplung.00256.2019.
22. *Tian D, Shiiya H, Sato M, Nakajima J.* Rat lung transplantation model: modifications of the cuff technique. *Ann Transl Med*. 2020; 8 (6): 407. doi: 10.21037/atm.2020.02.46.
23. *Rajab TK.* Anastomotic techniques for rat lung transplantation. *World J Transplant*. 2018; 8 (2): 38–43. doi: 10.5500/wjt.v8.i2.38.
24. *Jin X, Kaes J, Van Slambrouck J, Inci I, Arni S, Geudens V et al.* A Comprehensive Review on the Surgical Aspect of Lung Transplant Models in Mice and Rats. *Cells.* 2022; 11 (3): 480. doi: 10.3390/cells11030480.
25. *Roman M, Gjorgjimajkoska O, Neil D, Nair S, Colah S, Parmar J, Tsui S.* Comparison between cellular and acellular perfusates for *ex vivo* lung perfusion in a porcine model. *J Heart Lung Transplant.* 2015; 34 (7): 978–987. doi: 10.1016/j.healun.2015.03.023.
26. *Pan X, Yang J, Fu S, Zhao H.* Application of *ex vivo* lung perfusion (EVLP) in lung transplantation. *J Thorac Dis*. 2018; 10 (7): 4637–4642. doi: 10.21037/jtd.2018.07.95.
27. *Bassani GA, Lonati C, Brambilla D, Rapido F, Valenza F, Gatti S. Ex Vivo* Lung Perfusion in the Rat: Detailed Procedure and Videos. *PLoS One*. 2016; 11 (12): e0167898. doi: 10.1371/journal.pone.0167898.
28. *Esipova OYu, Bogdanov VK, Esipov AS, Kuleshov AP, Buchnev AS, Volkova EA et al*. Development of a new low-volume oxygenator and creation of a hydrodynamic test bench for *ex vivo* lung perfusion in small animals. *Russian Journal of Transplantology and Artificial Organs.* 2023; 25 (3): 106–112. [In Russ, English abstract]. https://doi.org/10.15825/1995-1191-2023-3-106-112.
29. *Esipova OYu, Buchnev AS, Drobyshev AA, Kuleshov AP, Grudinin NV, Bogdanov VK.* Evaluation of oxygen transfer performance of a small-size membrane oxygenator. *Medical technics*. 2023; 4: 21–25.
30. *Esipova OYu, Buchnev AS, Drobyshev AA, Kuleshov AP, Grudinin NV, Bogdanov VK*. Evaluation of the oxygen transfer performance of a small membrane oxygenator. *Biomedical Engineering*. 2023; 57: 260–264. https://doi.org/10.1007/s10527-023-10311-w.
31. *Esipova OYu, Kuleshov AP, Bogdanov VK, Esipov AS, Volkova EA, Grudinin NV.* Development of a low-volume stand for the procedure of isolated *ex vivo* perfusion of the lungs of small animals. *Russian Journal of Transplantology and Artificial Organs*. 2024; 26 (3): 176–182. [In Russ, English abstract]. https://doi.org/10.15825/1995-1191-2024-3-176-182.

The article was submitted to the journal on 29.08.2024

DOI: 10.15825/1995-1191-2024-4-201-211

NUMERICAL ASSESSMENT OF THE EFFECT OF XENOPERICARDIAL BIOPROSTHETIC HEART VALVE CALCIFICATIONS ON ITS BIOMECHANICS

P.S. Onishchenko[1], K.Yu. Klyshnikov[1], A.A. Khromov[2], A.E. Kostyunin[1], T.V. Glushkova[1], T.N. Akentieva[1], E.A. Ovcharenko[1]

[1] Research Institute for Complex Issues of Cardiovascular Diseases, Kemerovo, Russian Federation
[2] Kuzbass Cardiology Center, Kemerovo, Russian Federation

Objective: to conduct a pilot study of the effect of bioprosthetic heart valve leaflet calcification on biomechanics and to identify the "stress in the material – dysfunction" relationship. **Materials and methods.** The study's focus was on two commercially available UniLine bioprosthetic mitral valves sized 26 and 30 (NeoCor, Russia). The samples were subjected to microcomputer tomographic scanning in order to reconstruct calcium volumes. The resulting 3D models were correlated with prostheses of corresponding sizes and projected to the volume of the locking element in the Abaqus/CAE engineering analysis software (Dassault Systemes, France). **Results.** According to numerical modeling, the maximum principal stresses increased significantly to 90.8 MPa in the samples, the opening decreased qualitatively, and impact on the prosthetic frame increased. Comparison of stress diagrams of numerical simulation with samples demonstrates the relationship between peak amplitude and rupture and thinning localizations in the flap apparatus. **Conclusion.** The work presented demonstrated the findings of a pilot study of the connection between biomechanics in a patient-specific calcified mitral prosthetic heart valve UniLine and macroscopic characterization of explanted samples. The comparative stage showed that stress values correlate with localization of leaflet dysfunction.

Keywords: bioprosthetic heart valves, calcification, dysfunctions, numerical modeling, biomechanics.

INTRODUCTION

According to various sources, over 9,000 heart valve surgeries are performed annually in the Russian Federation, with bioprosthetic heart valves (BHVs) accounting for at least 19% of these procedures [1]. BHVs offer several advantages over mechanical valves, including the absence of a need for lifelong anticoagulant therapy and the ability to more closely replicate native hemodynamics due to the design and materials of the leaflet components [2–4]. However, more than 30% of BHVs require replacement within 10–15 years due to various dysfunctions, such as calcification, pannus formation, ruptures, and perforations [5]. This highlights the need to investigate the underlying mechanisms [6–8] and develop preventive strategies [8, 9] for degenerative changes in the biological tissues of prosthetic valve leaflets. The main research approaches to addressing bioprosthetic valve dysfunction include:

– imaging techniques (X-ray, computed tomography (CT), micro-CT) [10–12];
– histological analysis [13–16];
– immunohistochemistry and immunofluorescence [16–19];
– blotting and proteomic profiling [20–22];
– sequencing [23–25];
– scanning electron microscopy [16, 26, 27].

Most of the aforementioned methods are now integrated in contemporary research, enabling a comprehensive characterization of valve dysfunction, including tissue destruction, cellular and bacterial infiltration, and protein deposition. With the advancement of computer simulation technologies, biomechanical analysis of prosthetic heart valves – both at the level of individual components and the prosthesis as a whole – has become increasingly feasible [28–33]. A major focus of current research is the evaluation of the stress-strain state of the leaflet material and the progression of valve dysfunction over time [32–35].

Initial studies in valve biomechanics modeled the leaflet structure using shell-based approaches, where the material's thickness was a key parameter [28, 34]. More recent efforts have shifted toward volumetric modeling [32], which allows for more accurate representation of *in situ* mechanical behavior. Similarly, calcific deposits can be incorporated either as material properties within the computational mesh [28] or explicitly represented as three-dimensional bodies on the valve surface [32, 34]. However, literature evidence suggests that such degene-

Corresponding author: Pavel Onishchenko. Address: 6, Barbarash boulevard, Kemerovo, 650002, Russian Federation. Phone: (3842) 34-55-86. E-mail: onis.pavel@gmail.com

rative changes may also localize within the thickness of the leaflet tissue itself [36–39]. This highlights a notable limitation in current modeling approaches – the oversimplified mathematical representation of the structural complexities within the leaflet tissue.

To address the shortcomings identified in previous numerical modeling studies of BHV dysfunction, we developed a novel approach for conducting in silico experiments. This method was validated through a comparative analysis involving both an intact (initial) model and a patient-specific model of a BHV. Additionally, the numerical modeling results were compared against dysfunctions observed in explanted xenopericardial mitral prostheses.

MATERIALS AND METHODS

The study focused on two UniLine bioprosthetic mitral valves (NeoCor, Russia) [40, 41], with diameters of 26 mm and 30 mm (Fig. 1, a), which were electively explanted due to dysfunction after 4.3 and 5.3 years of *in vivo* use, respectively. Within four hours of explantation, photographic documentation of the dysfunctional regions was performed, followed by detailed macroscopic imaging to facilitate comparison with biomechanical simulation outcomes.

Subsequently, both specimens underwent microcomputed tomography using a previously established protocol [27]. The acquired tomographic slices were imported into the Mimics medical 3D engineering software (Materialise, Belgium), where volumetric models of calcific lesions (Fig. 1, b) were reconstructed based on radiodense regions, as described in earlier methodologies [42].

Subsequently, we developed a computational model within the Abaqus engineering analysis environment

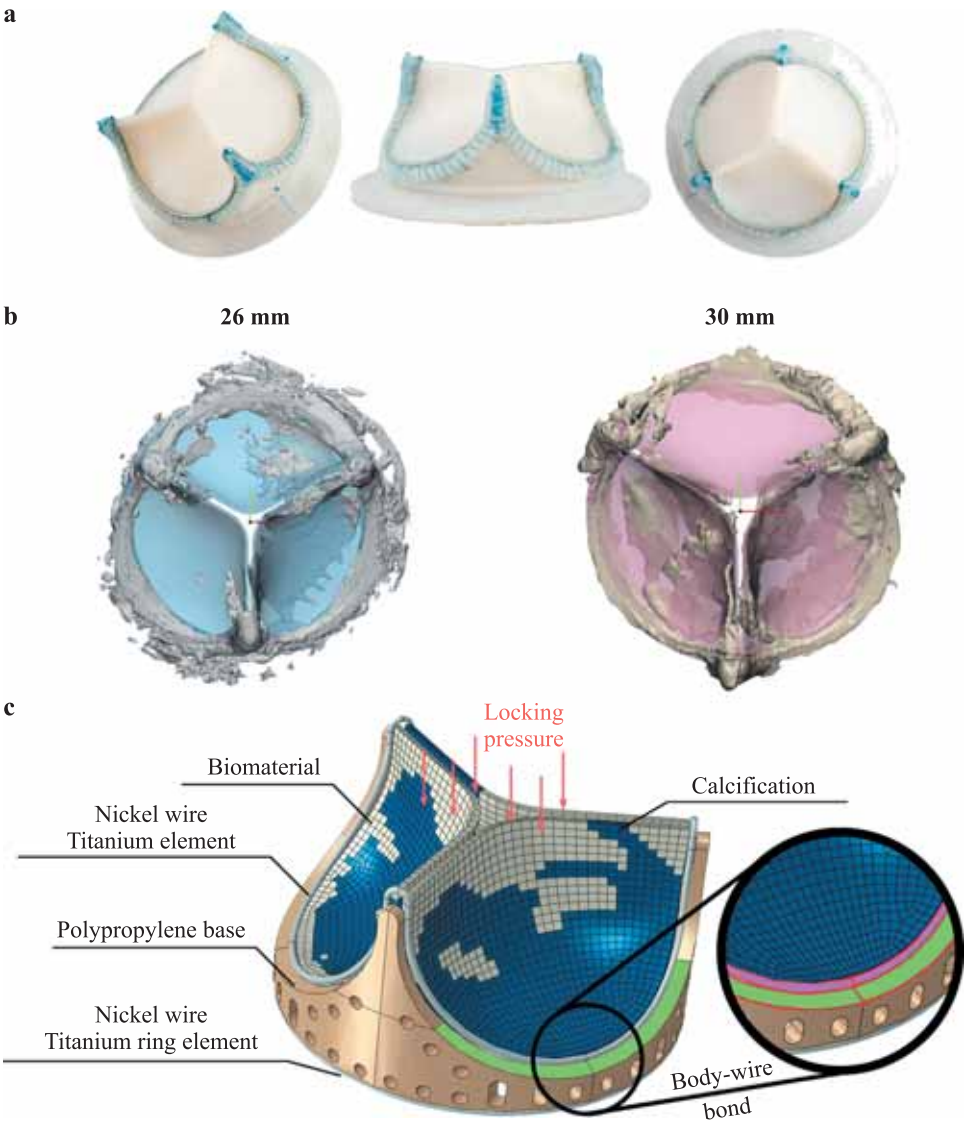

Fig. 1. UniLine bioprosthetic mitral valve: a, general view; b, comparison of the prosthesis model and calcifications reconstructed from micro-CT; c, description of the assembly components, visualization of applied pressure and interaction of the pairs of elements

(Dassault Systèmes, France), using the Dynamic/Explicit solver. The 3D model of the bioprosthesis, which included polypropylene and wire support structures along with 3 valve cusps (Fig. 1, b), was augmented with volumetric representations of calcifications (Fig. 2, b). A 3D finite element mesh was then constructed, comprising C3D8 hexahedral solid elements for the polypropylene frame and leaflet apparatus, and C3D4 tetrahedral elements for the wire components fabricated from titanium nickelide. The final meshes contained 15,862 and 21,031 elements for the 26 mm and 30 mm prostheses, respectively.

The biomechanical performance of the leaflet apparatus, including calcified regions, was assessed by simulating 2 complete cardiac cycles at a heart rate of 70 beats per minute, spanning a total simulation time of 0–1.8 seconds. Material properties were assigned in accordance with manufacturer specifications [43] and previously published data [44, 45]. Calcified regions were modeled as rigid bodies, following standard parameters for calcium deposits [44].

Uniaxial tensile test data for the leaflet material [46] were imported into the Abaqus/CAE environment, where coefficients were fitted for a nonlinear constitutive model (Table) using the following strain energy function:

$$W = \sum_{i=0}^{n} C_{i0}(I_1 - 3)^i,$$

where W is strain energy density, C_{i0} is Rivlin coefficient, and I_1 is first invariant of Green deformation tensor.

Table

Coefficients of the nonlinear biomaterial model

C_{10}, MPa	C_{20}, MPa	C_{30}, MPa	C_{40}, MPa
0.0071	0.5036	1.023	–0.651

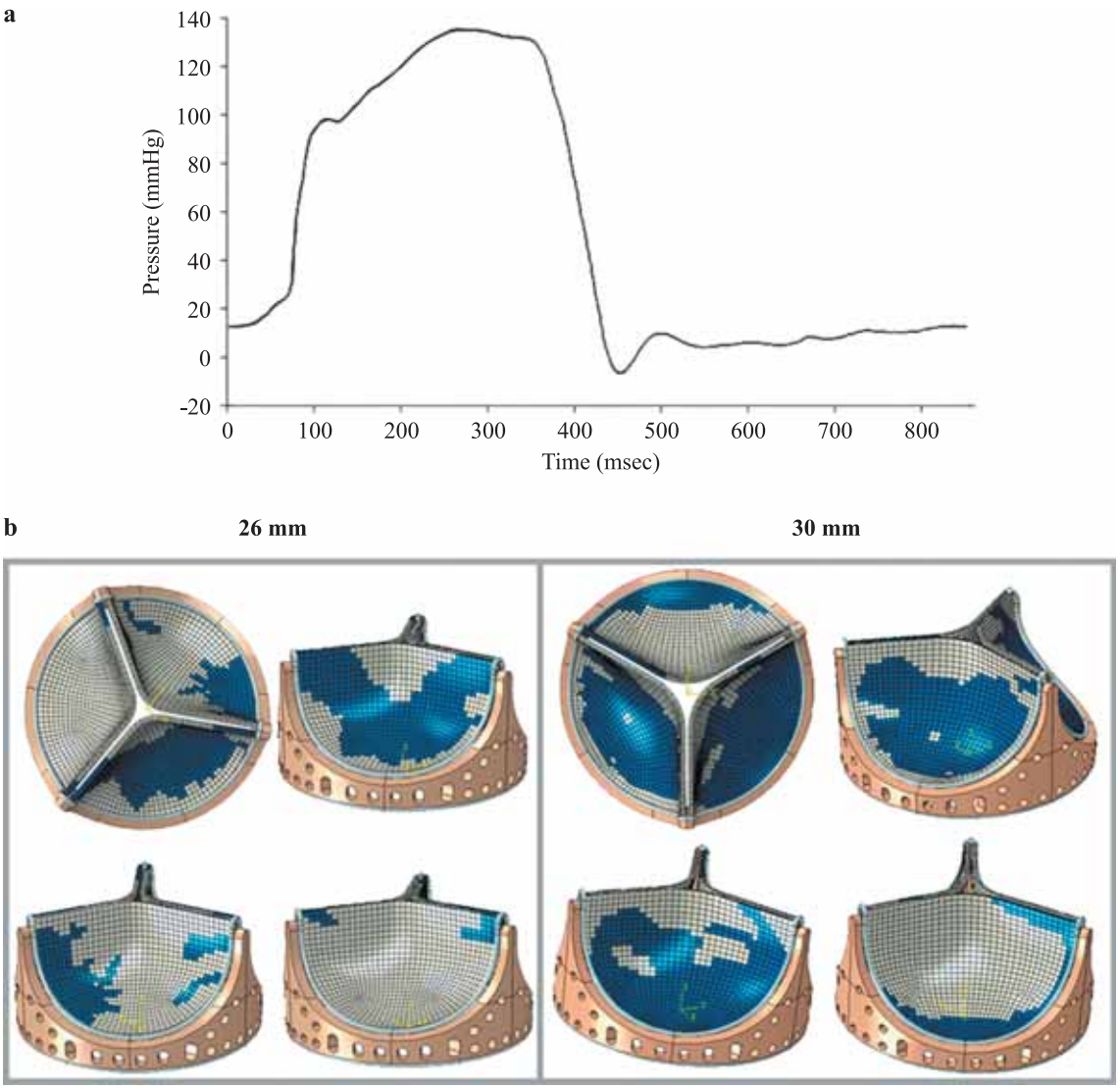

Fig. 2. Modeling methodology: a, pressure applied to the valve plug; b, location of calcifications (blue) in the biomaterial of the flap apparatus (gray)

Contact between the valve leaflets was modeled using a "hard contact" interaction with a coefficient of friction set at 0.2. All components of the prosthesis were integrated into a unified assembly via paired tie-type constraints: specifically, between the nodes of the polypropylene frame and the wire components, as well as between the upper wire component and the lower suture edge of the leaflet. Boundary conditions enforcing complete fixation – zero displacement and zero rotation – were applied to the lower annular wire component (Fig. 1, b). Hemodynamic loading was simulated by applying physiological pressure to the leaflet surface from the left ventricular side (Fig. 2, a, Fig. 1, b).

For comparison, UniLine valve models without calcification – featuring leaflets composed of a homogeneous xenopericardial material – were also simulated under identical conditions. In all modeled cases, the maximum principal stress was used as the key quantitative indicator to evaluate leaflet biomechanics.

RESULTS

Modeling of prosthetic biomechanics with no degenerative changes

At this stage, simulations were performed on BHV models in their intact state, without calcification of the leaflet apparatus. The results are presented in Fig. 3.

The analysis revealed increased stress concentrations at the commissural strut regions, with a uniform stress distribution throughout the volume of the polypropylene frame and symmetrical loading of the leaflet apparatus onto the wire component. During the entire cardiac cycle, peak stress did not exceed 11.5 MPa for the 26 mm prosthesis and 16.5 MPa for the 30 mm prosthesis. These values remain well below the threshold for irreversible deformation of the leaflet material [44, 47].

Modeling considering calcium deposits in the leaflet apparatus

The inclusion of leaflet calcification in the computational model significantly altered the biomechanical behavior of the bioprosthesis. Notably, there was a marked increase in peak maximum principal stress, accompanied by a qualitative reduction in leaflet opening amplitude (Fig. 4).

The most pronounced biomechanical changes were observed in the 26 mm UniLine bioprosthesis model. Peak maximum principal stresses within the calcified regions ranged from 30.5 MPa to 48.8 MPa, predominantly localized at sites of interaction with the wire frame. These elevated stress values are attributed to material stretching during the valve closure phase, with stress amplitudes reducing to an average of 20 MPa during valve opening.

Interestingly, larger-volume calcific deposits exhibited lower peak stress magnitudes compared to smaller clusters – 30 MPa in the closed state versus 6.3 MPa during opening. In addition, both the polypropylene base and wireframe elements experienced significantly increased loading compared to their intact counterparts.

The UniLine bioprosthesis with a 30 mm diameter, due to the greater volume of biomaterial in its leaflet structure, exhibited a more uniform stress distribution compared to the 26 mm model. However, maximum principal stresses in this model remained substantially elevated relative to the intact condition, reaching up to 90.8 MPa during closure and 55.9 MPa in the opening

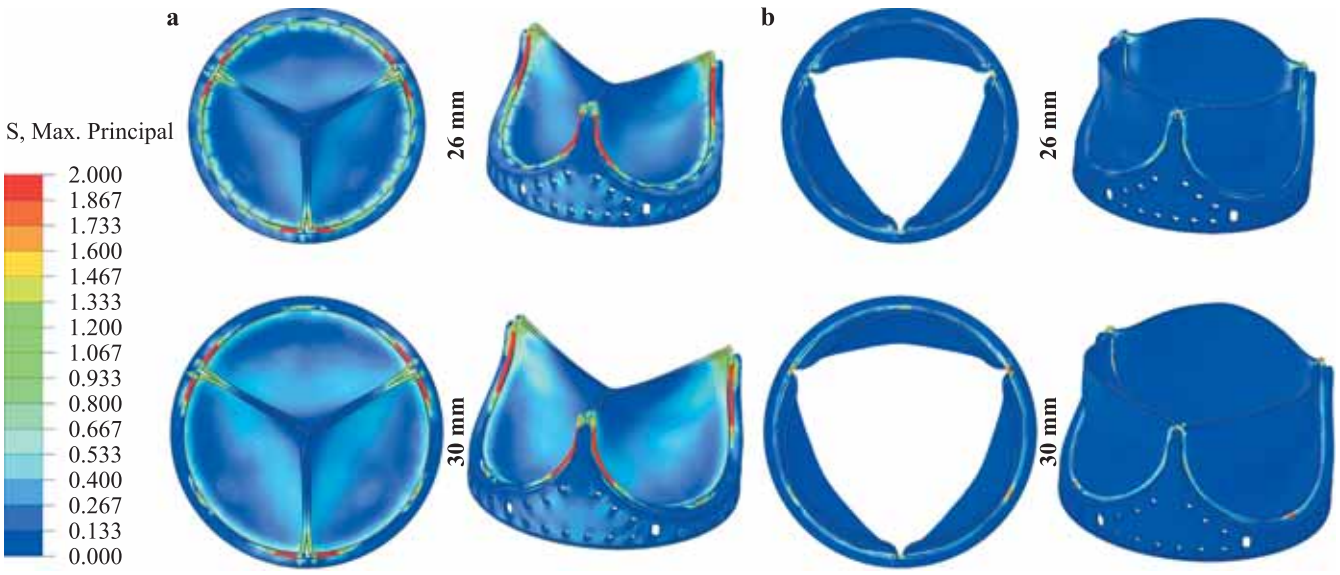

Fig. 3. Results of numerical modeling of the UniLine bioprosthetic valve of 26 mm (top row) and 30 mm (bottom row) diameter in an intact state at a: closure, T = 1.188 sec; b: maximum opening, T = 1.584 sec

phase, particularly in the region of the leaflet's free edge. There were no significant alterations in the stress experienced by the polypropylene framework component.

Correlation between biomechanical simulation and explanted bioprosthesis specimens

At this stage, we addressed a key question: to what extent do the simulated calcification zones within the leaflet apparatus, and the associated localized stress concentrations (Fig. 5, b, c), correlate with the structural dysfunctions observed in the explanted prostheses (Fig. 5, a)?

The study reveals irregularities and steep gradients in stress magnitude, which correspond to areas of tissue thinning (Fig. 5, b, c) and leaflet tears (Fig. 5, c). These changes are predominantly localized in the commissural regions, suggesting that mechanical stretching plays a critical role in the pathogenesis of structural degeneration.

One plausible mechanism underlying this dysfunction is the abrasion and subsequent disruption of the surface layer of the leaflet tissue at its attachment to the wireframe component. This disruption likely facilitates calcium penetration into the locking element.

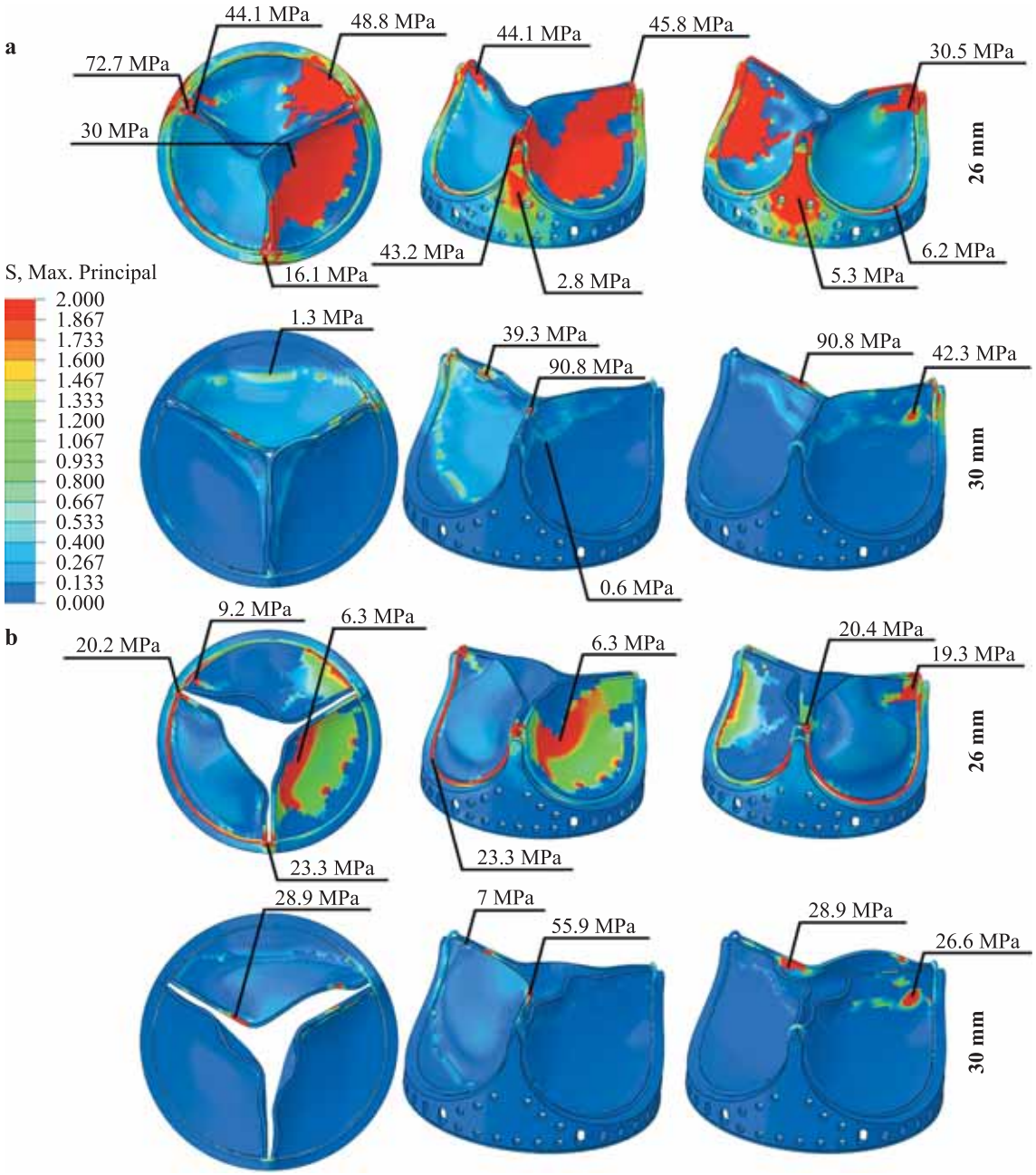

Fig. 4. Results of numerical modeling of the biomechanics of the UniLine bioprosthetic mitral valve with a diameter of 26 and 30 mm in a: closed state, T = 1.188 sec; b: open state, T = 1.584 sec

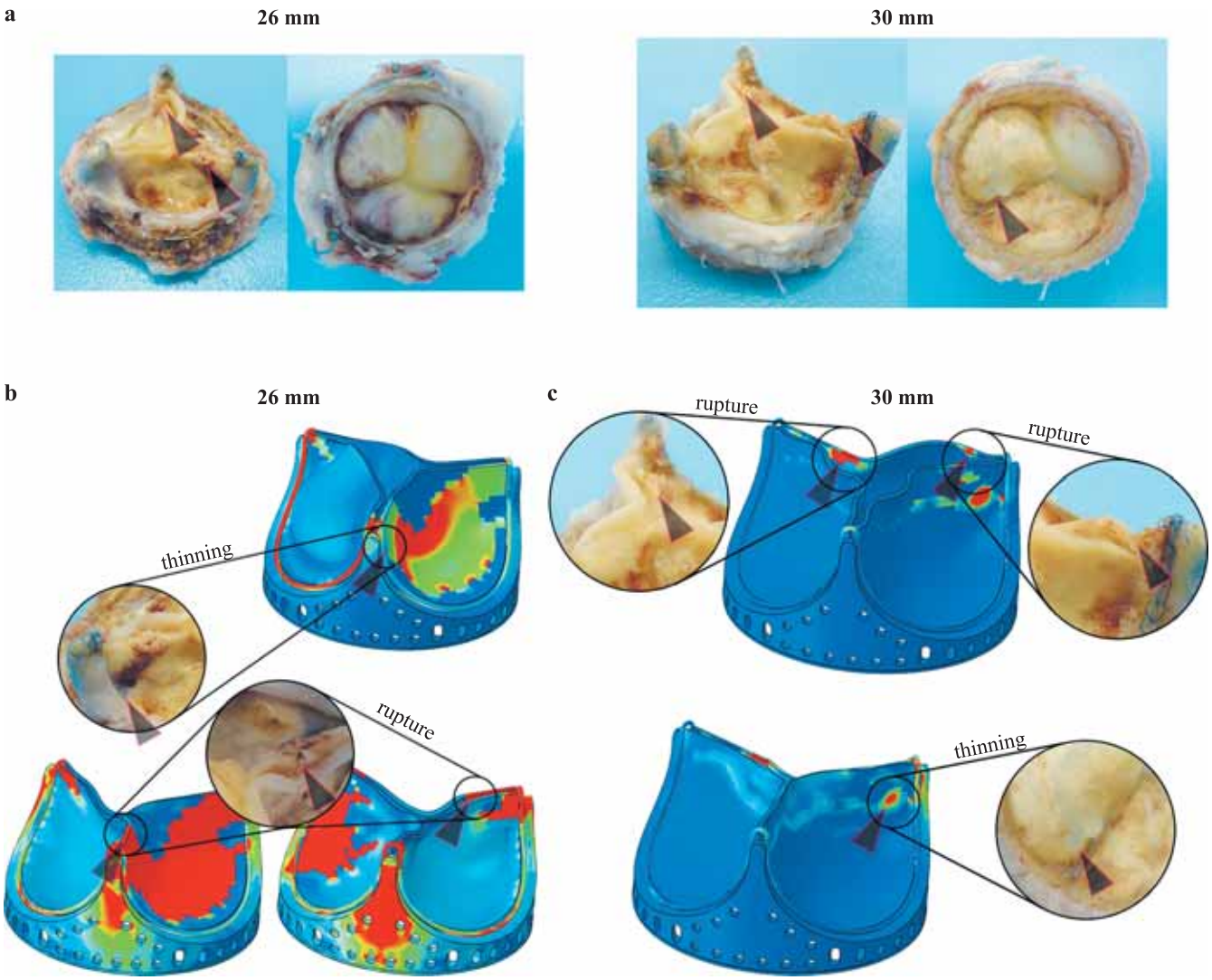

Fig. 5. Comparison of excised samples (a) and comparison of dysfunction areas with modeling results of the UniLine bioprosthetic valves of diameter 26 mm (b) and 30 mm (c). The corresponding comparison areas are highlighted with translucent pointers. The coloring of the diagrams corresponds to the scale of maximum principal stress [0, 2] MPa

DISCUSSION

On one hand, various research groups have demonstrated the significant impact of structural alterations on the performance of artificial heart valve substitutes. Hamid et al. (1987) [28] examined how the location of calcium deposits and the presence of perforations influence the vibrational behavior of the leaflet dome. Given the limited computational resources available at the time, the authors focused on estimating the fundamental natural frequency – a key parameter in assessing the mechanical stability and durability of BHVs. Their findings indicated that a central perforation reduced the natural frequency from 55 Hz (in a native, healthy valve) to 52 Hz. Inclusion of calcifications increased the frequency to 62 Hz, while damage involving all three leaflets caused a dramatic rise to 145 Hz.

With advancements in hardware and computing performance, more sophisticated simulations have become possible. In 2016, for instance, researchers presented a model simulating the implantation of a balloon-expandable prosthesis into a calcified native valve, using the commercial Edwards SAPIEN valve (Edwards Lifesciences Inc., USA) as a reference [34]. The study presents detailed stress distribution patterns and analyzes the biomechanical behavior of the leaflet apparatus as influenced by the implantation technique of the prosthesis. The findings demonstrate that stress amplitudes increase notably in regions with calcium accumulations, with the first principal stress component (σ_1) exceeding 0.5 MPa. In contrast, areas with an intact (“clean”) surface exhibit much lower stress, typically below 0.15 MPa. Further advancement of this modeling approach was presented by Qin et al. in 2020 [32], who investigated stenotic heart valves using patient-specific native valve models. Their study revealed a strong correlation between stress distribution and location of calcifications. Stress concent-

rations were localized at the interface between the leaflet dome and the calcified regions. Quantitative analysis indicated an average increase in stress amplitudes by about 1.4 ± 0.08 times compared to non-calcified models, depending on the extent of the lesion.

On the other hand, numerous histological studies involving both animal models and explanted BHVs have documented structural deterioration characterized by calcium deposits surrounded by a disrupted cellular matrix [36–39]. Microscopic examination of affected tissues reveals detachment of collagen fibers from the mineralized inclusions, a phenomenon attributed to repetitive mechanical impact during the cardiac cycle. This process is believed to underlie the development of ruptures and perforations in BHVs.

A similar observation was made in this study, where regions of tissue thinning and tearing in the excised bioprosthetic specimens corresponded with zones of elevated mechanical stress. The findings underscore the substantial impact of leaflet calcification on the biomechanical performance of the prosthesis. Specifically, calcific deposits markedly alter the distribution and magnitude of maximum principal stresses, thereby impairing the leaflet's ability to reproduce native hemodynamics. The two case studies presented here effectively illustrate the potential relationship between stress concentration and valve dysfunction. However, to establish more generalizable conclusions and to validate these findings, a multicenter study is warranted. Such a study should integrate advanced noninvasive imaging and calcium mapping techniques for biomechanical modeling, alongside modern immunophenotyping approaches. The methodology presented here demonstrates the feasibility of conducting pilot investigations using explanted samples, laying the groundwork for larger-scale research initiatives.

CONCLUSIONS

The biomechanical impact of calcification within the leaflet apparatus on stress distribution in both the supporting frame and the dome of the cusps was investigated using two UniLine bioprosthetic valves (26 mm and 30 mm in diameter) explanted due to structural degeneration. The analysis revealed a marked increase in peak stress amplitudes – reaching up to 90.8 MPa – in regions containing calcium deposits. These elevated stress concentrations negatively affected the surrounding tissue integrity, contributing to leaflet thinning and rupture. Furthermore, in the 26 mm UniLine valve, structural modeling that incorporated calcifications demonstrated increased mechanical loading on both the wire support elements and the polypropylene frame component.

This work was conducted as part of the fundamental research project of the Research Institute for Complex Issues of Cardiovascular Diseases, titled "Molecular, cellular, and biomechanical mechanisms of the pathogenesis of cardiovascular diseases in the development of new treatment methods based on personalized pharmacotherapy, the introduction of minimally invasive medical devices, biomaterials, and tissue-engineered implants" (Research Supervisor: Professor Leonid Barbarash, Fellow, Russian Academy of Sciences), subject code 0419-2022-0001.

The authors express their sincere gratitude for the support provided within the framework of the project "Foundation for Support of Young Scientists in Biomedical Sciences", and especially thank Professor E.V. Grigoriev (MD), Fellow, Russian Academy of Sciences, for his valuable assistance and guidance.

The authors declare no conflict of interest.

REFERENCES

1. *Bokeria LA, Milievskaya EB, Kudzoeva ZF, Pryanishnikov BB, Skopin AI, Yurlov IA.* Cardiovascular Surgery – 2018. Diseases and congenital anomalies of the circulatory system. Moscow, 2018; 270.
2. *Bonow RO, O'Gara PT, Adams DH, Badhwar V, Bavaria JE, Elmariah S et al.* 2020 Focused Update of the 2017 ACC Expert Consensus Decision Pathway on the Management of Mitral Regurgitation: A Report of the American College of Cardiology Solution Set Oversight Committee. *J Am Coll Cardiol [Internet]*. 2020 May 5 [cited 2023 May 26]; 75 (17): 2236–2270. Available from: https://pubmed.ncbi.nlm.nih.gov/32068084/.
3. *Nishimura RA, Otto CM, Bonow RO, Carabello BA, Erwin JP, Fleisher LA et al.* 2017 AHA/ACC Focused Update of the 2014 AHA/ACC Guideline for the Management of Patients with Valvular Heart Disease: A Report of the American College of Cardiology / American Heart Association Task Force on Clinical Practice Guidelines. *Circulation [Internet]*. 2017 Jun 20 [cited 2023 May 26]; 135 (25): e1159–e1195. Available from: https://www.ahajournals.org/doi/abs/10.1161/CIR.0000000000000503.
4. *Marom G, Einav S.* New insights into valve hemodynamics. *Rambam Maimonides Med J*. 2020 Apr 29; 11 (2): e0014. doi: 10.5041/RMMJ.10400.
5. *Velho TR, Pereira RM, Fernandes F, Guerra NC, Ferreira R, Nobre Â.* Bioprosthetic Aortic Valve Degeneration: a Review from a Basic Science Perspective. *Brazilian J Cardiovasc Surg*. 2022; 37 (2): 239–250. doi: 10.21470/1678-9741-2020-0635.

6. *Brockbank KGM, Song YC.* Mechanisms of bioprosthetic heart valve calcification. *Transplantation*. 2003; 75 (8): 1133–1135. doi: 10.1097/01.TP.0000062864.54455.E5.
7. *Scott Rapoport H, Connolly JM, Fulmer J, Dai N, Murti BH, Gorman RC et al.* Mechanisms of the *in vivo* inhibition of calcification of bioprosthetic porcine aortic valve cusps and aortic wall with triglycidylamine/mercapto bisphosphonate. *Biomaterials*. 2007; 28 (4): 690–699. doi: 10.1016/j.biomaterials.2006.09.029.
8. *Wen S, Zhou Y, Yim WY, Wang S, Xu L, Shi J et al.* Mechanisms and Drug Therapies of Bioprosthetic Heart Valve Calcification. *Front Pharmacol*. 2022 Jun 3; 13: 909801. doi: 10.3389/fphar.2022.909801.
9. *Timchenko TP.* Bisphosphonates as Potential Inhibitors of Calcification in Bioprosthetic Heart Valves (Review). *Modern Technologies in Medicine*. 2022; 14 (2): 68–79. doi: 10.17691/stm2022.14.2.07.
10. *Alwan L, Bernhard B, Brugger N, de Marchi SF, Praz F, Windecker S et al.* Imaging of Bioprosthetic Valve Dysfunction after Transcatheter Aortic Valve Implantation. *Diagnostics (Basel)*. 2023 May 29; 13 (11): 1908. doi: 10.3390/diagnostics13111908.
11. *Piérard S, Seldrum S, Muller T, Gerber BL.* Evaluation of aortic bioprosthesis stenosis by multidetector CT. *J Cardiovasc Comput Tomogr*. 2012; 6 (1): 62–65. doi: 10.1016/j.jcct.2011.11.005.
12. *Cartlidge TRG, Doris MK, Sellers SL, Pawade TA, White AC, Pessotto R et al.* Detection and Prediction of Bioprosthetic Aortic Valve Degeneration. *J Am Coll Cardiol*. 2019; 73 (10): 1107–1119. doi: 10.1016/j.jacc.2018.12.056.
13. *Lepidi H, Casalta JP, Fournier PE, Habib G, Collart F, Raoult D.* Quantitative histological examination of mechanical heart valves. *Clin Infect Dis*. 2005; 40 (5): 655–661. doi: 10.1086/427504.
14. *Sellers SL, Turner CT, Sathananthan J, Cartlidge TRG, Sin F, Bouchareb R et al.* Transcatheter Aortic Heart Valves: Histological Analysis Providing Insight to Leaflet Thickening and Structural Valve Degeneration. *JACC Cardiovasc Imaging*. 2019; 12 (1): 135–145. doi: 10.1016/j.jcmg.2018.06.028.
15. *Lepidi H, Casalta JP, Fournier PE, Habib G, Collart F, Raoult D.* Quantitative histological examination of bioprosthetic heart valves. *Clin Infect Dis*. 2006; 42 (5): 590–596. doi: 10.1086/500135.
16. *Prokudina ES, Senokosova EA, Antonova LV, Muhamadijarov RA, Koshelev VA, Krivkina EO et al.* Morphological features of biological and tissue-engineered vascular patches remodeling: results of tests on a sheep model. *The Siberian Journal of Clinical and Experimental Medicine*. 2023; 38 (4): 250–259. [In Russ., English abstact]. doi: 10.29001/2073-8552-2023-38-4-250-259.
17. *Bogdanov LA, Velikanova EA, Shishkova DK, Shabaev AR, Kutikhin AG.* Neointimal remodeling in carotid atherosclerosis: roles of matrix metalloproteinases-2 and -9 and different phenotypes of vascular smooth muscle cells. *Pathological physiology and experimental therapy*. 2020; (4): 20–30. [In Russ, English abstract]. doi: 10.25557/0031-2991.2020.04.20-30.
18. *Human P, Bezuidenhout D, Aikawa E, Zilla P.* Residual Bioprosthetic Valve Immunogenicity: Forgotten, Not Lost. *Front Cardiovasc Med*. 2022 Jan 4; 8: 760635. doi: 10.3389/fcvm.2021.760635.
19. *Marro M, Kossar AP, Xue Y, Frasca A, Levy RJ, Ferrari G.* Noncalcific mechanisms of bioprosthetic structural valve degeneration. *J Am Heart Assoc*. 2021; 10 (3): 1–13. doi: 10.1161/JAHA.120.018921.
20. *Shishkova DK, Glushkova TV, Efimova OS, Popova AN, Malysheva VY, Kolmykov RP et al.* Morphological and Chemical Properties of Spherical and Needle Calcium Phosphate Bions. *Complex Issues Cardiovasc Dis*. 2019; 8 (1): 59–69. doi: 10.17802/2306-1278-2019-8-1-59-69.
21. *Abramov A, Xue Y, Zakharchenko A, Kurade M, Soni RK, Levy RJ, Ferrari G.* Bioprosthetic heart valve structural degeneration associated with metabolic syndrome: Mitigation with polyoxazoline modification. *Proc Natl Acad Sci USA*. 2023 Jan 3; 120 (1): e2219054120. doi: 10.1073/pnas.2219054120.
22. *Smart I, Goecke T, Ramm R, Petersen B, Lenz D, Haverich A et al.* Dot blots of solubilized extracellular matrix allow quantification of human antibodies bound to epitopes present in decellularized porcine pulmonary heart valves. *Xenotransplantation*. 2021; 28 (1). doi: 10.1111/xen.12646.
23. *Asanov MA, Kazachek YV, Evtushenko AV, Teplova YE, Ponasenko AV.* Comparison of Microflora Isolated From Peripheral Blood and Valvular Structures of the Heart in Patients With Infective Endocarditis. *Acta Biomed Sci*. 2022; 7 (2): 91–98. doi: 10.29413/ABS.2022-7.2.10.
24. *Mohammadi MM, Bavi O.* DNA sequencing: an overview of solid-state and biological nanopore-based methods. *Biophys Rev*. 2022; 14 (1): 99–110. doi: 10.1007/s12551-021-00857-y.
25. *Rovery C, Greub G, Lepidi H, Casalta JP, Habib G, Collart F, Raoult D.* PCR detection of bacteria on cardiac valves of patients with treated bacterial endocarditis. *J Clin Microbiol*. 2005; 43 (1): 163–167. doi: 10.1128/JCM.43.1.163-167.2005.
26. *Mukhamadiyarov RA, Bogdanov LA, Glushkova TV, Shishkova DK, Kostyunin AE, Koshelev VA et al.* Embedding and backscattered scanning electron microscopy: A detailed protocol for the whole-specimen, high-resolution analysis of cardiovascular tissues. *Front Cardiovasc Med*. 2021 Oct 25; 8: 73954. doi: 10.3389/fcvm.2021.739549.
27. *Keklikoglou K, Arvanitidis C, Chatzigeorgiou G, Chatzinikolaou E, Karagiannidis E, Koletsa T et al.* Micro-CT for biological and biomedical studies: A comparison of imaging techniques. *J Imaging*. 2021 Sep 1; 7 (9): 172. doi: 10.3390/jimaging7090172.
28. *Hamid MS, Sabbah HN, Stein PD.* Vibrational analysis of bioprosthetic heart valve leaflets using numerical models: Effects of leaflet stiffening, calcification, and perfo-

ration. *Circ Res*. 1987; 61 (5): 687–694. doi: 10.1161/01.RES.61.5.687.
29. *Claiborne TE, Sheriff J, Kuetting M, Steinseifer U, Slepian MJ, Bluestein D. In vitro* evaluation of a novel hemodynamically optimized trileaflet polymeric prosthetic heart valve. *J Biomech Eng*. 2013 Feb; 135 (2): 021021. doi: 10.1115/1.4023235.
30. *Claiborne TE, Xenos M, Sheriff J, Chiu WC, Soares J, Alemu Y et al.* Toward optimization of a novel trileaflet polymeric prosthetic heart valve via device thrombogenicity emulation. *ASAIO J*. 2013; 59 (3): 275–283. doi: 10.1097/MAT.0b013e31828e4d80.
31. *Xuan Y, Dvir D, Wang Z, Mizoguchi T, Ye J, Guccione JM et al.* Stent and leaflet stresses in 26-mm, third-generation, balloon-expandable transcatheter aortic valve. *J Thorac Cardiovasc Surg*. 2019; 157 (2): 528–536. doi: 10.1016/j.jtcvs.2018.04.115.
32. *Qin T, Caballero A, Mao W, Barrett B, Kamioka N, Lerakis S, Sun W.* The role of stress concentration in calcified bicuspid aortic valve. *J R Soc Interface*. 2020 Jun; 17 (167): 20190893. doi: 10.1098/rsif.2019.0893.
33. *Kazik HB, Kandail HS, LaDisa JF, Lincoln J.* Molecular and Mechanical Mechanisms of Calcification Pathology Induced by Bicuspid Aortic Valve Abnormalities. *Front Cardiovasc Med*. 2021 May 26; 8: 677977. doi: 10.3389/fcvm.2021.677977.
34. *Sturla F, Ronzoni M, Vitali M, Dimasi A, Vismara R, Preston-Maher G et al.* Impact of different aortic valve calcification patterns on the outcome of transcatheter aortic valve implantation: A finite element study. *J Biomech*. 2016; 49 (12): 2520–2530. doi: 10.1016/j.jbiomech.2016.03.036.
35. *Weinberg EJ, Schoen FJ, Mofrad MRK.* A computational model of aging and calcification in the aortic heart valve. *PLoS One*. 2009 Jun 18; 4 (6): e5960. doi: 10.1371/journal.pone.0005960.
36. *Thubrikar MJ, Deck JD, Aouad J, Nolan SP.* Role of mechanical stress in calcification of aortic bioprosthetic valves. *J Thorac Cardiovasc Surg*. 1983; 86 (1): 115–125. doi: 10.1016/s0022-5223(19)39217-7.
37. *Van der Valk DC, Fomina A, Uiterwijk M, Hooijmans CR, Akiva A, Kluin J et al.* Calcification in Pulmonary Heart Valve Tissue Engineering: A Systematic Review and Meta-Analysis of Large-Animal Studies. *JACC Basic to Transl Sci*. 2023; 8 (5): 572–591. doi: 10.1016/j.jacbts.2022.09.009.
38. *Schoen FJ, Tsao JW, Levy RJ.* Calcification of bovine pericardium used in cardiac valve bioprostheses. *Am J Pathol*. 1986; 123: 134–145.
39. *Sakaue T, Koyama T, Nakamura Y, Okamoto K, Kawashima T, Umeno T et al.* Bioprosthetic Valve Deterioration: Accumulation of Circulating Proteins and Macrophages in the Valve Interstitium. *JACC Basic to Transl Sci*. 2023; 8 (7): 862–880. doi: 10.1016/j.jacbts.2023.01.003.
40. *Khalivopulo IK, Evtushenko AV, Shabaldin AV, Troshkinev NM, Stasev AN, Kokorin SG, Barbarash LS.* Comparison of Propensity Scores for Surgical Treatment of Bioprosthetic Mitral Valve Dysfunction Using Traditional and "Valve-in-Valve" Methods. *Complex Issues Cardiovasc Dis*. 2023; 12 (2): 57–69. doi: 10.17802/2306-1278-2023-12-2-57-69.
41. *Fedorov SA, Chiginev VA, Zhurko SA, Gamzaev AB, Medvedev AP.* Clinical and hemodynamic results of using different models of biological prostheses for correction of senile aortic valve malformations. *Modern Technologies in Medicine*. 2016; 8 (4): 292–296. (in Russ).
42. *Pestiaux C, Pyka G, Quirynen L, De Azevedo D, Vanoverschelde JL, Lengelé B et al.* 3D histopathology of stenotic aortic valve cusps using *ex vivo* microfocus computed tomography. *Front Cardiovasc Med*. 2023 Apr 25; 10: 1129990. doi: 10.3389/fcvm.2023.1129990.
43. ExxonMobil. Datasheet. 2022 [cited 2023 Jul 19]. p. 2 ExxonMobilTM PP1014H1 Polypropylene Homopolymer. Available from: https://exxonmobilchemical.ulprospector.com/datasheet.aspx.
44. *Finotello A, Gorla R, Brambilla N, Bedogni F, Auricchio F, Morganti S.* Finite element analysis of transcatheter aortic valve implantation: Insights on the modelling of self-expandable devices. *J Mech Behav Biomed Mater*. 2021 Nov; 123: 104772. doi: 10.1016/j.jmbbm.2021.104772.
45. *Capelli C, Bosi GM, Cerri E, Nordmeyer J, Odenwald T, Bonhoeffer P et al.* Patient-specific simulations of transcatheter aortic valve stent implantation. *Med Biol Eng Comput [Internet]*. 2012 Feb [cited 2022 Mar 16]; 50 (2): 183–192. Available from: https://pubmed.ncbi.nlm.nih.gov/22286953/.
46. *Onishchenko P, Glushkova T, Kostyunin A, Rezvova M, Akentyeva T, Barbarash L.* Computer models of biomaterials used for manufacture of flap apparatus of prosthetic heart valves. *Mater Sci*. 2023; 0 (7): 30–39. doi: 10.31044/1684-579x-2023-0-7-30-39.
47. *Guo S, Shi Y, Zhang H, Meng Q, Su R, Zhang J et al.* Design and fabrication of a Nb/NiTi superelastic composite with high critical stress for inducing martensitic transformation and large recoverable strain for biomedical applications. *Mater Sci Eng C Mater Biol Appl*. 2020 Jul; 112: 110894. doi: 10.1016/j.msec.2020.110894.

The article was submitted to the journal on 19.04.2024

INSTRUCTIONS TO AUTHORS

Articles should contain original information that has not been previously published and is not considered for publication in other editions. Fee for publication of manuscripts will not be charged.

The manuscript should be presented in Microsoft Word format A4, 1.5 spacing, and Times New Roman font size 12. Submit your article to the online submission system in accordance with the instructions on the journal's website https://journal.transpl.ru.

Structure of the article

The Title page should include:

– Initials (first name and patronymic) of the authors of the article should be specified before their respective last names.
– Author names (list the author's initials before listing his or her last name as when registering for ORCID, or Open Researcher and Contributor ID – a non-proprietary alphanumeric code that uniquely identifies scientific authors).
– Full official name of the institution, city and country.
– If authors from different institutions participated in writing of the manuscript, it is necessary to correlate those with the names of the authors by adding a digital index uppercase after last name, and right before the name of the institution.

Information about the authors

For each author fully specify the last and the first name, patronymic and position in the relevant department/institution.

For correspondence

Fully specify the last and the first name, patronymic of the author, who will be holding correspondence, address (including postal code), telephone, fax number, e-mail.

Abstract

Each article must be accompanied by an abstract. The amount of text for the abstract of the original article should be of no more than 300 words, for a literature review, clinical observation – no more than 200 words. The abstract must fully comply with the content of the work. The abstract should not use abbreviations without prior expansion.

Abstract of ***the original article*** should contain the following sections: ***Objective***, ***Materials and methods***, ***Results***, ***Conclusion***. The abstract should present the most important results of the research.

Do not write: "*A comparative analysis of the sensitivity and specificity was conducted …*"

Should write: "*The sensitivity was ... % and ...%, p = , specificity, respectively ...% and ...%, p =* ".

Keywords

At the end of the abstract keywords must be given. To select the keywords a thesaurus of U.S. National Library of Medicine should be used – Medical Subject Headings (MeSH) at http://www.ncbi.nlm.nih.gov/mesh.

Conflict of interest

The author should inform the editor about the factual or potential conflict of interest have included the information about such conflict into the respective section of an article.

If there is no conflict of interest, the author should say so in the form like the following: "Author declares unawareness of the conflict of interest".

This information is supposed to be placed before the article text.

Text of article

Original article should include the following sections:

- Introduction
- Materials and methods
- Results
- Discussion
- Conclusion
- References

Review article should include an analysis of the literature with the presentation of modern sources (mainly in the last 5 years).

Clinical observation should be well illustrated (to reflect the essence of the problem) and include discussion with the use of literature data.

References in the text are indicated by number in square brackets: [1], [2, 5], [14–18] and ***in the references section are presented in order of their appearance in the text.*** All values given in the article should be expressed or duplicated in **SI** units.

References

The author is solely responsible for the accuracy of the data included in the references section of the article. References to unpublished papers or papers in print works are not allowed.

References are presented on a separate page.

The names of journals can be contracted in accordance with an embodiment of reduction adopted by the specific journal.

If the article quoted has DOI (a digital object identifier) or/and PMID (Pub Med identifier) they must be specified after the description of the article. To compile descriptions in References section NLM bibliographic reference citation standard is used – U.S. National Library of Medicine (http://www.nlm.nih.gov/bsd/uniform_requirements.html). If the number of authors does not exceed 6, the bibliographic description includes all the authors. If the number of authors is more, only the first six authors should be indicated and then add et al.

Requirements for tables and figures

Tables should be placed into the text; they should have numbered heading and clearly labeled graphs, convenient and simple to read. Table's data must comply with the numbers in the text, but should not duplicate the information therein. Table references in the text are required.

Illustrations and drawings should be submitted in electronic format (JPEG or TIFF format with a resolution of at least 300 dpi and no smaller than 6 × 9 cm), in a volume of close to 1 MB. Drawings must include all copyright symbols – arrows, numbers, signs, etc. Figure captions should be submitted in a separate file with the extension *.doc. First, the name is given, then all arithmetic and alphabetical symbols (lettering) are explained.

Articles should be addressed
to the Russian Journal of Transplantology and Artificial Organs website:
https://journal.transpl.ru/vtio
E-mail: vestniktranspl@gmail.com

Издание зарегистрировано в Госкомпечати РФ, № 018616 от 23.03.99 г.

Подписано к печати 27.12.24.

Тираж 1000 экз.

ООО «Издательство «Триада».
ИД № 06059 от 16.10.01 г.
170034, г. Тверь, пр. Чайковского, 9, оф. 514,
тел.: +7 (915) 730-10-37, +7 (910) 647-49-85
E-mail: triadatver@yandex.ru
http://www.triada.tver.ru

Заказ 52271